

STRUCTURE AND PROPERTIES OF POLYMER BLENDS

BY

CHANGIZE SADRMOHAGHEGH

Submitted for the degree of DOCTOR OF PHILOSOPHY of
the University of Aston in
Birmingham

September 1979

SUMMARY

STRUCTURE AND PROPERTIES OF POLYMER BLENDS

Changize Sadrmohagheh

Submitted for the degree of PhD : September 1979

The mechanical properties, morphology, light and thermal stability of pure polymers (eg LDPE, PP etc) and blends of PE/PVC, PE/PP and PE/PS with and without additives have been studied using a variety of physical and chemical techniques. The change in mechanical properties occurring during the ultra-violet light accelerated weathering of these polymers and polyblends was followed by a viscoelastometric technique (Rheovibron), stress-strain and impact measurements in the solid phase at room temperature ($20 \pm 1^\circ\text{C}$). The results showed that tensile strength, elongation at break, impact strength and $\tan\delta$ (20°C) decreased with increasing PVC, PP and PS content. It was concluded that hydroperoxides are the most important initiators in normally processed polymers during the early stages of photo-oxidation. On exposure to uv light, the blends (PE/PVC, PE/PP and PE/PS) showed lower stability than pure LDPE.. A study of the mechanical properties during uv irradiation indicated that the tensile strength of the blends decreased initially but at a later stage increased with irradiation time. The elongation at break and impact strength decreased continuously with exposure time. In the thermal degradation of PE/PVC blends, PVC behaved as a stabiliser and this effect was significant at high concentrations of PVC (eg 20%).

Blends of PE/PVC, PE/PP and PE/PS which are found in domestic waste exhibit poor mechanical properties due to incompatibility. Therefore, reprocessing of such unseparated mixtures results in products of little technological value. The inclusion of some commercial block and graft copolymers which behave as solid phase dispersants (SPD's) increase the toughness of the blends. . Optical and electron microscopy were used to study the morphology of the blends in order to assist in the understanding of structure/property relationships of the blends.

Hydroperoxide

Photo-oxidation

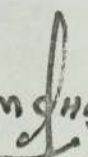
Thermal-oxidation

Solid phase dispersants (SPD's)- compatibilisers)

Recycling of polymer waste

The work described herein was carried out at the University of Aston in Birmingham between April 1976 and September 1979.

It has been done independently and has not been submitted for any other degree.


C. SADRMOHAGHEGH
C Sadr mohagheh

ACKNOWLEDGMENTS

I wish to express my gratitude to Professor Gerald Scott and Dr A Ghaffar for their guidance and encouragement throughout the course of this study.

I also acknowledge with thanks the co-operation of the Technical and Library Staff of the University of Aston in Birmingham together with friends and colleagues in the Chemistry Department.

C Sadrmohaghegh

CONTENTS

		<u>Page</u>
Chapter 1	General Introduction	1
1.1	Polymer waste statistics	5
1.2	Problems arising in polymer recycling	8
1.3	Technical aspects of polymer blends	10
1.4	Compatibility of polymers in blends	14
1.5	The effect of compatibility on transition behaviour	18
1.6	Mechanical properties of polymers and polyblends	21
1.6.1	Dynamic mechanical properties of polymers and polyblends	29
1.7	Microscopy	34
Chapter 2	Degradation of polymers and polymer blends	36
2.1	Photo-initiation	40
2.2	Thermal (non-oxidative) degradation of polymer blends	47
2.3	Mechanism of oxidative degradation of polyolefins	49
Chapter 3	Experimental	52
3.1	Materials	52
3.2	Melt processing	52
3.3	Preparation of films from processed samples	53
3.4	Evaluation of torque versus time curve	54
3.5	Determination of gel content in the processed polyethylene samples	56

3.6	Measurements of melt flow index (MFI)	56
3.7	Ultra-violet exposure cabinet	58
3.8	The accelerated thermal-oxidation of processed polymers	59
3.9	Measurements of brittle fracture time of polymer samples	61
3.10	Infra-red spectroscopy	61
3.10.1	Calculation of absorbance	63
3.11	Uv spectroscopy	65
3.12	Rheovibron (Dynamic Viscoelastometer)	65
3.12.1	Theory and derivation of basic dynamic equations	66
3.12.2	Principles involved in the rheovibron	70
3.13	Tensile strength	76
3.14	Impact strength	77
3.15	Estimation of peroxide in low density polyethylene and polypropylene	79
3.16	Microscopy examination	80
Chapter 4	The effect of processing and reprocessing on the thermal oxidation and photo-oxidation stability of low density polyethylene (LDPE)	83
4.1	Introduction: Structure of LDPE	83
4.1.1	Effect of processing on LDPE properties	86
4.2	Experimental	86
4.3	Results	89
4.4	Discussion	107
4.5	Processing of commercially stabilised polyethylene	114

4.6	Relation between mechanical properties and polymer morphology	121
Chapter 5	Effect of processing on thermal and photo-oxidation stability of polypropylene (PP)	125
5.1	Introduction	125
5.2	Experimental	128
5.3	Results	129
5.4	Discussion	147
5.5	Relation between mechanical properties and polymer morphology	157
Chapter 6	Study of blends of LDPE and PVC	159
6.A	Introduction	159
6.A.1	Experimental	160
6.A.2	Effect of PVC concentration on mechanical properties of LDPE/PVC blends	164
6.A.2.1	Results and discussion	164
6.A.3	Effect of PVC concentration on thermal oxidation of PE/PVC blends	182
6.A.3.1	Introduction	182
6.A.3.2	Results and discussion	187
6.A.4	Effect of PVC concentration on the photo-oxidation of LDPE/PVC blends	204
6.A.4.1	Results and discussion	204
6.A.5	The effect of some transition metal ions on thermal and uv oxidation of PE/PVC blends	219

6. A. 6	Introduction of some solid phase dispersants (SPD's) to improve the toughness of blends	219
6. A. 6. 1	Introduction	219
6. A. 6. 2	Experimental	228
6. A. 6. 3	Results and discussion	228
6. B	The effect of polypropylene concentration on mechanical properties of LDPE/PP blends	234
6. B. 1	Introduction	234
6. B. 2	Experimental	235
6. B. 3	Results and discussion	237
6. B. 4	Effect of polypropylene (PP) concentration on the photo-oxidation of LDPE blends	241
6. B. 4. 1	Introduction	241
6. B. 4. 2	Results and discussion	246
6. B. 5	Introduction of some solid phase dispersants (SPD _s) to improve the toughness of blends	260
6. B. 5. 1	Introduction	260
6. B. 5. 2	Experimental	261
6. B. 5. 3	Results and discussion	261
6. C	Effect of polystyrene (PS) concentration on mechanical properties of LDPE blends	261
6. C. 1	Introduction	261
6. C. 2	Experimental	268
6. C. 3	Results and discussion	270
6. C. 4	Effect of PS concentration on the photo-oxidation of LDPE blends	277

6. C. 4. 1	Introduction	277
6. C. 4. 2	Results and discussion	283
6. C. 5	Introduction of some solid phase dispersants (SPD's) to improve the toughness of blends	291
6. C. 5. 1	Introduction	291
6. C. 5. 2	Experimental	296
6. C. 5. 3	Results and discussion	296
Chapter 7	Mechanistic conclusions	303
7. 1	Effect of processing on the mechanical properties of polymer blends	303
7. 2	Photo-oxidation of polymers and polymer blends	303
7. 3	Thermal oxidation of polymer blends	304
7. 4	Modification of polymer blends by solid phase dispersants (SPD s)	304
7. 5	Suggestions for further work	305
References		306-319

CHAPTER ONE

GENERAL INTRODUCTION

Plastics like other materials such as paper, glass, metal, wood and ceramics, once they have fulfilled their primary functions and are no longer required, are discarded and have to be disposed of in some way. Depending on the manner in which the waste is discarded, one can distinguish, at least within the context of this thesis, between 'plastics waste' and 'plastics litter'. Whenever discarded material is treated by any of the approved disposal processes, such plastics discards represent 'waste'. By far the largest proportion of plastics items which we throw away appears as waste collected with general domestic or urban refuse. This also applies to industrial rejects and discards which, if not dealt with on the site of their production, can not readily be collected and become indiscriminately deposited and randomly scattered discards. Irrespective of their origin, these materials constitute 'litter'.

The disposal of solid waste, both municipal and industrial, has become a vexing problem and in the recent concern for the environment, attention has been focussed upon plastics because they present a pollution problem greater than their weight percentag in waste would suggest. This is due to a combination of their volume/weight ratio, their omnipresence and their seemingly indestructable nature. These factors prompted a number of research programmes which are investigating this problem from a variety of points of view. For example, separation into individual components, pyrolysis of mixtures and indirect degradation are among the methods proposed for

the disposal of waste.

The rate of generation of solid wastes in general has been documented over the years. Currently about 1.69×10^8 tons (UK tons) 380 billion pounds (US) are collected annually by disposal authorities in the US^(1,2). Reports on the role of plastics in solid waste are less complete, with the earliest thorough study dating back to 1967⁽³⁾. Several have appeared^(4,6) since then and it is not surprising to learn that the contribution of plastics is growing at a rate much faster than the overall growth of solid wastes. This is evident from the vigorous growth and product diversification exhibited by the plastics industry in recent years, especially in packaging. The exact weight percentage of plastics in solid waste is a little uncertain but is estimated to be about 2% currently in both the UK and USA⁽¹⁾. A comparison of growth rates indicates that this percentage will increase markedly in the coming years. A particularly sobering finding is that in Japan, plastics comprised 7% of all solid waste in 1968, and the disposal of industrial waste there costs about \$0.05 per pound⁽¹⁾. These facts lend considerable impetus to research in reuse of plastics as a means of solving certain disposal problems.

Generally, recycling of the various municipal and industrial solid waste streams is attractive, if marketable products can be made from them, since it will reduce the volume of refuse that must be disposed of by conventional techniques. These include incineration and landfilling, which are already over-burdened in some areas. It also conserves natural resources, since the products made from the waste may be a substitute for something that would otherwise require the consumption of virgin

resources. Currently, recycling is practical to varying degrees for some materials, eg glass, paper, metals and rubber. Recycling of plastics could be accomplished in a variety of ways. Approaches have been considered which destroy the polymeric molecular structure to produce useful chemicals⁽⁷⁻¹¹⁾ or energy⁽⁸⁻¹⁰⁾. The simplest sample of recycling plastics where the useful product is also a plastic is returnable cartons or bottles which may be reused in the same form⁽⁵⁾. This is certainly a preferred method where applicable. However, it is easy to see that many uses will not permit this, particularly where contamination is involved. The recycling must therefore generally involve melt reprocessing of the plastics. For years the plastics industry has practical in-house reuse of scrap plastics generated during manufacturing operations⁽¹²⁻¹⁴⁾. Numerous small companies in the US make a profitable business of dealing in scrap plastics. However, most of these efforts are restricted to scrap plastics of the same genetic types and frequently of the same grade, and the reuse of the plastics that might be recovered from municipal solid wastes is normally not considered. Consequently, these efforts make only a limited contribution to the general problem.

Only a few studies aimed at recycling plastics recovered from solid wastes by reprocessing have been reported⁽¹⁵⁻¹⁸⁾. To implement such an approach it is generally necessary to first separate the plastics from the rest of the solid waste stream. Currently, there is no method in operation which does this for the general municipal solid waste; however, there are experimental processes in operation designed to separate other parts of the solid waste stream which could potentially aid in the separation of plastics^(8,19). Some novel approaches

for the separation of a solid waste stream into basic components are being examined^(20,21). If the incentive were great enough, the crude technique of hand sorting could be employed, or if the public concern were high enough, segregation at source could be practiced. In the present study, this problem will not be considered further, since it is the aim here to evaluate the value of mixed plastics as a reusable material. Beyond the separation of 'plastics' from the rest of the refuse, lie other profound problems, since the plastics recovered would be composed of a variety of generic polymer types such as the polyolefins, polystyrene and poly-(vinyl chloride), as well as a multiplicity of grades of each of these polymers. It is generally known that a mixture of thermoplastic polymers results in a considerable down-grading of properties when processed compared to pure polymers. Separation of these waste plastics into their generic types would be desirable and efforts are being directed towards this objective^(15,16,21). Further segregation into pure polyethylene polystyrene etc may be possible in certain cases. Even if sophisticated techniques are developed for this purpose, it is highly unlikely that they would be 100% efficient, and thus each stream would still be composed of an assortment of chemical types with a preponderance of one. The objective of this research is to explore the potential for recycling without generic separation. The first step is to make a thorough determination of the properties of the blends that might be recovered. The second step is to investigate approaches to upgrade these properties and the third step is to investigate the effect of reprocessing on the degradation of the final products.

1.1 Polymer Waste Statistics

Several studies^(22, 5, 6, 18) have considered the percentage of the total solid waste stream which may be classed generally as plastics. Such information is invaluable for assessing the overall economics but they are not very useful in the planning of research on recycling at this time. Of more critical concern is the generic breakdown, ie what fraction of the plastics segment is polyethylene, polystyrene, poly(vinyl chloride), etc? The answer to this question is also dependent on the specific segregation-reuse scheme considered, since certain components will necessarily be excluded because the segregation mechanism does not identify them as plastics or because the reprocessing scheme cannot accommodate them. Further, this breakdown will fluctuate both in place and in time, except for certain commercial wastes. Regardless of these factors, some characterisation of the plastics in municipal solid waste is desirable and numerous estimates have been published^(5, 6, 18, 22). Most of these are based on an analysis of production statistics and end-use patterns with some limited sampling of actual refuse. From perusal of production figures, it is ascertained⁽²³⁾ that low density polyethylene, high impact polystyrene and poly(vinyl chloride) (PVC) are the main polymers used in domestic packaging applications.

	<u>1974</u>	<u>1975</u>
Low density polyethylene	295.0	232.0
High density polyethylene	79.0	70.0
Poly(vinyl chloride)	58.0	48.0

(in '000 tonnes)

(Source: 'Packaging Review', 1976, UK).

At the present time, there is no estimate of the fraction of the plastic which is combined with other materials such as metal or paper, which would severely limit the possibility of reprocessing them. The character of commercial wastes is peculiar to each situation.

Within each general chemical type of plastic there are many variations of grades which arise from tailoring the materials to meet spectrum of uses. These fractions, however, are likely to be of some importance in plastics reprocessing and reuse and therefore more information is needed. For polyethylene, the principle factors are density, molecular weight, and molecular weight distribution. For the purpose of initial characterisation, density and melt index range are probably adequate. An analysis⁽²⁴⁾ of available sales statistics yielded the rough breakdown shown in Table 1. It reflects the large use of polyethylene in film and bottles.

For poly(vinyl chloride) the major factors are molecular weight, copolymer versus homopolymers, plasticised versus rigid, and the presence of impact modifiers and processing aids. Data are not available to characterise fully the waste PVC. Packaging uses account for essentially half of the waste PVC where nearly comparable amounts of flexible and rigid polymers are employed. Much of the rigid PVC is impact modified grades.

For polystyrene these variables are molecular weight and general purpose versus impact modified grades, and again suitable data for full characterisation of this segment of the waste is not readily available. Most general purpose polystyrene in waste appears as disposable foamed products. Probably a

Table 1: Estimated analysis of grades of polyethylene in solid waste

Melt index	density	
	Low	High
1	1%	17%
1-5	60%	4%
5	12%	4%

similar amount of impact modified polystyrene will also be present in the waste. At this present time it is not known to what extent copolymers such as SAN or ABS contribute to waste although it is not thought to be large.

1.2 Problems Arising in Polymer Recycling

The desirability of recycling of waste is considered to bear no reason to doubt the economic viability. In America the Environmental Protection Agency (EPA), is already positively promoting the recycling of town refuse and in February 1973 the EPA, in a report presented to Congress⁽²⁵⁾, stressed the necessity for recycling. Part of the conclusions are quoted below.

- (1) In manufacturing processes using reclaimed materials obtained by recycling as 'raw materials', it is considered that, compared with the case of using virgin raw materials, there are generally decreases in environmental pollution, occurrence of waste material and consumption of energy.
- (2) Recycling is greatly influenced by economics. The cost of producing articles from recycled material is generally greater than when using virgin raw materials. Therefore, at present, there is only marketability when using as 'raw material' town refuse which is of high quality and also easy to obtain.
- (3) Today technically it is possible to obtain material for recycling from mixed town refuse. However, since the cost of collection is high, the recycling business is only

attractive in cities where the waste disposal cost is great, or in cities where a market for recycled material is in the close vicinity.

- (4) To obtain material for recycling from town refuse is, as a general concept, the ideal solution. However, it is necessary to lower the equivalent manufacturing cost and it is necessary to improve the quality of the recycled material. Also it is necessary to establish an economic and social system which makes recycling economically attractive.

Recent production figures reveal that four major thermoplastics make up about 75 percent of the total US plastics output⁽²⁶⁾.

<u>US Production Figures</u>	<u>%</u>
High density polyethylene (HDPE)	9.5
Low density polyethylene (LDPE)	20.2
Polypropylene (PP)	7.4
Poly(vinyl chloride) (PVC)	16.5
Polystyrene (PS)	18.3

Together these 'volume' thermoplastics accounted for 6,300 million lbs of the urban and industrial waste mix in 1970, and this figure is expected to rise to 18,000 million lbs in 1980. Of this total, the polyolefins (LDPE, HDPE, PP) account for around 66%, with the remaining 34% split nearly evenly between PS and PVC.

It is clear then, that any large-scale attempts to recycle plastics

will have to deal mainly with the materials discussed above. Unfortunately, the thermodynamic incompatibility of these chemically different polymers results in very poor mechanical properties of mixtures compared to the virgin material⁽²⁷⁾, limiting such mixtures to a few low-grade, non-critical applications.

1.3 Technical Aspects of Polymer Blends

Some of the polymers discussed above are more important in industry, notably polystyrene (PS) and poly(vinyl chloride) (PVC) have disadvantages in use in that they are brittle and show poor resistance to impact. This is at present overcome by the use of modifiers, themselves polymers, which are blended with the polymer in small proportions (normally not more than 5-20%). These materials normally contain a polymer with a low glass transition temperature such as polybutadiene or copolymers of polybutadiene with other monomers such as styrene, acrylonitrile, methacrylonitrile, methylmethacrylate to improve compatibility with the main polymer matrix.

The simplest method involves simple mechanical blending of the two polymeric components in the molten state⁽²⁸⁾. The earliest form of high impact polystyrene (HIPS) was made by this technique.

While the impact resistance of mechanical blends is clearly superior to that of the parent polystyrene, they have two important deficiencies that cause them to be inefficient. First due to the high viscosity of the melts, the problem of attaining intimate mixing cannot be entirely overcome. As a result, the

dispersed phase maintains a relatively large particle size⁽²⁸⁾. Secondly, the two phases are bonded together only by a weak Vander Waals force, so that the material as a whole exhibits poor cohesion.

Still higher levels of toughness in rubber-modified polystyrene can be obtained by the graft polymerisation techniques, which give both more intimate mixing and better interfacial bonding than is possible by mechanical blending. In effect, the efficiency of the rubbery component in toughening the matrix is considerably increased. In general, the graft polymers are prepared by bulk polymerisation processes in which the rubber component is first dissolved in the styrene monomer to a level of 5-10% by weight. For such bulk processes, efficient mixing is required during polymerisation of the styrene monomer until the mass has a fairly high viscosity, that is, until a conversion of about 50% is reached (Malace and Keskkula, 1968⁽²⁹⁾). During this time, the rubber (eg polybutadiene) while soluble in the pure styrene monomer, becomes insoluble as the polystyrene concentration increases and undergoes phase separation and later phase inversion. When this occurs, both polymer phases contain considerable quantities of styrene monomer.

After polymerisation is complete, a complex cellular structure exists (Huelck and Covitch, 1971⁽³⁰⁾), with polystyrene in the continuous phase. However, the styrene monomer that remains within the polybutadiene phase after phase separation forms discontinuous droplets upon polymerisation within the polybutadiene phase. It is believed that most grafted polymer formed is located at the interfacial regions of the cellular structure⁽³⁰⁾. If mixing is not carried out during the early stages of polymerisation, a

gross honeycomb-like or cellular structure may result, in which the rubber remains as the continuous phase. This is true even though the rubber is present at a level of only 5-10%⁽³¹⁾. A product of this type is usually softer and lower in impact strength than the phase-inverted materials just discussed. Scott and his co-workers investigated the mechanical properties of this copolymer and also studied the effect of uv light on mechanical properties of HIPS^(32,33,34).

Like the rubber-polystyrene blends, ABS (acrylonitrile-butadiene-styrene) resins are two phase systems in which an elastomeric phase is finely dispersed in a glassy matrix of a styrene-acrylonitrile (SAN) resin. The rubbery phase usually consists of polybutadiene, NBR (acrylonitrile-butadiene rubber), or a random copolymer of styrene and butadiene (SBR), which may itself be modified by grafting of a third monomer (for example acrylonitrile) in order to alter its compatibility with the matrix. A wide range of resins may be produced that combine good resistance to heat and chemicals with ease of processing, stiffness, and toughness. Indeed, the ABS resins are considered to be true engineering plastics, suitable for many applications requiring a high level of mechanical performance and durability⁽³⁵⁻⁴⁴⁾.

The simplest type of ABS is made by mechanically blending the two polymers⁽⁴²⁾. In this case the two copolymers always have a certain fraction of one monomer, styrene, in common to improve compatibility.

Poly(vinyl chloride) (PVC) homopolymer is a stiff, rather brittle plastic with a glass transition temperature of about 80°C,

which is somewhat more ductile than polystyrene and hence has somewhat improved toughness. For example, methyl methacrylate-butadiene-styrene (MBS) elastomers can impart impact resistance and also optical clarity^(45,46). ABS resins are also frequently employed for this purpose. Another of the impact mechanical blends of elastomeric polymers with plastic resins is based on poly(vinyl chloride) as the plastic component and random copolymers of butadiene and acrylonitrile (AN) as the elastomer⁽²⁸⁾. On incorporation of this elastomeric phase, PVC, which is ordinarily a stiff, brittle plastic, can be considerably toughened. A non-polar homopolymer rubber such as polybutadiene (PB) is incompatible with the polar PVC. Indeed electron microscopy shows a well-defined two-phase system for simple blends of PVC with PB⁽²⁸⁾. However, the introduction of a small amount of AN as a comonomer in the PB component results in more polar and more compatible, acrylonitrile-butadiene rubber. As shown by Matsuo⁽²⁸⁾, the addition of 20% AN to PB (NBR-20) causes the phase boundaries to become less distinct—an indication of enhanced compatibility. Addition of AN to a level of 40% (NBR-40) destroys the phase boundaries entirely, resulting in the micro-heterogeneous system shown by Matsuo⁽²⁸⁾.

One of the typical developed polyblends is EPR (ethylene-propylene rubber) with PP (polypropylene)⁽⁴⁷⁾. The blend is not a molecular dispersion; at low EP content, PP is the continuous phase of high crystallinity in which the EPR particles are embedded. As shown by the work of Onogis^(48,49) in which dynamic viscoelasticity was measured as a function of temperature and PP-EPR blend compositions. Stress-strain curves as well as orientation function were studied, was

measured and phase immersion occurs in the blend when the EPR content exceeds 50%. However, even at low EPR concentration in the system the crystallisation of polypropylene (PP) is influenced by the EPR content and leads to changes of initial Young's moduli for crystalline deformation and microscopic deformation. The lower EPR content also influences the temperature dependence of both the initial Young's moduli and the size of the supermolecular structures obtained by the slow and fast cooling processes in which samples were prepared.

1.4 Compatibility of Polymers in Blends

It has been found experimentally that a glass-rubber polymer system in which the components have such a strong affinity so that they are mutually soluble is of no value as high impact resistance plastic. On the other hand, a two polymer system in which the affinity of the components is so low that they cannot be mechanically blended in a uniform fashion are also worthless as impact modified plastics. An optimum compatibility between the phases must be achieved, great enough to provide necessary adhesion at the glass rubbery interface, yet not so great that discrete two-phase character is destroyed by solubility.

In general, the change in Gibbs free energy of a mixture of two phase polymers at constant temperature and pressure to form a true molecular solution can be given by:

$$\Delta G = \Delta H - T \Delta S$$

where ΔH is the change of enthalpy and ΔS represents the change in entropy which occurs in the system and T is the absolute temperature, if ΔG is negative, the solution process is thermodynamically favoured, if positive, the two-phase system is stable. The change in entropy ΔS for a mixing process is always positive, since mixing is associated with increasing the randomness or disorder of the system. With increase absolute temperature, it is seen that the entropy contribution to the free energy change, $T \Delta S$ always favours the solution. The important point here, however, is that because of their high molecular weights, the entropy change which occurs when two polymers are mixed is quite small, orders of magnitude less than that for mixing equivalent masses of low molecular weight liquids⁽⁵⁰⁾. The enthalpy of mixing is a measure of the affinity of the molecules for their environment, so that a negative value indicates a decrease in energy of the system upon mixing, ie the molecules prefer the environment of the mixture to that in their pure state. Such a situation is exceedingly rare in the case of polymer molecules which almost invariably prefer their own kind⁽⁵¹⁾.

The exception arises when there are strong hydrogen bonded interaction between different components. A qualitative means of predicting the affinities of the polymer-pairs has been designed in terms of easily measured properties of the compounds. One possibility is through the use of the solubility parameter (δ) which has proved useful in the study of the dissolution and swelling of polymers in low molecular weight liquids. For non-polar liquids, the internal energy change upon solution is given by:

$$\Delta E = Q_1 Q_2 (\delta_1 - \delta_2)^2 \text{ cal/cc of solution}$$

where the Q_1, Q_2 are the volume fractions of the components. Realising that amorphous polymers are essentially liquids and assuming that the volume change upon mixing is negligible, this is an expression for change in enthalpy on solution since $\Delta H = \Delta E$ for a constant volume, constant pressure process^(52, 53).

Whilst not too much work has been done on the compatibility of the polymer-pairs alone, there has been extensive work done on polymer-polymer solvent system in which the individual polymers are dissolved in a common solvent, and should aid the formation of a single phase system. In almost all cases, however, at polymer concentration of a few percent when initially homogeneous solutions are mixed, a two-phase system is formed, one liquid phase containing all of one polymer and the other layer all of the second polymer⁽⁵⁴⁾. This result applies even when the polymer-pairs are quite similar. As predicted by the theory, as the molecular weight of polymers decreases and the ΔS term increases, compatibility becomes greater⁽⁵⁵⁾. Also as expected hydrogen bonding exerts a favourable influence on compatibility but even so, only a few completely soluble polymer-polymer solvent systems have been reported and it is doubtful whether they would maintain compatibility at higher concentrations. These facts are of interest in conjunction with the graft polymerisation in bulk technique. Although the initial rubber solution may be homogeneous, as soon as an appreciable amount of second component has been formed, a two-phase system will result. In fact it has been found that there is only one rubber glass pair for which adequate evidence has been presented to indicate complete compatibility in the

bulk phase (PVC and NBR-40 blends) compatibility is undoubtedly the result of the strong interaction between the polar-chlorides and nitrile groups. Since true solubility will rarely (if ever) be a problem, the design of successful two-phase impact system by means of polymer blends focusses on achieving the greatest compatibility or adhesion between the phases. The first approach to this would be to match the solubility parameters as closely as possible. This may be done by varying the proportion of a monomer common to both phases, but this method often presents drawbacks. For example a 60/40 butadiene-styrene rubber is more compatible with polystyrene than a 75/25 copolymer but it has a higher glass transition temperature and low temperature impact resistance suffers.

The most successful method of improving phase adhesion has been to graft glassy monomers to the rubber backbone. The grafted material is quite compatible with the surrounding glass phase and is chemically bound to the rubber resulting in excellent adhesion and improved impact strength.

It has been reported that cross-linking of the rubber phase improves impact strength. Although it does improve melt processability, reasons for the impact improvement are not clear unless the polymers were soluble to begin with. Cross-linking the rubber would eliminate this solubility and also eliminates this viscose flow which might aid in the initiation of drawing.

1.5 The Effect of Compatibility on Transition Behaviour

Another technique which has recently been used to study the two-phase polymer system is dynamic mechanical tests^(43,56). Basically, it consists of subjecting a sample to an oscillating stress (or strain) and measuring the resulting strain (or stress) as a function of frequency (time) and/or temperature. Two fundamental quantities are obtained from this test:

- (i) a storage modulus E' which is a measure of the amount of applied energy stored in the material elastically, and
- (ii) loss modulus or damping decrement E'' which is a measure of the amount of applied energy dissipated by materials as heat.

Such time or temperature dependent quantities in the case of polymer blends yield particular information about compatibility of two phase polymers. For incompatible polymer pairs, each polymer exhibits its own characteristic glass transition temperature. A good example of this case is PVC/PBD polymer blends (Fig 1.5.3). The T_g for the PBD is observed at temperatures in the range of -100°C depending on PBD concentration. While only a slight decrease in ϵ' can be observed in this temperature range, the value of ϵ'' exhibits distinct peaks with temperature increase when PBD is present. On the other hand, at $+80^{\circ}\text{C}$ the continuous phase PVC undergoes its T_g resulting in a much larger change in ϵ' the material which softens from a plastic to viscoelastic mass and ϵ'' exhibits a separate loss peak. Similarly, in the blends of PVC and NBR-20 (Fig 1.5.2), the presence of an E'' peak

corresponding to the T_g of NBR-20 at -40°C is evident; however, its upper tail overlaps with that of the PVC transition. This could indicate that although the rubber phase exists independently in this semi-compatible system, the interaction between the two phases is marked. The values of E' do not exhibit two transition; instead the glass transition is broadened and shifted to lower temperatures.

The PVC and NBR-40 systems show a third distinct type of behaviour somewhat reminiscent of the behaviour of random copolymer compositions (Fig 1.5.1). Values of E' exhibit only one transition, which systematically moves down the temperature scale as the NBR-40 content is increased. Further the glass transition for the NBR-40 blends assumes a sharpness characteristic of homopolymers or random copolymers. Clearly an increase in the AN content of NBR results in an increased compatibility with PVC.

Idealising the above somewhat, it can be said that a blend of two incompatible homopolymers results in two sharply defined phases, each with its own glass transition temperature. As the two polymers attract each other more (but remain incompatible) so that extensive mixing is obtained, the two glass transitions shift inward towards each other and broaden. A point is reached where one very broad transition is noted, which may span the temperature range between two components. On the other hand, if the mixing is complete on the molecular level and a true solution is formed, the single glass transition tends to revert to a narrow transition again, at a temperature controlled by the weight fraction of the components.

Figure 3.14. Temperature dependence of dynamic modulus E' and dynamic loss modulus E'' for PVC/NBR-40 blends (a nearly compatible system): (—) 100/0; (---) 100/10; (----) 100/25; (· · ·) 100/50. (Matsuo *et al.*, 1969a.)

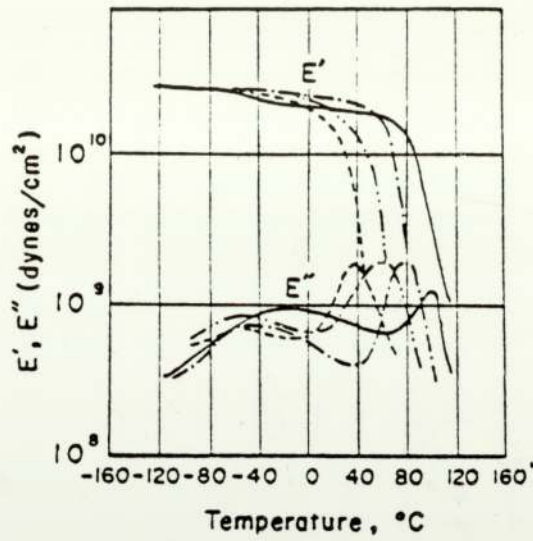


Fig 1.5.1

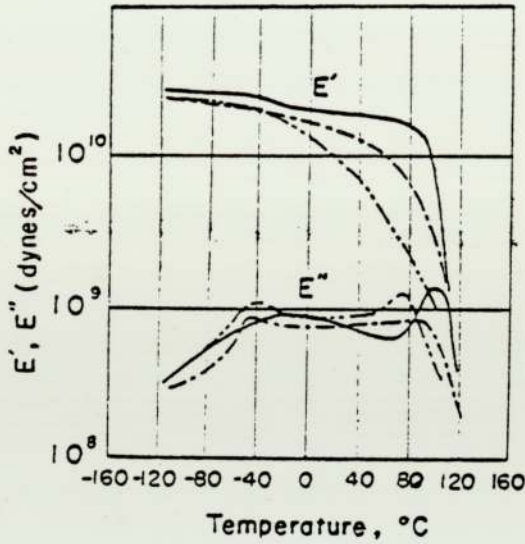


Fig 1.5.2

Figure 3.13. Temperature dependence of dynamic modulus E' and dynamic loss modulus E'' for PVC/NBR-20 blends (a semicompatible system): (—) 100/0; (---) 100/15; (----) 100/25. Such behavior is preferred in order to achieve high impact strength. (Matsuo *et al.*, 1969a.)

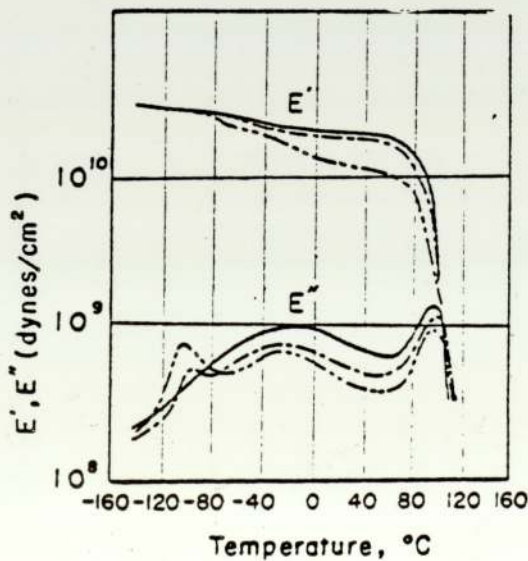


Figure 3.12. Temperature dependence of dynamic modulus E' and dynamic loss modulus E'' for PVC/PBD blends (an incompatible system): (—) 100/0; (---) 100/5; (----) 100/15. Note the two distinct loss peaks near -100°C ; these correspond to the PBD phase. This transition does not appear clearly in the E' curve because the PBD is the dispersed phase. (Matsuo *et al.*, 1969a.)

Fig 1.5.3

While most polymer pairs exhibit pronounced incompatibility, several important pairs are apparently either compatible or nearly so^(56, a, b, c) (see Tables 2 and 3).

1.6 Mechanical Properties of Polymers and Polyblends

The mechanical properties of polymers are of interest in any applications where they are used as a structural material. Changes in mechanical properties provide information as to the useful service life of polymers. They are also important, however, because they show how mechanical behaviour is related to different physical structures that may be produced under varying conditions.

Thermoplastics are viscoelastic materials whose properties are very dependent on temperature. Their behaviour depends on the relative values of the viscous and elastic components of the dynamic mechanical spectrum. On the application of stress there follows:

- (a) an instantaneous elastic deformation (owing to the bending and stretching of primary valence bonds),
- (b) a retarded, and recoverable, elastic deformation (owing to the molecular configuration moving to the new based equilibrium associated with an elongated or orientated stressed state),
- (c) an irrecoverable deformation (owing to polymer chains or segments slipping past one another).

Table 2: Some compatible or semi-compatible polymer pairs

Component 1	Component 2	References
poly(vinyl chloride)	poly(butadiene-co-acrylonitrile)	57-59
poly(vinyl acetate)	poly(methyl acrylate)	60, 61
poly(methyl methacrylate)	poly(ethyl acrylate)	61, 62
polystyrene	poly(α -methyl styrene)	63
polystyrene	poly(2,6-dimethyl phenylene oxide)	64-66
polystyrene	Isotactic poly(vinyl methyl ether)	67
poly(vinyl chloride)	poly(δ -caprolactone)	69

Table 3: Selected incompatible polymer pairs

Polymer 1	Polymer 2	References
polyethylene	polyisobutylene	69
poly(methyl methacrylate)	poly(vinyl acetate)	70
natural rubber	poly(styrene-co-butadiene)	71
polystyrene	polybutadiene	72
polystyrene	poly(vinyl chloride)	73
poly(methyl-methacrylate)	polystyrene	63
poly(methyl-methacrylate)	cellulose triacetate	74
nylon 6	poly(methyl-methacrylate)	75
nylon 66	poly(ethylene-terephthalate)	76
polystyrene	poly(ethyl acrylate)	77, 78
polystyrene	polyisoprene	79
polyurethane	poly(methyl methacrylate)	80

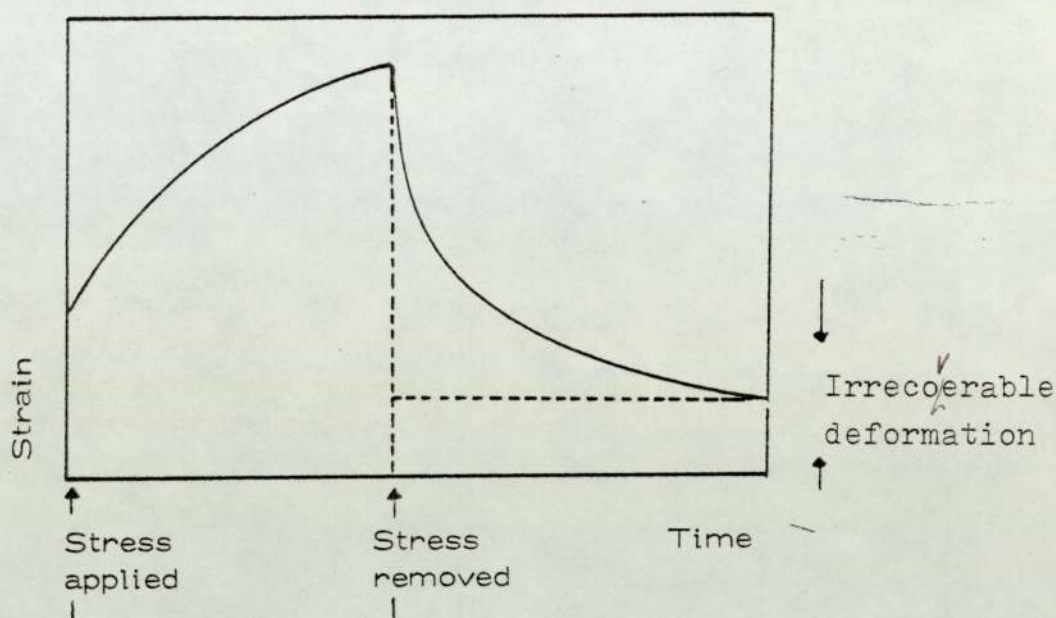
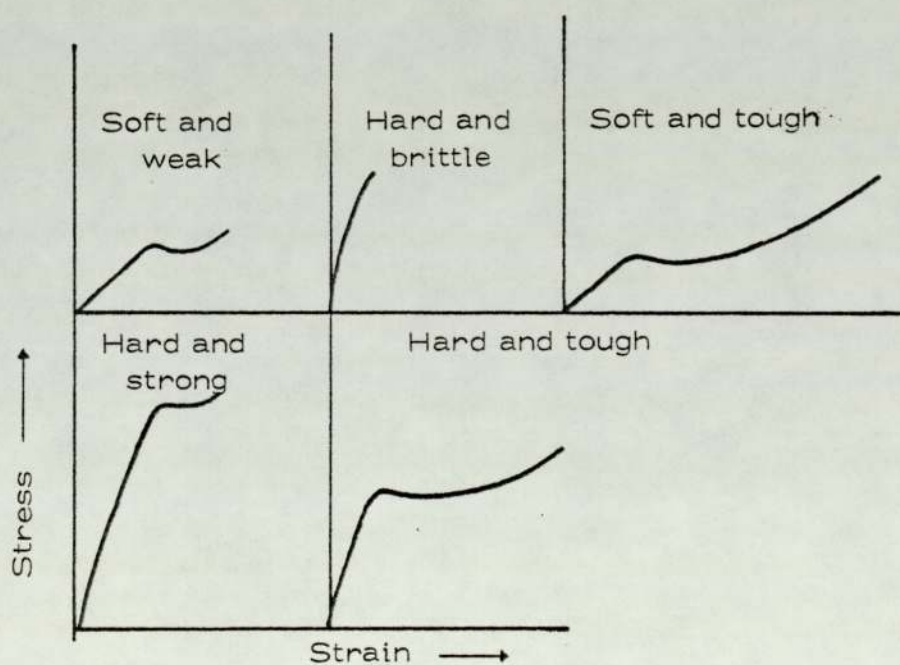
These effects can be shown diagrammatically by showing the variation of strain with time when a stress is applied and then removed (Fig 1.6.1).

A number of mechanical tests may be used to study visco-elastic materials⁽⁶⁰⁾. The most important tests include creep, stress-relaxation, stress-strain (tensile test), and dynamic mechanical behaviour.

For creep measurements, a load is applied to a test specimen and its length is measured as a function of time. In stress-relaxation measurements, the test specimen is rapidly stretched to a given value and the force required to hold the length constant is measured as a function of time.

Tensile tests, are made by stretching the sample at a constant rate of elongation until failure occurs. The stress is gradually built up until the specimen either breaks or yields. From the stress-strain curve one can calculate a modulus (ratio of stress/strain over the initial part of the curve at low strains), the ultimate elongation and the breaking or ultimate tensile strength of the material. The stress-strain curve also indicates whether a material is brittle or ductile in nature⁽⁶⁰⁾. The types of stress-strain curves obtained with polymers are often divided into five classes. These classes are: soft-weak, hard-brittle, soft-tough, hard-strong and hard-tough. The various types are illustrated in Fig 1.6.2. If the rate of strain is very high, this type of test becomes similar to an impact test which measures toughness or energy required to break the test specimens. The area under a stress-strain curve is proportional to the energy absorbed in breaking the material.

Fig 1.6.1 Variation of strain with time

Fig 1.6.2 Tensile stress-strain curves for several types of polymeric materials⁽⁸¹⁾

The speed at which test pieces are stressed is important, since their mechanical properties are time-dependent by virtue of their long chain structure. At very slow speeds, molecules will tend to slip past each other and the magnitude of the force between the molecules. At very high speeds however there will be no time for the molecules to move relative to one another and the specimen will break only when the individual molecular chains are broken. The tensile stress will generally be higher in the latter case.

Brittle materials have low toughness while ductile materials with cold drawing are very tough because of the large elongation to break. Two phase polymeric systems such as polyblends and block copolymers are important for their stress-strain behaviour in at least two major areas of application:

- (1A) where high toughness and elongation at break is required a rubbery phase is added to a brittle polymer; and
- (2A) where an increase in tensile strength and reduced tendency to flow is required a rigid phase (often as part of a block polymer) is added to a rubber⁽⁸²⁻⁸⁵⁾.

Fig 1.6.3 illustrates the usual changes in stress-strain curve on adding increasing amounts of the rubber phase to a brittle polymer such as polystyrene. The same general trends are found with polyblends, block polymers and graft polymers in the temperature interval between the glass transition temperature of the two components. Small amounts of rubber produce a rigid material which has a yield point and shows necking or cold-drawing. The yielding phenomenon is largely the result of

crazing or breaking up of the rigid continuous phase⁽⁸⁶⁻⁸⁸⁾. Large amounts of rubber produced indistinct yield points with uniform elongation. High elongation is generally the result of the rubbery phase being the continuous phase. Crazing may still occur, but it is more likely that cavitation occurs with the production of voids resulting from phase separation at the rubber-rigid polymer interface.

There are also other types of polyblends such as mixtures of two rubbers^(82,89-91) in which the components are less miscible to form one phase systems⁽⁹²⁻⁹⁵⁾ and mixtures of rubbers and crystalline polymers whose T_g is below room temperature⁽⁸⁹⁾. Such polyblends generally behave as rubbers or crystalline polymers with a reduced degree of crystallinity⁽⁶⁰⁾.

Most commercial high-impact polymers, including ABS polymers, are complex polyblends of a rigid polymer with a rubbery graft polymer⁽¹⁰⁰⁻¹⁰²⁾. The grafted chains on the rubber are similar to the matrix, and these grafted chains promote good adhesion between the phases. Good adhesion is one of the requirements for a tough polymer with high impact strength⁽⁹⁶⁻⁹⁹⁾.

The properties of block polymers have been reviewed by Estes, Cooper, and Tabolsky⁽¹⁰³⁾ and by Aggarwal⁽¹⁰⁴⁾. There are a number of other papers which discuss the stress-strain properties of block polymers^(84,85,105). Graft polymers have been reviewed by Battaerd and Tregear⁽¹⁰⁶⁾.

Fig 1.6.3 Typical stress-strain behaviour of polyblends of a rubber in a brittle polymer (numbers refer to the approximate percent of rubber in the polyblends)

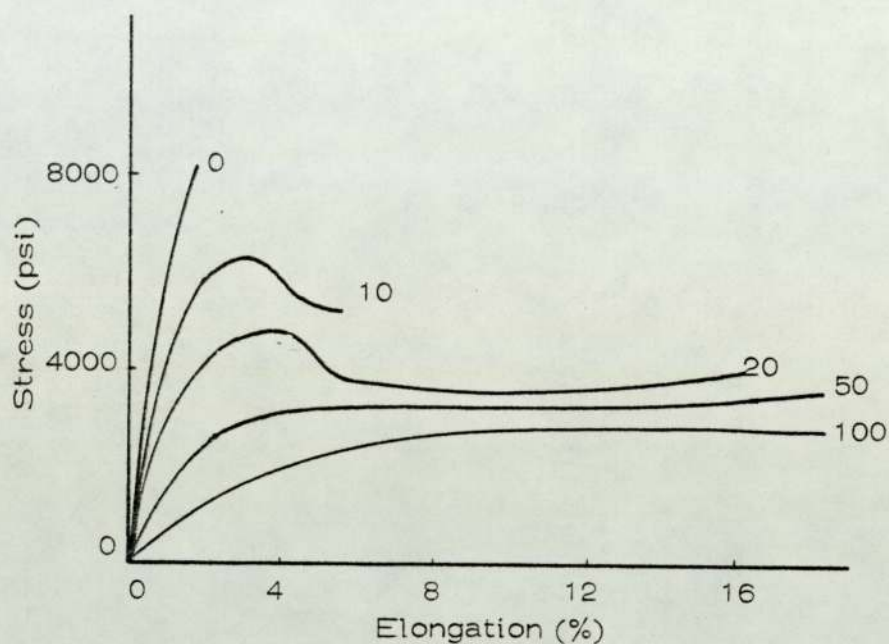
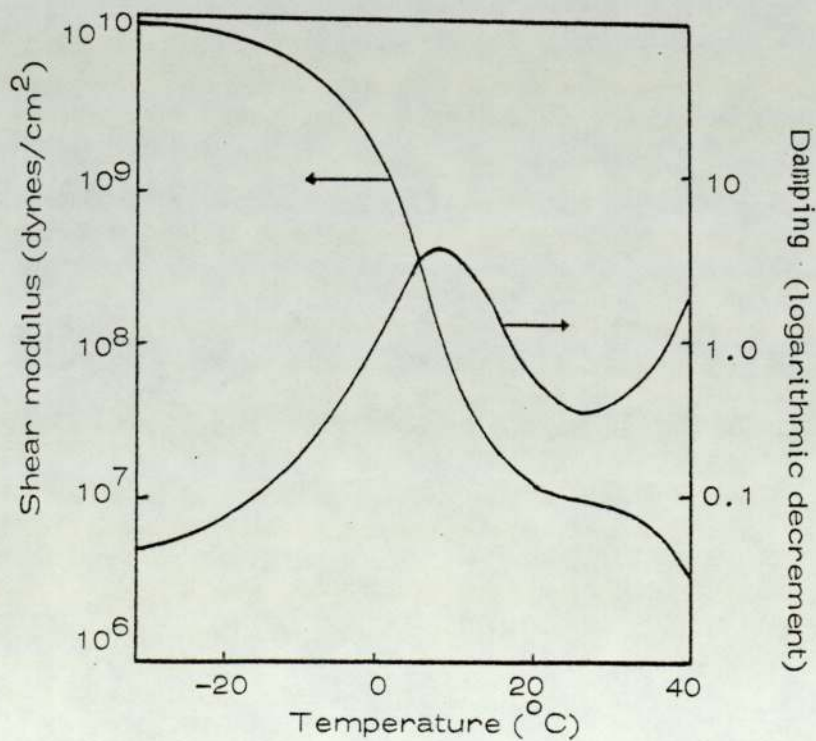


Fig 1.6.1.1 Typical dynamic mechanical behaviour -vs- temperature



1.6.1 Dynamic Mechanical Properties of Polymers and Polyblends

Nielsen⁽⁶⁰⁾ shows a typical graph of dynamic mechanical properties -vs- temperature for an amorphous uncross-linked polymer (Fig 1.6.1.1).

It can be seen that initially the modulus decreases very slowly as the temperature increases until in the region of the glass transition the modulus decreases by a factor of about a thousand in a short temperature interval. The modulus takes another drop at still higher temperatures due to the increasing role of viscous flow. The damping goes through a maximum and then a minimum as the temperature is raised. In the transition region the damping is high because some of the molecular chain segments are free to move while others are not. Below and above the glass transition, the chain segments are frozen and free to move respectively and both states can store energy without dissipating it into heat.

Cross-linking has a dramatic effect on the dynamic mechanical properties over T_g . The vulcanised rubbers are typical of relatively low degrees of cross-linking. If the frequency of the test is too high, the modulus does not reach an equilibrium value and the expected increase in modulus with degree of cross-linking becomes partly obscured by entanglements and imperfections such as trapped entanglements on pendant cross-linked structures^(107,108). However, the damping is a sensitive indication of cross-linking⁽¹⁰⁹⁻¹¹¹⁾. At temperatures well above T_g , the damping decreases with increasing degree of cross-linking as illustrated in Fig 1.6.1.2 where the swelling ratio is an inverse function of the degree of cross-linking.

Damping (logarithmic decrement) at 50°C is a function of the swelling ratio for cross-linking SBR rubber. Benzene was the solvent for the swelling tests⁽⁶⁰⁾.

Crystalline polymers generally show more complex dynamic mechanical behaviour than do amorphous polymers.

Crystalline polymers always have a glass transition and generally at least one or two secondary transitions. There may also be transitions within the crystalline phase. In addition according to Nielsen, the mechanical properties are strongly dependent upon the degree of crystallinity, the size of the crystallinities and the melting of the crystallinities. The modulus decreases as the crystallinity decreases. Crystallinities containing short chain sequences of polymer melt before crystallinities which contain long chain sequences. Thus, small and imperfect crystallinities melt at a lower temperature than large and more perfect crystallinities. For this reason, the temperature dependence of the modulus above the glass transition temperature gives an estimate of the distribution of crystallinities size. The difference between a highly crystalline isotactic polypropylene and a slightly crystalline nearly atactic one, is illustrated in Fig 1.6.1.3. The high crystallinity of the isotactic polymer is reflected in its high modulus. The small size or imperfections of the crystallinities in the nearly atactic material is partly responsible for its low melting point. Increasing crystallinity shifts the main damping peak to a higher temperature.

The damping above T_g is also strongly dependent upon molecular weight as illustrated in Fig 1.6.1.4. The value of the damping at the minimum above T_g decreases as the molecular weight

Fig 1.6.1.2 Damping (logarithmic decrement) at 50°C as a function of the swelling ratio for cross-linked SBR rubber. Benzene was the solvent for the swelling tests⁽⁶⁰⁾

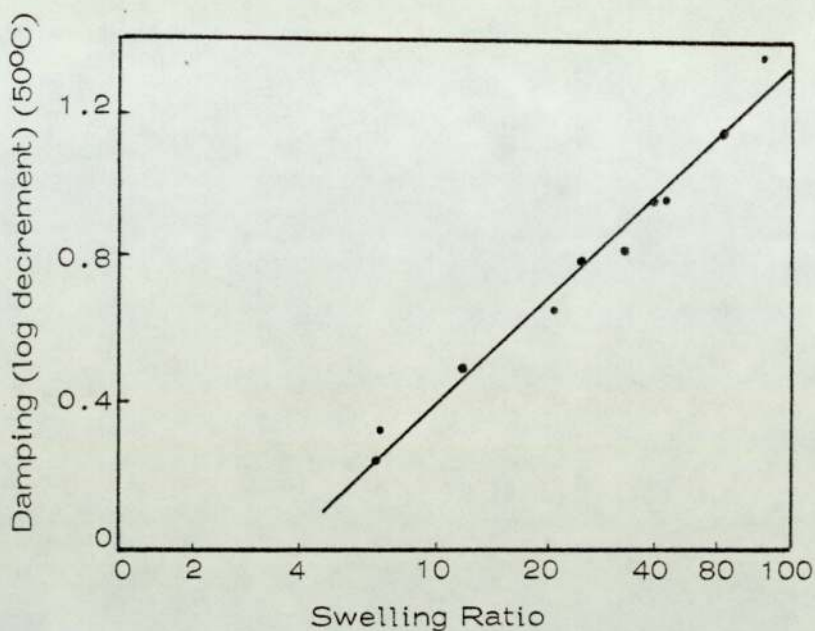
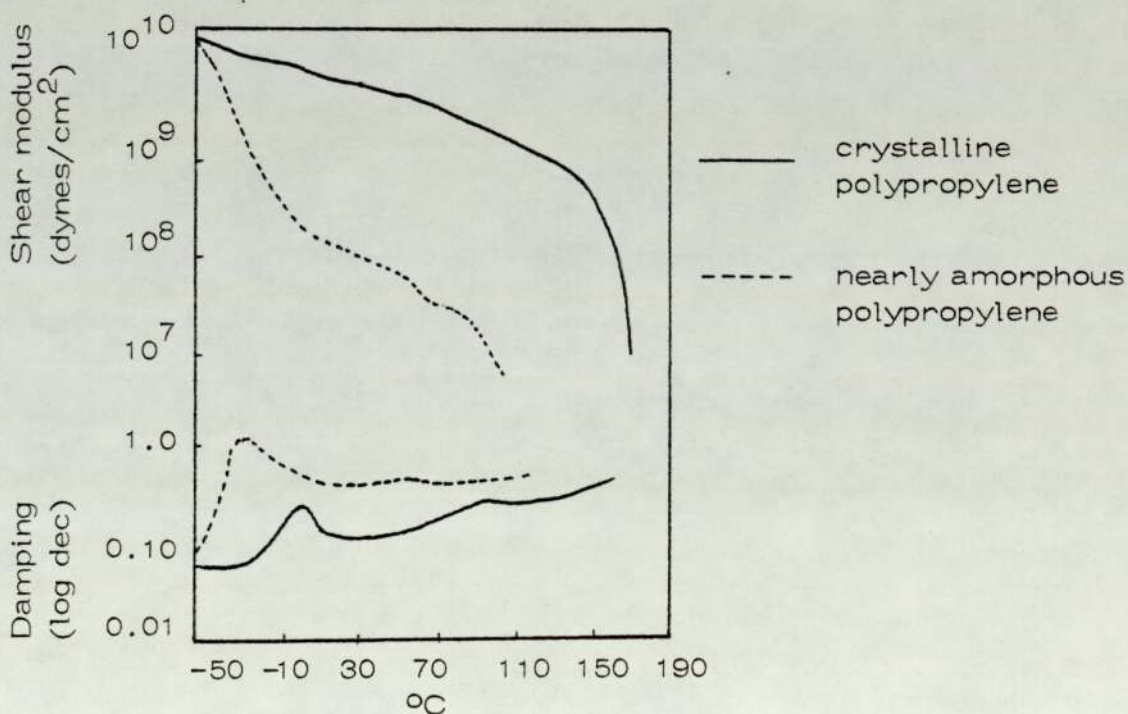


Fig 1.6.1.3 Dynamic mechanical properties of polypropylenes⁽⁶⁰⁾



increases⁽¹¹²⁻¹¹⁵⁾. The minimum occurs near the mid-point of the rubbery plateau region where the modulus curve has an inflection point. In contrast to what might be expected, Cox, Isaksen and Merz⁽¹¹³⁾ found that the damping is a function of the number average molecular weight rather than the weight average molecular weight. They also found that the valley around the minimum in damping broadened as the ratio of the weight to number average molecular weight increased.

However, Oyanogi and Ferry^(116a) found that the minimum was relatively insensitive to very low molecular weight polymer. Marvin^(116b) developed a theory and predicted that:

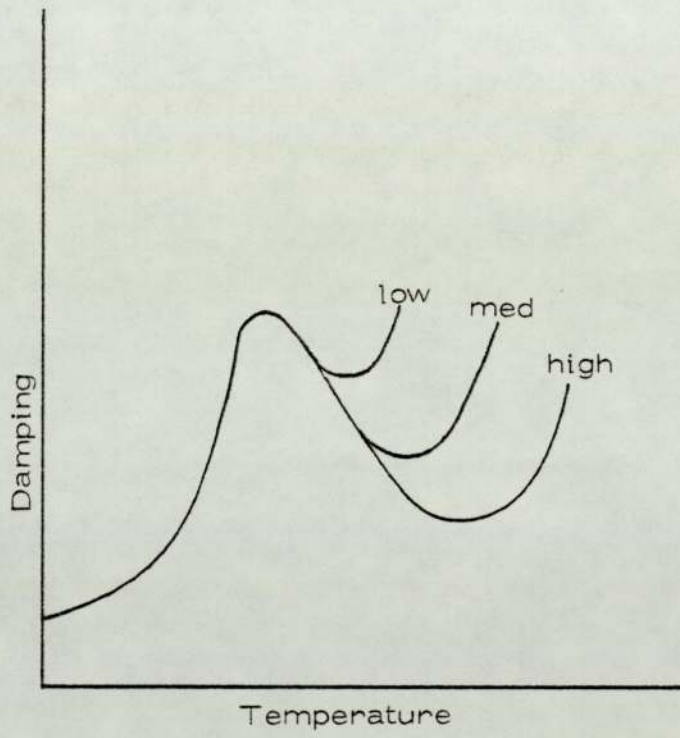
$$\frac{G''}{G'} = 1.04 \left(\frac{2Me}{M_n} \right)^{0.80}$$

(G'', G' refers to imaginary modulus and real modulus respectively)

where Me is the molecular weight entanglement as determined from the equation for the kinetic theory of rubber elasticity. The factor should be omitted if Me is determined from the break in log viscosity versus molecular weight curve.

Dynamic mechanical measurements have been widely used to study the thermo-mechanical properties of polymers and polyblend^(60, 117) changes during oxidative degradation⁽¹¹⁸⁻¹²⁰⁾ and to study the curing of resins⁽¹²¹⁾ but little literature information is available on the change in dynamic mechanical properties of polymers during uv irradiation. Scott and co-workers⁽¹¹⁸⁻¹²⁰⁾ studied the changes in dynamic mechanical properties of some commercial polyblends such as HIPS (high impact polystyrene) and ABS during uv and thermal oxidation. They also attempted to

Fig 1.6.1.4 Damping versus temperature for a polymer of three different molecular weights



improve those changes in dynamic mechanical properties by adding different stabilisers^(122, 123).

Many instrumental techniques have been developed to determine the dynamic mechanical properties of polymers. Details were reported in the literature⁽⁶⁰⁾. The choice of instrument for a particular polymer system is judged by the initial physical state of the polymer (eg glass or rubber) size and shape of the specimen, experimental conditions used. It also depends on which of the variable parameters such as temperature, frequency etc are to be followed. Torsional braid analysis (TBA) has been used for studying cross-linking reactions in polymers by Gillham and Lewis^(121, 124) which has been further modified by Plant and Scott⁽²³⁷⁾ to follow the thermal degradation of polypropylene both during processing and on accelerated oven ageing.

1.7 Microscopy

This is a powerful tool for visually studying the distribution of the two phases in the polyblend. One can tell not only the domain size of the dispersed phase but also which polymer forms the dispersed phase from refractive index. A phase contrast light microscope can detect heterogeneity at the 0.2-10 μ level. If the sample can be stained preferentially and sectioned with micro tome, then under favourable conditions electron microscopy can show heterogeneity on the fine microscopic scale. In a study of PVC-poly(butadiene-co-acrylonitrile) blends, Matsuo, Nozaki and Jyo⁽¹²⁵⁾ showed that heterogeneity at 100 \AA scale and finer can be detected readily. Thus, microscopy can offer a measure of heterogeneity down

to 0.01μ which is much smaller than the domain size of most polyblends. Results of microscopy have established convincingly that nearly all polyblends are heterogeneous two-phase systems. A major problem is to interpret the results since heterogeneity as revealed by microscopy is a relative property. If compatibility is used in a qualitative sense, a polyblend with a fine domain size will be more compatible than one with a larger domain size provided equilibrium size distribution has been attained in both cases.

Of the methods listed, glass transition temperature, dynamic mechanical measurements and microscopy undoubtedly give the most useful information on the compatibility of polyblends. Phenomenologically, compatibility can best be described by the degree of homogeneity of the polyblend as measured and compared by the domain size of the dispersed phase. The finer the distribution of the dispersed phase in the continuous phase, the better will be the compatibility. Since the fineness of a dispersion is relative, compatibility will also be a relative and not an absolute attribute of the polyblend systems. As in the case of small molecules, if two polymers have a strong affinity for each other owing to strong intermolecular interaction, they will mix more intimately. In other words, compatibility is a relative measure of the affinity of two polymers for each other. Shutz⁽¹²⁶⁾ has reviewed rigorously the thermodynamic nature of this interaction. We can generalise that where two polymers show strong affinity for each other, they can be dispersed to small domain size and the smaller the domain size the more compatible the system.

CHAPTER TWO

DEGRADATION OF POLYMERS AND POLYMER BLENDS

The first important publication concerned with the weathering of a commercial high polymer appeared in the Journal of the Chemical Society for 1861, when A.W.Hoffman reported upon his examination of the gutta serena covering of cable used in the construction of the East Indian Telegraphs which had deteriorated rapidly after installation, involving a substantial financial loss. The history of synthetic plastics is usually accepted as dating from the following year when Alexander Parks presented his plasticised nitrocellulose, later known as Parkesine, at the Great International Exhibition. Hoffman's earlier work on the naturally occurring materials did illustrate a number of fundamental facts which are quite generally true of the modern synthetic plastics as well as of the naturally occurring high polymers. His work showed, for example, that deterioration could be associated with the absorption of oxygen and that it is accelerated by heat and also by light. As a result of these chemical changes, such effects as discolouration, surface cracking and deterioration of mechanical and electrical properties are manifested. Surface cracking or embrittlement can lead to drastic reduction in toughness, tensile strength and ultimately to mechanical failure.

The important accelerating environmental influences apart from oxygen which are deleterious to polymer stability are heat, light, contamination by metal ions, ozone and mechanical deformation⁽¹²⁷⁾.

The absorption of several types of energy by polymers initiates or accelerates those chemical reactions responsible for deterioration. Various forms of radiation and mechanical stress contribute to polymer failure. Acceleration of deterioration by heat is a general phenomenon responsible for the degradation of polymers both in the presence and absence of chemical reactants. Ultra-violet radiation initiates the deterioration of many polymers and mechanical stress also contributes to failure, particularly in combination with thermal energy during processing or fabrication.

Deterioration of polymers takes place in two phases of their life⁽¹²⁸⁾. Firstly, during fabrication, in processes like moulding and extruding into the form in which it is to be used. This period is characterised by exposure to relatively high temperatures over short intervals of time. Deterioration of some polymers can and probably does occur even during synthesis but protection at this stage is generally impractical, since stabilisers that inhibit deterioration usually retard polymerisation. Conditions encountered during fabrication can be extreme, both in temperature and in mechanical stress. Sensitising groups are often introduced into small fraction of the total number of molecules, and their trace impurities can accelerate deterioration of the polymer during its service life.

Secondly, during the subsequent useful life of the fabricated article, it is usually subjected more or less continuously to air and light and oxidative and photodegradative processes are therefore most important. During this period the polymer is exposed to conditions of actual use and deterioration is more

gradual. Exposure conditions usually vary in cycles in contrast to the more constant conditions of fabrication. This phase also includes storage. In many applications polymers may be stored at temperatures above those encountered during the service life. Also, on a time scale, storage can be significant portion of the overall life of a polymer. Although temperature and mechanical stress are usually lower during ageing than during fabrication, the time of exposure is much longer and failure usually occurs during this period.

Although the energy distribution in the solar spectrum in space extends to wave length below 200 nm^(129,130) almost all the radiation of wavelength less than 290 nm is absorbed in the earth's atmosphere; therefore very little of the shorter wave length radiation reaches the earth's surface^(130,131). Most of the absorption at the shorter wavelength is caused by a layer of ozone which exists at higher altitudes. Therefore only light having a wavelength exceeding 290 nm reaches the earth surface. The energy distribution of solar radiation as a function of wavelength (λ) is shown in Fig 2.A^(131,132). Curve (A) represents the energy which would reach an object on the surface of the earth if there were no atmosphere to absorb part of the radiation. Curves (B) and (C) represent the energy distribution reaching the earth after passing through the atmosphere at high noon when the angle of the sun is 30° to the horizontal respectively. It is readily apparent that no radiation with a wavelength shorter than 2900 Å is transmitted by the atmosphere. Fig 2.B shows the proportion of the sun's total energy greater than hc/λ is plotted as a function of E_λ . Values of the strength of several chemical bonds are included for reference. It is evident from the figure that although

Fig 2.A The energy distribution of solar radiation as a function of wavelength (λ)

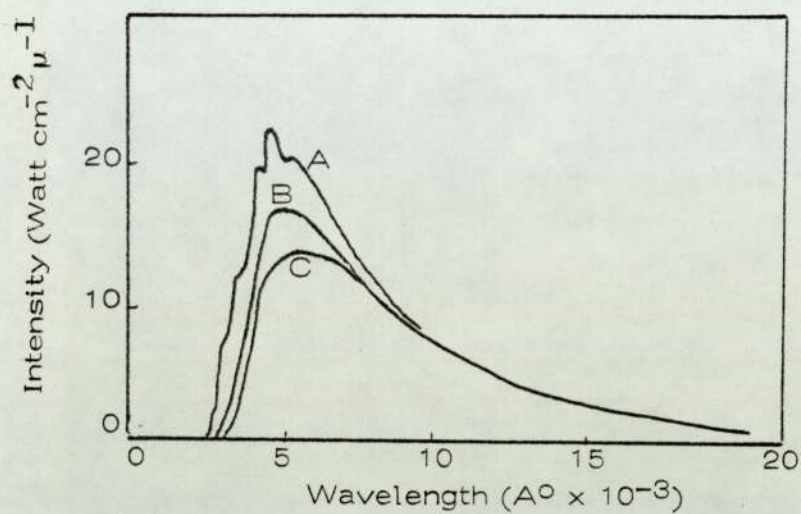
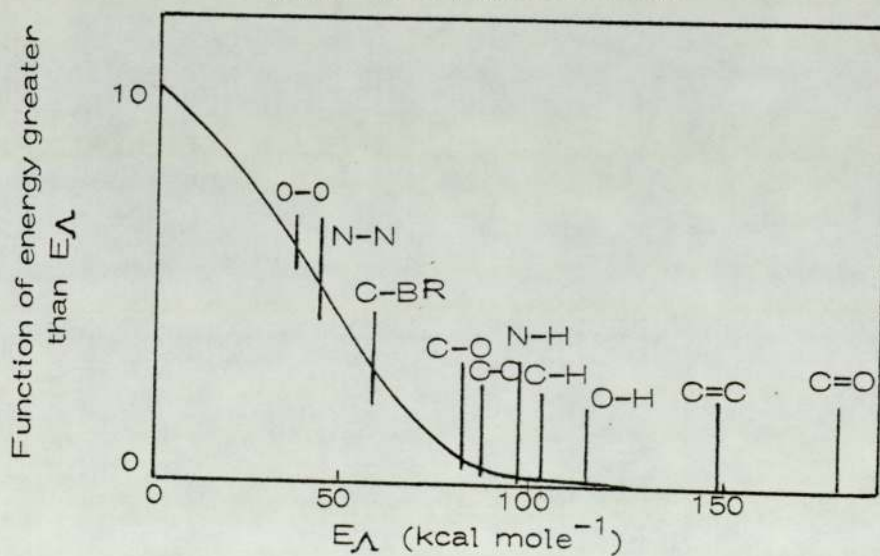


Fig 2.B The proportion of the sun's total energy greater than hc/λ as a function of E_λ



over half of the sun's radiation has sufficient energy to break weak bonds such as the O-O in a peroxide or N-N bond, very little of the total radiation is sufficiently energetic to break strong bonds such as the C-C bond and none is expected to break strong bonds such as C-H, O-H, C=C and C=O which have energies greater than 100 Kcal/mole. Therefore pure polyolefins containing only C-C and C-H bonds are not expected to show any uv absorption^(133,134). Consequently, they should not be affected by sunlight when exposed to the atmosphere. The fact that free radicals are formed and photodegradation reactions occur after irradiation of polyolefins with uv light in the wavelength range 290-350 nm which constitutes about 5% of the total solar radiation reaching the earth's surface indicates that some kind of chromophores must be present in these polymers. Presumably these are introduced during polymerisation and processing resulting in light absorption by the polymer which may initiate photochemical reactions.

The most important chromophoric groups and impurities which can initiate photochemical reactions are believed to be hydroperoxide and carbonyl groups formed during processing. Other agents which may photo-sensitise polymers include aromatic compounds absorbed from the urban atmosphere, metallic impurities during polymerisation and processing and oxygen polymer charge transfer complexes with the polymer.

2.1 Photo-initiation

- (1) Initiation due to the metal impurities: The polyolefins obtained by polymerisation in the presence of Ziegler-Natta

catalysts always contain transition metal (eg titanium) residues, which cannot easily be removed. The concentration of such metal impurities (generally < 50 ppm) and their nature generally depend on the purification process.

It is well known^(135,136) that transition metal ions act as sensitisers promoting the photo-oxidation of polyolefins. Japanese authors⁽¹³⁷⁾ have recently found that the degradation of polypropylene induced by uv light (3650, 2537, 1800 Å) depends on the oxygen concentration and on the residues of the polymerisation catalyst. They concluded that photo-oxidation in an oxygen atmosphere is sensitised by metallic iron catalyst residues.

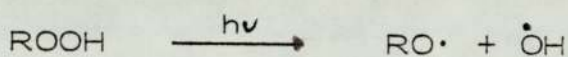
The available data suggests that the transition metal compounds extend their sensitising action by uv light absorption and the generation of free radicals that initiate photo-oxidation. Electronic transitions, constituted by electron transfer from one ion to another (or to the solvent) are responsible for most inorganic photochemical reactions⁽¹³⁸⁾.

- (2) Initiation due to oxidation products of polyolefins: A large amount of the uv light absorbed by the polyolefins between 300 and 340 nm is commonly attributed to absorption by peroxidic groups and by two types of carbonyl groups^(139,140). These groups are introduced into the polymer by air oxidation during polymerisation, or processing (moulding, extrusion, spinning etc) or by very slow metal catalysed oxidation at room temperature^(141,142). Also

copolymerisation with carbon monoxide during the preparation of the polyolefins has been proposed⁽¹⁴³⁾ as a source of carbonyl groups in the polymer. Therefore, the primary photochemical reactions in polymers may be understood only when the effect of light on the carbonyl and hydroperoxidic groups is known, also how such an effect depends on the chemical and physical nature of the medium.

- (3) Initiation due to hydroperoxidic groups: Alkyl hydroperoxides show the maximum of the first absorption band in the 200 nm region, but the tail of the band extends to about 320 nm. Therefore, they can absorb a part of the sunlight that reaches the earth (≥ 300 nm).

Thus light absorption by peroxides is due to transitions that probably involve the two chosen lying levels $n_{px,y}^* \rightarrow \sigma_{pz}$, reflected in the absorption shift to the longer wavelengths⁽¹⁴⁴⁾. Therefore the sunlight they absorb breaks the O-O bonds and created the two radicals according to the scheme⁽¹⁴⁴⁾:



The quantum efficiency for this reaction is found to be near unity^(145,146).

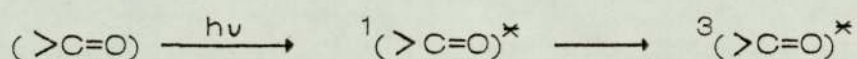
Carlsson and Wiles^(147a) studied the photolysis of polypropylene hydroperoxide generated by prior thermal oxidation of the polymer. These workers found a quantum efficiency of about four for hydroperoxide photolysis in polypropylene. They postulated that photolysis of tertiary

hydroperoxides present in the polymer is a key step in the photodegradation mechanism. Their postulation of hydroperoxide initiated photodegradation of polypropylene was later supported by evidence from ESR studies^(147b).

According to Scott and co-workers⁽¹⁴⁸⁻¹⁵²⁾ the hydroperoxides formed during processing are the main photo-initiators in the early stages of photo-oxidation of commercial polyolefins. The initial photo-oxidation rate of polyolefins is found to be directly proportional to the hydroperoxide concentration in the polymer formed during processing. Scott also concludes that the hydroperoxides formed during thermal processing of polyolefins are the precursors to carbonyl formation. When carbonyl compounds are formed by thermolysis or photolysis of hydroperoxides, they take part in the later stage of photo-oxidation.

- (4) Initiation due to carbonyl groups: Aliphatic ketones and aldehydes show in the near uv a relatively weak absorption band with a peak around 280 nm and with tails that extend beyond the region of 300 nm as far as 320-330 nm for the ketones and 340-343 nm for the aldehydes (eg the molar extinction coefficient at 313 nm of diethylketone in isoctane is 2.07). This absorption is due to a forbidden singlet-singlet transition, involving the promotion of an electron from a non-bonding n orbital localised on the oxygen atom to a more delocalised antibonding π^* orbital distributed over the entire carbonyl group⁽¹⁵³⁾. The same process of light absorption may be assumed to occur in polyolefins containing carbonyl groups in their chain.

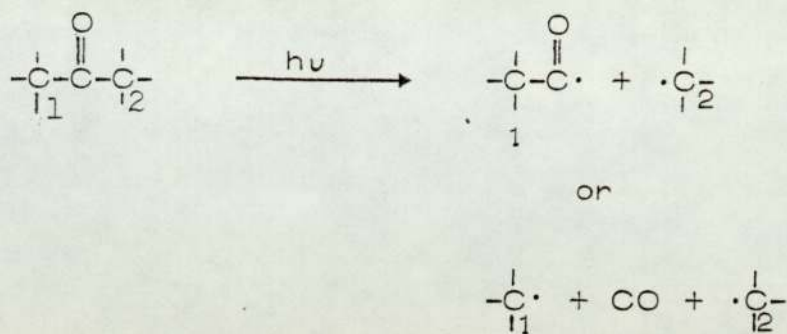
Before dissipation of the excitation energy a part of the carbonyl groups that are present in the excited singlet state $^1(n, \pi^*)$, may undergo a radiationless transition (Intersystem crossing) and pass to the triplet state $^3(n, \pi^*)$ with lower electronic energy. The number of individuals populating the triplet state will also depend on the reactivity of the carbonyl compound in the singlet state.



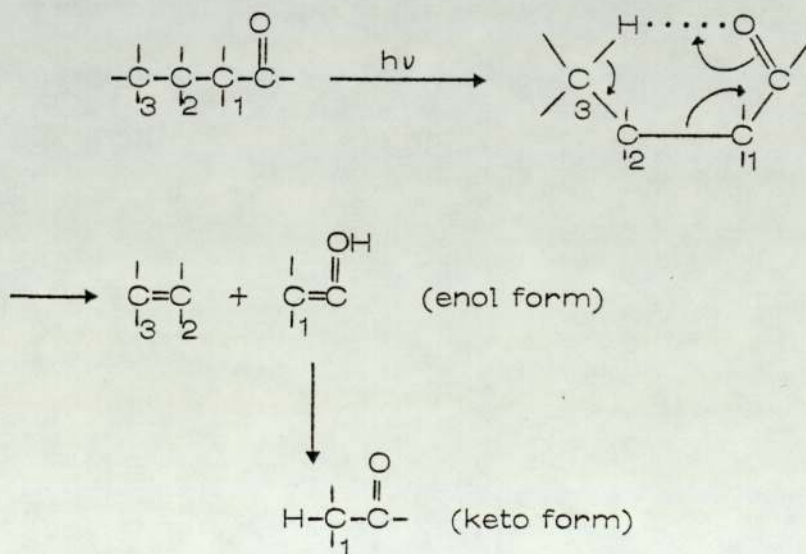
This reactivity, in its turn, is influenced by the structure of the carbonyl compound and by the presence of molecules in its close neighbourhood capable of interacting with it.

The known photo-chemistry of aliphatic ketones suggest that the principle reactions involving ketone are Norrish I type and Norrish II type reactions^(154, 155).

Norrish type I process: It has been shown⁽¹⁵⁶⁾ that both the excited singlet states and the excited triplet states of ketones are the precursors of this reaction. However, intensive investigation are still being carried out in order to establish the contribution of each of these two states^(157, 158). In the type I reaction, the bond between the carbonyl group and adjacent α -carbon, is homolytically cleaved producing two radicals.



Norrish type II process⁽¹⁵⁴⁾: This reaction may occur provided that the ketone possesses at least one hydrogen atom on the carbon atom in γ -position with respect to the carbonyl group. The type II reaction proceeds by intermolecular hydrogen transfer to yield one olefin and one enol, which then rearranges to the final ketone of smaller size^(159,160). It was demonstrated that the hydrogen transfer takes place via a six-membered cyclic intermediate^(161,162). Although the cyclic intermediate proposed allows a convenient representation of the process, alternative mechanisms for the type II scission are possible^(161,162).



The importance of type I and type II processes in the photolysis of polyolefins is obvious; their occurrence may cause, by rupture of the main chains, considerable decreases in the molecular weights with consequent failure of the physical properties of the polymer.

It is now generally accepted that photodegradation of polymers involves the same free radical chain mechanism as thermal oxidative degradation^(128, 127) which is largely similar to simple hydrocarbon oxidation⁽¹⁶³⁻¹⁶⁵⁾. Hydroperoxides are key initiators for the process of oxidative degradation of polymers both during thermal oxidative degradation and uv initiated degradation. The main difference between thermo-oxidation and photo-oxidation lies in the rate of the initiation step. Cicchetti⁽¹⁶⁶⁾ observed that rate of uv initiated oxidation (both in polymers and in model compounds) is very much faster than that of thermo-oxidation. The high rate of oxidation in uv light is believed to be due to rapid homolytic cleavage of initially formed hydroperoxide by light, forming radicals.

All types of polymers tend to degrade on weathering at least to some extent (Gesner, 1965⁽¹⁶⁷⁾, Hirai, 1970⁽¹⁶⁸⁾, Shimada and Kabuki, 1968⁽¹⁶⁹⁾). The analysis of weathering behaviour becomes quite complicated in the case of polyblends, because not only do the two phases age at different rates, but continuing interactions between the two phases remain of prime importance.

The most important target of oxidative attacks involves carbon-carbon double bonds. In fact, at the initial stage of oxidation

of rubber modified plastics it is possible to consider that only the rubber phase oxidises, with no attack in the plastic portions. Hirai⁽¹⁶⁸⁾ has shown that polymers with a high double bond concentration are more oxygen sensitive than those having a low or zero concentration of double bonds.

The recent developments and the prominence of a new class of materials has stimulated an interest in the stability of polymer blends. It is often surprising how the polymers in the blend influence the stability of each other in spite of the fact that this influence must usually act across the discrete phase boundary which exists between the constituents of the blend. This is quite different from the situation in copolymers in which the constituent monomers are chemically bonded to each other.

2.2 Thermal (non-oxidative) Degradation of Polymer Blends

The possibility of interactions between a polymer on its degradation products and a second polymer in the same environment (eg polymer blends) has been examined in a number of recent thermal degradation studies. Some pairs of polymers for example PS and PMMA⁽¹⁷⁰⁾ show no evidence of interaction in the degradation of a blend. In other cases, it has been found that the products of degradation of one polymer can greatly influence the degradation behaviour of the other. Thus polymethyl methacrylate depolymerises much readily in the presence of degrading PVC and this effect has been used as evidence in favour of a radical mechanism for PVC dehydrochlorination in a bulk system^(171,172). In further investigation⁽¹⁷³⁾, it has been found that several

polymers form block and graft copolymers when degraded with polypropylene. The deacetylation of PVA is substantially accelerated by the presence of PVC and other chlorine containing polymers⁽¹⁷⁴⁾.

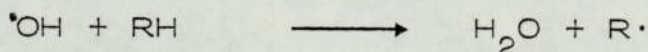
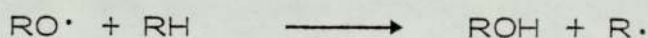
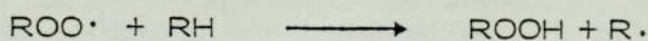
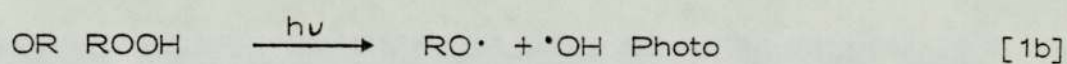
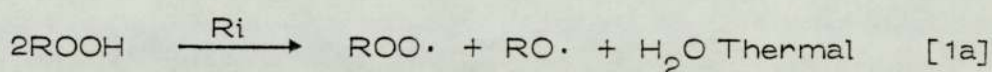
For the PVA-PVC systems, it has been suggested that⁽¹⁷⁵⁾ since it is unlikely that the polymers themselves could interact across the phase boundary between them, an explanation of these phenomena has been given in terms of catalysis by the volatile products, acetic acid and hydrogen chloride, which will readily diffuse across the phase boundaries. The degradation of blends of PVA and PMMA in the form of films cast from a common solution of the two polymers has been studied by thermal volatilisation analysis and analysis of evolved gas for acetic acid⁽¹⁷⁶⁾. Volatile degradation products were characterised by spectroscopic and GLC techniques. These blends behaved in a closely analogous manner to PVC-PMMA blends and the results suggest that the PMMA component of the heterogeneous blend is modified in two ways:

- (1) in a destabilisation reaction series initiated by attack of acetate radicals generated in the PVA phase which migrate into PMMA phase, and
- (2) in a stabilisation reaction involving conversion of ester side groups to acid and subsequently to anhydride ring structures which act as blocking points for depolymerisation.

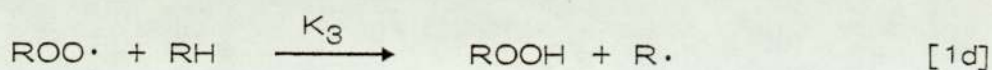
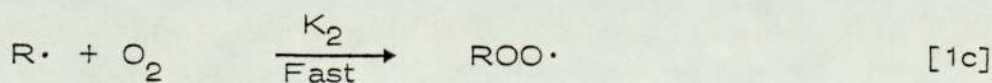
2.3 Mechanism of Oxidative Degradation of Polyolefins

It is generally accepted that the breakdown of polyolefins in ultraviolet light is an oxidative chain reaction and proceeds through the same free radical mechanism as thermal-oxidative degradation^(128, 148) which is essentially similar to simple hydrocarbon oxidation⁽¹⁶³⁻¹⁶⁵⁾. Hydroperoxides are key initiators for the process of oxidative degradation of polymers both during thermal oxidative degradation and uv initiated degradation. The basic reaction scheme consists of three steps: initiation, propagation and termination.

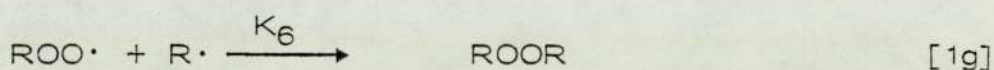
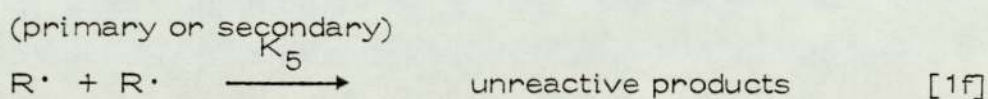
Initiation:



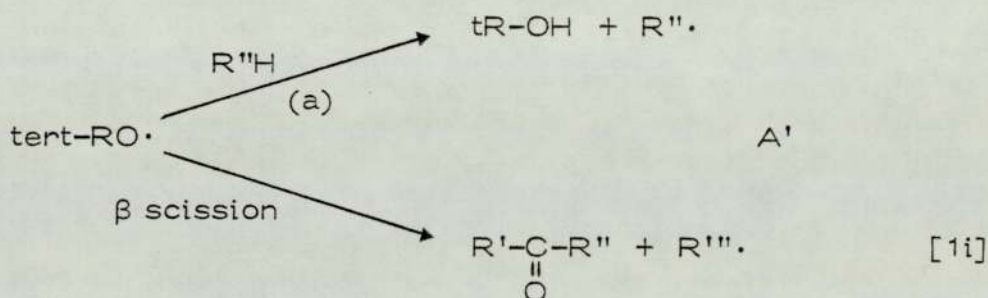
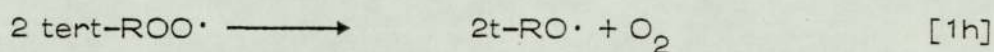
Propagation:



Termination:



Radical forming termination:



The main difference between thermo-oxidation and photo-oxidation lies in the nature and rate of initiation steps. On the basis of recently published results⁽¹⁶⁶⁾ it is observed that the rate of uv initiated oxidation (both in polymers and in model compounds) is very much faster than that of thermo-oxidation, but the nature of the initiation is not yet fully established. The high rate of oxidation in uv light (even in hydrocarbons without any added activator) is believed to be due to rapid homolytic cleavage of initially formed hydroperoxide by light, forming radicals (reaction [1b]).

At partial pressures of oxygen equivalent to air or higher, the

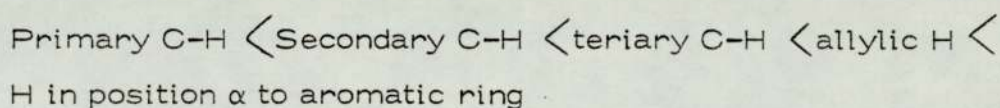
rate of combination of $R\cdot$ with O_2 (reaction [1c]) is so fast that $[R\cdot] \ll [RO_2\cdot]$ and the only termination reaction of consequence will be the bimolecular combination of the two $RO_2\cdot$ radicals (reaction [1e]).

Since the rate of uv initiated oxidation is higher, the rate of termination is also higher and the kinetic chain is shorter.

Under steady state conditions, and under normal atmospheric pressure, a general expression for the rate of oxidation of the above reaction scheme was observed⁽¹²⁸⁾ and is given as:

$$\text{Rate of oxidation: } [R_{ox}] = \sqrt{R_1 \frac{K_3}{K_4}} [RH] \quad [1i]$$

Under these circumstances the reaction rate depends on the chemistry of the hydrocarbon RH. The easier it is for hydrogen to be abstracted from RH, the higher will be the value of K_3 and faster will be the rate of oxidation. The ease of abstraction of hydrogen from different types of carbon atom has been shown by Bolland⁽¹⁷⁷⁾ to increase in the following order:



Therefore it might be expected that small amounts of chain branching or unsaturation in the polymer might be responsible for initiating degradation by slowing peroxidising or by providing easily oxidisable sites.

CHAPTER THREE

EXPERIMENTAL

3.1 Materials

The polymers used were:

- (i) Two grades of low density polyethylene (LDPE) in granular (bead) form, one containing no antioxidant and identified as 'Alkathene' polyethylene WJG 47 and the other in the stabilised form supplied commercially as 'Alkathene' (no 806) were obtained from Imperial Chemical Industries Limited. The polymers were of 0.913 gm/cm^3 density and of melt flow index 2.0 originally.
- (ii) Unstabilised polypropylene (PP) in powder form identified as 'propathene' HF 20C, CV 170 supplied by Imperial Chemical Industries Limited.

Grades of polyvinyl chloride and polystyrene used are described in Chapter 6.

3.2 Melt Processing

The samples were processed on a RAPRA torque rheometer⁽¹⁷⁸⁾ which is essentially a small mixing chamber, containing mixing screw contrarotating at different speeds. Throughout the processing operation for various blends high shear rate (72 rpm) were used. The hot melt was chilled in water on removal from the rheometer to avoid uncontrolled thermal

oxidation. If the blending was carried out on a two-roll mill the melt would be exposed to air, whereas in the torque rheometer mixing takes place in the closed chamber, free from air. The processing time was kept constant at 5 minutes from the time the cavity was closed until the polymer melt was taken out.

The additives and polymers were mixed at room temperature by tumble mixing for one hour before processing in the torque rheometer, or extruder. An operating temperature of 180°C was maintained throughout the mixing cycle.

Continuous film of even thickness was extruded using an 18 mm Betol (Betol Machinery Limited, Luton, Bedfordshire). Both polymer and polyblends were extruded. Fixed temperature settings were used throughout all operations. These were as follows: barrel zone 3 at 180, barrel zone 2 at 170, barrel zone 1 at 160, die zone 1 and 2 at 180°C. A 10°C temperature gradient was used on the take off rollers. The step rollers were set at 60°C and the bottom at 40°C. Take-off speed was fixed at 5.0 ft/min and screw speed at approximately 20 rpm was adjusted to produce various thickness of extrudate ranging from 0.0135–0.024 cm. Film produced from both the torque rheometer and extruder were examined and compared.

3.3 Preparation of Films from Processed Samples

Polymer films were prepared for ir and uv spectroscopy measurements, tensile measurements, dynamic and impact tests by compression moulding.

The films were pressed out of the polymer samples, removed from the torque rheometer at the times stated, using a special grade of cellophane as a mould releasing agent between two stainless steel glazing plates. Control of film thickness was achieved by using a definite amount of material, about 5-6 gm of material was found to produce film of approximately $(1.3-2.0) \times 10^{-2}$ cm thickness. The weighed amount of polymer was placed between the glazing plates in two cellophane sheets and inserted into the press.

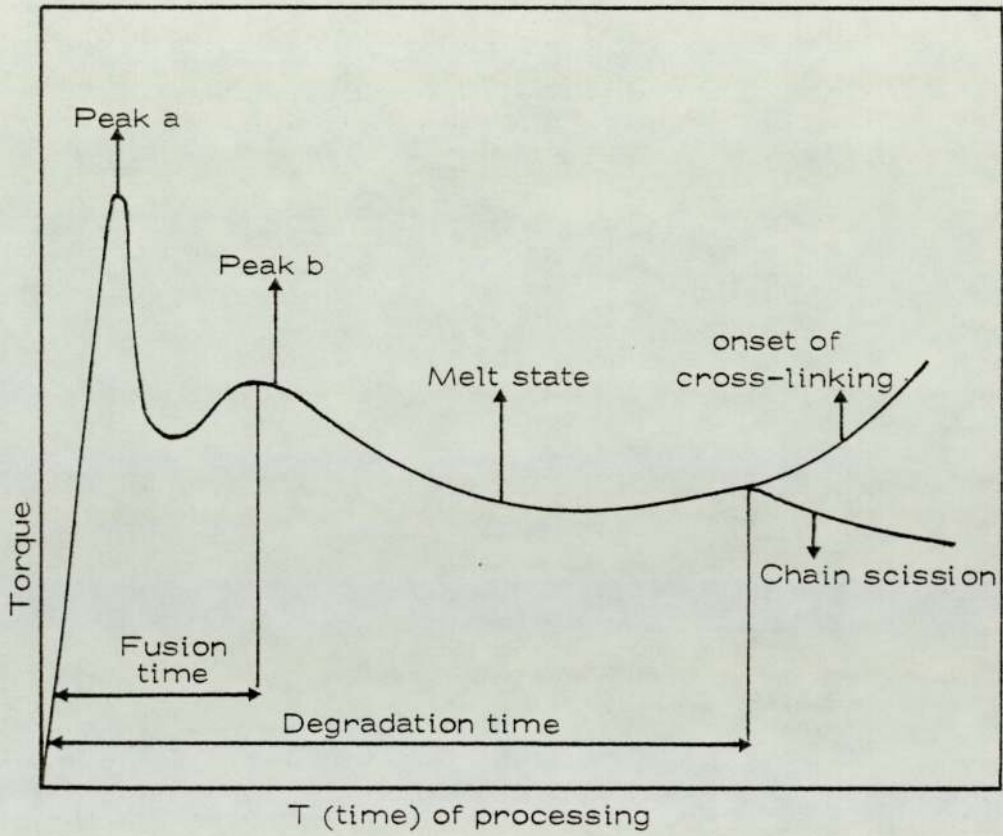
The pressing of films involved three stages:

- (a) preprocessing for 1 minute with a platen temperature of $180 \pm 5^{\circ}\text{C}$ to a thickness of about 0.045 cm (5-7 tons),
- (b) final pressing, for 2 minutes, with a platen temperature of $180 \pm 5^{\circ}\text{C}$ and maximum ram pressure (30.0 tons), to a film thickness of between $(1.3 - 2.0) \times 10^{-2}$ cm, and
- (c) water cooling the plates to $50 - 60^{\circ}\text{C}$ and removing the plates from the press and the films stored in the dark at 0°C . The thickness of each film over its entire area was measured with a micrometer in order to select portions of uniform thickness.

3.4 Evaluation of Torque versus Time Curve

Idealised torque -vs- processing time curve⁽¹⁷⁹⁾ is illustrated in Fig 3.4). When the polymer is introduced into the torque rheometer the torque rises sharply. The polymer is heated and when it reaches its glass transition temperature (T_g) it

Fig 3.4 General shape of the torque-time curve



becomes rubbery. The torque then decreases and reaches a minimum which gives rise to a peak 'a' (Fig 3.4). This stage is followed by the gelation of the material. The polymer starts to melt causing the torque to increase. When the melting (or gelation) is completed the torque increases again giving rise to a peak 'b'. The time to reach the peak 'b' is called fusion or flux time. The fusion time for a particular polymer mainly depends on mechanical stress, temperature and the presence of additives. Cross-linking or chain scission of polymer is also reflected from torque vs- processing time curve.

3.5 Determination of Gel Content in the Processed Polyethylene Samples

Gel content in the processed low density polyethylene sample were determined in chlorobenzene at 90°C. 0.5 gram of polymer films (in small pieces) were placed in the Erlenmeyer flask and 50 ml chlorobenzene was added. After heating for 30 minutes at 90°C, under nitrogen the solution was filtered, hot, gel was collected and vacuum dried to constant weight.

3.6 Measurement of Melt Flow Index (MFI)

Melt Flow Index was determined on low density polyethylene and blends samples which have been processed with or without additives. The apparatus used was Davenport polyethylene grader.

The melt flow index is a measure of the melt viscosity of the polymer which in turn is related to the molecular weight. The

melt flow index (MFI) is defined as the amount of polymer in grammes extruded through a standard die in a given time (usually 10 minutes). A low melt flow index corresponds to a high melt viscosity and since melt viscosity is directly related to the molecular weight of the polymer a low MFI corresponds to a high molecular weight and vice-versa⁽¹⁸⁰⁾. A strict relationship obviously only applies to polymers of the same chemical constitution, but it also is restricted to polymers of the same density since density also effects melt viscosity. In the case of the polyethylene and EVA the standard temperature is 190°C but for polypropylene the temperature is 230°C in order to allow for its higher melting point.

The appropriate relationship of MFI with molecular weight (\bar{M}_n) and melt viscosity (η^*) are given by the following two equations respectively (in case of LDPE)⁽¹⁸¹⁾.

$$\sqrt{\bar{M}_n} = 188 - 30 \log \text{MFI}$$

$$\eta^* \text{ (POISE)} = 7.5 \times 10^4 \frac{1}{\text{MFI}}$$

Since thermal oxidation brings about changes in the molecular weight of the polymer by virtue of such reactions as chain-scission, cross-linking etc, these are expected to be reflected in the melt flow index values. Hence melt flow index measurement provides a means of detecting any oxidation which may occur during heat treatment of the polymer.

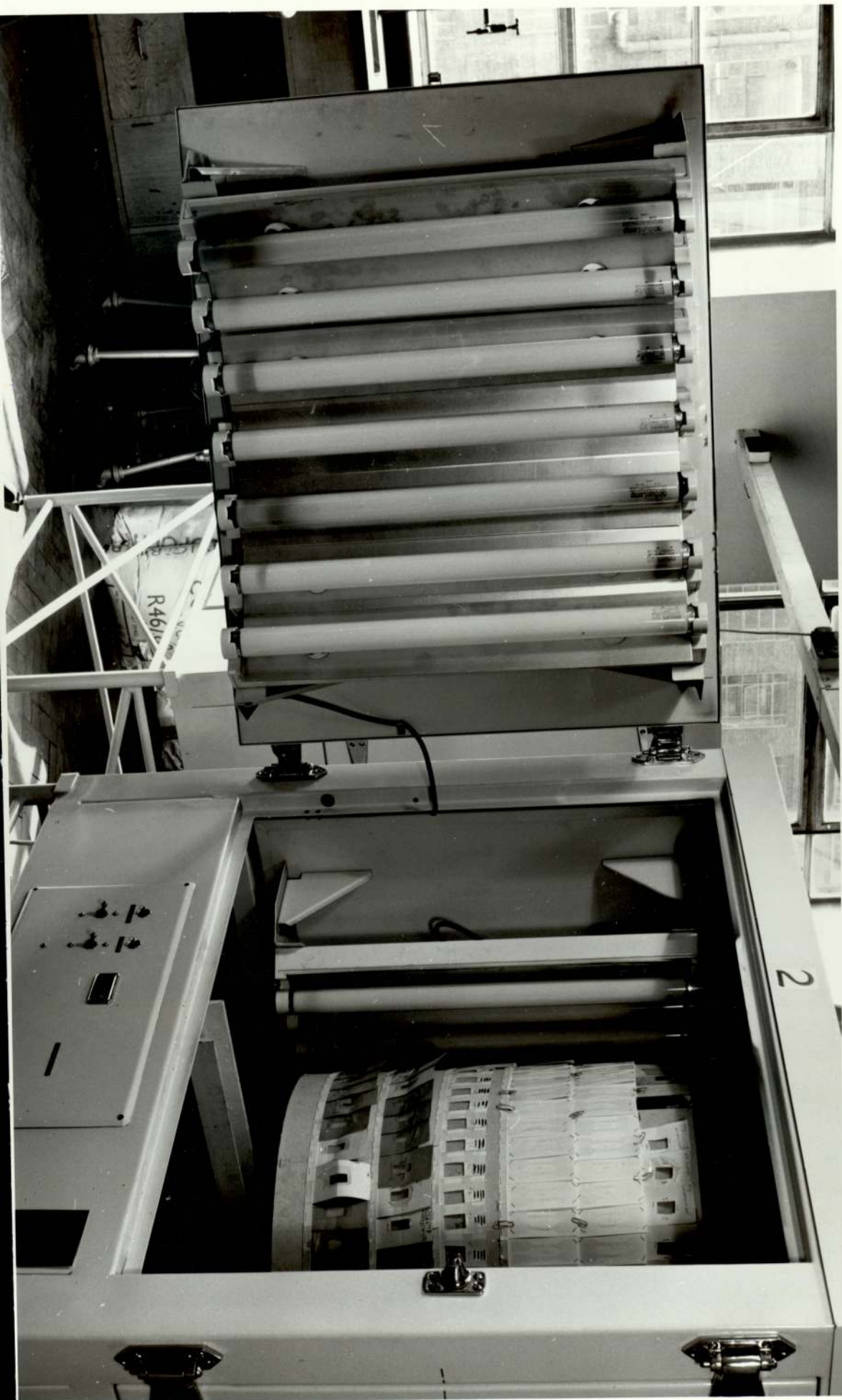
The apparatus was brought to a steady extrusion temperature of $190 \pm 0.5^\circ\text{C}$ before beginning an experiment. The barrel was then charged with 4.0 gm of polymer, tamping down with the

changing tool to exclude air. The time taken to charge the barrel should not exceed one minute. The barrel was closed airtight and nitrogen gas was passed from the cylinder to the barrel. The pressure of nitrogen gas was maintained at 160 lb/in^2 and the polymer was allowed to extrude through 0.2095 cm diameter die. The extrudate was cut with a suitable sharp-edged instrument. The time interval for the first extrudate was 60 seconds and was discarded; then 6 successive cut-offs were taken each at the end of 30 seconds; any cut-off that contained air bubbles was rejected and each cut-off was weighed separately and their average weight was determined. If the difference between the maximum and minimum values of the individual weighings exceeded 10% of the average, the test result was discarded and the test repeated on a fresh portion of the sample. The melt flow index was calculated from the following relation:

$$\text{MFI} = \frac{600 \times \text{average wt of cut-off in grm}}{(\text{interval of time in sec})}$$

3.7 Ultraviolet Exposure Cabinet

Uv irradiation of the samples was carried out in the ultraviolet cabinet. Ultraviolet cabinet comprised a metal cylinder of about 110 cm in outer diameter and having a concentric circular rotating sample drum whose circumference was 15 cm from the periphery of the metal cylinder (photograph number 1). Thirty-two fluorescent tube lamps were mounted on the inside of the cylinder. The rotating arrangement of the samples allows an identical amount of total radiation to fall on every



PHOTOGRAPH NO. 1

sample. The cylindrical cabinet was opened to the atmosphere on both the lower and upper sides, and the circulation of the air in the cabinet was ensured by the driven ventilator situated under the rotating frame.

The samples were attached to a separately made hard brown paperboard with aluminium foil backing which was mounted vertically on the circumference of the rotating wheel fixed inside the cabinet. In this position the light beam fell perpendicularly on the surface of the film. The temperature recorded inside the cabinet with the lamp on was $30 \pm 1^\circ\text{C}$.

The radiation source consisted of the cylindrical array of 20 W fluorescent tube lamps, positioned on the inner side of the cabinet. 24 lamps, type C (Phillips actinic blue OS) and 8 lamps, type A1 (Westinghouse sunlamps FS20) were used and these were symmetrically distributed so that the combination was one lamp type A1 for every 3 lamps of type C. The spectral distribution of both types of lamps used is shown in Figs 3.7A and 3.7B for the lamp A1 and lamp C respectively. The maximum in the relative intensity of the lamp A1 is at 317 nm and of the lamp C, 374 nm. The available wavelength with the above combination of lamps was between 280 nm - 500 nm and the radiation intensity I_0 at the sample surface was $I_0 = 44.3 \text{ W/m}^2$.

To minimise the problem of decline in lamp output, the tubes were replaced sequentially every 2000 hours of exposure.

3.8 The Accelerated Thermal Oxidation of Processed Polymers

Experiments on low density polyethylene and blends were carried out in a Wallace oven at $110^\circ\text{C} \pm 2^\circ\text{C}$. Polypropylene

Fig 3.7.A Spectral distribution of fluorescent lamp type A1 (Westinghouse Sunlamp FS20)

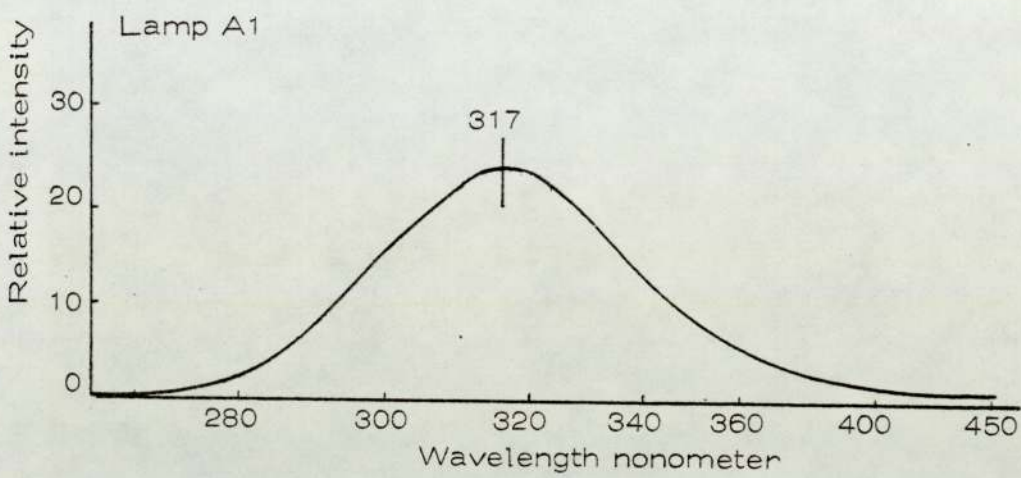
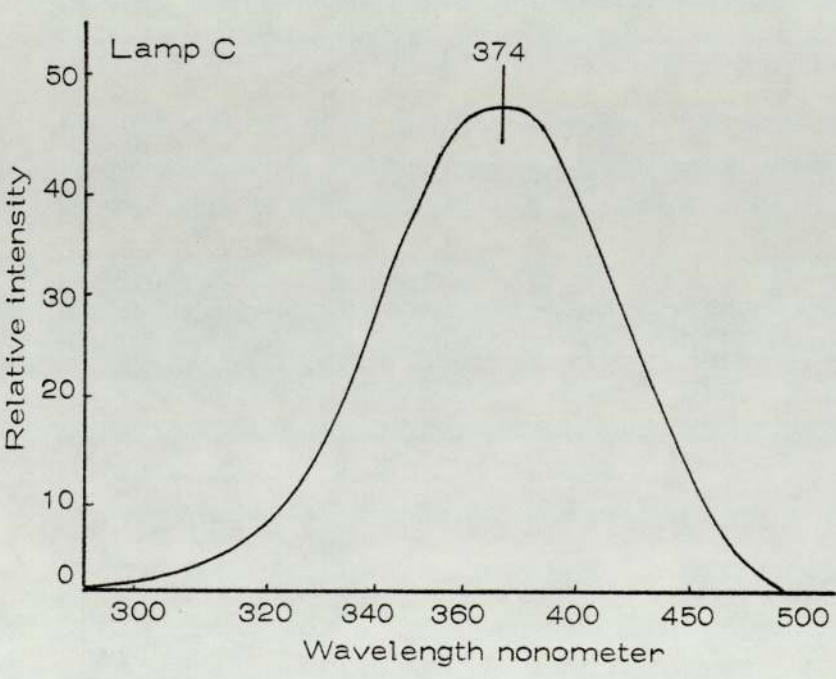


Fig 3.7.B Spectral distribution of fluorescent lamp C (Phillips Actinic Blue 05)



films were examined at $140 \pm 2^\circ\text{C}$. This has separated seven cells and has very good temperature control. There is an arrangement for controlling air flow through the cells. Each sample film was contained in a separate cell. Air flow was maintained between 3-4 CFH/hour.

3.9 Measurement of Brittle Fracture Time of Polymer Samples

This is a destructive test method. Film of identical size (2-5 cm) and of uniform thickness (0.015 cm) containing different additives and percentages of second polymer along with a control sample were irradiated and were periodically checked and their time to embrittlement was determined by folding the film back on itself 180° manually. The method was found to be inconsistent in some cases and reproducibility was not very good. This was perhaps due to phase separation of blends and slight variation in thickness along the different parts of the sample and also due to unequal application of force at the time of testing which was done by hand.

3.10 Infra-Red Spectroscopy

All the infra-red spectra were recorded using a Perkin-Elmer grating infra-red spectrophotometer model 457. The spectra from 4000 to 250 cm^{-1} were recorded at medium scan speed.

Infra-red spectroscopy has been widely used to determine the nature of oxidation products and rate of formation of these products during thermal and photo-oxidation of polymers. It is a non-destructive test and particularly useful for

quantitative purposes since the same test sample can be used repeatedly.

Since thermal and photo-oxidation of polymers results in the build up of different oxidation products, for example hydroxyl, carbonyl, carboxyl, vinyl etc the kinetics of the growth of these functional groups, as the irradiation proceeds have been followed by observing the change in the characteristic absorption peaks at different wavelengths and these were assigned by a comparison with the values for the long chain ketones, aldehydes, acids, esters, etc⁽¹⁸²⁾.

Procedure

In all quantitative analyses, the following combined form of Beer-Lambert's equation was used⁽¹⁸³⁾

$$A = \log_{10} I_0 / I = EC l$$

where:

A = absorbance or optical density

I_0 = intensity of radiation effectively entering the sample

I = intensity of radiation emerging from the sample

E = extinction coefficient expressed in litres mole⁻¹ cm⁻¹

C = concentration of absorbing group present in the sample in mole/litre

l = path length of radiation in the sample in cm

The samples were exposed for regular intervals of time and the spectra were run on the same chart paper for comparison

purposes.

To minimise errors due to variation in film thickness as well as errors due to the instrument, and internal standard, a characteristic absorption peak at 1895 cm^{-1} for low density polyethylene and 905 cm^{-1} for polypropylene were used. These peaks remained constant during irradiation. The growth or decay of observed absorption peaks (for functional groups) were expressed as indices which were defined as the ratio of the absorbance of functional group peaks to that of the reference peak.

$$\text{Index} = \frac{\text{Absorbance of the functional group}}{\text{Absorbance of a standard peak}}$$

3.10.1 Calculation of Absorbance

The base line technique⁽¹⁸⁴⁾ was used to calculate the optical density or absorbance due to various functional groups. This was done as shown in Fig 3.10A, by drawing a straight line (base line) tangential to adjacent absorption maxima or shoulders, then erecting a perpendicular through the analytical wave length until it intersects the base line. At 'A' the concentration of the functional group to be determined is zero and at 'B' there appears an absorption peak whose height serves to calculate the concentration. Before putting the sample in, the spectrophotometer was adjusted to read 100% transmission (background line).

However, with an absorption such as shown in Fig 3.10B, the

Fig 3.10.A

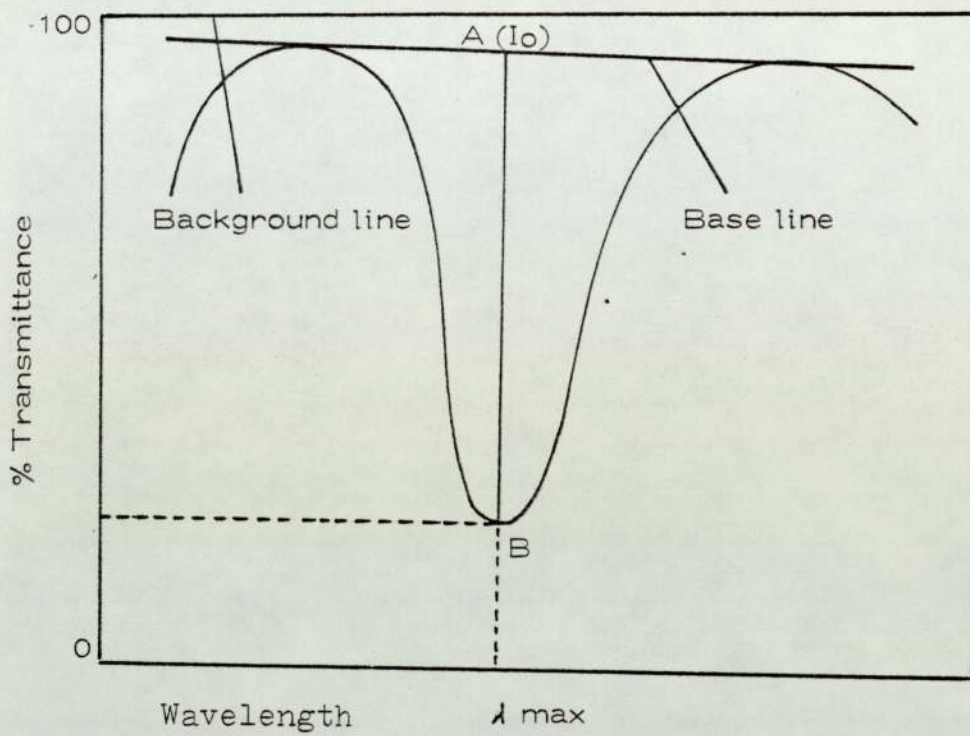
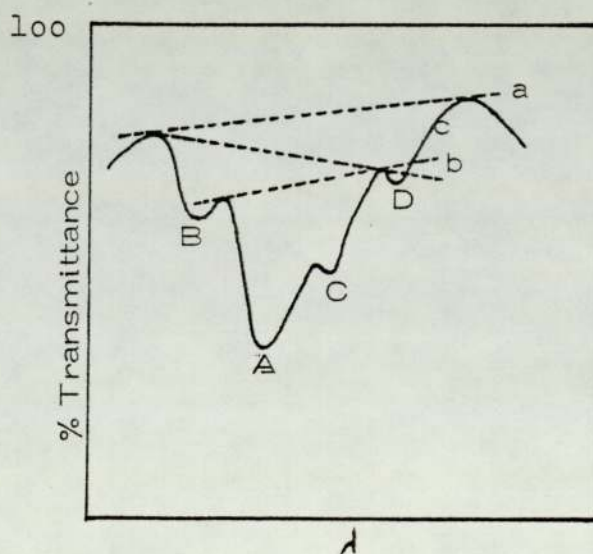


Fig 3.10.B



proper location of base line is less obvious but in the present work to determine the absorbance of peak 'A', the base line is taken to be either a, b or c, depending on the width of the shoulders, B, C, and D. If all three shoulders, B, C and D are narrow, 'a' is used as the base line and so on. And in this situation which frequently occurs, one particular way to draw the line is adopted in all the samples for the same functional group.

3.11 Uv Spectroscopy

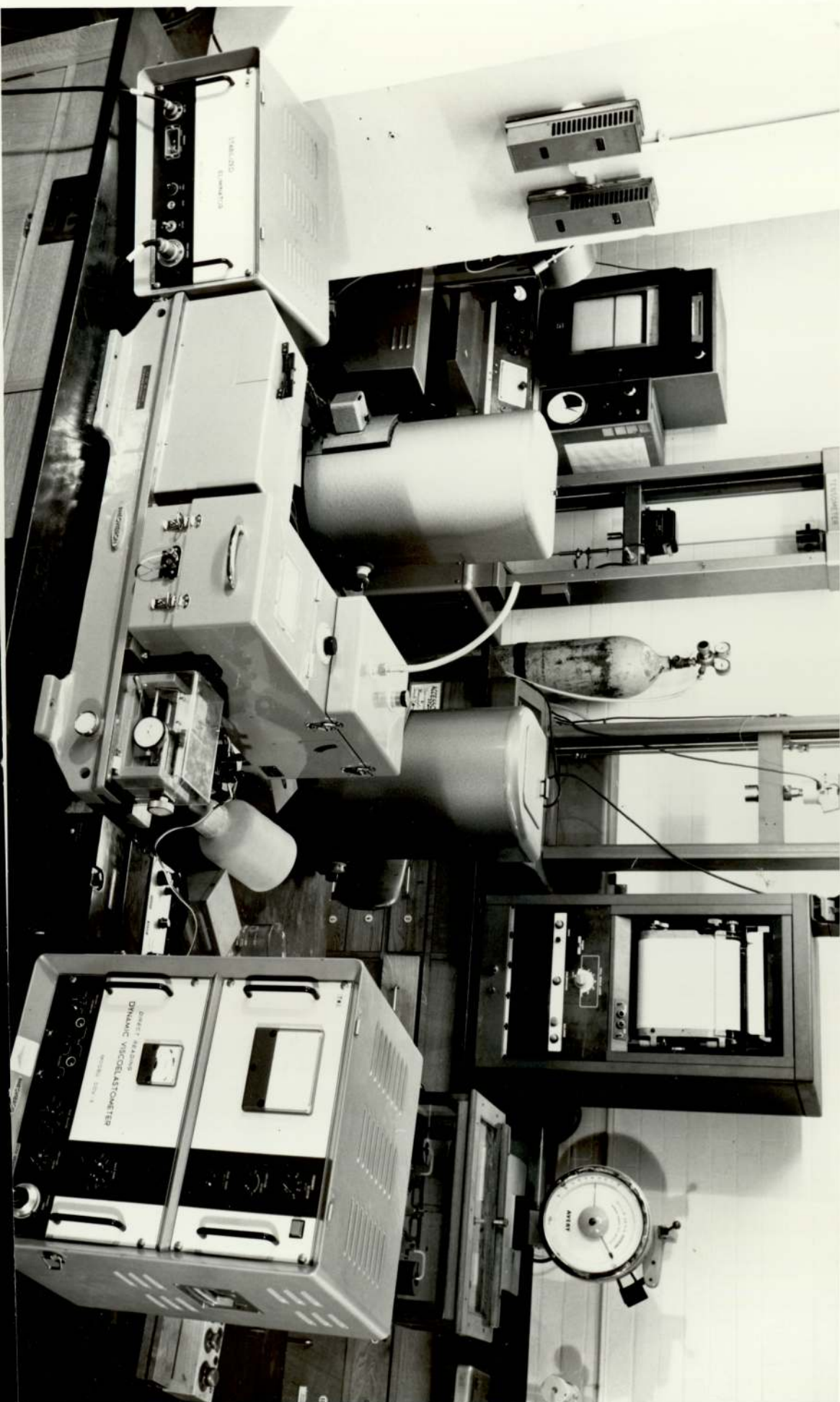
Ultra-violet spectra of polymers and polyblends with or without additives were recorded using Perkin Elmer 137 Ultraviolet Visible Spectrophotometer. For obtaining compensated spectra of films containing additives, a film of unprocessed polymer of identical thickness without additive was used in the reference beam.

3.12 Rheovibron (Dynamic Viscoelastometer)

A direct reading dynamic viscoelastometer was used for the measurement of the temperature or frequency dependence of dynamic mechanical properties of polymers in both amorphous and crystalline state. The Rheovibron used in the present study was Model DDVII, Toyo Measuring Instruments Company Limited (TMI), Tokyo⁽²⁸⁸⁾ (photograph number 2).

The sample in the form of films (having dimensions of length between 0.5 - 6 cm, breadth maximum 0.5 cm and thickness maximum 0.1 cm) is set horizontally in the furnace with both its ends attached to the two gauges (T-1 stress and T-7 strain)

PHOTOGRAPH NO. 2



with the help of a chuck and connecting rod. Of the two gauges, one is a transducer of displacement (T-7) and has a maximum force and displacement of 8 grm - 0.3 mm and an output of 4000×10^{-6} strain. The other is a transducer of generated force (T-1 stress). It has a maximum force of 550 grm and output of approximately 4000×10^{-6} strain. Both the amplitude of displacement and the main magnitude of the load applied on the specimen is measured by T-7 and T-1 gauges respectively and when they are adjusted to unity, their phase angle $\tan \xi$ can be read directly from the main meter.

3.12.1 Theory and Derivation of Basic Dynamic Equations

Dynamic mechanical methods measure the ability of a material to store and to dissipate energy on mechanical deformation. In such measurements, free or forced sinusoidal vibrations are set up in a specimen. These may be shear, flexural or compression vibrations and changes in the frequency or in the amplitude of such vibrations is followed using a suitable instrument. The changes in the frequency of free vibrations arise from motions of molecules and molecular segments which, in turn depend on the physical and chemical state of the material being investigated. Two quantities may be obtained from dynamic tests:

- (i) Modulus of elasticity is a measure of stress accompanying a unit deformation and for material obeying Hook's law, is the ratio of stress to strain. It also provides a measure of recoverable potential energy. However, not all materials perfectly follow Hook's law and the energy utilised in deforming a body is not fully recoverable, a

part is always lost as heat. The extent of this energy dissipation, however, varies from material to material.

- (ii) Mechanical damping is a measure of loss of energy as heat and is defined by the ratio of the energy dissipated as heat to the energy stored as potential energy. The mechanical damping can be calculated as logarithmic decrement (Δ) which is the logarithmic ratio of amplitudes of two successive damped oscillations (Fig 3.12.1.1).

A perfectly elastic material (eg the ideal spring) has no mechanical damping. Here the stress applied in deforming or stretching is stored as potential energy and is fully recoverable when the applied load is removed. Viscous liquids are examples of the other extreme where all the energy used in deforming is dissipated into heat. High polymers are the best known examples of the class of material known as viscoelastic, having the characteristics of both the viscous liquid and elastic spring. If a stress is suddenly applied to a polymeric material the resulting strain reaches some value immediately and then decays or relaxes over a period of time. Thus sinusoidal experiments involving viscoelastic material appear to show two stress components, one in phase with the applied strain (ϵ') (or parallel to the direction of strain, Fig 3.12.1.2) and the other, out of phase with the applied strain (ϵ'') (or perpendicular to the direction of the strain).

The magnitude of two stresses is given by:



Fig 3.12.1.1 Schematic representation of typical damped oscillation curve

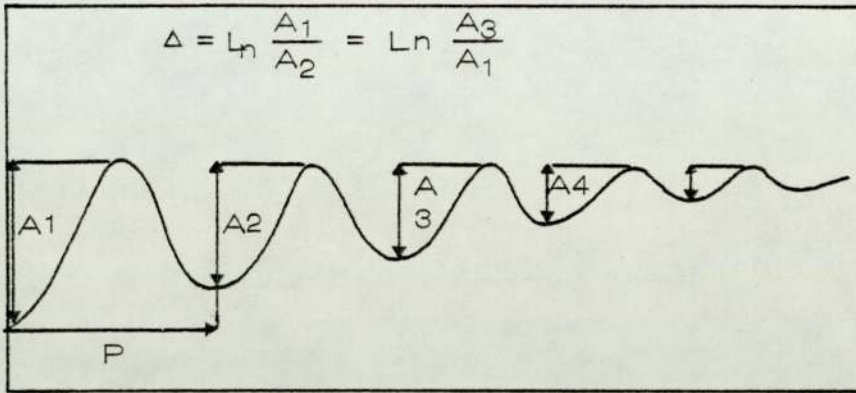
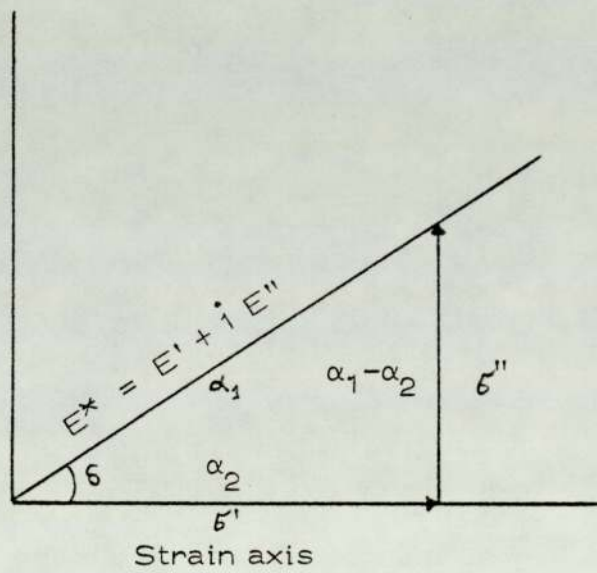


Fig 3.12.1.2 Vector diagram



$$\sigma' = E' \times \text{strain} \quad (3.1)$$

$$\sigma'' = E'' \times \text{strain} \quad (3.2)$$

where E' and E'' are real and imaginary parts of the complex modulus defined as $E^* = E' + i E''$.

The quantity of E' and E'' are also called storage and loss modulus respectively. The former is related to the stored and recoverable energy and the latter is related to the damping terms which determine the dissipation of energy into heat when the material is deformed.

The equation $E^* = E' + i E''$ can also be expressed in terms of the absolute value of complex modulus of elasticity $|E^*|$ and phase angle δ between the stress and strain

$$|E^*| = E' + i E'' = \sqrt{(E')^2 + (E'')^2} = \frac{\sigma_{\max}}{\epsilon_{\max}} \quad (3.3)$$

$$|E^*| = |E^*| (\cos \delta + i \sin \delta) \quad (3.4)$$

$$\text{where } E' = |E^*| \cos \delta \quad (3.5)$$

$$E'' = |E^*| \sin \delta \quad (3.6)$$

being the real and imaginary parts of the complex tensile modulus $|E^*|$ respectively. In the case of very low damping, (ie $\delta \rightarrow 0$) $\cos \delta = 1$ and $E' = |E^*|$ (ie E' is the same as modulus). From the equations 3.5 and 3.6,

$$\frac{E''}{E'} = \tan \delta \quad (4.7)$$

The term E''/E' is called mechanical dissipation factor and is proportional to the ratio of the energy loss to the energy stored during a cycle of deformation.

3.12.2 Principles Involved in the Rheovibron

The procedure used in the measurement of dynamic mechanical properties by 'rheovibron' involves the production of an oscillatory motion in the specimen with the help of the driving device which deforms the specimen sinusoidally. In the viscoelastic state (as has been discussed above) the sinusoidal stress is developed at the other end of the specimen but out of phase with the applied strain and differing by a phase angle, $\tan \delta$. To obtain the angle, δ , both the magnitude of the oscillating displacement ΔL and oscillatory force ΔF are measured by transducers (T-7 and T-1 respectively). When the absolute values of the electrical outputs of both deformation and load transducers are adjusted to unity (full scale deflection of meter), vector subtraction is made by changing the connection of the output circuit of the output circuit of two strain gauges (T-7 and T-1). If $|\alpha_1|$ and $|\alpha_2|$ are output voltage of the T-1 and T-7 respectively, then $|\alpha_1| = |\alpha_2| = 1$ is satisfied, $\tan \delta$ is given by Fig 3.12.1.2.

$$|\alpha_1 - \alpha_2| = \sqrt{\alpha_1^2 + \alpha_2^2 - 2\alpha_1\alpha_2 \cos \delta} \quad (\text{by cosine rule})$$

$$= \sqrt{2(1 - \cos \delta)}$$

$$= \sqrt{4 \sin^2 \delta} / 2$$

$$= 2 \sin \delta / 2$$

$$\cong \tan \delta \quad (\delta \text{ being very small})$$

The operation $|\alpha_1| = |\alpha_2| = 1$ can be performed using the dividers G_1 and G_2 (Fig 3.12.2.1). The value of $\tan \delta$ can therefore be directly read from the meter.

The absolute value of the complex modulus $|E^*|$ can be calculated from the following equations:

$$|E^*| = \frac{\sigma_{\max}}{\epsilon_{\max}} = \frac{\frac{\Delta F}{S}}{\frac{\Delta L}{L}} = \frac{\text{force}}{\text{area}} / \frac{\text{length}}{\text{elongation}} =$$

$$= \frac{\Delta F}{S} \cdot \frac{L}{\Delta L} \quad (3.8)$$

where: ΔF = oscillating load or amplitude of tensile force
 S = cross-section of sample in cm^2
 L = length of the sample
 ΔL = oscillating displacement of the sample or amplitude of elongation

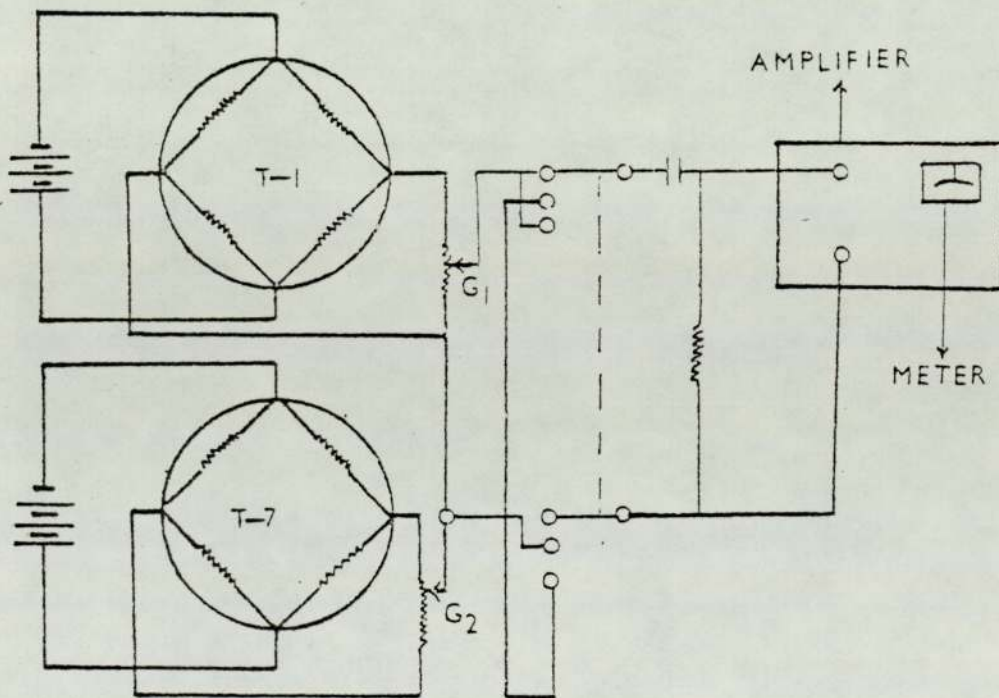
If the supply and output voltages of the transducers T-1 and T-7 are E_1 , E_2 and C_1 , C_2 respectively, then the relation of ΔF and ΔL can be calculated as follows:

$$\Delta F = \frac{C_1}{E_1 f_1} \quad , \quad \Delta L = \frac{C_2}{E_2 f_2}$$

where f_1 and f_2 are the calibration factors of the transducers T-1 and T-7 respectively.

Putting these values in the equation 3.8,

Fig 3.12.2.1 General concept of rheovibron



$$|E^*| = \frac{C_1}{C_2} \cdot \frac{L}{S} \cdot \frac{f_2}{f_1} \cdot \frac{E_2}{E_1} \quad (3.9)$$

By adjusting the dividers G_1 and G_2 , condition $\frac{C_1}{C_2} = \frac{G_2}{G_1}$ is set, since the products of $C_1 G_1 = C_2 G_2$ are made equal at the time of measuring $\tan \delta$ ($|\alpha_1| = |\alpha_2| = 1$).

Replacing these values in the equation 3.9,

$$|E^*| = \frac{f_2}{f_1} \cdot \frac{L}{S} \cdot \frac{E_2}{E_1} \cdot \frac{G_2}{G_1} \quad (3.10)$$

Now $\frac{L f_2}{f_1 S}$ is constant for the sample and transducer used and E_2/E_1 is previously calibrated. Therefore $|E^*|$ is only dependent on the reading of G_1 and G_2 .

Calculation of oscillating load, ΔF

This is obtained from the following equation:

$$F = 10^4 \text{ dynes} \cdot \frac{10^3}{D} \cdot N$$

where 10^4 dynes = calibration value of T-1 gauge (≈ 10 grm)

D = value of the dynamic force dial (D.F) at the time of measuring $\tan \delta$

N = the value of the $\tan \delta$ range at the time of measuring $\tan \delta$ and obtained from Table 3.1

Calculation of oscillating displacement, ΔL

$$\Delta L = 5 \times 10^{-3} \text{ A.N.cm}$$

Table 3.1

Tan δ range or amplitude factor	\bar{N} or A
0 db	31.6
10	10.0
20	3.16
30	1.0
40	0.316
50	0.1
60	0.0316

where: 5×10^{-3} cm = calibration value of T-7 gauge

A = the value of the amplitude factor when
measuring $\tan \delta$ and obtained from
Table 3.1

Putting the above values of ΔF and ΔL in the equation of
complex modulus equation 3.8

$$|E^*| = 2 \times \frac{L}{A \cdot D} \times \frac{L}{S} \times 10^9 \text{ dynes/cm}^2 \quad (3.11)$$

Since during the displacement of the sample, there is also a slight
displacement in the chuck rod and T1 rod which give an error
in the final ΔL values. To eliminate this, an error constant,
'K' is included in the above equation and the final equation of
complex modulus of elasticity takes the form:

$$|E^*| = 2 \times \frac{1}{A \cdot (D-K)} \times \frac{L}{S} \times 10^9 \text{ dynes cm}^{-2} \quad (3.12)$$

The real and imaginary parts of the complex modulus E^* ,
however, are obtained from the equations 3.5 and 3.6, where:

- L = sample length (cm)
- S = cross-sectional area (cm^2)
- A = value corresponding to amplitude factor
selected (usually A was equal to 1.0)
- D = dynamic force reading on dial
- K = error factor

3.13 Tensile Strength

The tensile tests were carried out on an Instron Tensile Tester (model TM. SM) using a cross head speed of 2 cm per minute.

Tests were carried out on 6-8 samples from each run and the average result was taken. The error involved in the measurement was in the region of 15%. The dimensions of the dumb-bell test piece was as follows:

Length	5.0 cm
Breadth	0.35 cm
Thickness	0.012-0.019 cm
Gauge length	3 cm
Temperature	21-23°C

Specimen number, average thickness and blend composition was recorded for every test. From the stress-strain curves obtained, modulus, tensile strength, yield strength and elongation were measured. The result being calculated from the equation given below:

$$\text{Tensile strength (TS)} = \frac{\text{force at break}}{\text{thickness} \times \text{width}}$$

$$\text{Yield strength (YS)} = \frac{\text{force at yield}}{\text{thickness} \times \text{width}}$$

$$\text{Percentage elongation (\%E)} = \frac{\text{chart length} \times \text{cross head speed} \times 100}{\text{chart speed} \times \text{gauge length}}$$

$$\text{Modulus} = \frac{\text{chart length} \times \text{gauge length} \times \text{initial slope}}{\text{cross head speed} \times \text{thickness} \times \text{width}}$$

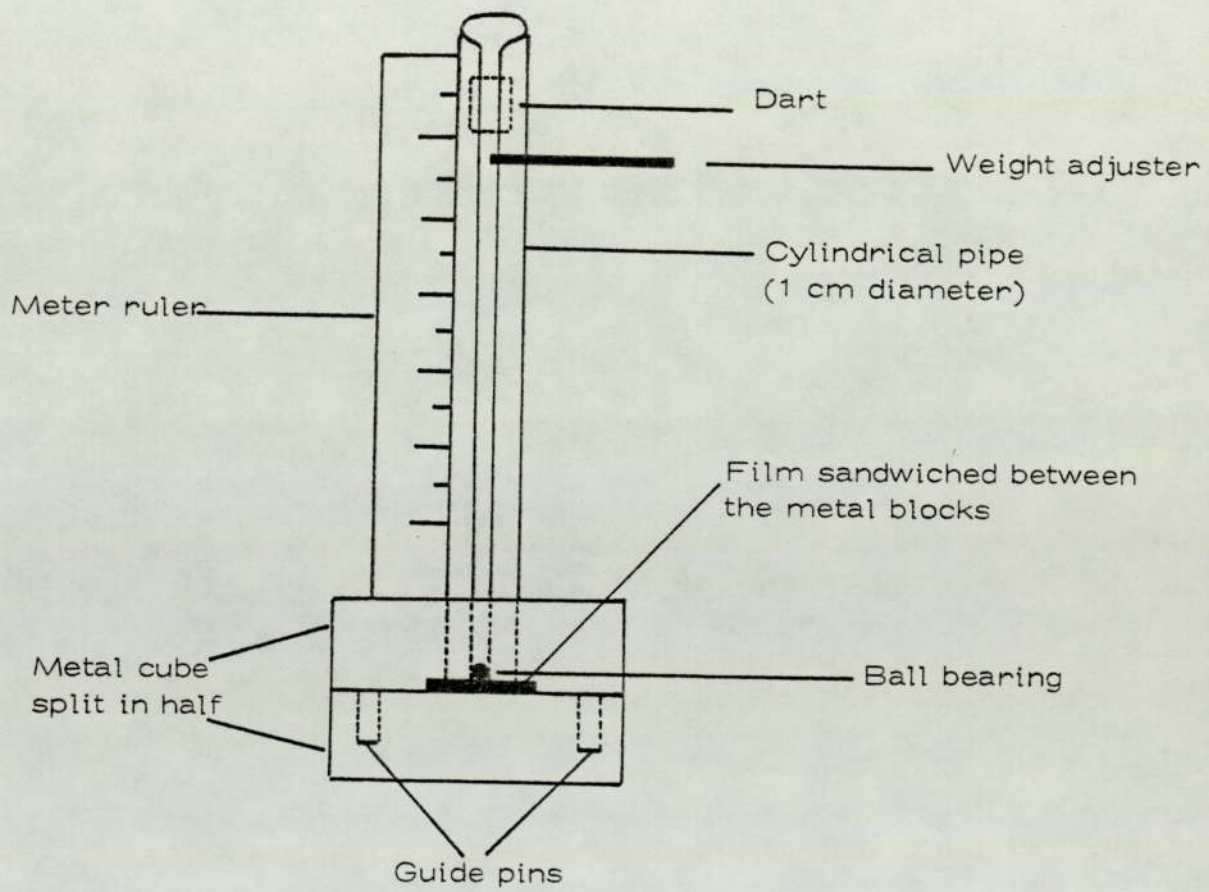
3.14 Impact Strength

The falling dart method was used. It involves raising a dart of known weight to a certain height and dropping it on the film which is firmly clamped (see Fig 3.14.1).

A relatively simple laboratory-made impact tester was used. It consists of two metal blocks with concentric drilled holes in the middle. A metal pipe with a slit along its length is mounted directly above the hole of the upper metal block. A meter ruler is attached closely beside the pipe. Metal rods of different lengths (and therefore different weights) were used to act as falling darts.

To perform the impact test, the film is clamped between the two metal blocks. A ball bearing is dropped from the top of the pipe to rest on the film. A suitable falling dart (metal rod) is supported by a spatula and the height adjusted before letting go

Fig 3.14.1 Impact tester



to drop on the ball bearing which is in contact with the film. The breaking of films was examined visually. The result was recorded as 'broken' if the specimen tore through from one surface to the other.

The impact resistance of the film would then be the potential energy of the dart which would just break the film, ie:

$$E = \text{impact resistance} = m \times g \times h \text{ Joules}$$

where: m = mass of dart in kg, g = acceleration due to gravity, 9.81 m/sec and h = height of the dart in meters.

It was found that impact strength was very sensitive to film thickness. Hence, in every film thickness of exactly 0.015 cm was used. Five tests were performed for each sample and the average impact resistance computed. The error involved in the measurement was in the range of 15%.

3.15 Estimation of peroxide in low density polyethylene and Polypropylene

(a) Chemical method: Iodimetric method based on the oxidation of sodium iodide was used. Liberated molecular iodine was determined by titration with standard 0.01 N sodium thiosulphate. The method used by Manasek et al⁽¹⁸⁵⁾ and Geddes⁽¹⁸⁶⁾ was modified as follows. 0.5-1 gram of polymer film (in small pieces) was introduced into 21.7 ml (approximately) of chloroform and purged with nitrogen for half an hour. This was then allowed to swell for 18 hours (this time was determined to give a maximum hydroperoxide concentration),

3.3 ml of glacial acetic acid was then added and the solution was purged with nitrogen for 5 minutes before and after addition of 2 ml of a freshly prepared deaerated 5% solution of sodium iodide in methanol. In addition to deaeration during carrying out hydroperoxide determination, all solvents were also deaerated in bulk prior to use with nitrogen gas and the procedure using rubber seals was employed. After storage for 4 hours (low density polyethylene) and 2 hours (polypropylene) in the dark for complete reaction the liberated iodine was titrated using standard 0.01 N sodium thiosulphate.

(b) Ir method: Thermally oxidised LDPE gives a sharp band in the ir spectra at 3555 cm^{-1} which is due to O-H stretching of free hydroperoxide^(182,186,187). This band is measured as index (defined as A_{3555}/A_{1895}). No such sharp band was found in polypropylene.

3.16 Microscopy Examination

The versatility of the Vicker's photoplan optical microscope enables both polarised light and phase contrast microscopy to be used to investigate the polymer and the degree of dispersion of second polymer in the first polymer matrix (continuous phase). The instrument had provisions to take photographs of the slide in view. Photographs were taken under polarised light and phase contrast conditions.

Phase contrast microscope specimens were photographed using a piece of the polyblend which sandwiched between the object lamp of the microtone. With the use of solid carbon dioxide the polyblend was cooled. This made the material 'hard' and

therefore facilitates easy cutting with a microtome blade. The microtome knife was tilted and set at a slicing angle of 45° . The piece of polyblend was sliced until a flat surface appeared. The automatic feed was then locked at 2μ . Now, it was necessary to cut slowly but steadily in order to produce a sample of uniform thickness.

The slice was removed from the blade with a single bristle from a brush and transferred to a hot glycerol bath. The slice rolled out on contact with the hot liquid. The glycerol was maintained at $90 \pm 5^{\circ}\text{C}$ and this was found to be suitable for the polyblends used. Polyblends with a higher or lower heat distortion temperature would need a higher or lower bath temperature. However, the use of a heated bath destroys any orientation in the blends.

The roll out slice was taken onto a microscope slide and after reaching the room temperature, transferred to another microscope slide with the aid of a bristle. A cover slide was placed on top of the specimen and pressed gently with a glass rod. The specimen was sandwiched between the cover slide and the glass slide and the glycerol on the surface of the polyblend acts as the mounting medium.

Polarised microscope specimens were examined using glass slides which were cleaned by putting them into a saturated solution of sodium hydroxide and methanol for 24 hours. The slides were taken out and washed with distilled water.

A glass slide was placed on a hot plate and above it another slide was placed. The first slide acts as a heat transfer medium

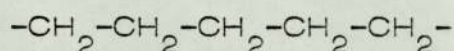
and prevents any dirt from the hot plate getting on to the second slide. A small piece of the polyblend is placed on the second slide and it is melting a cover slide placed above it. Using a glass rod the cover slide is pressed and when the glass cools the polyblend is firmly sandwiched between the glass slides.

CHAPTER FOUR

THE EFFECT OF PROCESSING AND REPROCESSING ON THE THERMAL OXIDATION AND PHOTO-OXIDATION STABILITY OF LOW DENSITY POLYETHYLENE (LDPE)

4.1 Introduction: Structure of LDPE

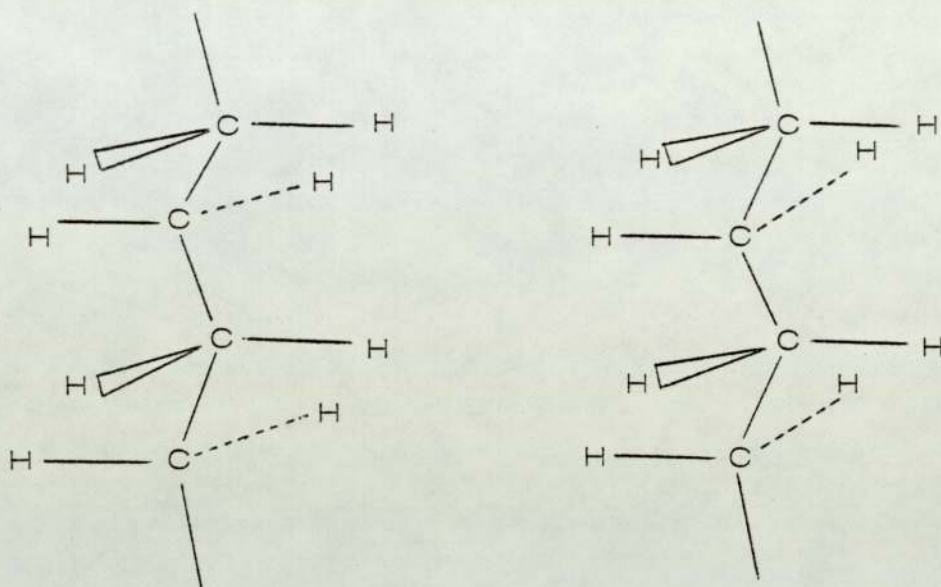
The simplest structure for the polyethylene molecule is completely unbranched chain of $-\text{CH}_2-$ units as shown:



The vigorous nature of the high pressure process, however, militates against the straight forward process of chain growth and a great deal of chain branching occurs which has an important bearing on the properties of low density polyethylene. Both the short and long chain branches are produced and investigation of low density polyethylene prepared by high pressure process using infra-red spectroscopy⁽¹⁸⁹⁾ indicates the presence of about 20-30 methyl groups per 1000 carbon atoms. The quantitative determination of methyl content based on the measurement of the intensity of absorption band at 1378 cm^{-1} (7.26μ) was reported by Cross, Richard and Willis⁽¹⁹⁰⁾. From their results it was shown that a typical LDPE of molecular weight 32000 and MFI 1.8 contained 23 methyl groups per 1000 carbon atoms and 52 methyl groups per molecule, indicating about 50 branch points in the chain. Although the presence of branches in LDPE has been established, the length of such branches is still under debate. It is generally assumed that both short and long branches are

present in polyethylene. Fox and Martin⁽¹⁹¹⁾ assumed branching to be methyl but Elliot et al⁽¹⁹²⁾ suggested that the branches were longer than the methyl group. Careful quantitative analysis of the ir spectra of low density polyethylene (LDPE) indicated^(193, 194) the presence of ethyl and butyl branches in the polymer. The structure of low density polyethylene molecule also effects the physical and chemical properties of the polymer. One important property is crystallinity. Many factors limiting both the crystallisation rate and attainable degree of crystallinity⁽¹⁹⁵⁾. These include such considerations as chain length and repeat unit symmetry, stereospecificity, size and flexibility of side groups and chain stiffness.

Polyethylene in the crystalline state takes up the extended conformation in which the carbon atoms in the backbone are in zig-zag arrangement⁽¹⁹⁶⁾. The hydrogen atoms take up the staggered conformation (see below) so that they are as far apart as possible and are thus in position of minimum energy. In the crystal, these chain pack so that the hydrogen atoms on alternate carbon atoms are stacked vertically above each other; this arrangement also helps lateral packing.



Packaging of polyethylene chain in the crystal⁽¹⁹⁶⁾.

In addition to chain branching, low density polyethylene also contains unsaturation. Three different olefinic double bonds normally terminal or vinyl group ($\text{RCH} = \text{CH}_2$ absorbing at 909 and 1640 cm^{-1} in the infra-red spectra), internal chain double bonds ($\text{RCH} = \text{CHR}'$, absorbing at 964 cm^{-1}) and vinylidene or side chain methylene groups ($\text{R}_1\text{R}_2\text{C} = \text{CH}_2$, absorbing at 888 cm^{-1}) are found to be present in LDPE.

Low density polyethylene is a tough, slightly translucent material and is waxy to touch. The density can vary between about 0.916 g/cm^3 to 0.935 g/cm^3 . Low density polyethylene film has a good balance of properties such as tensile strength, burst strength, impact resistance and tear strength.

4.1.1 Effect of Processing on LDPE Properties

It has been shown that commercial processing operations have a deleterious effect upon the mechanical properties and subsequently light stability of polyolefins unless the effects of thermal oxidation during processing are minimised by the use of antioxidants^(149,197-199). Thermal oxidation of polyethylene differs from photo-oxidation in the nature of the chemical species produced in the two processes. Thermal oxidation involves the small amount of unsaturation initially present in the polymer in the formation of allylic hydroperoxides^(149,200,197) which subsequently break down to give aldehydes and ketones with destruction of the unsaturation⁽¹⁹⁷⁾. Photo-oxidation leads to the rapid photolysis of peroxides and of subsequently formed aldehydes and ketones with the formation of vinyl unsaturation and of carboxylic acids^(149,200). Vinyl unsaturation, particularly in the presence of hydroperoxides accelerates the thermal and photo-oxidation of polymers⁽²⁰¹⁾ during processing and in service.

4.2 Experimental

Stabilised and unstabilised low density polyethylene (LDPE) were processed at 180°C in the RAPRA torque rheometer in a closed chamber for 5 minutes. The polymers were then compression moulded at 180°C for 2 minutes on photographic glazing plates of thickness 0.015 ± 0.001 cm. Reprocessing was carried out on chopped up film under similar conditions to that used in processing. This was carried out 5 times for each polymer and reprocessed samples were indicated as number 2, number 3, number 4 and number 5. The

number 0 and number 1 were compression moulded and initially processed samples respectively.

Infra-red examination of the processed and reprocessed and subsequently photo-oxidised film were carried out using Perkin Elmer 457 spectrophotometer. The carbonyl index at $1710/1895\text{ cm}^{-1}$, vinyl index at $909/1895\text{ cm}^{-1}$ and vinylidene index at $889/1895\text{ cm}^{-1}$ were measured as discussed in Chapter 3.

Hydroperoxide content of processed and reprocessed samples were measured chemically (see Chapter 3). Melt flow index and gel content of processed and reprocessed unstabilised low density polyethylene samples were determined as discussed in Experimental Chapter 3.

The deterioration of the physical properties was followed by measuring the stress-strain parameters as a function of exposure time. The tensile test carried out on an Instron Tensile Tester (model TMSM) using cross-head 2 and chart speed 5 cm per minute at room temperature ($22 \pm 1^\circ\text{C}$).

The dynamic mechanical tests were carried out using a direct reading viscoelastometer (Rheovibron) (see Chapter 3). The tests were carried out at room temperature ($20 \pm 1^\circ\text{C}$) and at constant frequency ($\text{Hz} = 110$).

4.3 Results

The change of torque with processing time of low density polyethylene in the RAPRA torque rheometer at 180°C in

closed chamber is shown in Fig 4.1, curve 6 (see Chapter 3 for details of measurement). Fig 4.1 (curve 1) shows the gel which formed after each processing time increase with time and torque when the polymer was processed in closed chamber.

Melt flow index (MFI) of the polymer decreased in an autoretarding mode from the beginning of processing at 180°C (Fig 4.1, curve 2). This is associated with changes in mechanical properties such as $(\tan \delta)_{20^{\circ}\text{C}}$, % elongation and strength at break. The % elongation at break increased with an increase in gel content and processing time as shown by Fig 4.1, curve 4. Tensile strength at break increased for the first 30 minutes of the processing time and then decreased as shown in Fig 4.1, curve 5. $(\tan \delta)_{20^{\circ}\text{C}}$ also decreased with processing time (Fig 4.1, curve 3) in the same way as MFI.

The ir spectra (Fig 4.2B) of reprocessed unstabilised low density polyethylene gives a band at the 3555 cm^{-1} which is due to $-\text{O}-\text{H}$ stretching of free hydroperoxide^(182,187). This band was calculated as an index $(A_{3555}/A_{1890}\text{ cm}^{-1})$ (see Chapter 3). A good correlation was found between hydroperoxide measured chemically and hydroperoxide measured by infra-red (ir) method for unstabilised low density polyethylene (Fig 4.3).

The behaviour of LDPE on reprocessing (Fig 4.4) is rather different from LDPE processed continuously for the same length of time (Fig 4.4, curves 1-4). The reduction in MFI and increase in gel content were both lower (Fig 4.4, curves 1, 4).

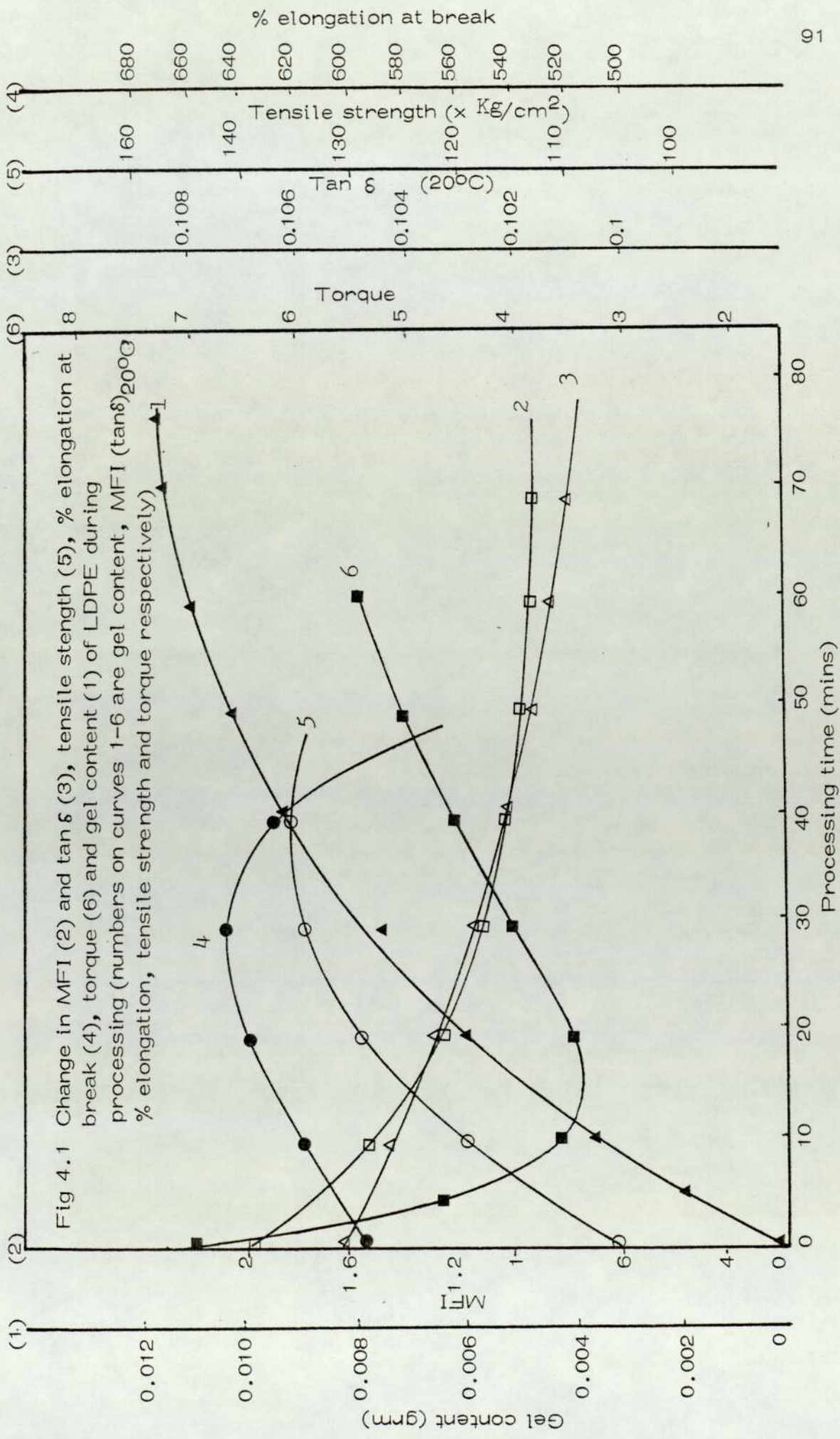


Fig 4.2.A Change in the carbonyl formation of LDPE at 1710 cm^{-1} during uv irradiation (numbers on curves are exposure time in hours and No.1, No.3 and No.5 are processing cycles respectively)

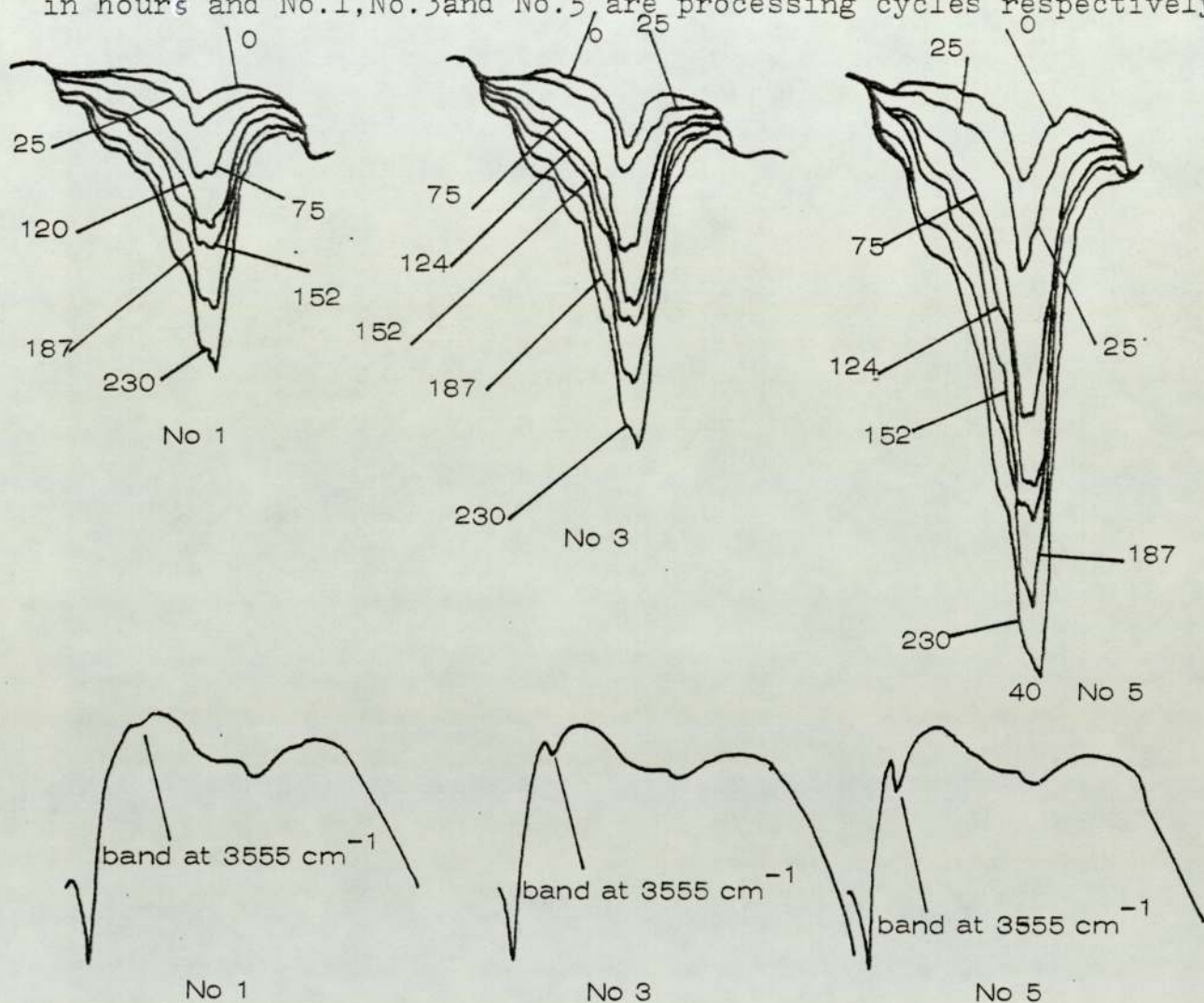
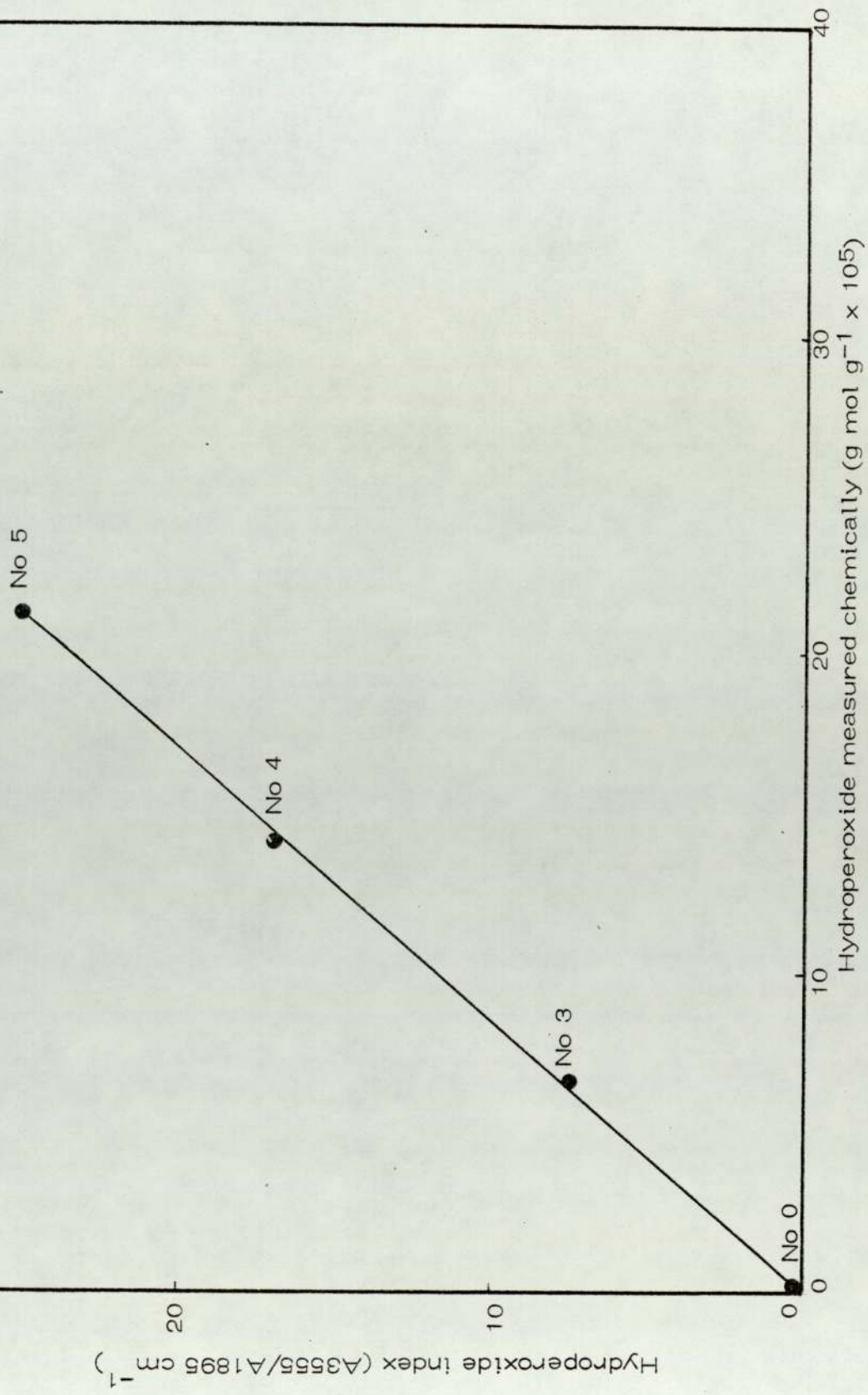


Fig 4.2.B Change in hydroperoxide (3555 cm^{-1}) of LDPE during processing cycles (numbers No.1, No.3, and No.5 are processing cycles)

Fig 4.3 Relationship between chemical (iodometric) and ir method of hydroperoxide estimation in LDPE (numbers 0,3, 4 and 5 are represent processing cycles)



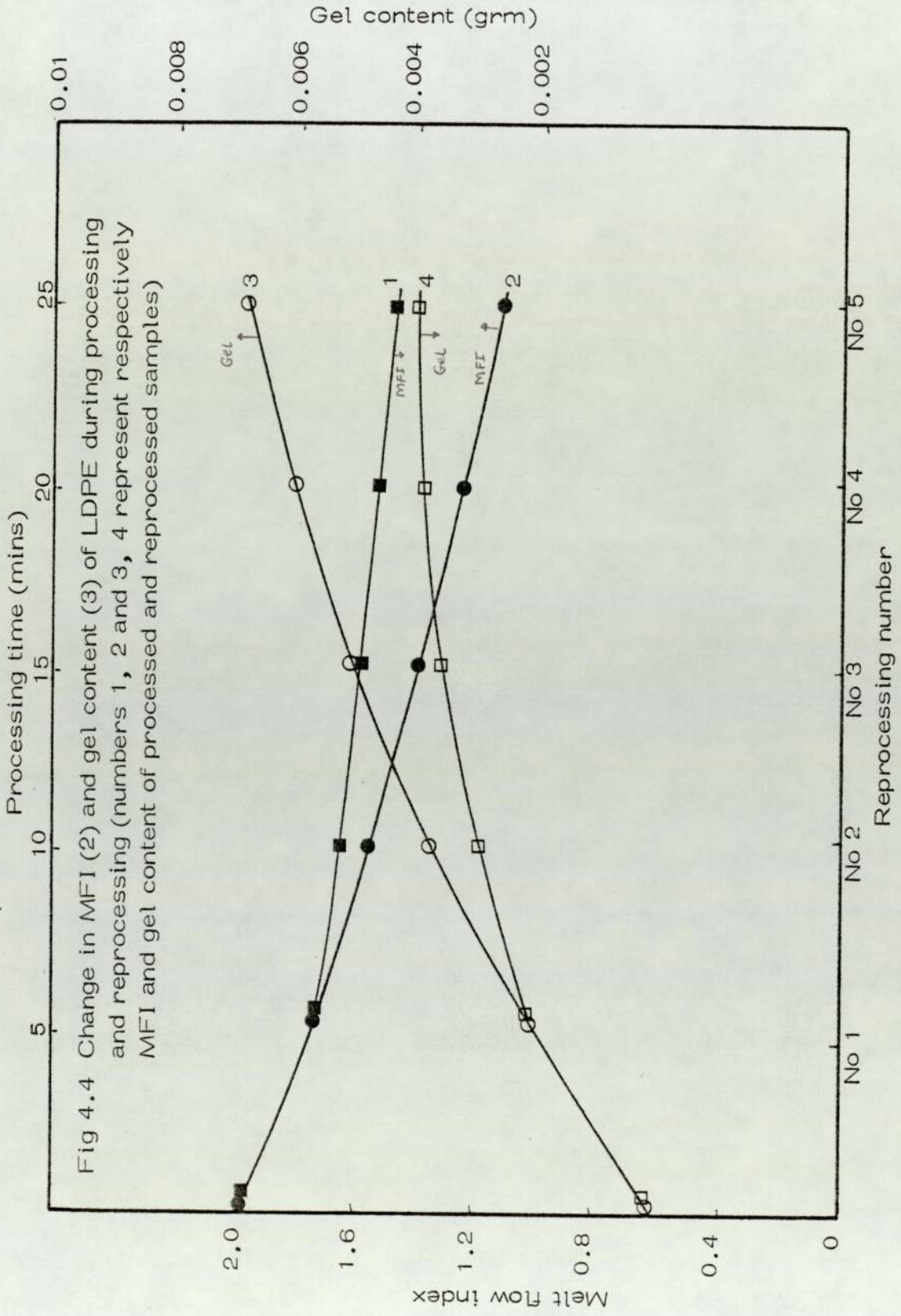


Fig 4.4 Change in MFI (2) and gel content (3) of LDPE during processing and reprocessing (numbers 1, 2 and 3, 4 represent respectively MFI and gel content of processed and reprocessed samples)

Infra-red absorption spectrophotometry has previously been used to determine the nature of oxidation products and the rate of their formation during thermal and photo-oxidation of polyethylene^(147,202). Since photo-oxidation results in the build-up of different oxidation products, for example, hydroxyl, as well as bringing about changes in unsaturation in the polyethylene polymer, the kinetics of the growth of these functional groups, as the irradiation proceeds were followed by observing the change in the characteristic absorption peaks at a definite wave lengths⁽¹⁸²⁾. Table 4 shows the absorption frequencies of various carbonyl compounds and olefinic unsaturation groups which are studied in the present work.

Fig 4.2A shows the effect of uv irradiation on the carbonyl absorbance of polyethylene film reprocessed at 180°C for 5 minutes in a closed chamber. The rate of photo-oxidation of LDPE as measured by the rate of formation of carbonyl in the polymer is shown in Fig 4.5. The most significant effect of reprocessing is the increase in the initial rate of photo-oxidation in the third reprocessing compared with polyethylene which has been subjected to a normal single processing operation (Fig 4.5). The formation of vinyl at 910 cm^{-1} (Fig 4.6) which has a negligible concentration in the processed polymer increased in an auto-accelerating mode with uv irradiation time. This is the expected sequence of events if vinyl is formed by Norrish II photolysis of carbonyl compounds⁽¹⁵⁵⁾. The vinylidene index at $890/1985\text{ cm}^{-1}$ decreased rapidly to a low value during the early part of photo-oxidation sequence (Fig 4.7). Vinylidene index cannot be measured accurately during the later stages of photodegradation due to interference from the growing vinyl

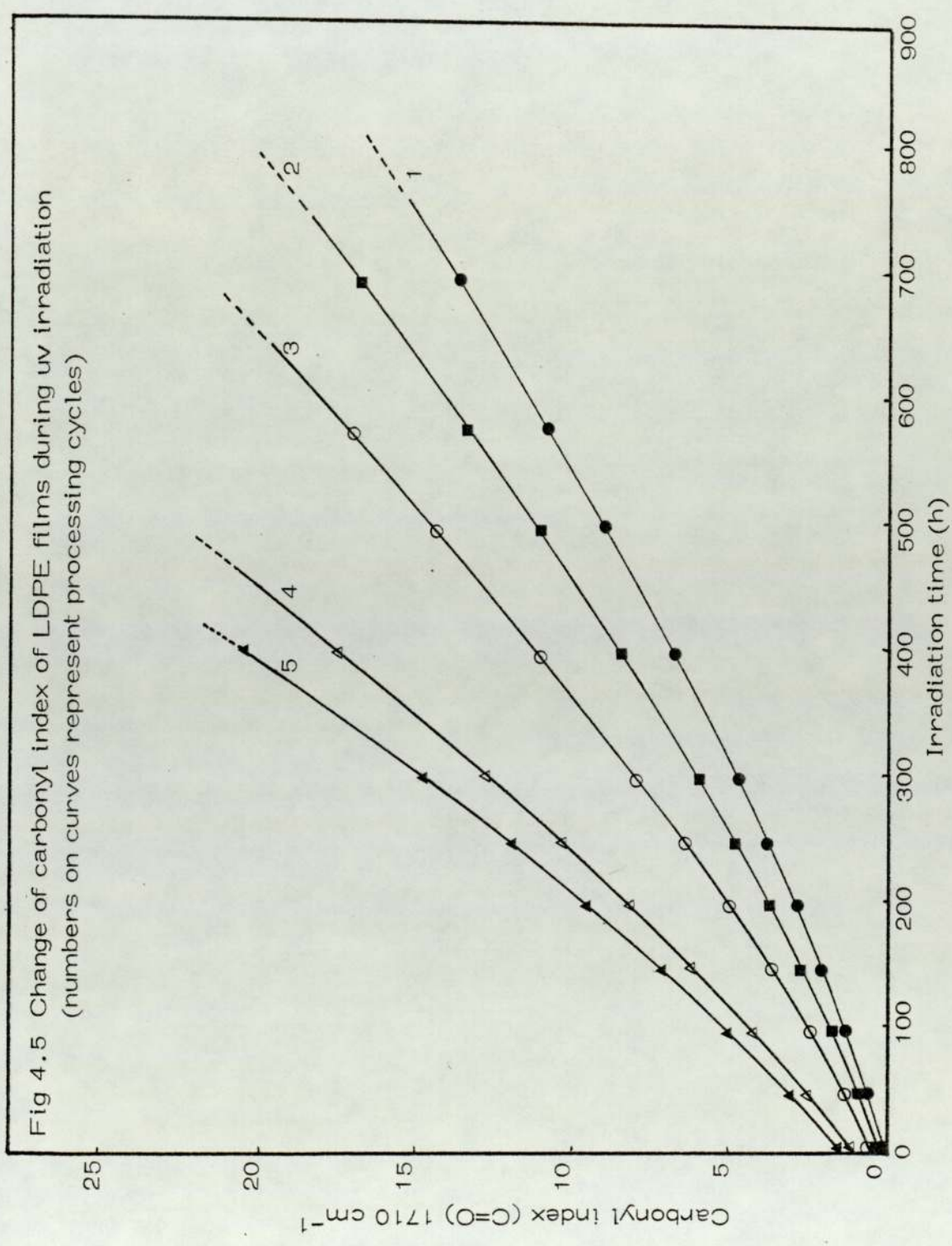


Fig 4.5 Change of carbonyl index of LDPE films during uv irradiation (numbers on curves represent processing cycles)

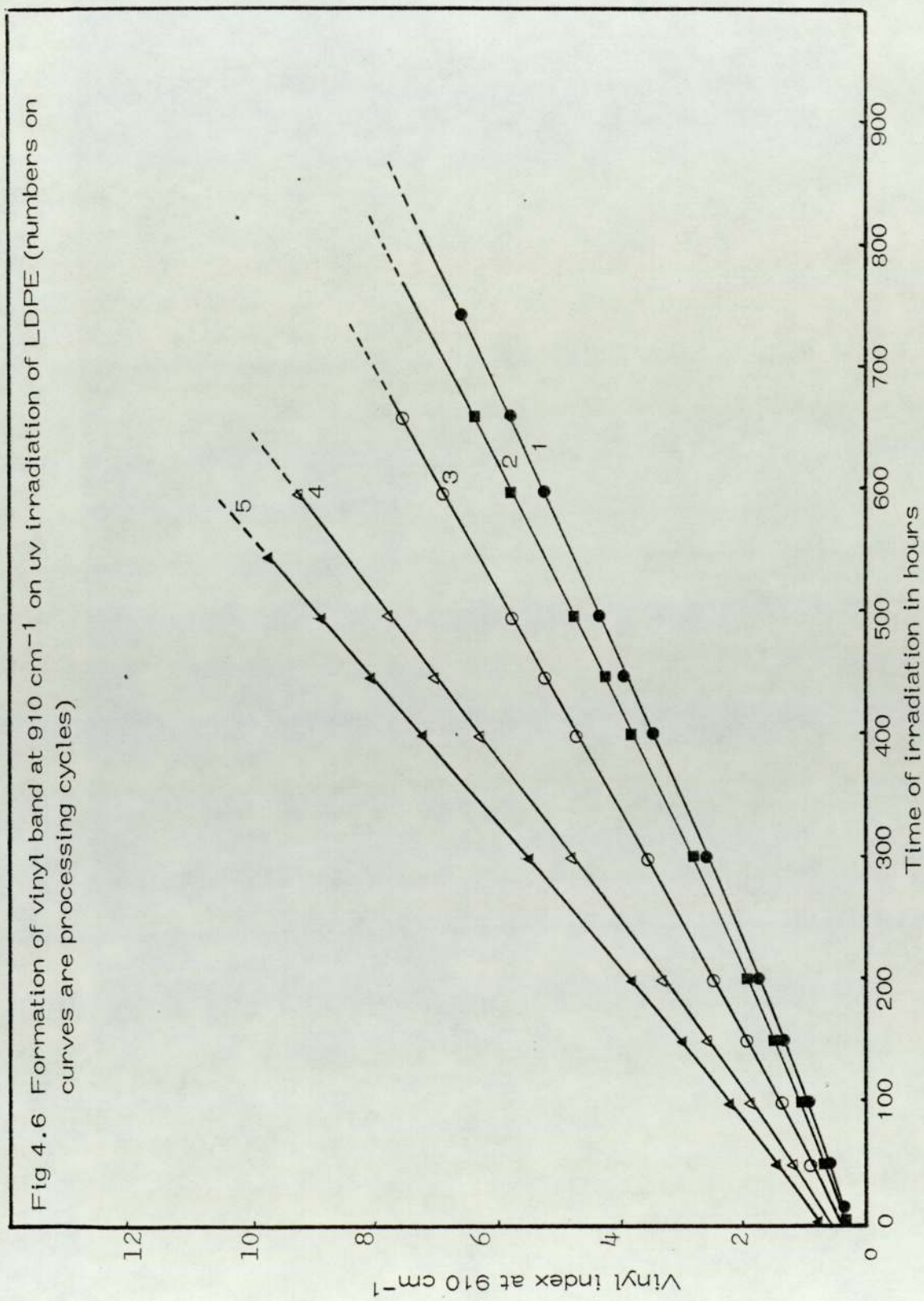


Fig 4.7 Change in vinylidene index of LDPE films during uv irradiation (numbers on curves are processing cycles)

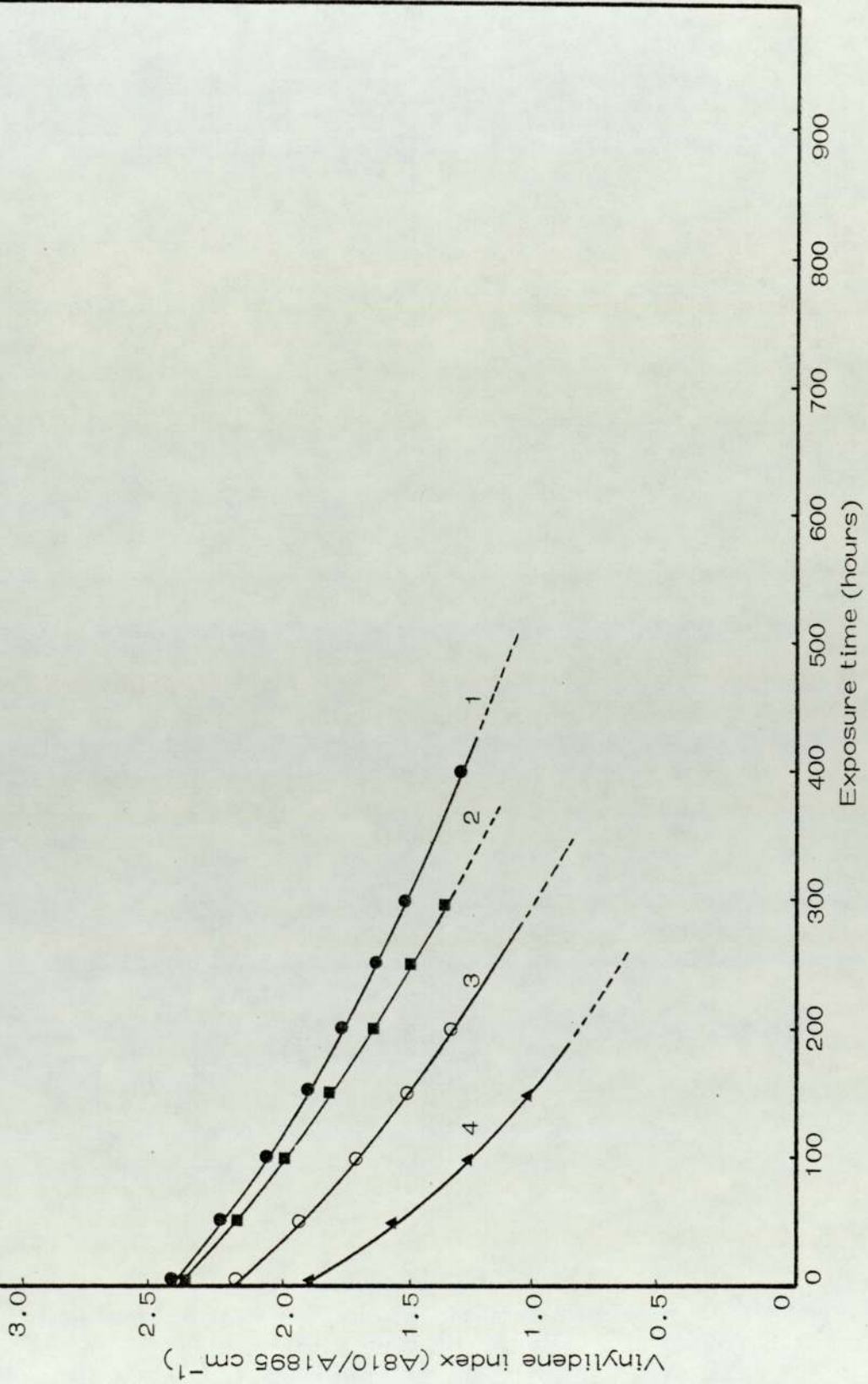


Table 4:

Wavelength (cm ⁻¹)	Functional group	Intensity	Reference
3555	-OOH (free)	Sharp	182, 187, 203
3380	Polymeric associated -OH	Strong	204
3628	Phenol	Variable, sharp	205
3632	Primary alcohol	"	205
1725	Terminal, ketone or methyl ketone $\text{CH}_3-\overset{\text{O}}{\parallel}{\text{C}}-\text{CH}_2-$	Strong	147(a)
1720 \pm 1	Internal ketone $-\text{CH}_2-\overset{\text{O}}{\parallel}{\text{C}}-\text{CH}_2-$	"	182, 187
1730	Long chain aldehyde $-\overset{\text{O}}{\parallel}{\text{C}}-\text{H}$	"	182, 187
1745	Ester $\overset{\text{O}}{\parallel}{\text{C}}-\text{OR}$	Strong	182, 187
1785	Peracid $\overset{\text{O}}{\parallel}{\text{C}}-\text{O}-\text{OH}$		187
1765	Perester $\overset{\text{O}}{\parallel}{\text{C}}-\text{OOR}$		187
1685	α, β -unsaturated ketone $-\text{CH}=\text{CH}-\overset{\text{O}}{\parallel}{\text{C}}-$		182, 206

Continued ...

Table 4 Continued

1645	Internal double bond R-CH=CH-R (non-conjugated)	Weak	182
1185	C-O in carboxylic acid	Weak	190
887 \pm 1	$\begin{array}{c} R_1 \\ \diagdown \\ C=CH_2 \\ \diagup \\ R_2 \end{array}$ vinylidene group	Strong	182
909	Vinyl group R ₁ CH=CH ₂	Variable	182
964	Vinylene group on disubstituted trans- alkene R ₁ CH=CH-R ₂	Variable	182
990	Disubstituted cis- alkene -CH=CH-	Variable	82
1378	-CH ₃ group content in PE	Weak	207
1305	CH ₂ - chain in amorphous phase	Weak	207
1080	(C-C) in long chain in the amorphous phase	Weak	207

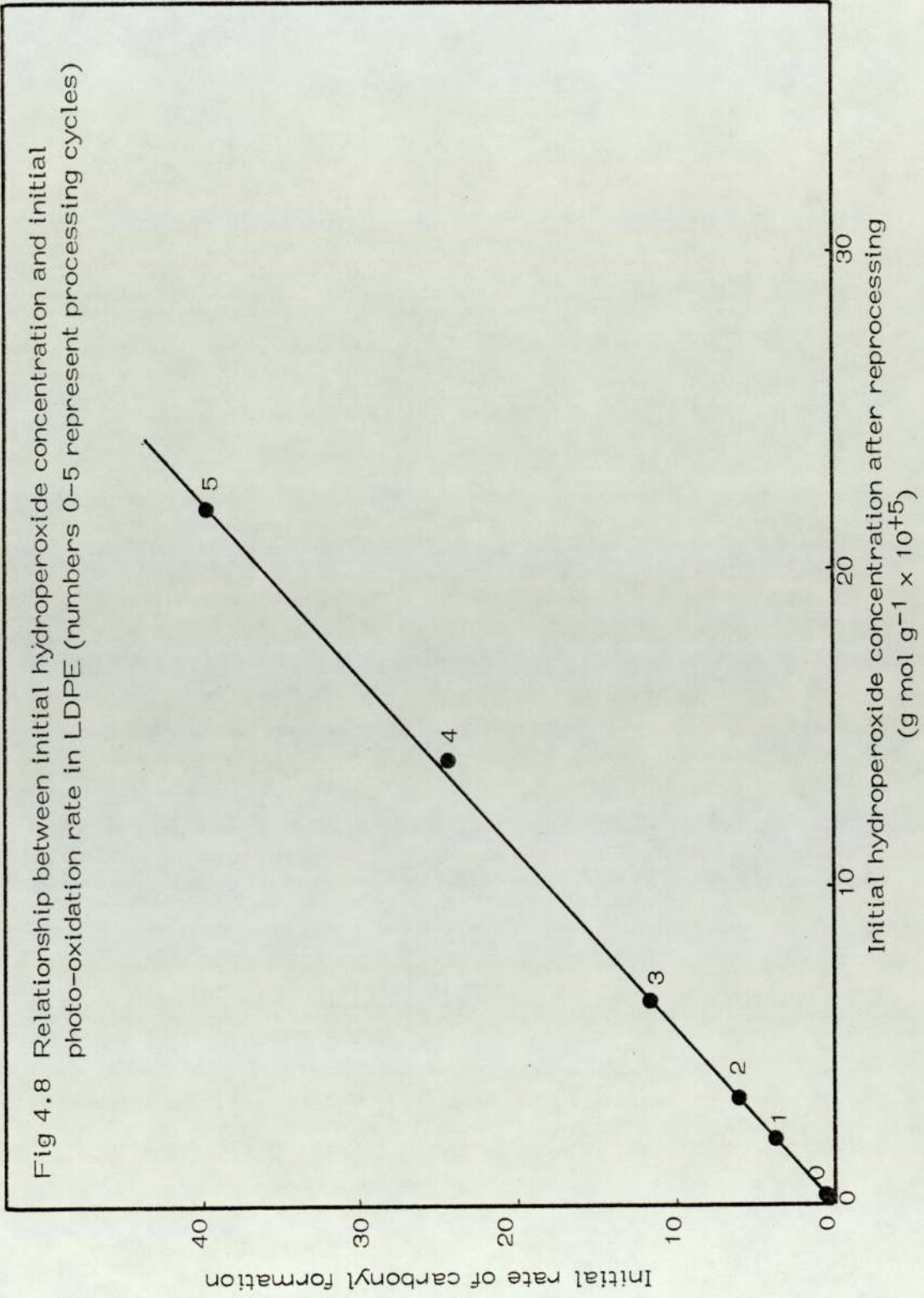
band at 910 cm^{-1} resulting from Norrish II photolysis of ketone. Decrease of vinylidene on uv irradiation proceeded the formation of significant amounts of carbonyl (Fig 4.5) in accordance with earlier studies⁽¹⁹⁸⁾. The initial rate of photo-oxidation as measured by carbonyl formation was found to be linearly related to the initial hydroperoxide concentration (Fig 4.8). This was also observed by other workers⁽¹⁹⁹⁾.

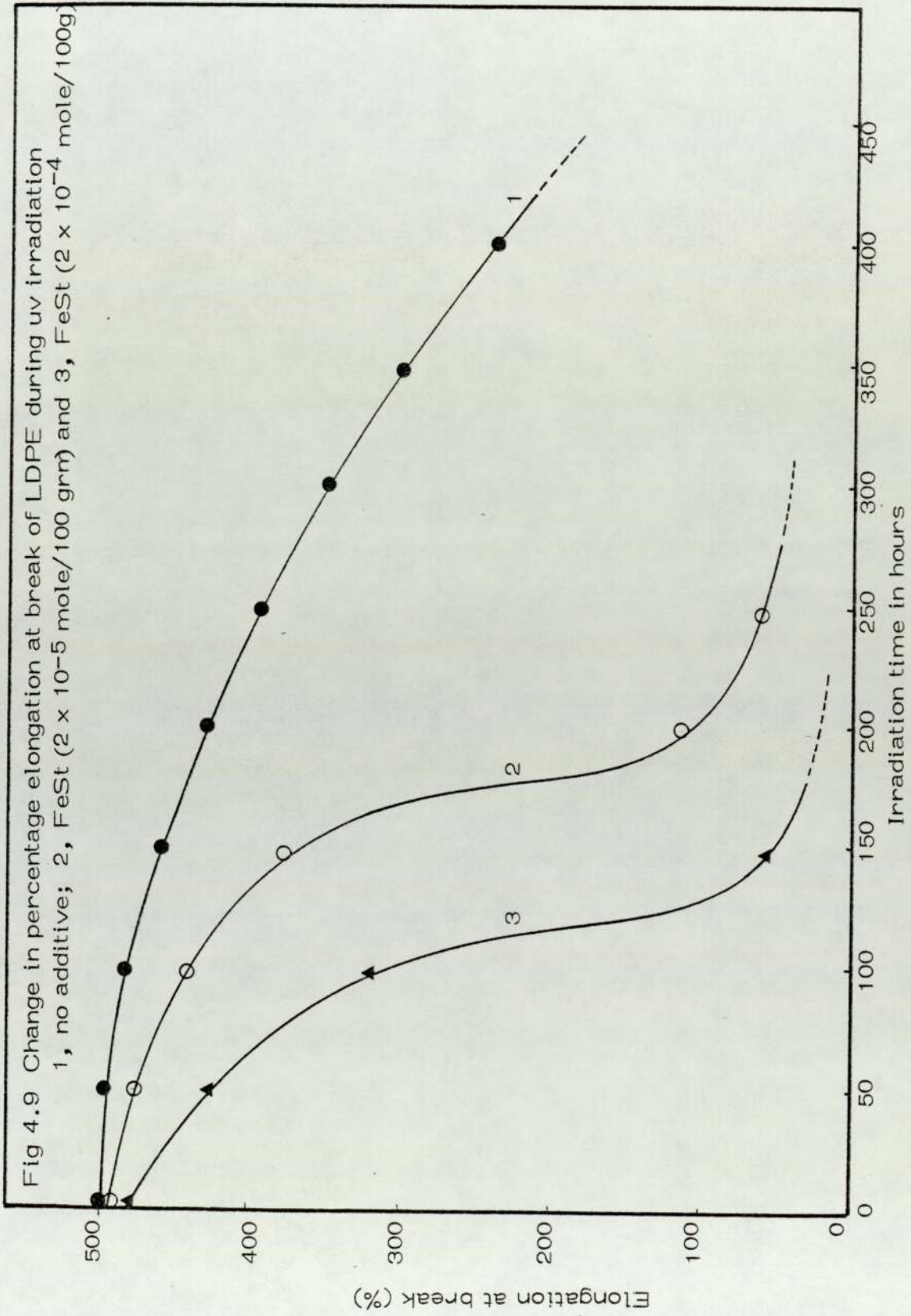
The mechanical properties of LDPE are intimately related to the physical structure of the polymer (eg, crystallinity and morphology). The change in the mechanical properties of LDPE processed at 180°C for 5 minutes were followed during uv irradiation with and without additive. Fig 4.9 (curve 1) shows that the loss of elongation at break is auto-accelerating. Tensile strength decrease follows a similar course (Fig 4.10).

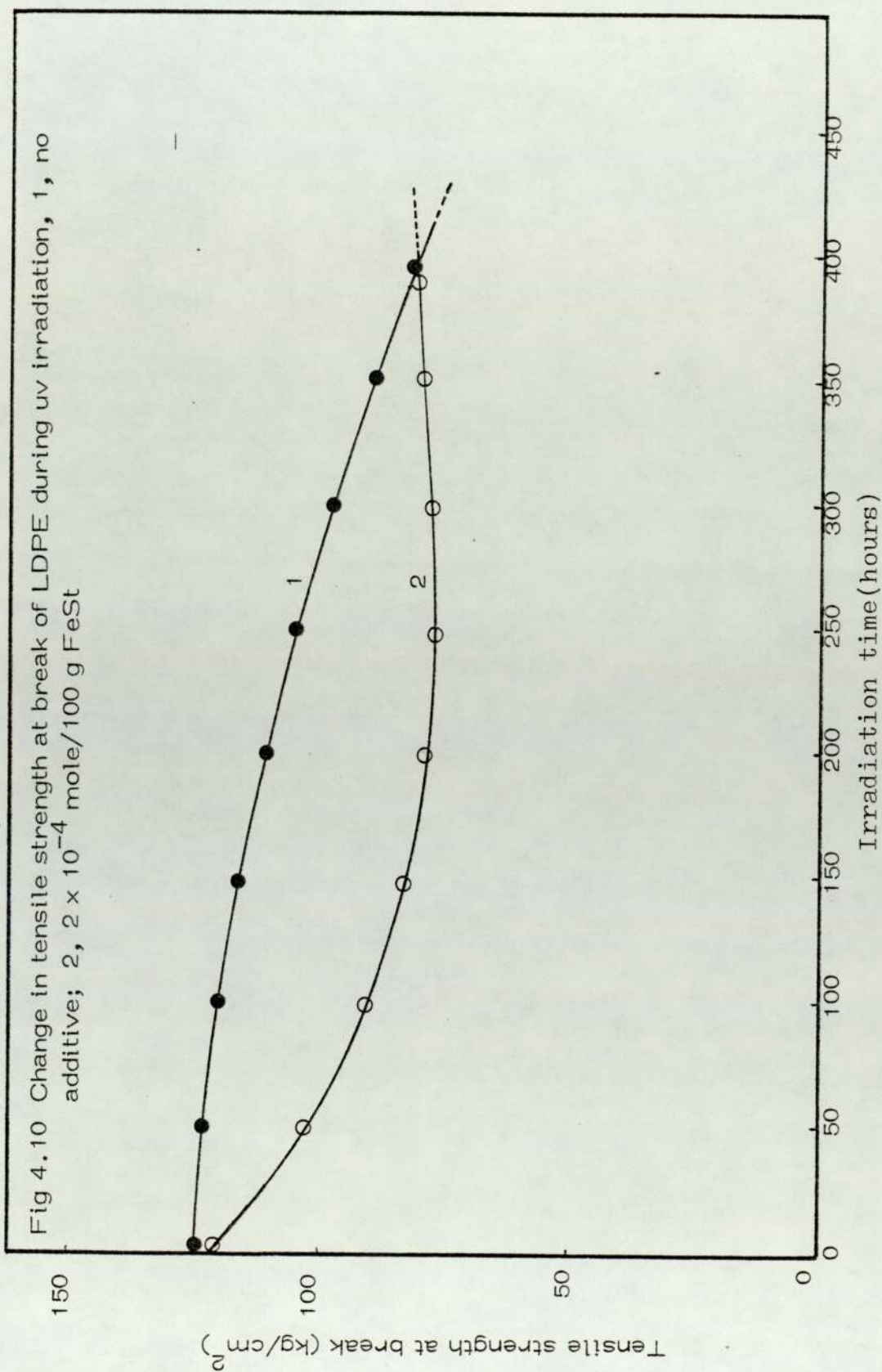
In order to simulate commercially used polymeric products with reprocessed polymer the stabilised polyethylene or polypropylene was initially processed in the RAPRA torque rheometer and subsequently uv irradiated for 90 hours. These samples were then processed in the torque rheometer for 5 minutes. Figs 4.11 and 4.12 show the change of carbonyl index and complex modulus for the processed and reprocessed polymer samples after subjecting to uv light (90 hours). (The reason for 90 hours irradiated polymers is to produce an artificially 'used' polymer which has had some environmental exposure.)

Most polymers produced on an industrial scale contain metallic impurities since it is not possible to avoid

Fig 4.8 Relationship between initial hydroperoxide concentration and initial photo-oxidation rate in LDPE (numbers 0-5 represent processing cycles)







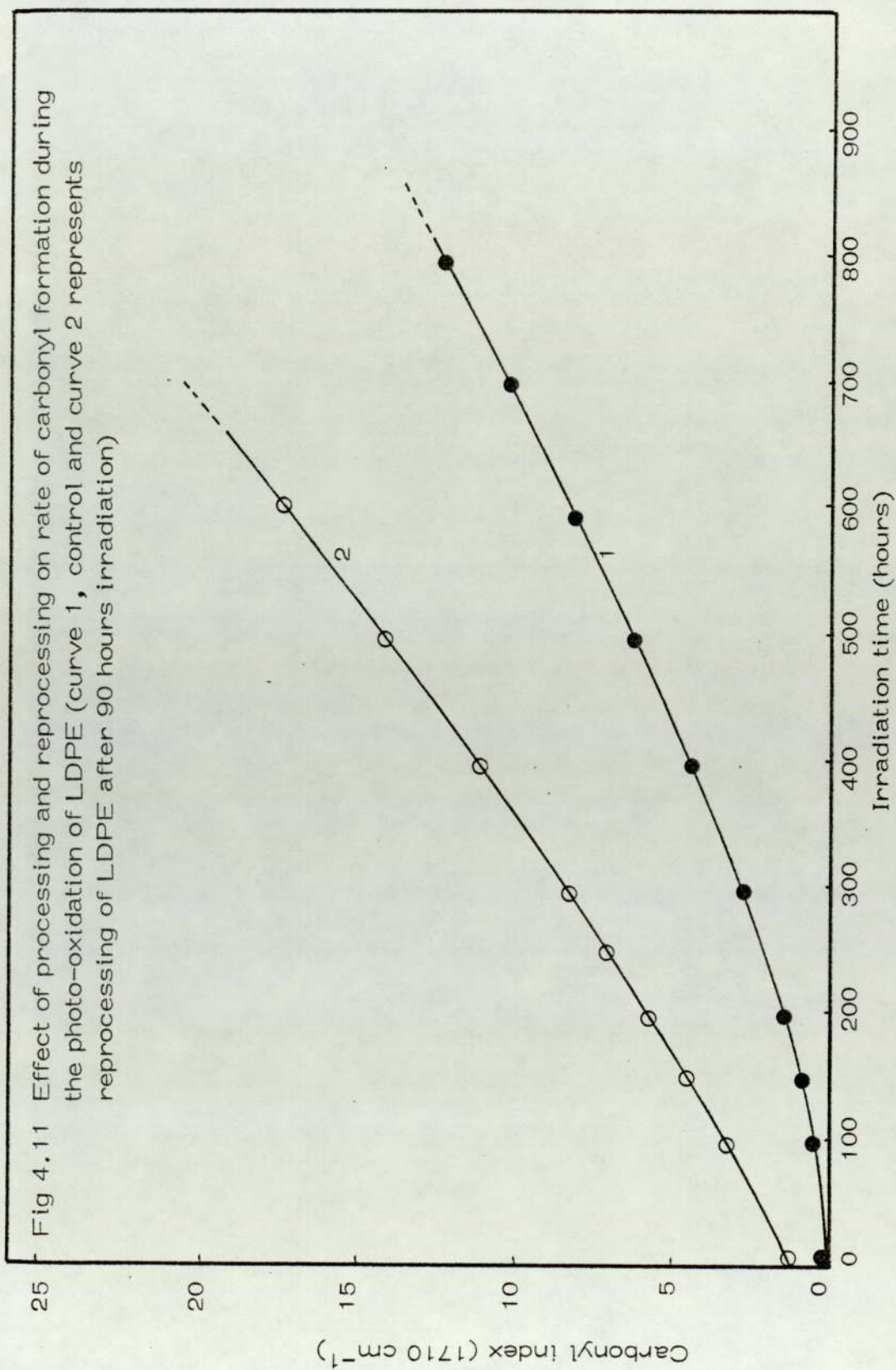
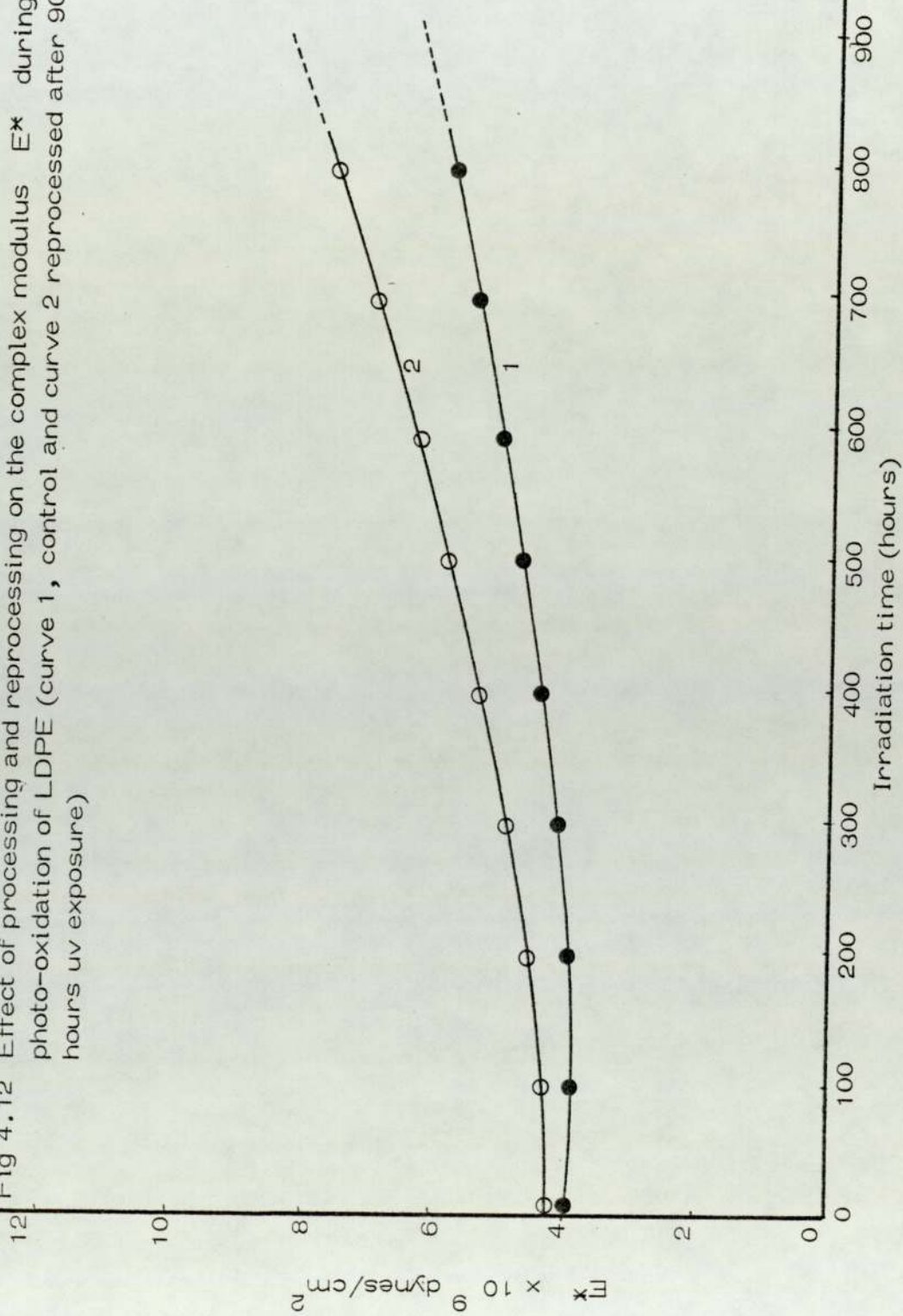


Fig 4.12 Effect of processing and reprocessing on the complex modulus E^* during photo-oxidation of LDPE (curve 1, control and curve 2 reprocessed after 90 hours uv exposure)



contamination during processing or reprocessing it, particularly in the presence of small amounts of acid. Fig 4.13 shows the effect of transition metal ions (eg, ferric stearate, FeSt) on the rate of oxidation of low density polyethylene during uv irradiation.

The increased rate of oxidation has a powerful effect on the rate of mechanical property change. Fig 4.9 (curves 2 and 3) shows the % elongation at break decreased much more rapidly than LDPE without any transition metal ions. Tensile strength decrease followed a similar course to elongation at break, up to a certain point and then began to increase (Fig 4.10) (see more details in Chapter 6).

$(\tan \epsilon)_{20}$ also increased rapidly with irradiation time but then fell rapidly after reaching a maximum (Fig 14, curves 2 and 3). Complex modulus increased from the beginning of uv exposure whereas the control showed an initial drop (Fig 4.15).

4.4 Discussion

The above results show marked changes in the torque (Fig 4.1, curve 6), melt flow index (Fig 4.1, curve 2), $(\tan \epsilon)_{20}$ (Fig 4.1, curve 3), % elongation at break (Fig 4.1, curve 4) and tensile strength (Fig 4.1, curve 5) in LDPE subjected to relatively mild processing conditions. This indicates a very delicate balance of cross-linking and chain scission reactions during the early stages of thermal oxidation of LDPE which has previously been observed in LDPE by Scott and co-workers⁽¹⁹⁸⁾ They observed a significant increase in average molecular weight (Fig 4.16)⁽¹⁹⁸⁾ even at 20 minutes of processing in a

Fig 4.13 Effect of ferric stearate (FeSt) on the rate of carbonyl formation during the photo-oxidation of LDPE (numbers on curves are concentrations of FeSt in mol/100 grm)

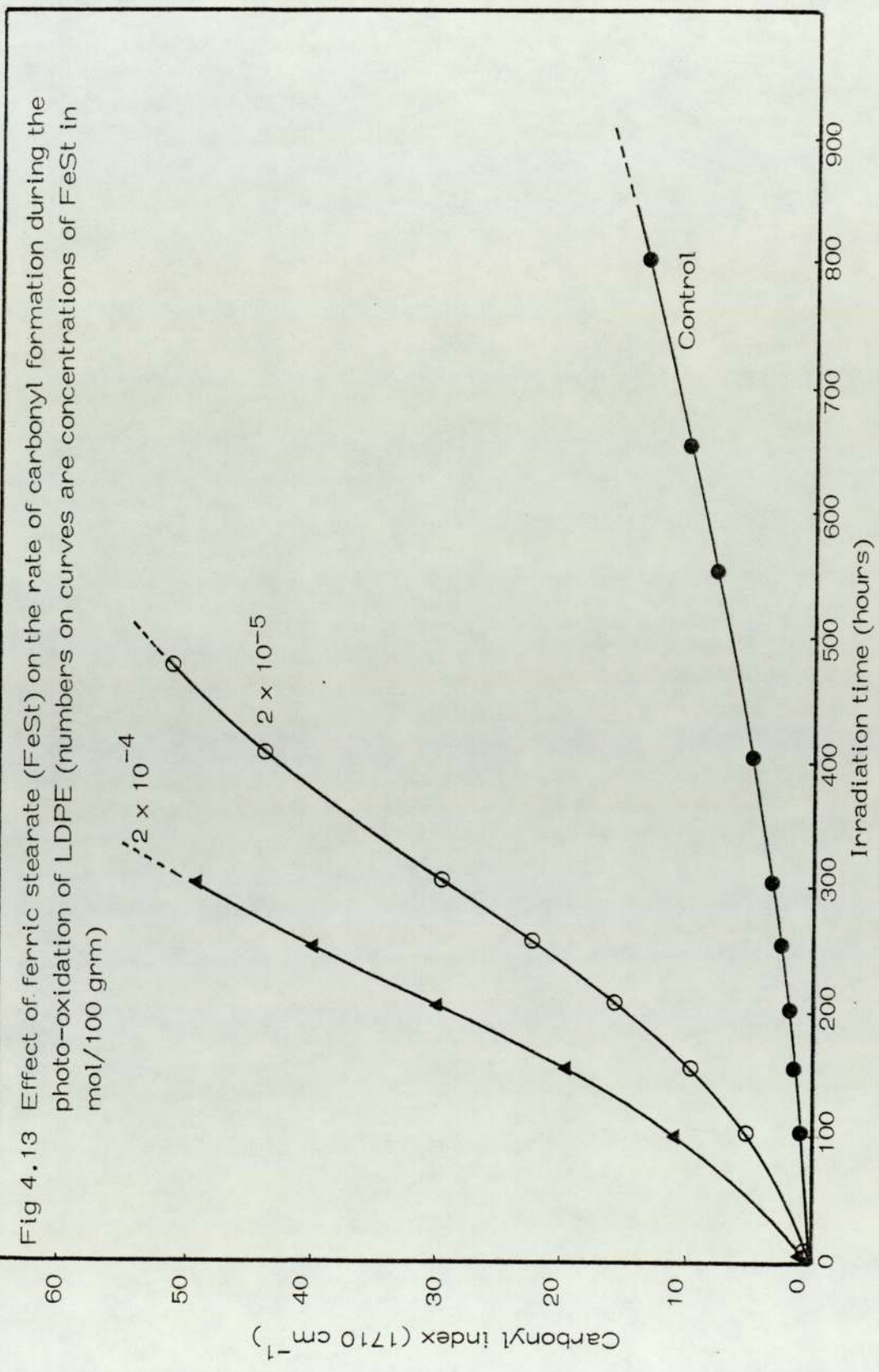


Fig 4.14 Effect of ferric stearate concentration on the $\tan \delta$ (20°C) during the photo-oxidation of LDPE (numbers on curves are concentration of FeSt in mol/100 g)
 1, no additive; 2, 2×10^{-5} mol/100 g; 3, 2×10^{-4} mol/100 g

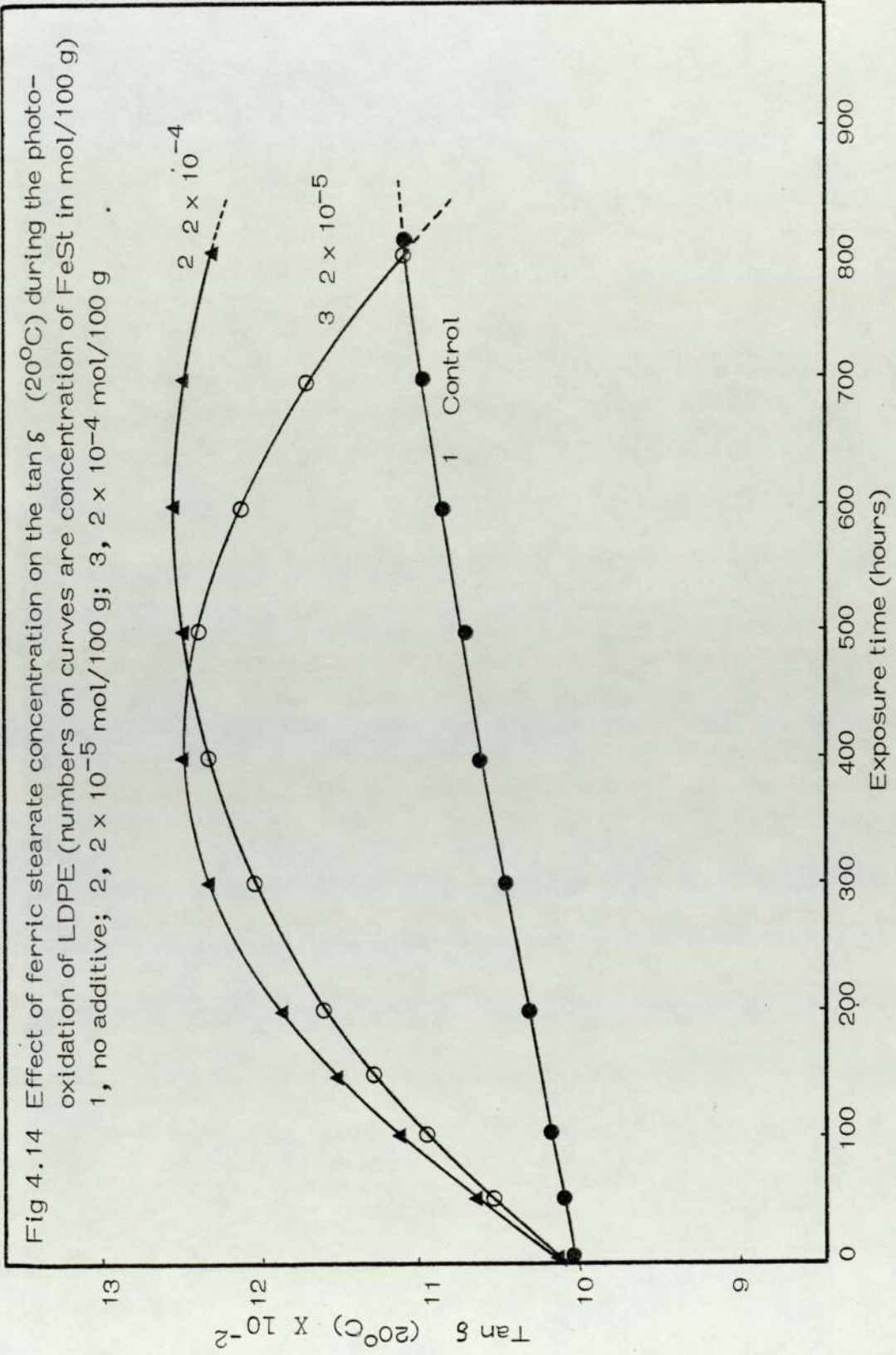


Fig 4.15 Effect of ferric stearate on the complex modulus E^* during the photo-oxidation of LDPE (numbers on curves are concentration of ferric stearate in mole/100 g)

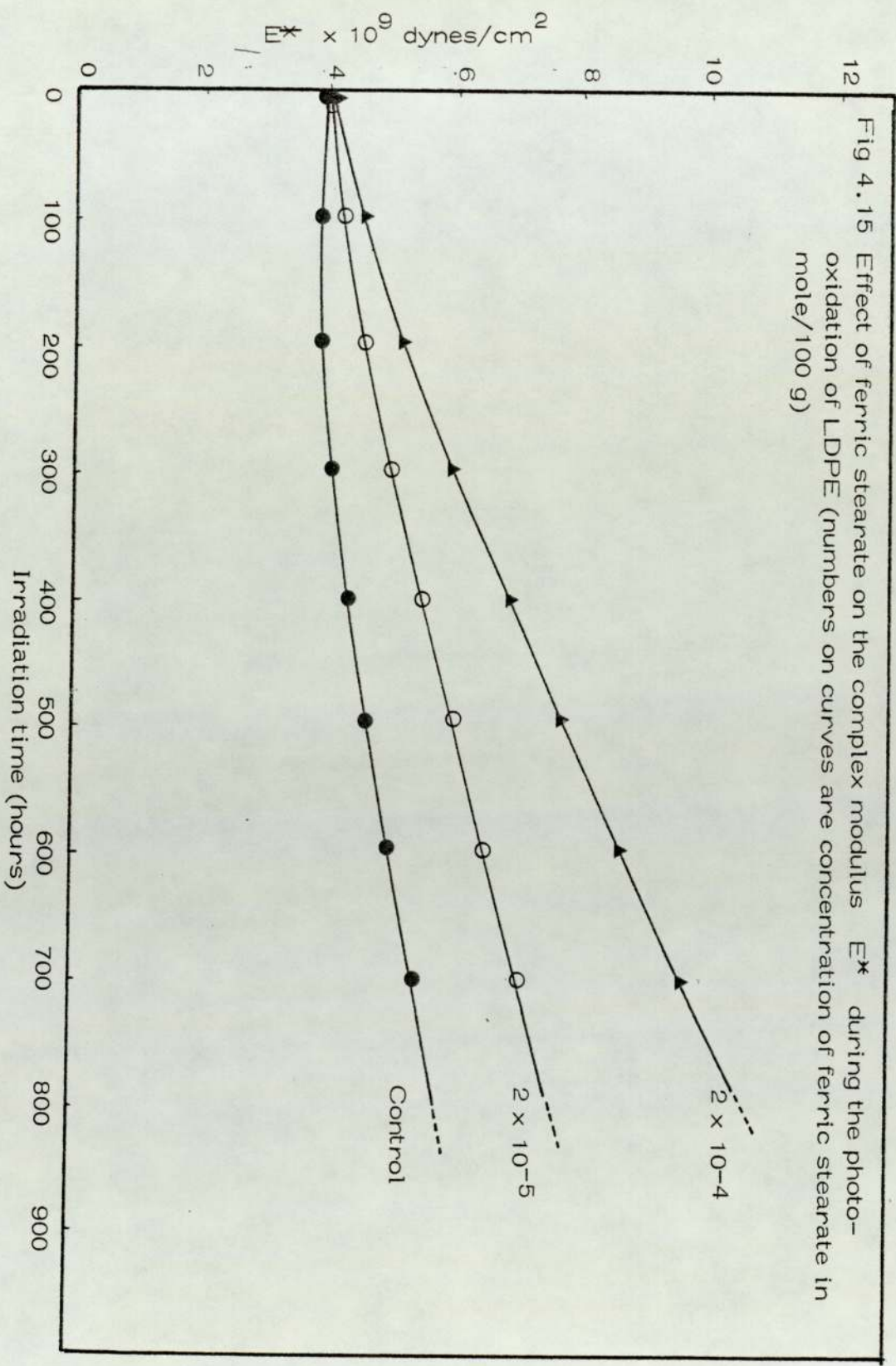
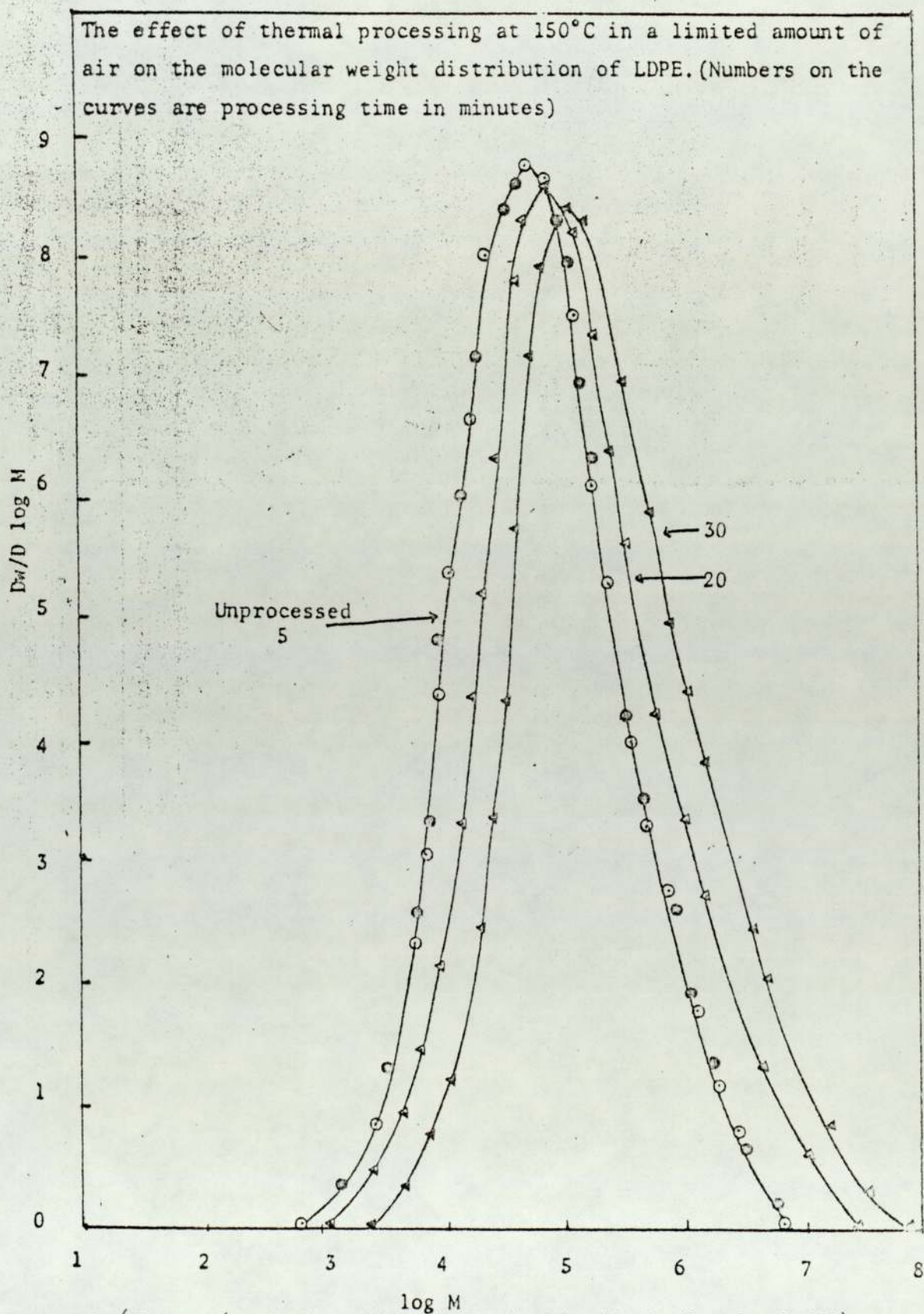


Fig 4.16

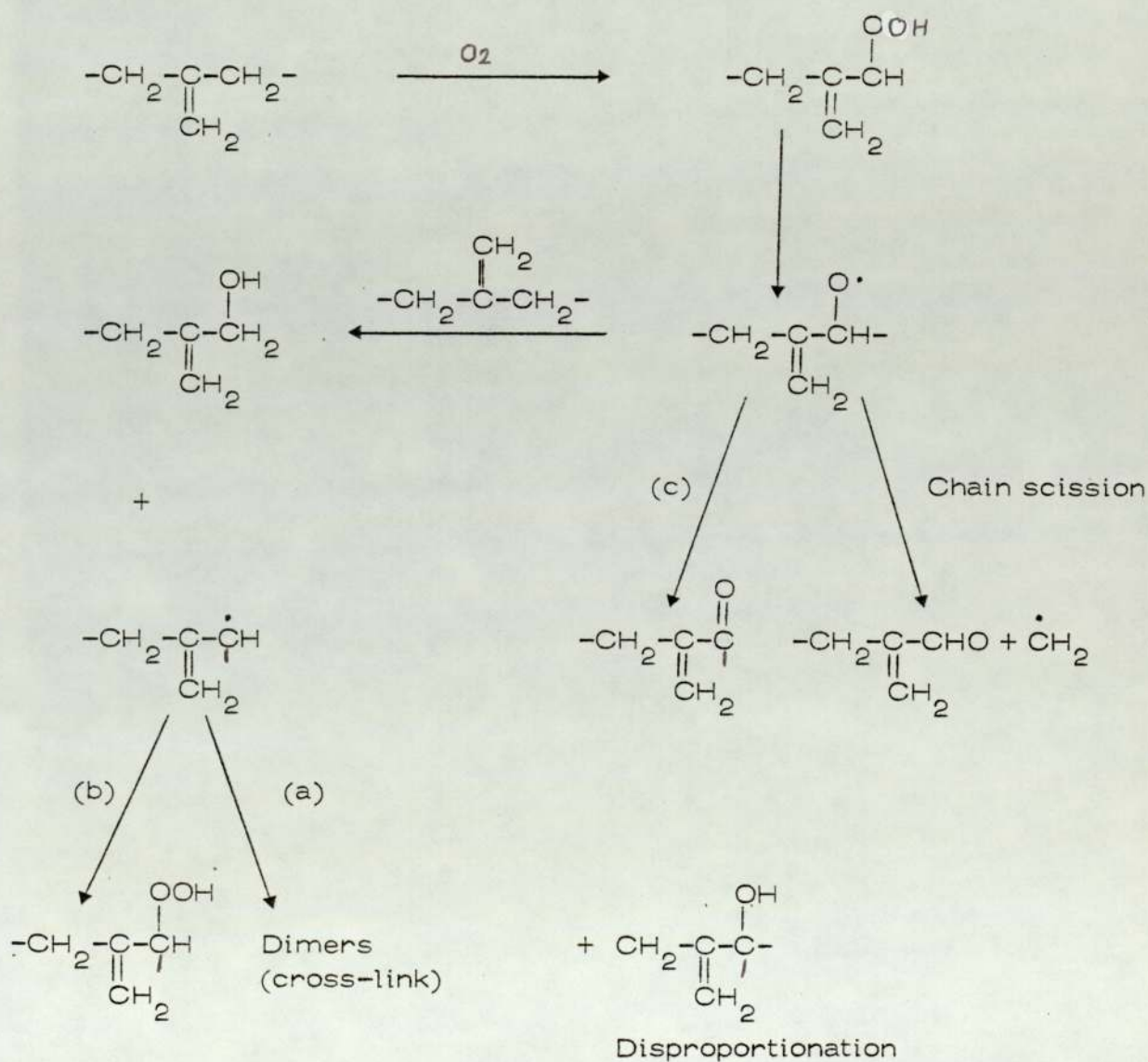


(Reproduced from K B Chakraborty Ph.D thesis 1977)

closed chamber. This increase in molecular weight and the formation of solvent insoluble gel under conditions of limited oxygen supply (closed chamber) can probably be related to the similar cross-linking reactions observed in the photo-oxidation of LDPE at ambient temperature⁽²⁰⁰⁾. It was previously suggested⁽⁶⁰⁾ that the cross-linking process must be intimately related to the changes in mechanical properties. The mechanical damping value of LDPE at 20°C changes rapidly during the early stages of processing (Fig 4.1, curve 3). It has been shown by Nielsen^(60b) that the damping above T_g is strongly dependent upon molecular weight (Chapter 1, Fig 1.6.1.4). The value of $\tan \delta$ in the region just above T_g decreases as the molecular weight increases (see Fig 1.6.1.4⁽¹¹²⁻¹¹⁵⁾). Conversely, hence cross-linking has a dramatic effect on dynamic mechanical properties above T_g ⁽¹⁰⁷⁻¹⁰⁸⁾ (Chapter 1). However it is a sensitive indication of cross-linking⁽¹⁰⁹⁻¹¹¹⁾. At temperatures well above T_g , damping decreases with increasing cross-linking. Vulcanised rubber is typical of materials having a relatively low degree of cross-linking and the measurement of the damping of vulcanised rubber is a rapid method of determining cross-linking⁽⁶⁰⁾. Decreasing $\tan \delta$ is therefore related to the cross-linking of LDPE during processing (Fig 4.1, curve 3). A similar decrease in $\tan \delta$ is observed in the rubber modified polymers^(201,209) and in PVC^(210,119), both of which contain significant amounts of cross-linking. Initial cross-linking during thermal oxidation of LDPE has also been observed by Turi and his coworkers⁽²¹¹⁾ as indicated by an initial increase in elongation at break and tensile strength and by Gan and Scott⁽²¹²⁾ in the initial formation of gel. Changes in MFI (Fig 4.4, curves 1, 2) also reflect the cross-linking reaction occurring in continuously

processed and reprocessed LDPE for the same length of time. The difference between the two is that the reprocessed polymer has been subjected to greater oxygen contact and it has been shown previously⁽¹⁹⁸⁾ that the effect of oxygen is to reduce the extent of cross-linking during processing. It was also suggested by Scott and his co-workers^(198,123) that the addition of alkyl and alkoxy radicals to the double bonds could account for cross-linking through a dimerisation of allylic radicals (Scheme 1).

Scheme 1



This reaction will predominate in an oxygen deficient system until all the oxygen is used up whereas further hydroperoxide (followed by carbonyl formation and chain-scission) will occur when Scheme 1(b), 1(c) in the presence of excess oxygen.

The hydroperoxide measured by infra-red at 3555 cm^{-1} shows an increase during the reprocessing operation (Figs 4.2 and 4.3) and acts as a powerful initiator when the polymer is subsequently subjected to uv light. Fig 4.3 shows a linear relationship between chemically measured hydroperoxide and the infra-red absorbance at 3555 cm^{-1} .

4.5 Processing of commercially stabilised polyethylene

The primary purpose of the present study is to simulate the effect of repeated processing on polyethylene in order to determine the effect of recycling operation on the behaviour of such polymers. Most commercial polymers contain small amount of antioxidants added during manufacture and it is important to examine commercially available stabilised products. In Fig 4.17 is shown the change with irradiation produced in the spectrum of polyethylene film without any additive. The three regions in the spectrum, viz $3500 - 3000\text{ cm}^{-1}$, $1850-1600\text{ cm}^{-1}$ and $1200-850\text{ cm}^{-1}$ where the changes were found to be most pronounced, have been related broadly to the absorption frequencies associated with O-H stretching vibration in carbonyl oxidation products and C-H bending or deformation modes in olefinic compounds respectively. The band at 3380 cm^{-1} which is typical of hydrogen bonded alcohol and hydroperoxide groups was initially present in the polymer but of weak intensity and as

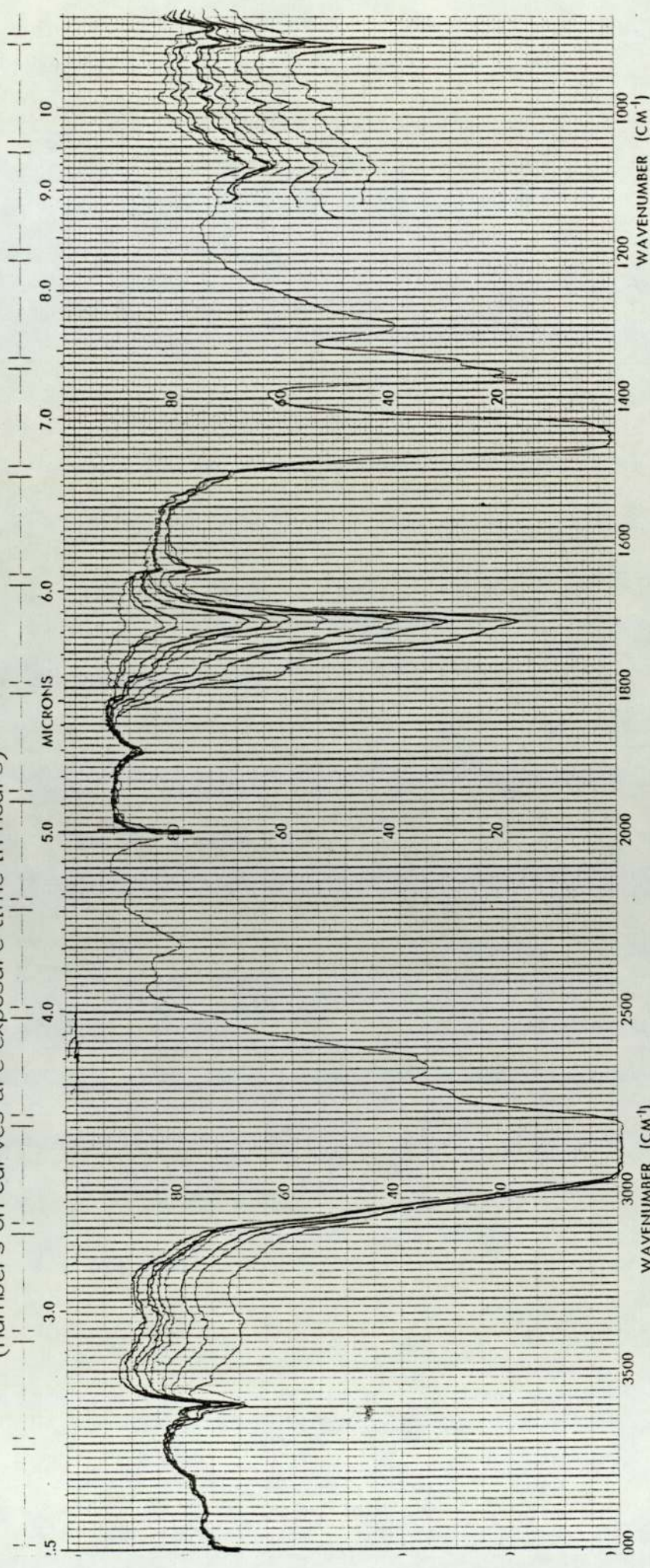
the reaction progressed, the intensity of absorption around 3400 cm^{-1} frequency increased gradually and finally became much more broad indicating formation of more hydroxyl compounds as a result of photo-oxidation. The determination of the nature of the hydroxyl group was very difficult by ir because of various overlapping hydroxyl group bands. It is generally accepted that the rate of hydroxyl group production is however, much slower as compared to carbonyl formation⁽¹⁸⁸⁾. No free hydroperoxide groups (at 3555 cm^{-1}) were detected by ir methods although such groups were detected in thermally oxidised film (Fig 4.2. B). This may be as suggested by Winslow⁽²¹³⁾ because hydroperoxides photolyse more rapidly than they are formed in polyethylene. This does not mean that all hydroperoxides are removed from the system but that their concentration is low to be detected by the ir method. This has been confirmed by Chakraborty and Scott⁽²⁸⁹⁾ who found that thermally induced hydroperoxide disappeared rapidly from LDPE during uv irradiation.

In the carbonyl region ($1800\text{--}1680\text{ cm}^{-1}$), photo-oxidised polyethylene showed a complex absorption with a large number of bands. The intensity of which increased with exposure time. Each of these bands was due to a different type of carbonyl compounds formed during photo-oxidation (Table 4). During prolonged irradiation the absorption peaks were dominated by doublets at 1710 and 1730 cm^{-1} (due to acid and aldehyde respectively). The formation of acid in highly photo-oxidised film was further substantiated by the occurrence of another band at 1185 cm^{-1} which was accounted for by the single bonded (C-O) vibration within the carboxyl group. In the later stages of photo-oxidation, the

absorption due to the carboxylic group predominated, indicating the formation of this species as one of the major oxidation products in the uv degradation of LDPE. Other carbonyl compounds such as peracid (1785 cm^{-1}) (Fig 4.17), perester (1763 cm^{-1}) and conjugated carbonyl (1690 cm^{-1}) were also found as shoulders in the main peak (Fig 4.17). Another major effect of uv irradiation on polyethylene was observed in the region $1650\text{--}800\text{ cm}^{-1}$ corresponding to different types of olefinic unsaturation. These groups, viz vinyl (910 cm^{-1}), vinylidene (890 cm^{-1}) and internal double bond (1645 cm^{-1}) have been shown to be present in the polymer as impurities. Cross et al⁽¹⁹⁰⁾ have shown a markedly different behaviour of carbon-carbon unsaturation in polyethylene during photo-oxidation compared with that during heat oxidation. In the present work, relative changes in absorption due to various olefinic double bonds was also used as a measure of changes caused by photo-oxidation and the results obtained were consistent with previous work⁽²¹⁴⁾. In summary, vinylidene group concentration decreases gradually where as both vinyl unsaturation and internal double bond increase during irradiation. These results are shown in Fig 4.5, 4.6 and 4.7.

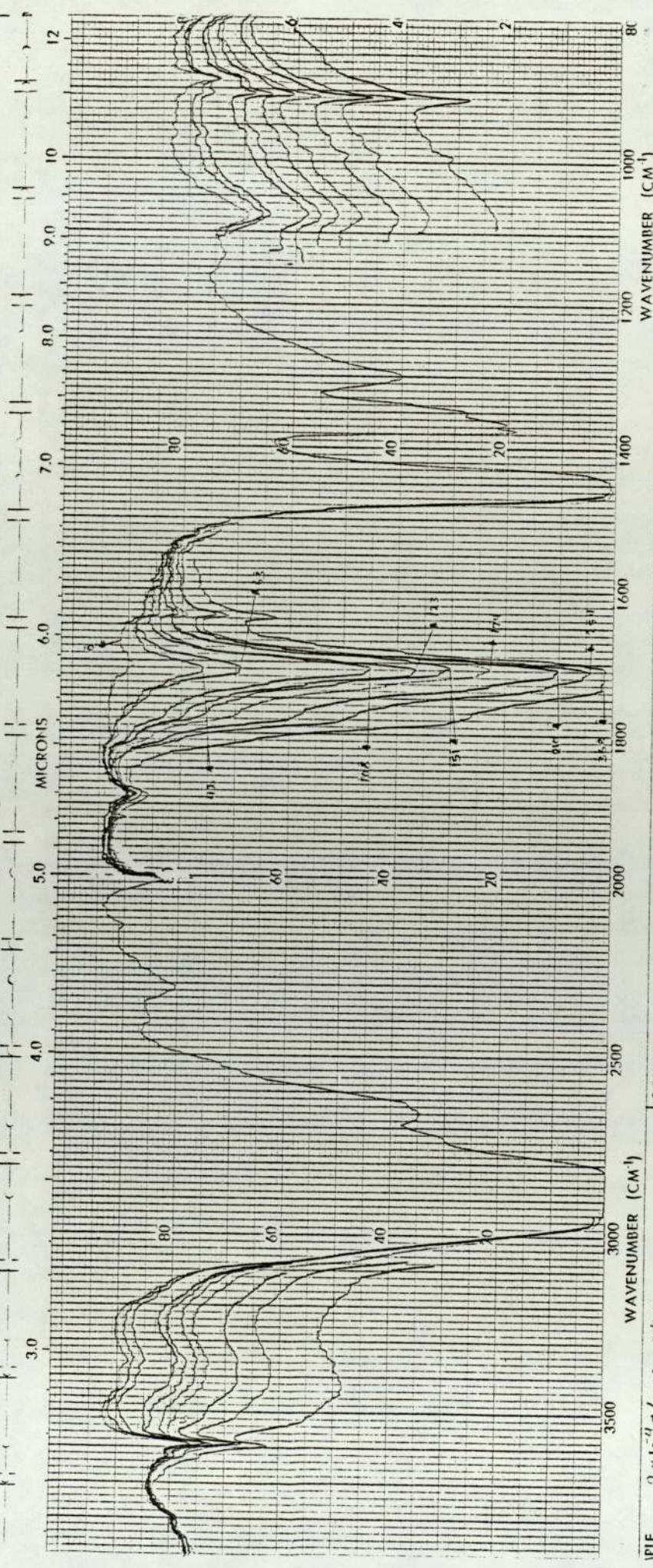
Figs 4.18 and 4.19 show the general change in the ir spectra of commercial LDPE films containing ferric stearate during uv exposure. The overall absorption pattern was the same as in the control film, but the rate of development of oxidation products functional groups was strongly influenced by the addition of activators. The common transition metal ions are, however, likely contaminants during processing and particularly reprocessing operations due to inadequate removal from waste plastics. The effect of a typical pro-oxidant transition metal

Fig 4.18 Infra-red spectra of photo-oxidised LDPE film containing 2×10^{-5} mol/100 g Ferric Stearate (FéSt) (numbers on curves are exposure time in hours)



SCAN	SUIT	No 45
REMARKS		
SAMPLE	2 x 10 ⁻⁵ / 100 g - polyene FéSt / 1cc/8t	SOLVENT
ORIGIN		CONCENTRATION
		CELL PATH
		REFERENCE

Fig 4.19 Infra-red spectra of photo-oxidised LDPE film containing 2×10^{-4} mol/100 g Ferric Stearate (FeSt) (numbers on curves are exposure time in hours)



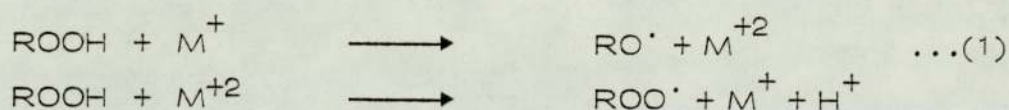
SAMPLE 2×10^{-4} mol/100g Ferric Stearate
 SOLVENT _____
 CONCENTRATION _____
 CELL PATH _____
 REFERENCE _____

WAVENUMBER (cm^{-1})
 MICRONS
 WAVENUMBER (cm^{-1})

SCAN SPEED _____
 SLIT _____
 No 457-500

REMARKS

ions complex on the uv stability of LDPE and polypropylene (see Chapter 5) are shown in Figs 4.17 - 4.19 and Fig 4.13. It is clear that ferric stearate has a catastrophic effect on the uv stability of such polymers. Copper, manganese, cobalt and iron are particularly powerful thermal pro-oxidants in the form of soluble salts on metal complexes and their effect is to catalyse the breakdown of hydroperoxides to free radicals (see equation 1).



The overall reaction is identical to normal thermal breakdown but it occurs much more rapidly, effectively removing the induction period (Fig 4.13). Ferric ions also powerfully catalyse this process which partially explains their uv pro-oxidant effect. However, a direct photolysis (equation 2) of the ferric salt also seems to be involved in the photo-pro-oxidant effect⁽¹⁴⁸⁾.



The removal of the induction period by addition of FeSt has the same effect on the mechanical properties. If samples of polymer containing varying amounts of ferric stearate (2×10^{-4} and 2×10^{-5} mol/100 grm polymer) are exposed to photo-oxidation it is found that the rate of decay of mechanical properties is related to the concentration of ferric stearate (Figs 4.11 and 4.9).

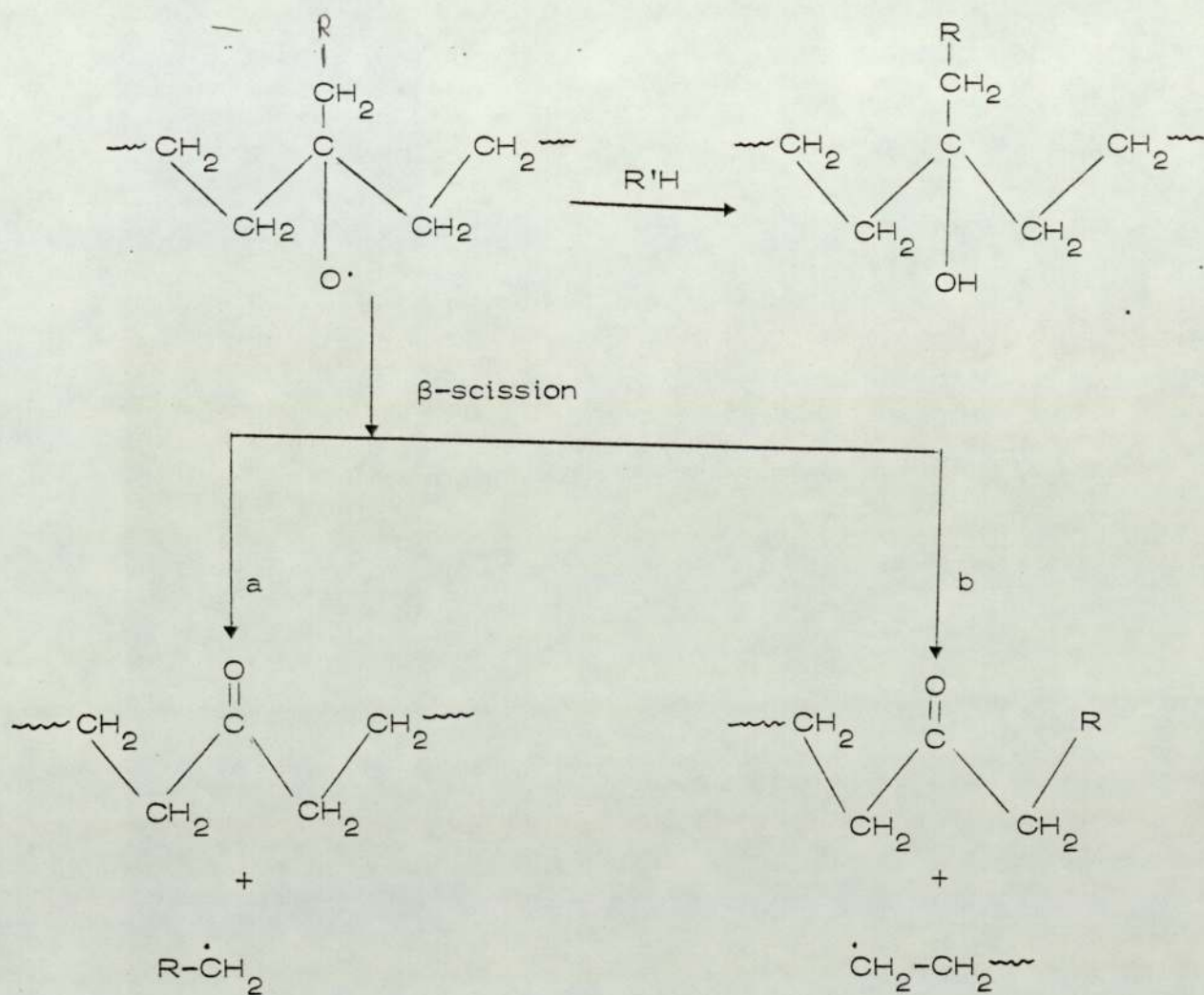
4.6 Relation between mechanical properties and polymer morphology

It is evident from Chapter 1 that mechanical properties are intimately related to the crystallinity and morphology of the polymer. Nielsen⁽⁶⁰⁾ has established a good correlation between the modulus of a series of polyethylenes having different crystallinity and the specific volume of the polymer at the same temperature and has shown that modulus is directly proportional to crystallinity; that is, the greater the crystallinity, the higher is the modulus. In the present case, it is found that photo-oxidation resulted in an increase in dynamic modulus. The rate of such increase in modulus however was greatly influenced by the presence of an activator in the polymer sample and differed with different concentrations used. The increase in the modulus in LDPE during uv irradiation may be correlated with an increase in crystallinity of the polymer. Surprisingly it was also observed that prior to attaining a steady rate of increase in modulus, there was an initial drop in modulus. This is attributed to the fact that pro-oxidant of polyethylene proceeds through a competition between cross-linking and chain-scission⁽¹⁹⁸⁾ and during the initial exposure time, it seems possible that cross-linking predominates. The initial cross-linking during uv irradiation of LDPE has been observed by other workers^(215,211).

An additional explanation for the initial drop in modulus due to cross-linking is as follows. Polyethylene is a typical semi-crystalline polymer, made up of small regions of ordered structures. It is generally accepted that photo-oxidative degradation primarily starts in the amorphous region where the

diffusion of oxygen is easier than in the crystalline region . For a high modulus polymer, deformation occurs by the movement of segments of a chain when the stress is applied. For a segment to move, it must have free volume to move into and this will in turn depend on the degree of packing of the molecules. For lightly cross-linked material (as it occurs in the amorphous region of LDPE during photo-oxidation) there is still enough free volume for segmental rotation and consequently deformation will be longer for a small applied stress and thereby the modulus should be low. For highly cross-linked material, however, there will be an increase in modulus since network structure will resist segmental rotation. Jenkins⁽²¹⁶⁾ also reported an initial decrease in modulus during gamma irradiation of silicone and bipolar elastomers before a steady rate of cross-linking was obtained (when the modulus increased).

As the irradiation time is increased the modulus should rapidly increase due to secondary crystallisation. This process which is sometimes referred to as chemi-crystallisation is a result of predominant chain scission in the amorphous phase leading to realignment of the chains into crystalline structures. It has been shown that⁽²⁰⁶⁾ crystallinity in polyethylene greatly depends on chain branching. Since bulky side groups inhibit the close packing of molecules, they therefore reduce the crystallinity and hence density of the polymer. The photo-oxidation of LDPE is found to be accompanied by a reduction in chain branching (see below)⁽¹²³⁾ which is favourable for close packing of molecules and gives rise to high density and crystallinity.



Another factor influencing crystallinity is the mobility of the chain segments. Short chain segments or repeating units of high symmetry formed through photo-oxidative chain scission permit the chain to align themselves more readily than long chain repeating units of low symmetry.

The mechanical damping ($\tan \delta$) (20°C) of low density polyethylene shows appreciable change during early stages of irradiation (Fig 4.14). After prolonged exposure, however, the damping

values passed through a maximum as the embrittlement time was approached. Damping finally fall off after embrittlement. In polyethylene samples containing ferric stearate, damping attained a maximum value before the control, the maxima appeared earlier with increasing concentration of ferric stearate in LDPE.

Scott et al⁽²⁰⁰⁾ found an increase in % elongation at break up to 200 hours of uv irradiation with an associated initial drop in modulus for metal ion sensitised uv degradation of LDPE. This was much higher than that of commercial LDPE and it appears that cross-linking may not be very important for commercial LDPE. In commercially stabilised polymers, change in crystallinity and molecular weight seem to be important factors during uv irradiation. The mechanical damping behaviour of crystalline polymers is generally more complex than that of amorphous polymers⁽⁶⁰⁾. Since the damping is due primarily to the amorphous phase, the damping above Tg is strongly dependent on molecular weight. The value of the damping above Tg decreases as the molecular weight increases⁽⁶⁰⁾ (see Fig 1.6.14 in Chapter 1).

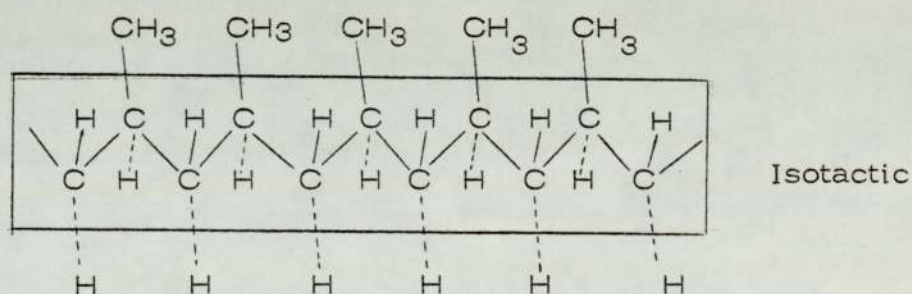
CHAPTER FIVE

EFFECT OF REPROCESSING ON THERMAL AND PHOTO-OXIDATION STABILITY OF POLYPROPYLENE (PP)

5.1 Introduction

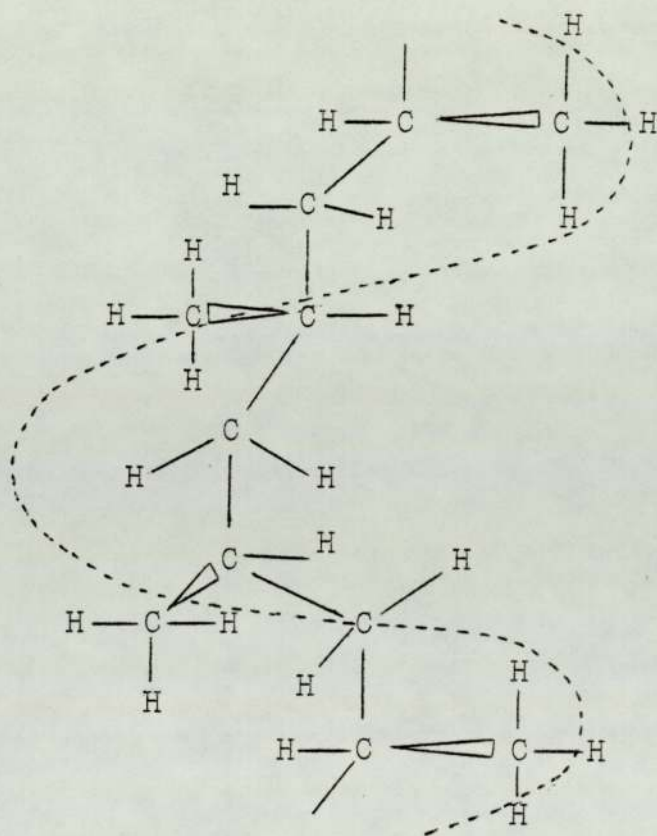
Polypropylene has found wide commercial application in the form of fibres and films, despite the problem of thermal and photo-oxidative instability associated with this polymer. A partial solution of these problems has been achieved by the development of ultraviolet (uv) stabilisers and antioxidant systems for use with polypropylene^(199,217).

The crystalline phase has been shown to be mostly isotactic whereas the amorphous phase is considered to be mostly atactic. Isotactic polypropylene has the following structure:



Both the isotactic and syndiotactic forms of the polymer are easily crystallised. The alternating CH₃- groups in the syndiotactic polymer can be easily packed together in the planar zig-zag crystal form typical of polyethylene. In the case of the isotactic form, the polymer molecules in the crystal take the form of a helix, as shown in Fig 5.1.1. This staggers the CH₃- side groups and allows the chains to pack

Fig 5.1.1 Helical packing of isotactic polypropylene chain in the crystal (196)

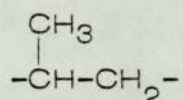


together without strain. It can be seen that there is one complete turn of the helix for every three monomer units. In atactic polypropylene because of the random arrangement of the CH_3 side groups, the chains cannot pack together closely and so it is non-crystalline.

The last five years have seen steady advances in polypropylene technology. This has been encouraged by the increasing competitiveness of isotactic polypropylene compared with polyethylene and PVC in that the price of polypropylene on a weight basis is now only just above that of polyethylene. Isotactic polypropylene competes on almost level terms in injection moulding and film applications and has considerable advantages in fibre applications⁽²¹⁸⁾. As far as blow moulding is concerned, polypropylene is still less easy to process than polyethylene, but it has the advantages of higher temperature stability (for hot fill applications), higher clarity and the absence of stress cracking. Polypropylene is more susceptible to oxidation than polyethylene due to the presence of labile hydrogens on the tertiary carbon in each repeating unit^(128, 197).

The infra-red spectra of oxidised isotactic polypropylene have been studied thoroughly by a number of workers⁽²¹⁹⁻²²⁴⁾. Many bands in the infra-red spectra, eg 1450, 1370, 1171, 975 and 890 cm^{-1} were found to be nearly independent of the temperature. Bands whose intensity decreased at higher temperatures were found at 1330, 1305, 1220, 1105, 995, 846 and 810 cm^{-1} . In view of the sharp drop of these intensities in the melting region of the polymer, and from a comparison of the spectra of crystalline and fully amorphous polypropylene,

it was concluded that the temperature sensitive bands are connected with the crystalline domains^(221,224). Blais and Carlsson have shown surface restructuring during photo-oxidation of polypropylene films⁽²²⁵⁾. The 977/974 cm^{-1} absorbance ratio of the film surface was found to increase steadily during uv degradation and was related to an increase in helical ordering resulting from backbone scission during irradiation⁽²²⁵⁾. This was also shown by an increase in density. The 974 cm^{-1} absorbance is due to the CH_3 unit⁽²²⁶⁾,



and the ratio 997 cm^{-1} /974 cm^{-1} is a measure of the isotactic content of the polymer which is in turn related to percentage crystallinity of the polymer^(224,227). The increase in crystallinity is expected to be greatest in areas of extensive photo-oxidation such as film surfaces⁽²²⁵⁾. This was confirmed by the data where 977/974 cm^{-1} ratio at the surface approached a maximum with increasing exposure time and the same ratio acquired a constant value towards the interior of the film⁽²²⁵⁾.

5.2 Experimental

Unstabilised polypropylene was processed at 180°C in the RAPRA torque rheometer in a closed chamber for 5 minutes. The polymers were then compression moulded at 180°C for 2 minutes on photographic glazing plates of thickness 0.015 ± 0.001 cm. Reprocessing was carried out on chopped up film under similar conditions to the initial processing. This was

carried out four times for each polymer and reprocessed samples were indicated as number 2, number 3, number 4; number 0 and number 1 were compression moulded and initially processed samples respectively.

Infra-red examination of the processed and subsequent photo-oxidised films were carried out using 457 and 599 Perkin Elmer spectrophotometer. The rate of photo-oxidation was measured by the following carbonyl index⁽¹⁵⁰⁾:

$$\text{expressed as } A_{1710}/A_{905} \text{ cm}^{-1}$$

and the hydroperoxide content of the processed and reprocessed samples were measured chemically (see Chapter 3).

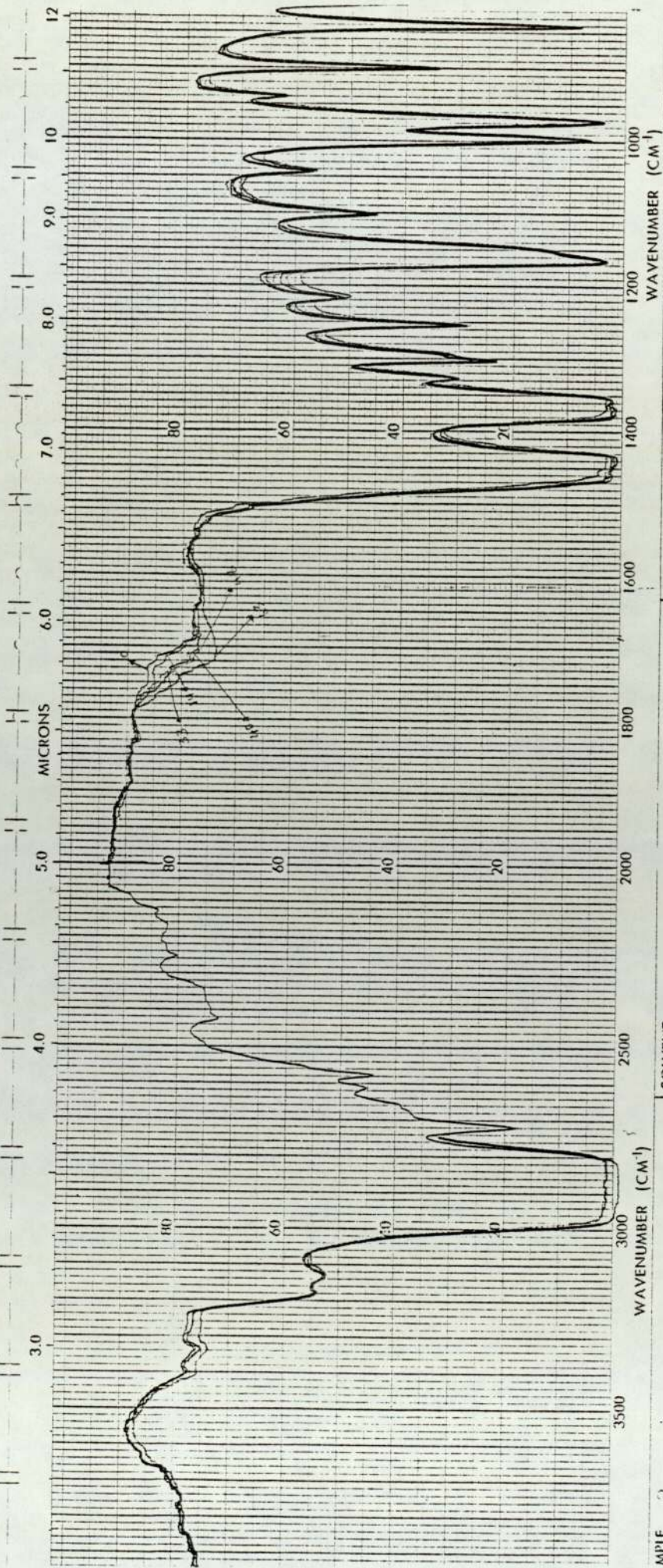
The deterioration of physical properties was followed by measuring the stress-strain parameters as a function of exposure time. The tensile tests were carried out on an Instron Tensile Tester (see Chapter 3) using cross-head 2 and chart speed 5 cm per minute at $22 \pm 1^{\circ}\text{C}$.

The dynamic mechanical tests were carried out using the Rheovibron (Chapter 3). The tests were carried out at room temperature ($20 \pm 1^{\circ}\text{C}$) and at a frequency of 110 Hz.

5.3 Results

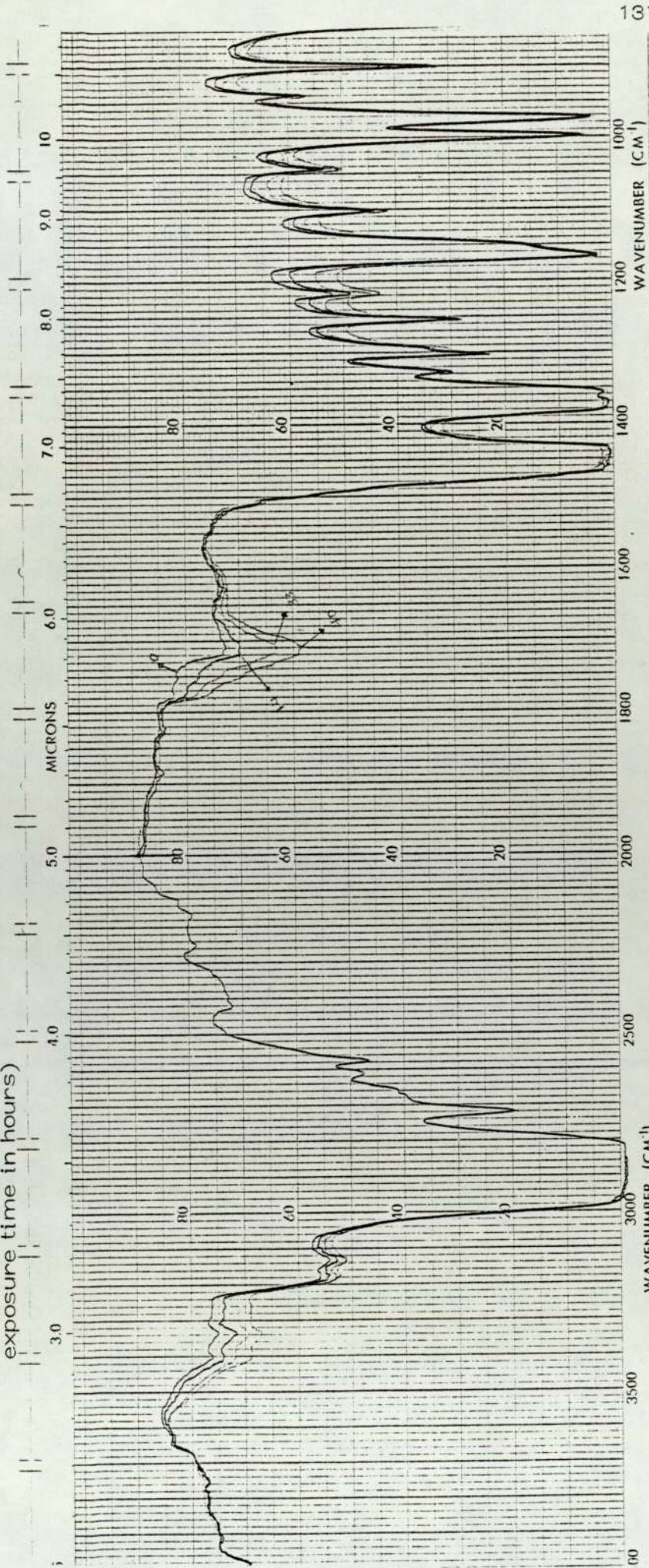
The ir spectra from processed and reprocessed samples of polypropylene are shown in Figs 5.1 and 5.2. The first point of interest is the $4000\text{--}3000 \text{ cm}^{-1}$, OH stretching region of the

Fig 5.1 Infra-red spectra of photo-oxidised unstabilised polypropylene (PP) (numbers on curves are exposure time in hours)



SAMPLE Photo-oxidized PP SOLVENT _____ REMARKS _____
 No. 1 CONCENTRATION _____ _____
 CELL PATH _____ _____
 REFERENCE _____ _____
 SCAN SPEED _____ No. 457-51
 SLIT _____

Fig 5.2 Infra-red spectra of photo-oxidised unstabilised polypropylene (PP) (numbers on curves are exposure time in hours)



SAMPLE	Representative of PP			SCAN #	SIIT
	SOLVENT	CONCENTRATION	CELL PATH	REMARKS	
ORIGIN	No. 4			No 457	

spectrum. A broad band from $3500\text{--}3300\text{ cm}^{-1}$ with two peak heights at 3400 and 3350 cm^{-1} respectively was observed in the ir spectra (Figs 5.1 and 5.2). Both the peak heights continued to increase steadily with time of irradiation.

The carbonyl region, from 1850 to 1650 cm^{-1} is also shown in Figs 5.1 and 5.2. The carbonyl index at 1710 to 1715 cm^{-1} increased in an auto-accelerating mode as the number of reprocessing increased. The conjugated carbonyl shoulder band at 1685 cm^{-1} which was found to present initially in the unprocessed polymer, disappeared either on extended reprocessing or on uv irradiation (Figs 5.1 and 5.2).

Like low density polyethylene (Chapter 4), the main carbonyl band in photo-oxidised polypropylene has a number of shoulders indicating the presence of various carbonyl species. Although the typical -C=O bands due to aldehyde, esters and ketones were merged into a single broad band between 1715 and 1750 cm^{-1} , the band due to carboxylic acid near $1710\text{--}1715\text{ cm}^{-1}$ was quite distinct. This peak began to form almost from the beginning and remained the major carbonyl absorption during oxidation, showing carboxylic acid to be the major oxidation product of polypropylene. Adams⁽²²⁸⁾ also found various carbonyl products in photo-oxidised polypropylene and he calculated the concentration of various carbonyl products by infra-red spectroscopy and chemical reactions.

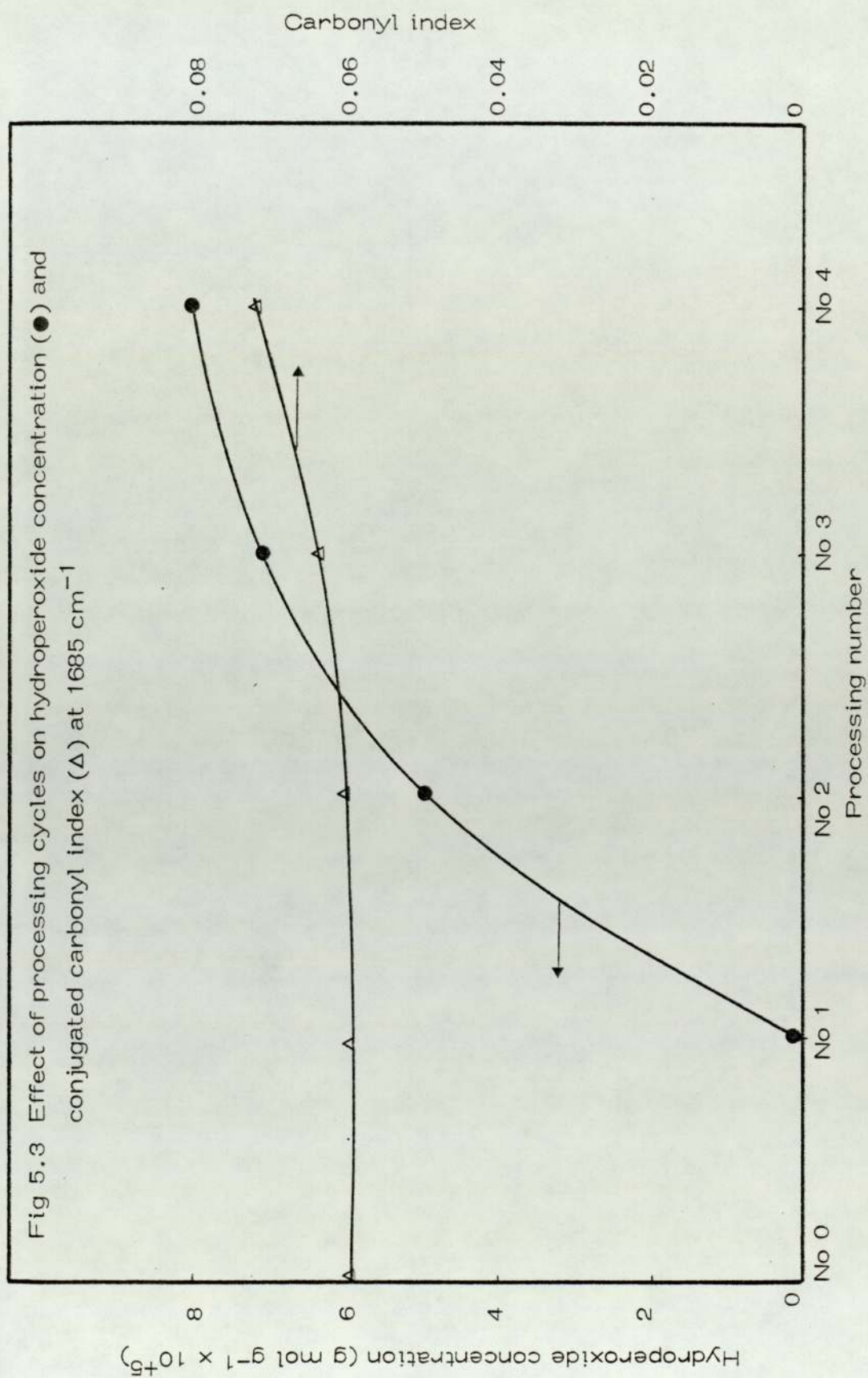
The infra-red spectra from oxidised and unoxidised polypropylene have not shown any bands for specific olefinic unsaturation. Bands at 964 cm^{-1} for ethylinic unsaturation, 910 cm^{-1} for vinyl and 888 cm^{-1} for pendant type unsaturation

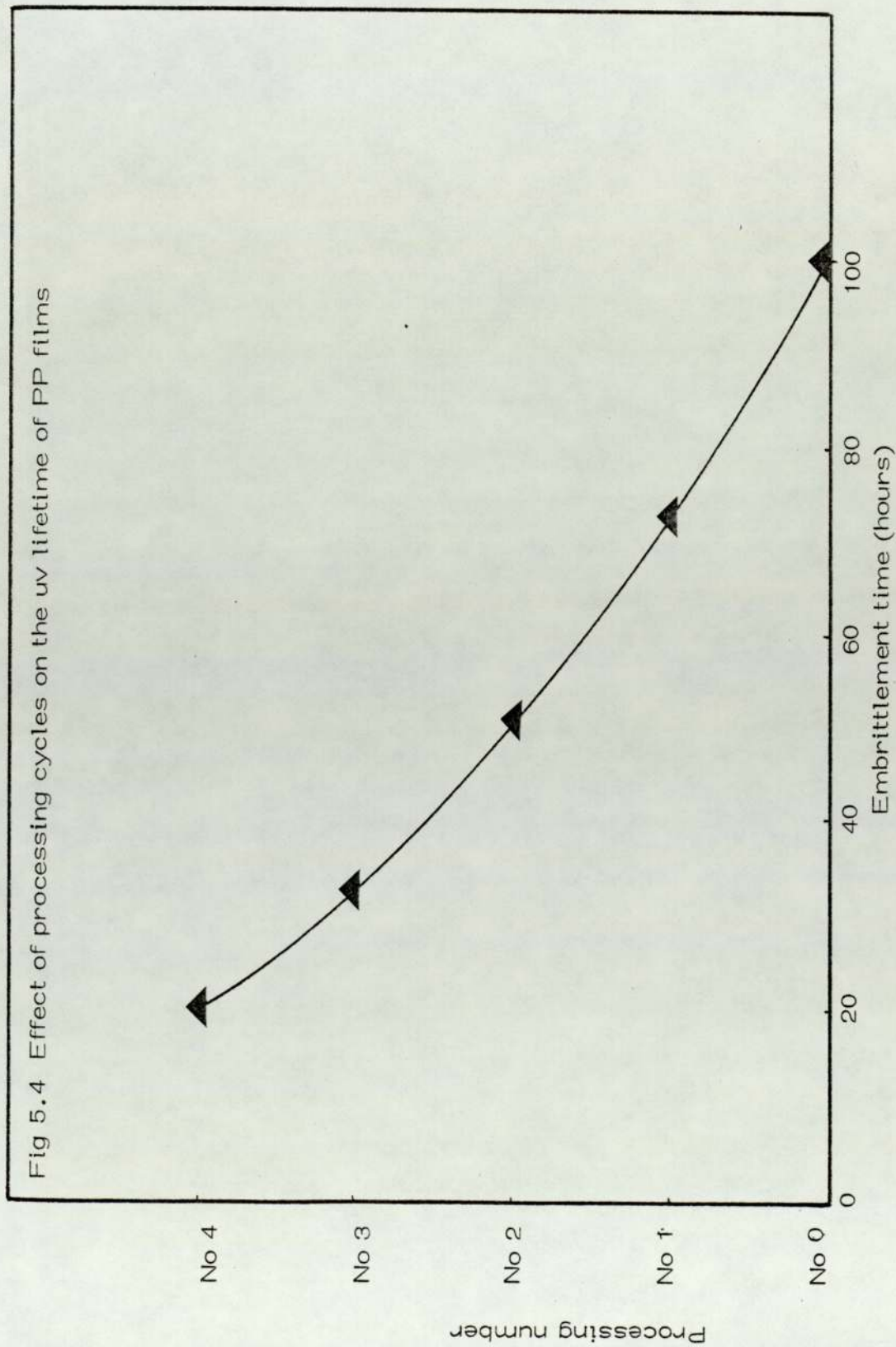
were not detected due to the presence of various bending or wagging bands of polypropylene itself in those regions. But a broad band at 1645 cm^{-1} indicated the presence of olefinic unsaturation in polypropylene (Figs 5.1 and 5.2). Moreover, the presence of conjugated carbonyl in unprocessed polypropylene also confirms the presence of unsaturation, although the nature of the unsaturation is not known.

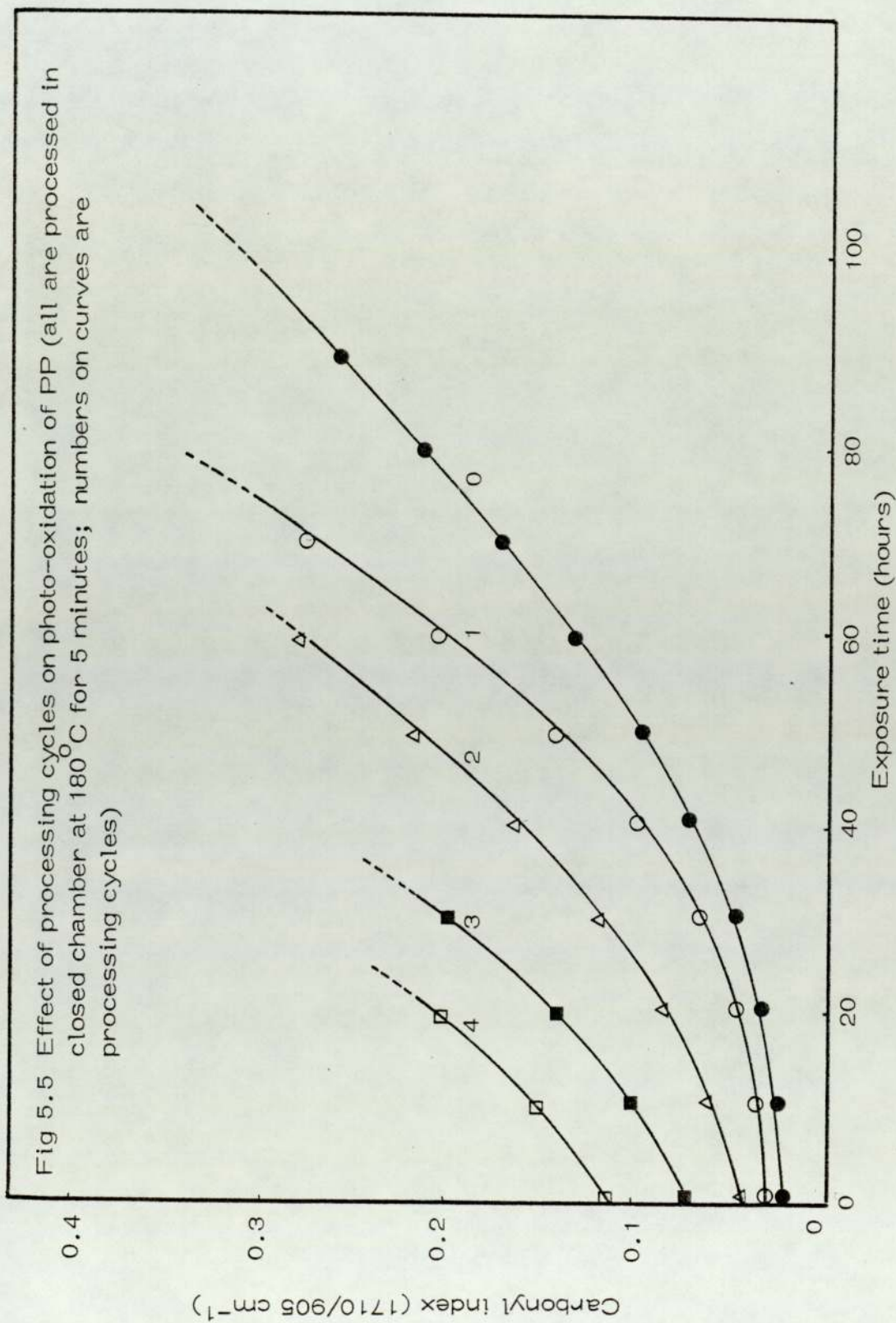
No band at 3555 cm^{-1} (due to non-hydrogen bonded hydroperoxide group) was observed either in photo-oxidised or thermally oxidised polypropylene film as was observed in thermally oxidised LDPE (Chapter 4 and Chapter 6). The absence of this peak from the polypropylene film spectra may be due to the presence of predominantly hydrogen bonded hydroperoxide. Chien⁽²²⁹⁾ has shown from the infra-red spectra of ethylene-propylene copolymer that about 70% of hydroperoxides are intramolecularly hydrogen bonded. The broad band in the hydroxyl region is probably due to hydrogen bonded alcohols and hydroperoxides.

The hydroperoxide concentration (measured chemically, see Chapter 3) showed an induction period up to the first processing and then rapidly increased with reprocessing (Fig 5.3). The shortest uv lifetime was observed at the highest hydroperoxide concentration for reprocessed polypropylene (Fig 5.4).

The rate of photo-oxidation was measured by following the carbonyl index at $1710\text{--}1715\text{ cm}^{-1}$, and Fig 5.5 shows that the rate of oxidation is highest for reprocessed samples, eg No 4, which had the highest initial hydroperoxide concentration (see Fig 5.3).

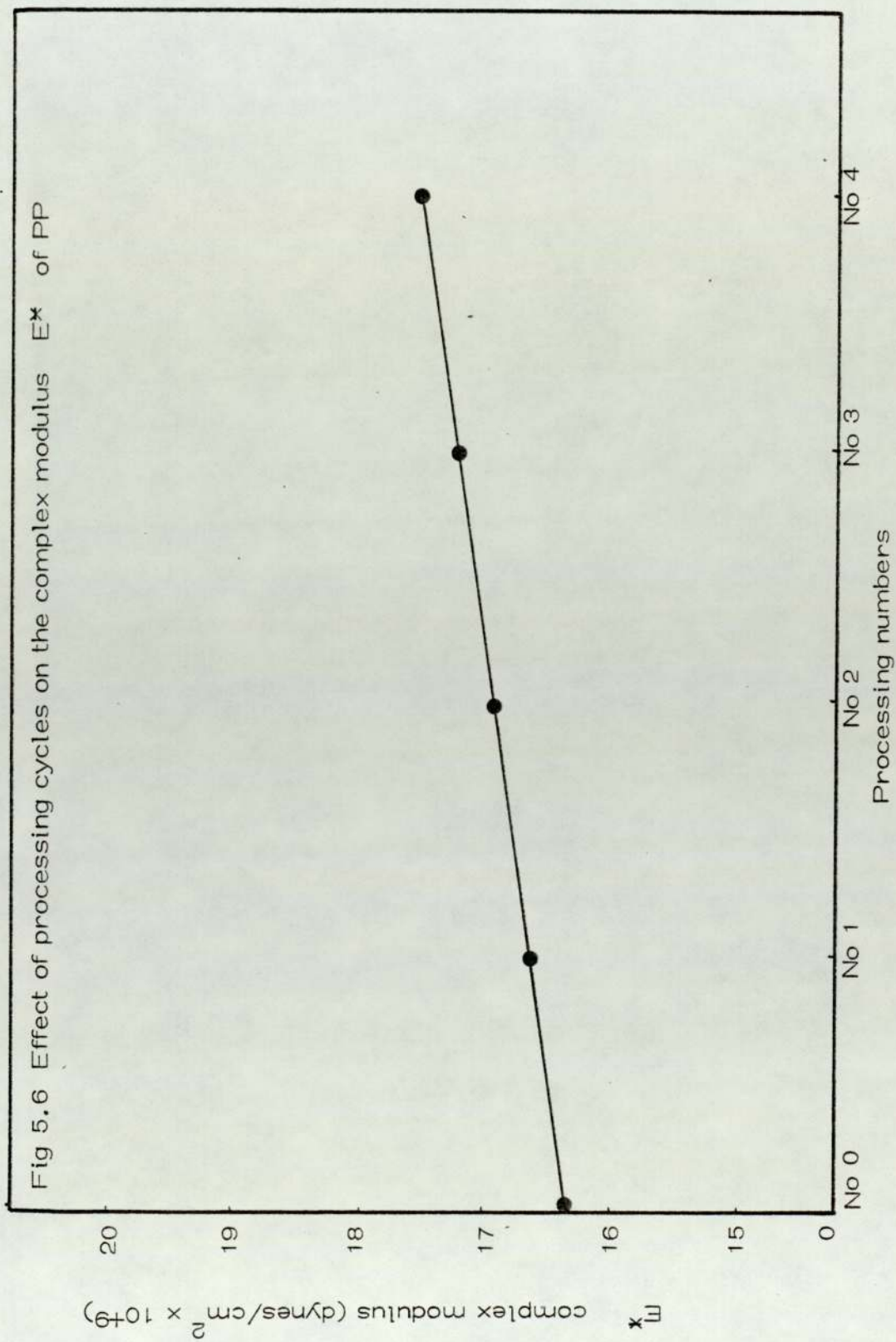


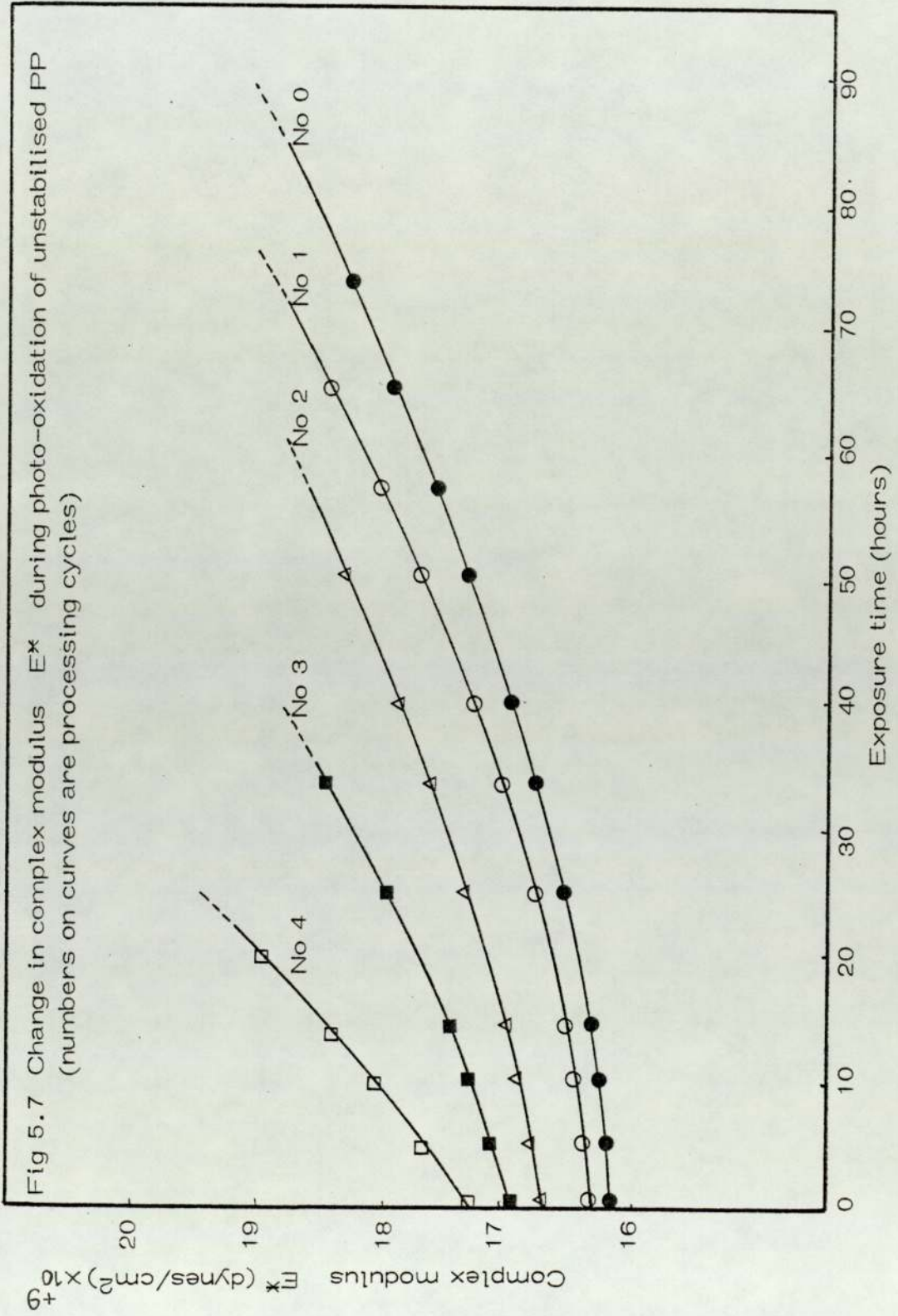


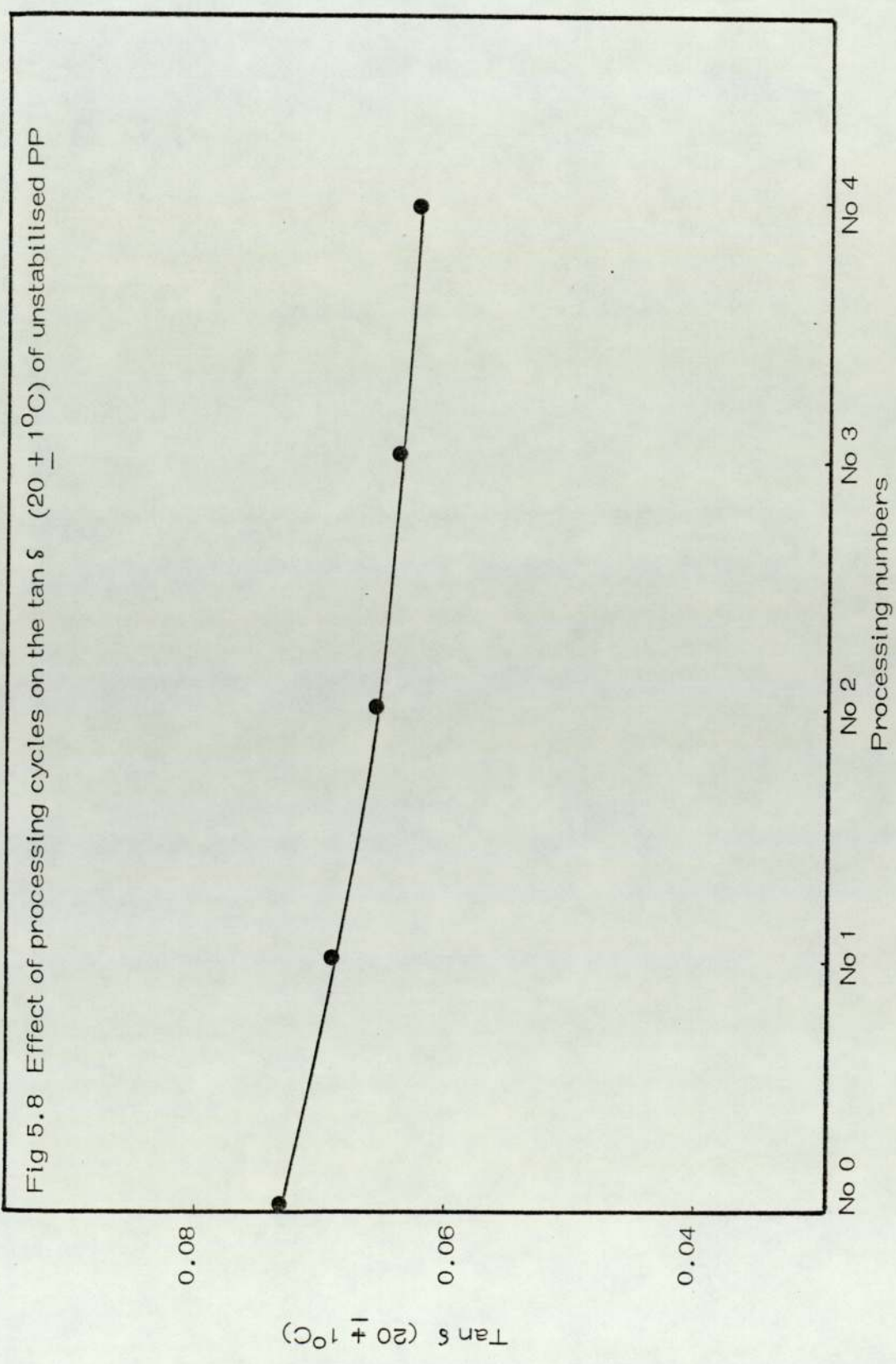


The deterioration of the mechanical properties of polypropylene with reprocessing has been followed by measuring complex modulus and $\tan \delta$ at $20 \pm 1^\circ\text{C}$. Figs 5.6 and 5.7 show that the complex modulus increases with the number of reprocessings and with exposure time. $\tan \delta$ (20°C) shows a related decreasing relationship for reprocessing and uv exposure time (Figs 5.8 and 5.9). A linear relationship between hydroperoxide concentration and complex modulus (Fig 5.10) of reprocessed polypropylene was also observed.

Figs 5.11 - 5.14 show the infra-red spectra of reprocessed polypropylene samples which were thermally oxidised for various times at 110 and 140°C in an oven (flow rate). In the carbonyl region ($1800 - 1600 \text{ cm}^{-1}$) (Figs 5.11 - 5.14), thermally oxidised polypropylene showed a complex absorption with a large number of bands, the intensities of which increased with heating time. Each of these bands was due to a different type of carbonyl compound formed during thermal oxidation in air. The initial weak carbonyl absorption in the unprocessed film was observed at $1710 - 1715 \text{ cm}^{-1}$. The growing carbonyl increased towards $1710 - 1715 \text{ cm}^{-1}$ (acid) with increasing heating time. This increase of carbonyl was faster for the samples at 140°C (Figs 5.14 and 5.15). Other carbonyl products were also observed as shoulders in the later stages of thermal oxidation. The shoulders on the main carbonyl band were identified as peracid (1780 cm^{-1}), perester (1760 cm^{-1}) and conjugated carbonyl ($1680 - 1685 \text{ cm}^{-1}$). Luongo⁽¹⁸⁷⁾ suggested that all oxygen containing groups formed are breakdown products of hydroperoxide. Fig 5.15 shows the formation of carbonyl in polypropylene film which has been reprocessed. The heavily reprocessed samples, No 4, and







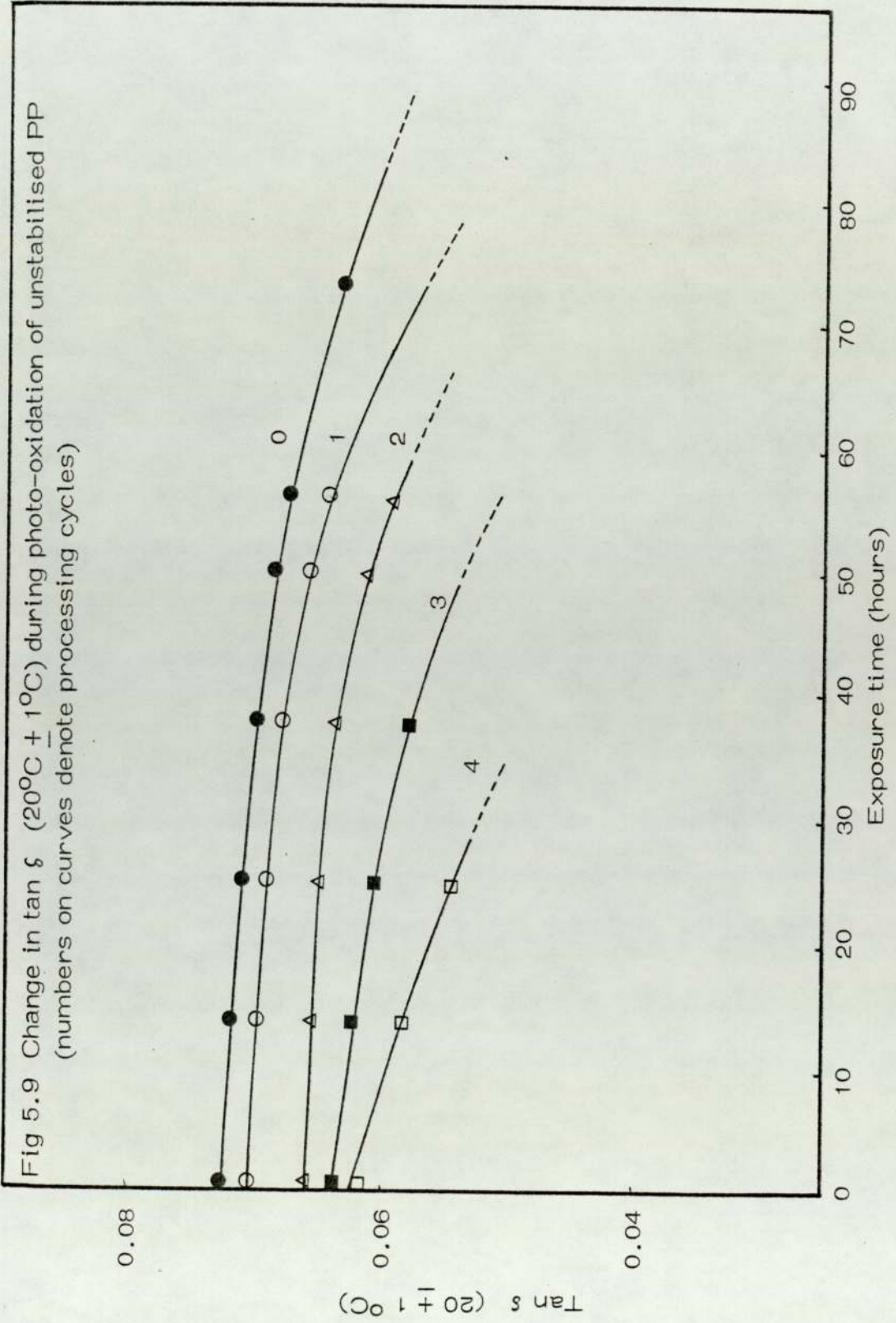


Fig 5.10 Relationship between hydroperoxide concentration and complex modulus E^* in unstabilised polypropylene

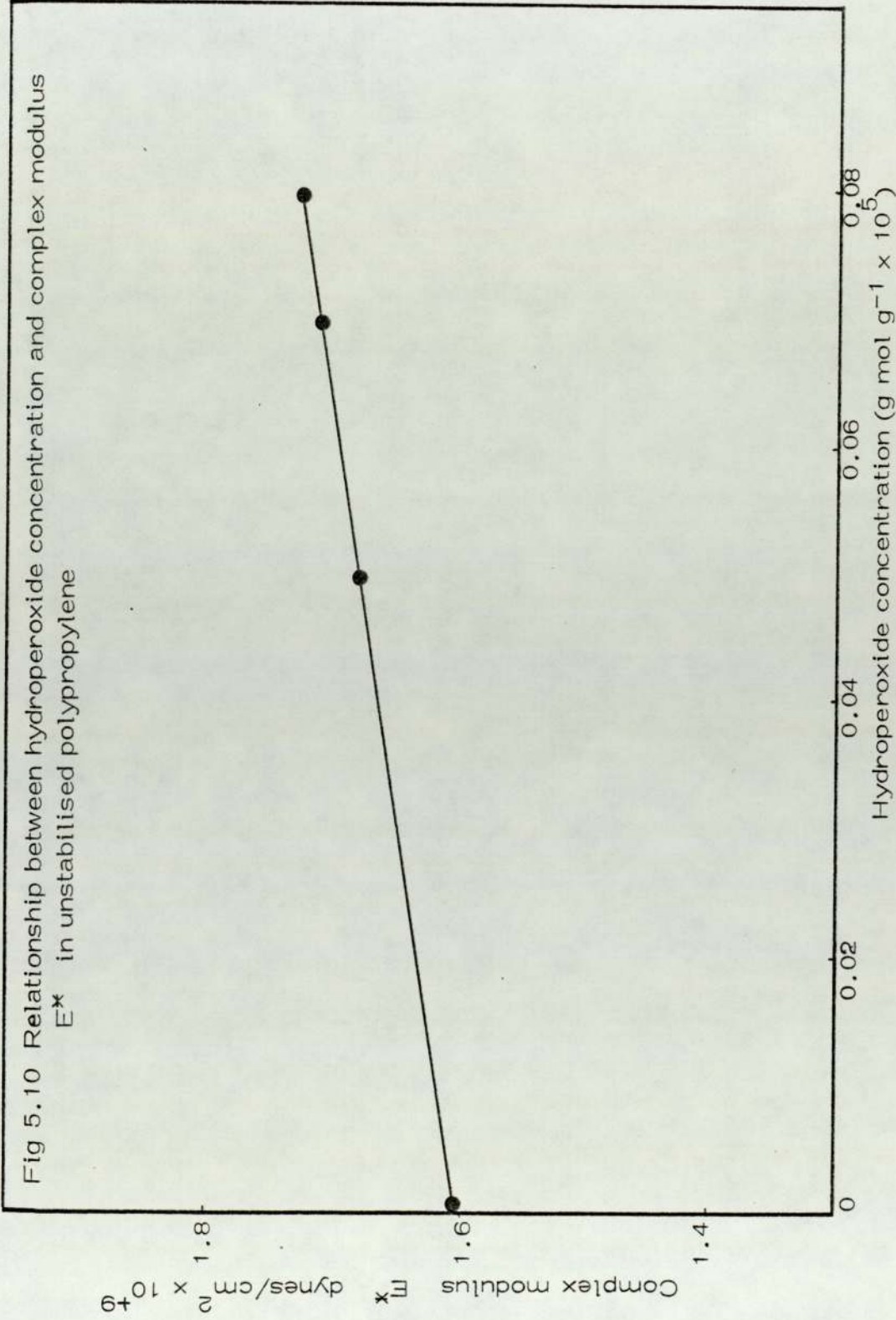
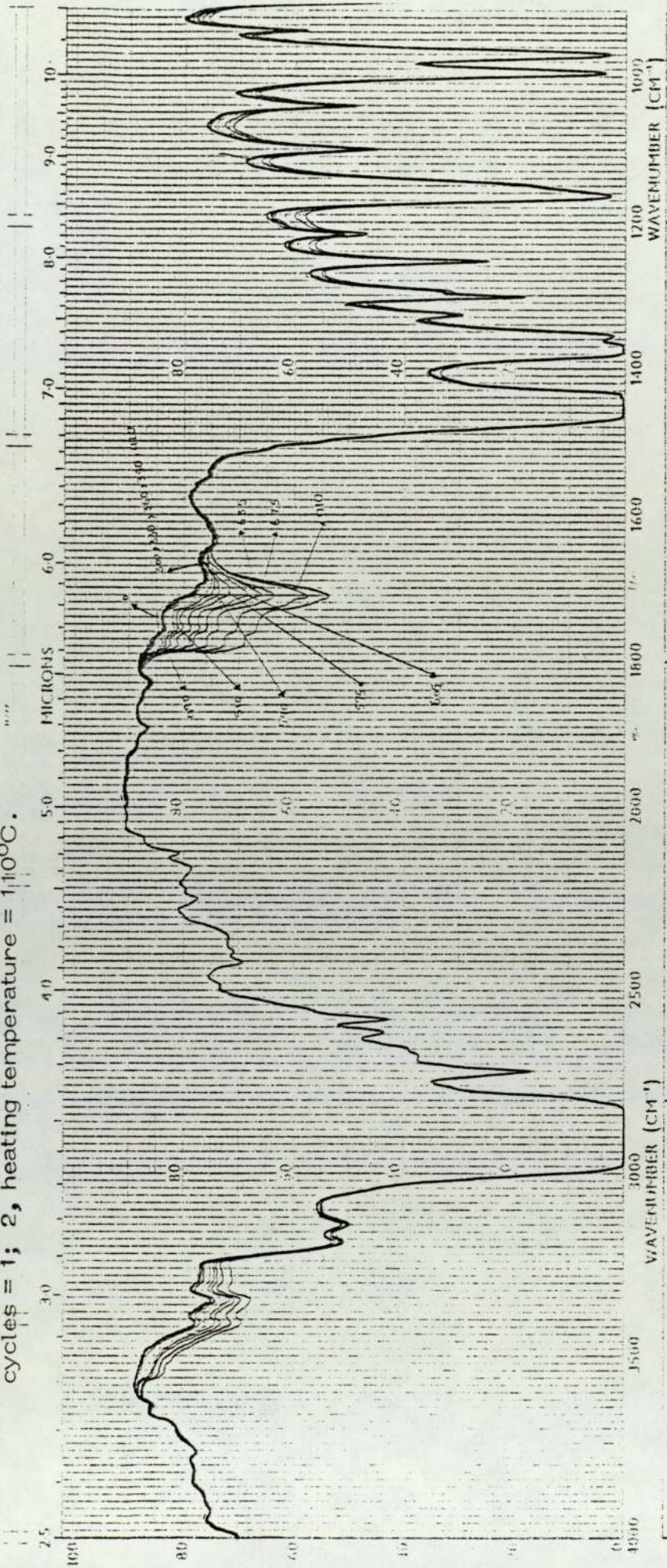


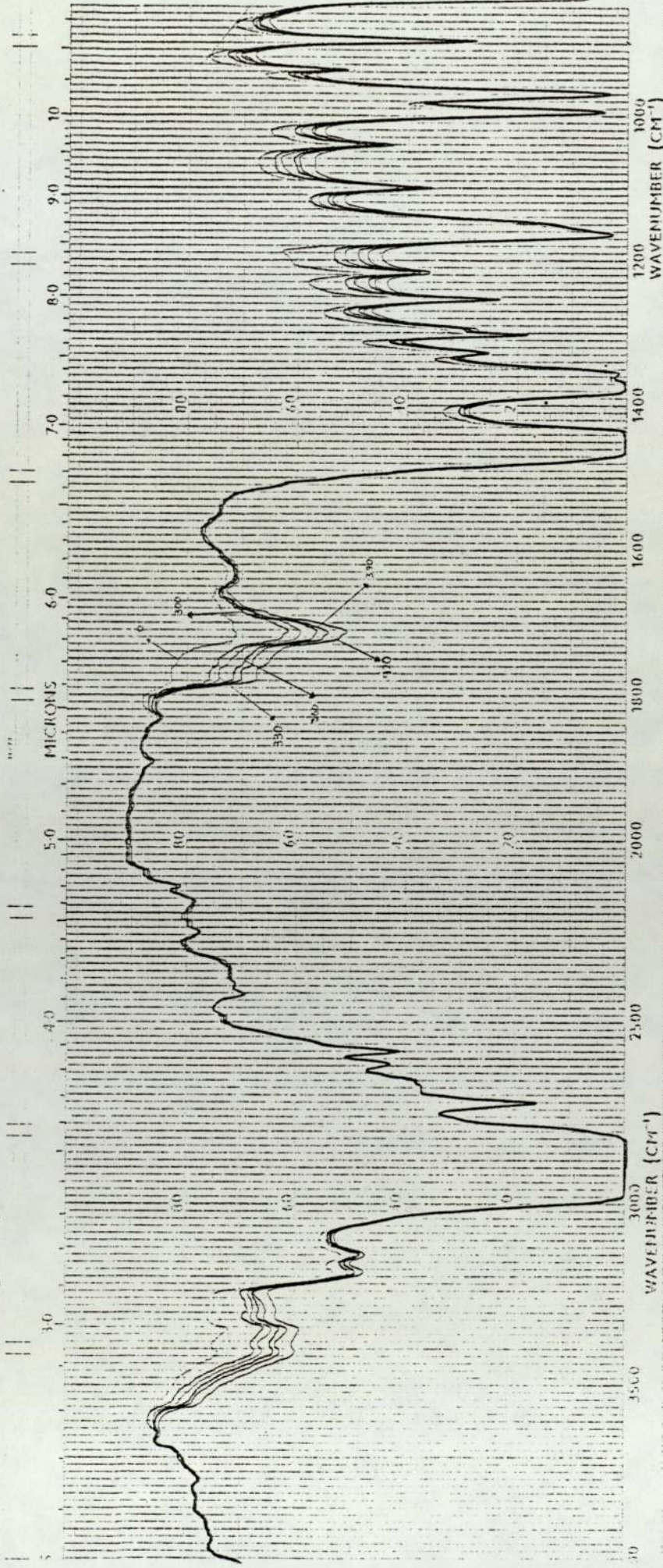
Fig 5.11 Change in hydroxyl (3500-3000 cm^{-1}) and carbonyl (1800-1600 cm^{-1}) absorptions during thermal oxidation of an unstabilised PP film (numbers on curves are heating time in mins). 1, processing cycles = 1; 2, heating temperature = 110°C.



148

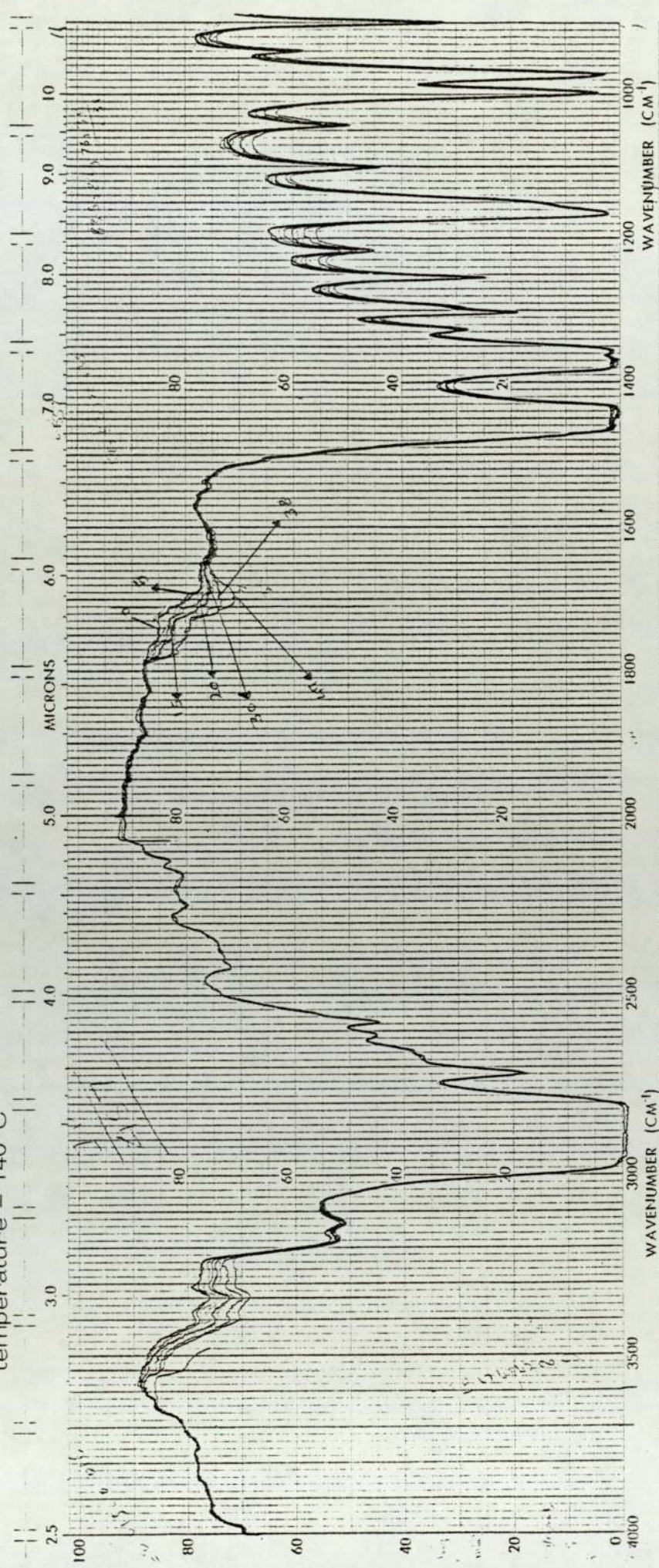
SAMPLE <u>Resin 1/PP</u>	SOLVENT _____ CONCENTRATION _____ CELL PATH _____ REFERENCE _____	REMARKS _____ _____ _____
OPERATOR _____	SCAN TIME _____ SLIT _____	OPERATOR _____ DATE _____

Fig 5.12 Change in hydroxyl (3500-3000 cm⁻¹) and carbonyl (1800-1600 cm⁻¹) absorption during thermal oxidation of reprocessed PP (numbers on curves are heating time in mins). Processing cycles = 4, heating temperature = 110°C



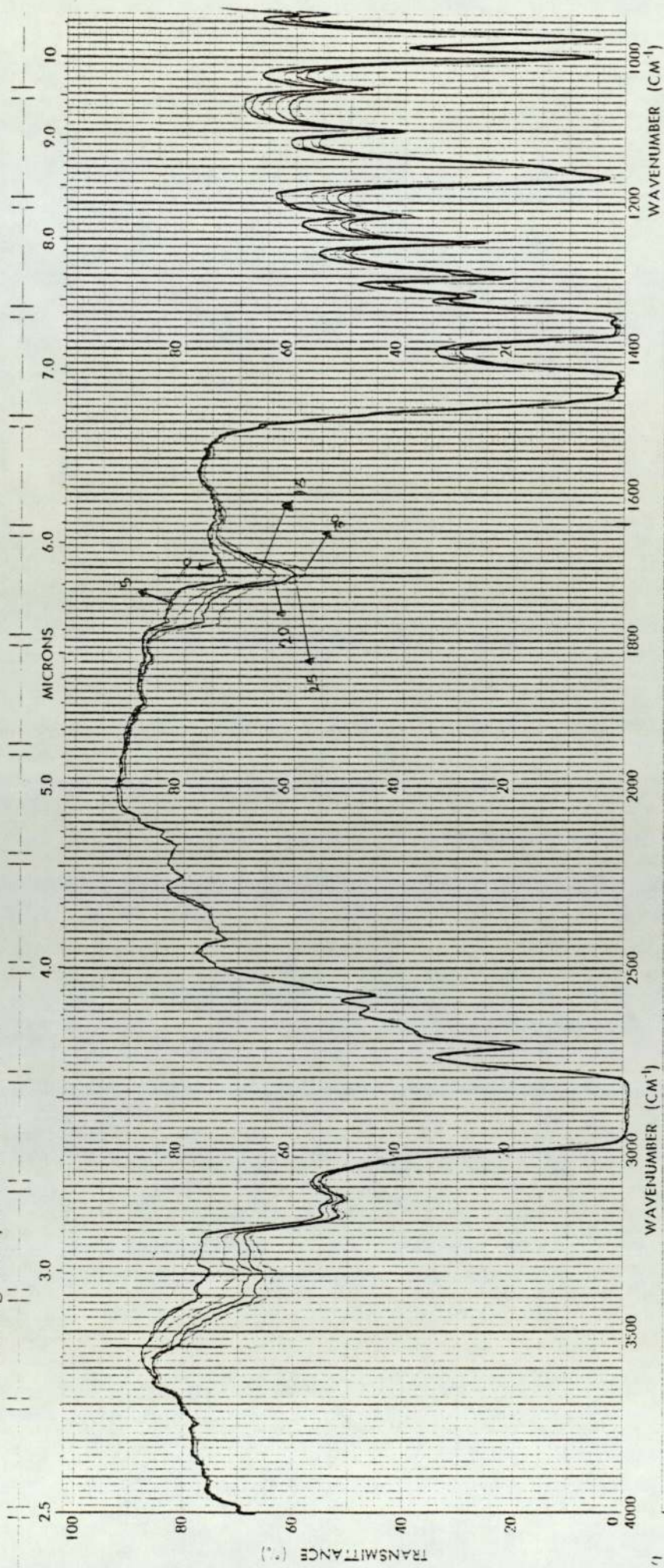
SAMPLE	SOLVENT	REMARKS	SCAN TIME	OPERATOR	DATE
	CONCENTRATION		SPLIT		
CURVE	CELL PATH				
	REFERENCE				

Fig 5.13 Change in hydroxyl ($3500-3000\text{ cm}^{-1}$) and carbonyl absorption during thermal oxidation of an unstabilised PP (numbers on curves are heating times in mins). Processing cycles = 1, heating temperature = 140°C



SAMPLE	SOLVENT	CONCENTRATION	CELL PATH	REFERENCE	REMARKS	SCA
						SUIT
ORIGIN						No

Fig 5.14 Change in hydroxyl ($3500-3000\text{ cm}^{-1}$) and carbonyl ($1800-1600\text{ cm}^{-1}$) absorption during thermal oxidation of reprocessed PP (numbers on curves are heating time in mins). Processing cycles = 4, heating temperature = 140°C



SAMPLE	REMARKS		
	SOLVENT	CONCENTRATION	CELL PATH
ORIGIN			REFERENCE

very mildly reprocessed samples, No 1, at two different temperatures, 110 and 140°C in an air oven showed a significant difference in carbonyl formation on heating (Fig 5.15).

As mentioned in the previous chapter (4), it is not possible to avoid contamination by transition metal ions during processing and reprocessing⁽²⁰⁰⁾. Therefore it is necessary to study the effect of some common transition metal ions (eg Fe, Co, Cr, Mn, Cu, Zn) during thermal and photo-oxidation of processed and reprocessed polypropylene. Figs 5.16 and 5.17 show the effect of such transition metal ions on the stability of polypropylene when subjected to uv light and thermal ageing. Fig 5.18 shows also how transition metal ions act when polypropylene undergoes reprocessing.

5.4 Discussion

Both the rate of development of carbonyl and the time to embrittlement of polypropylene subjected to uv exposure are markedly dependent on previous thermal treatment (Figs 5.4 and 5.5). It has also previously been observed by Scott and co-workers⁽¹⁹⁷⁾ that polypropylene is markedly sensitised to photo-oxidation by the thermal processing sequence involved in its conversion to fabricated products.

Hydroperoxides^(150, 151, 230) and ketonic carbonyl^(147, 231, 140) and conjugated carbonyl⁽²³²⁾ have all been proposed as photo-initiators during the early stage of photo-oxidation of polypropylene. All these impurities are formed as a result of thermal oxidation during processing or fabrication of

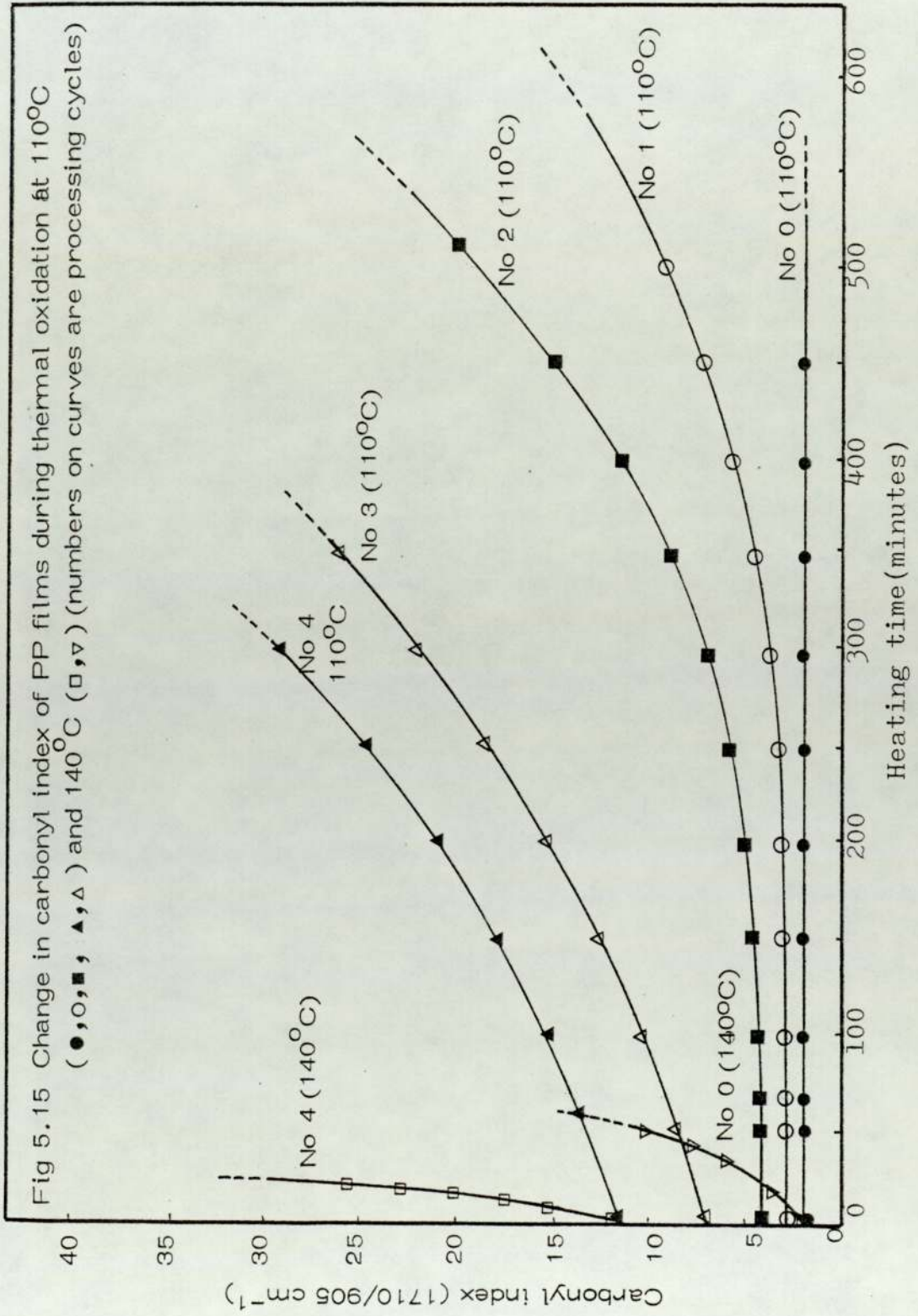


Fig 5.16 Effect of additives on photo-oxidation of polypropylene processed at 180°C in the closed chamber for 5 mins (concentration of additives, 3×10^{-5} mol/100 g)
 1, CoSt; 2, M nSt; 3, CrSt; 5, FeSt; 6, PP (no additive); 7, NiSt, 8, ZnSt

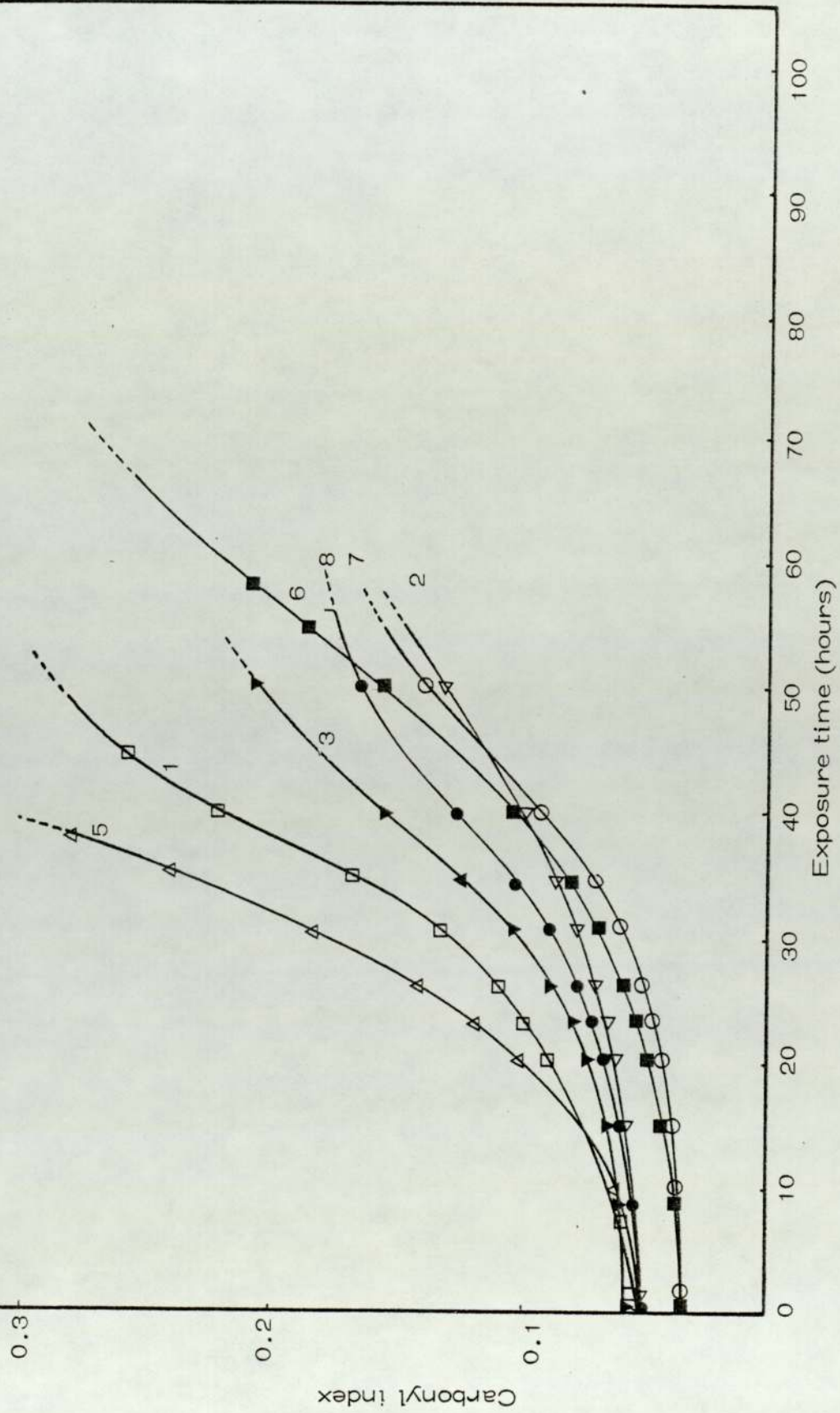
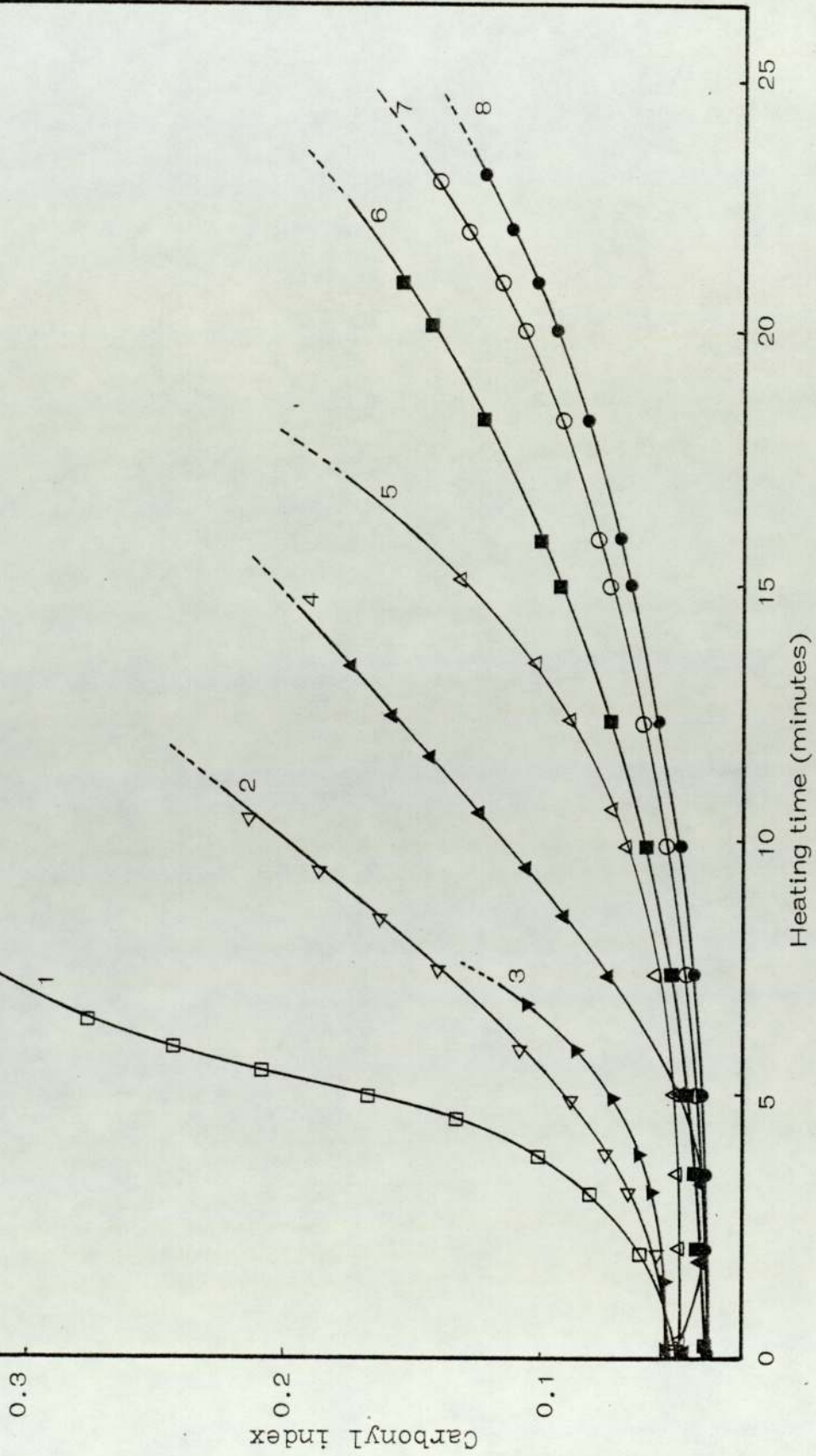


Fig 5.17 Effect of transition metal ions on thermal oxidation of PP (all processed at 180°C, 5 mins in closed chamber, concentration of additives 3×10^{-5} mol/100 gm) (numbers on curves are 1, CoSt; 2, MnSt; 3, CrSt; 4, CuSt; 5, FeSt; 6, PP (no additive); 7, NiSt; 8, ZnSt respectively)



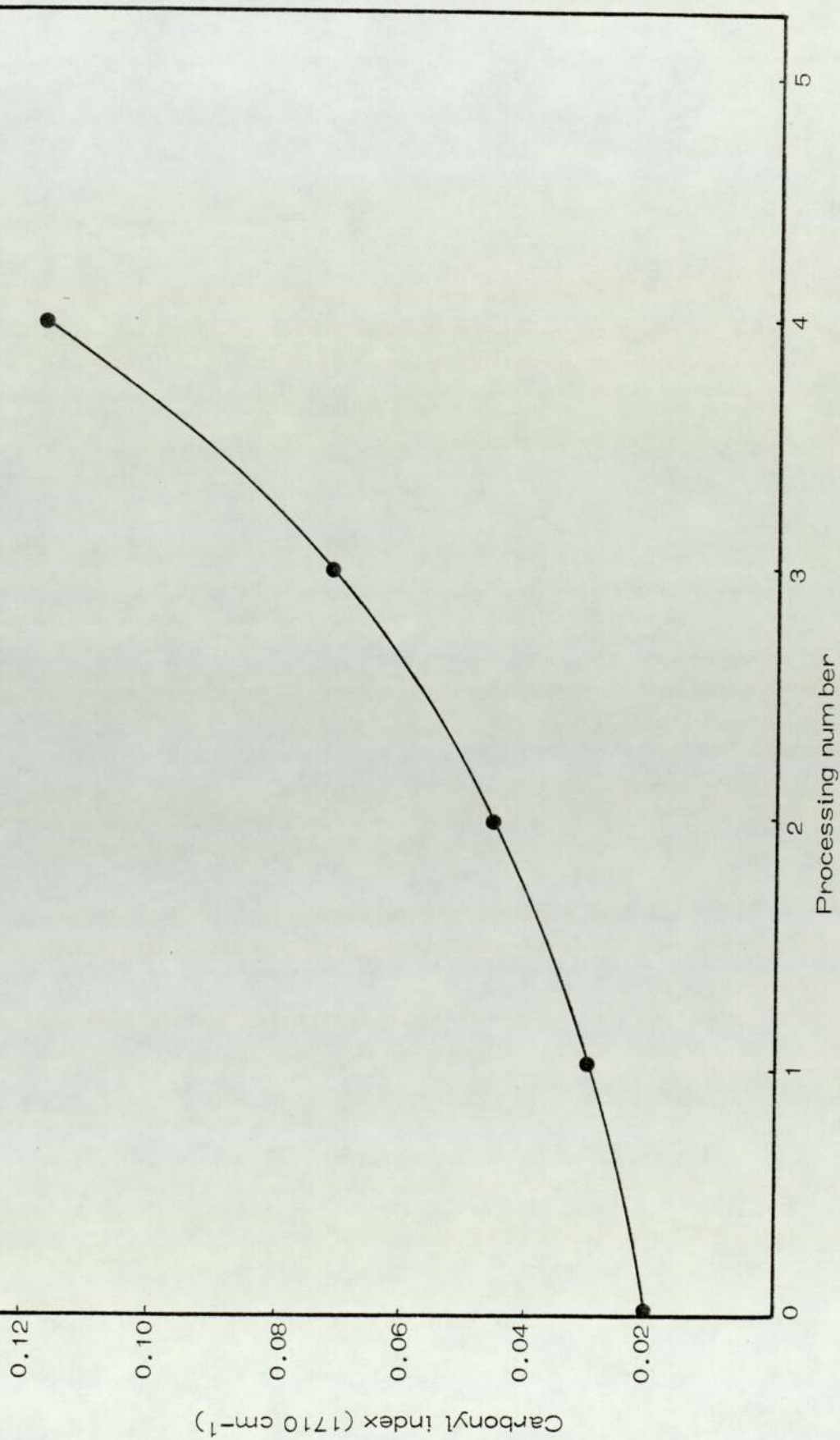
polypropylene. It is seen (Fig 5.3) that the further growth of conjugated carbonyl (index A1710/A905 cm^{-1}) shows an induction period. Hydroperoxide rather than saturated carbonyl or conjugated carbonyl is the main photo-initiator during the early stages of photo-oxidation of polypropylene. Furthermore, the rate of photo-oxidation as measured by carbonyl formation can be directly related to the concentration of peroxides (Fig 5.5).

Scott and co-workers⁽²⁸⁹⁾ observed a linearity of $[\text{ROOH}]^{1/2}$ with time of initial uv irradiation, implying that hydroperoxides initially formed are alone responsible for the photo-oxidation kinetics. More recently, Carlsson et al⁽²³³⁾ showed a similar type of half order hydroperoxide concentration dependence on initial irradiation time and concluded that the low hydroperoxide level detectable in a commercial unstabilised polypropylene sample is alone adequate to account for the photo-initiation kinetics and additional initiation by carbonyl impurities is insignificant. Emanuel⁽²³⁴⁾ also demonstrated the formation of hydroperoxide on uv irradiation of polypropylene which precedes the formation of carbonyl. There is now a great deal of evidence to suggest that hydroperoxide formed during the processing operation (Fig 5.3) are responsible for the photo-sensitisation during photo-oxidation.



Samples of reprocessed polymer containing varying amounts of carbonyl (Fig 5.21), when subsequently exposed to photo-oxidation show rapid carbonyl formation (Fig 5.5), the rate

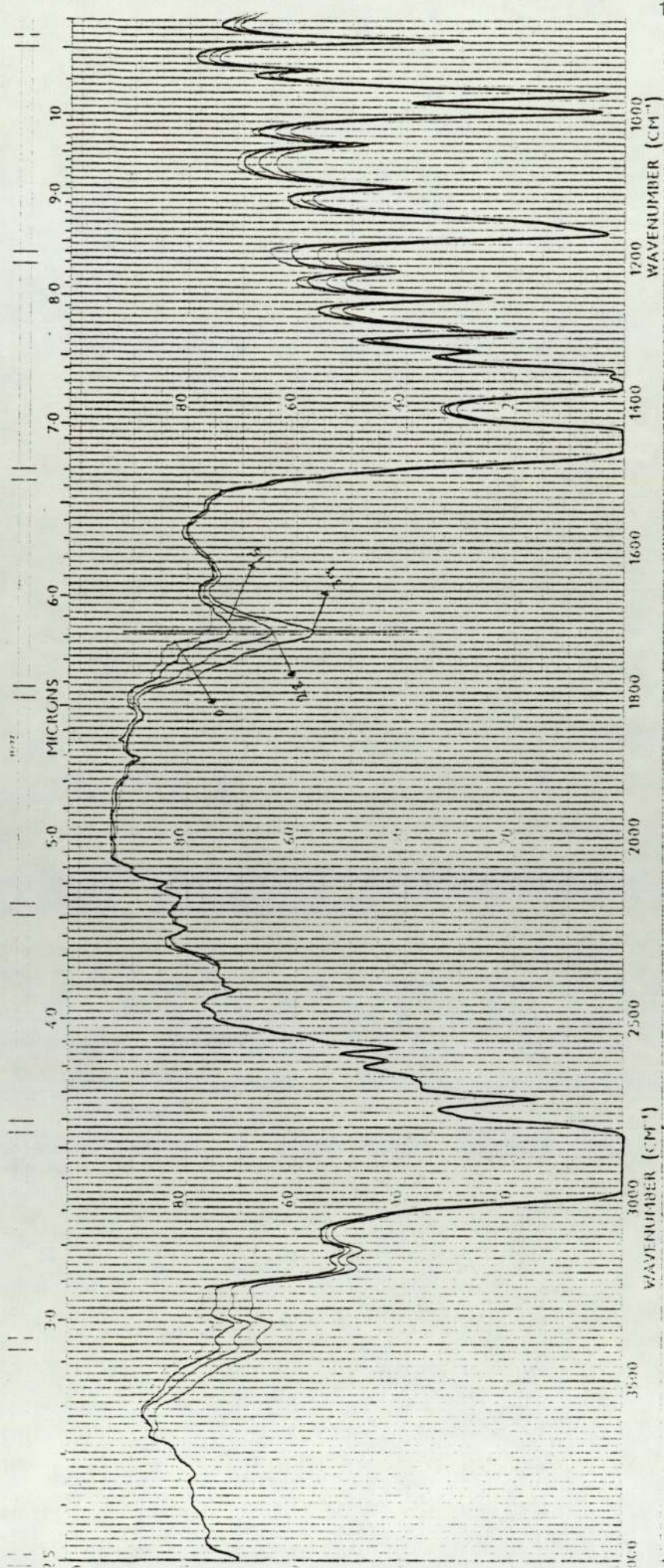
Fig 5.21 Effect of processing cycles on the rate of carbonyl formation of unstabilised polypropylene



of formation being related to the severity of processing and initial carbonyl concentration in the polymer⁽¹⁴⁹⁾. The embrittlement time also decreased as the number of processing operations increased (Fig 5.4).

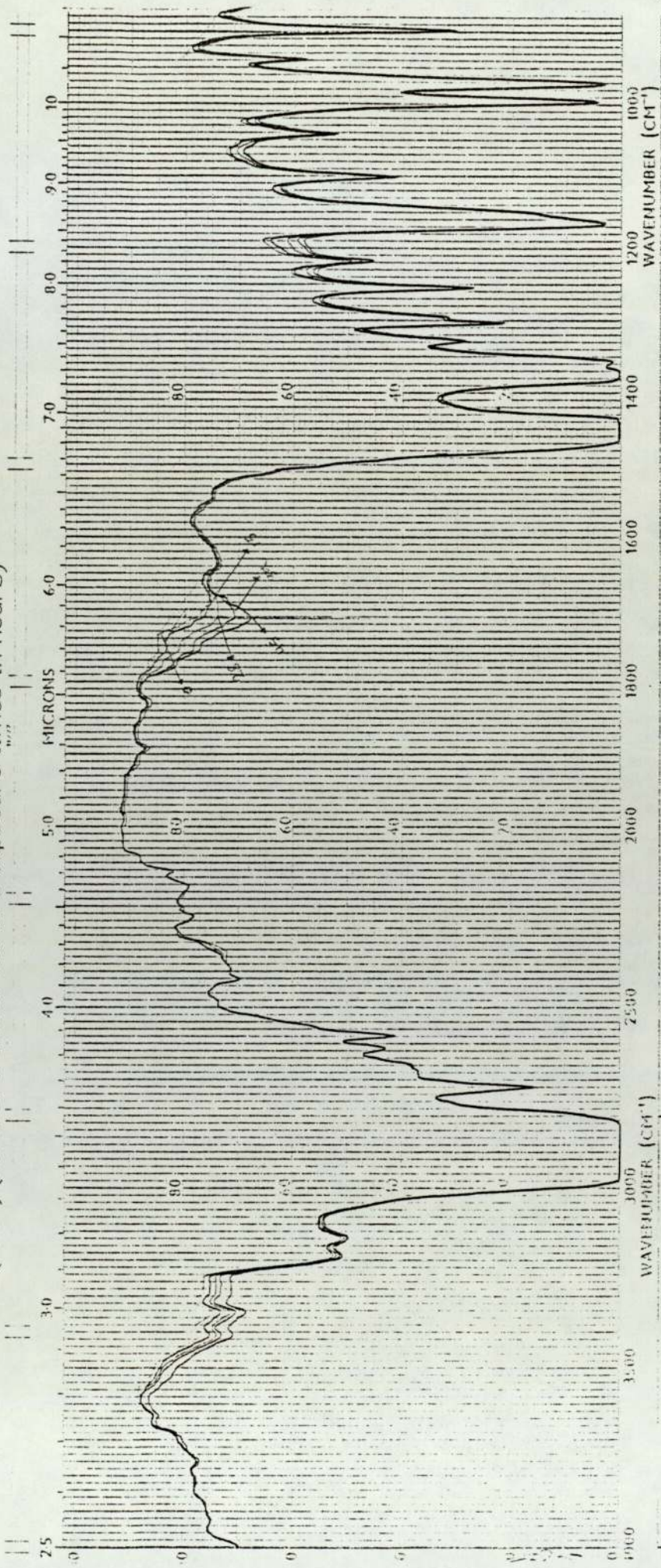
Infra-red spectra showed the general change in the polypropylene films containing transition metal ions during uv irradiation. The overall absorption pattern was the same as in the control film, but the rate of development of oxidised product functional groups was strongly influenced by the addition of activators (eg nickel, stearate and ferric stearate) (Figs 5.1, 5.2, 5.19 and 5.20), showing that ferric stearate is a more powerful photo-pro-oxidant than other transition metal stearates. The effects of thermal oxidation are different from that of photo-oxidation. In the carbonyl region $1800 - 1600 \text{ cm}^{-1}$ (Fig 5.11 - 5.14), thermally oxidised polypropylene showed a complex absorption with a large number of bands, the intensity of which increased with heating time. Each of these bands was due to a different type of carbonyl compound and some but not all were observed in photo-oxidised polypropylene. The growing carbonyl band shifted towards acid ($1710 - 1715 \text{ cm}^{-1}$) with increased heating time. Other carbonyl products were also observed as shoulders in the later stage of oxidation (Figs 5.11 - 5.14) at 1780 , $1760 - 1763$ and 1725 cm^{-1} (for detailed characterisation, see Table 4, Chapter 4). Co, Cr, Mn and Cu stearates are more powerful thermal pro-oxidants than ferric stearate (Fig 5.17), which was however more effective as a photo-pro-oxidant (Fig 5.16). The effect of soluble salts such as metal complexes is to catalyse the breakdown of hydroperoxide to free radicals (see Chapter 4). Scott and co-workers observed similar results in LDPE showing that cobalt was a powerful thermal

Fig 5.19 Infra-red spectra of photo-oxidised polypropylene film containing 2×10^{-5} mol/100 g polymer ferric stearate (numbers on curves are exposure times in hours)



APPLY		FERRIC STEARATE (Fe ³⁺)	
SOLVENT		2 x 10 ⁻⁵ mol/100g polymer	
CONCENTRATION			
CELL PATH			
REFERENCE			
REMARKS			
SCAN TIME			
SLIT			
OPERATOR			
DATE			

Fig 5.20 Infra-red spectra of photo-oxidised polypropylene film containing 2×10^{-5} mol/100 g polymer nickel stearate (NiSt) (numbers on curves are exposure times in hours)



SAMPLE	SOLVENT	REMARKS	SCAN TIME
ORIGIN	CONCENTRATION		SLIT
	CELL PATH		OPERATOR
	REFERENCE		DATE

Nickel stearate Mist -5
2 x 10⁻⁵ mol/100g polypropylene

pro-oxidant for LDPE⁽¹²³⁾. Therefore, reprocessed polypropylene which contains different transition metal ions when subjected to uv light shows different carbonyl formation characteristics initially and at the later stages of photo-oxidation (Figs 5.16, 5.17 and 5.18). Fig 5.18 shows that the initial carbonyl index for cobalt stearate is higher than for ferric stearate but at the later stages of photo-oxidation, ferric stearate produced a higher concentration of carbonyl than cobalt stearate.

5.5 Relation between mechanical properties and polymer morphology

The dynamic mechanical properties, mechanical damping and complex modulus of polypropylene change rapidly during the early stages of irradiation. After prolonged exposure, however, the damping value decreased (Fig 5.9) and went through a minimum as the embrittlement time was approached. Since photo-oxidation started in the amorphous phase this led subsequently to an increase in crystallinity^(227,226,224). Nielsen⁽⁶⁰⁾ has shown different values of damping with polypropylene of different degrees of crystallinity.

The damping behaviour of crystalline polymers is generally more complex than that of amorphous polymers since crystalline polymers have a damping peak corresponding to the glass transition. However, since part of the polymer is in the crystalline state, the intensity of the damping peak is reduced. The intensity of the damping peak is given by⁽²⁹⁰⁾:

$$G''/G' = W_c (G''/G')_c + (1 - W_c)(G''/G')_a$$

where subscripts c and a refer to the contribution of the pure

crystallinity and amorphous phases respectively. Also Nielsen has related the modulus of polypropylene to the degree of crystallinity (W_c)⁽⁶⁰⁾ as the complex modulus increased with crystallinity (Fig 5.7). Fig 5.10 also shows a linear relationship between hydroperoxide (measured chemically) and complex modulus E^* (for further discussion of the effect of photo-oxidation on mechanical properties of polymers, see Chapters 4 and 6).

CHAPTER SIX

STUDY OF BLENDS OF LDPE AND PVC

6.A Introduction

Blending of incompatible plastics usually gives a reduction in mechanical properties compared with their polymer components⁽²⁷⁾. As mentioned previously, the interest in the study of these systems partly arises from the re-use of polymer waste. Segregation into generic types is an expensive operation and it was proposed that the blend be used without separation. Research was carried out⁽²³⁵⁾ to upgrade the inferior mechanical properties of the blends by controlling the domain sizes as well as the addition of compatibilisers and fillers etc.

Han et al have found⁽²³⁶⁾ that in PE/PVC systems (45:55), PVC was dispersed in the PE matrix. This structure accords with the results of Han et al⁽²³⁶⁾ who showed that material with the lower melt viscosity would constitute the continuous phase.

There is an optimum mixing time. Refinement of the domains size decreases with increasing mixing time up to a stage where coarsening in the structure takes place⁽²³⁶⁾. The effect of increasing the mixing temperature had a similar effect^(236,235). Furthermore, there is a limitation since high temperature and or long mixing times increases the risk of degradation and discoloration of the blends.

It was found⁽²³⁵⁾ that the tensile strength increased with

decreasing domain size. In general, coprecipitation gave a higher tensile strength product than melt blendings. The reason is that the domain size increases on melt blending. The precipitated sample also showed an improved elongation at break over the melt-blended samples⁽²³⁷⁾. This was explained in terms of improved dispersion and the existence of a similar stress concentration around the similar PVC particles⁽²³⁵⁾. In melt mixing, there was a limit to the reduction of domain sizes. The blend properties were found to be further improved by the use of various fillers and cross-linking agents⁽²³⁵⁾.

PVC has a higher tensile strength than PE⁽²³⁵⁾. If PE and PVC were to be truly compatible, the tensile strength of the blend would be expected to increase linearly from minimum (100% PE) to maximum (100% PVC) with increasing PVC content. It was shown⁽²³⁸⁾ that a blend of mutually compatible polymers (eg, PPO and PS) exhibited such a linear relationship and directly related to the specific ratio selected.

6.A.1 Experimental

Materials: Stabilised low density polyethylene was used as the base polymer market under the trade name of Alkathene 805 and produced by the Imperial Chemical Industries (ICI).

BP Brean M90/50 (mass polymerised grade PVC) was used to blend with low density polyethylene.

The solid phase dispersants (SPD's) to improve the toughness of blends consisted of EPDM, ABS, ACS, SBS, NR, BR, HIPS

and CPE (20% and 42% Cl) (see Table 6.1).

Processing: The blends were processed at 180°C in the RAPRA torque rheometer for 5 minutes in a closed chamber. Samples were then compression moulded at 180°C for two minutes into sheets as discussed in the Experimental Chapter (3).

Processing additives: (a) Commercial dibutyltin maleate based stabiliser (Irgastab T290), manufactured by Ciba-Geigy (UK) Limited. Infra-red spectroscopy analysis suggested that this stabiliser may contain 'hindered' phenol component. (b) Calcium stearate, BDH Chemicals Limited (analar grade). (c) Lubricant Wax E (trade name of Hoechst AG) was obtained from RAPRA, Shawbury, Shrewsbury, Shropshire. Wax E was obtained in the form of flakes and prior to use was produced in a mortar.

Table 6.2 shows the formulations with varying proportions of PVC (0.5, 10, 15 and 20%). The formulations used were all based on 35 g of polymers.

Tensile strength was measured as described in Chapters, 3, 4 and 5. Impact strength and rheovibron were used as discussed in Chapter 3.

Microscopy: Optical and scanning electron microscopy examination were performed on the blends, in each case photographs were obtained of unoxidised and oxidised samples.

The percentage of grafted PVC was calculated from infra-red

Table 6.1

EPDM	Ethylene-propylene diene rubber, supplied by Esso Petroleum under trade name of ENJAY 4608
NR	Natural rubber supplied by Dunlop Ltd, under trade name of SMR (CV)
BR	Butyl rubber, supplied by Polysar under trade name of Butyl 100
ABS	Acrylonitrile-butadiene-styrene terpolymers, produced by Monsanto
SBS	Styrene-butadiene-styrene (which contains 72% butadiene) was supplied by Shell Industry
CPE	Chlorinated polyethylene made from Union Carbide DGU5320, 42% and 20% (C1) were supplied by ICI
ACS	Acrylonitrile-chlorinated polyethylene-styrene supplied by Showa Denko KK
HIPS	High impact polystyrene used under the trade name of BI 1003 containing 6.5% polybutadiene and 1% phenolic antioxidant
PU	Polyurethane which was supplied by Porvair Ltd

Table 6.2

No	Compositions (%)		Charge weight mixer (g)	
	PE	PVC	PE	PVC
1	100	0	35.00	0
2	95	5	33.25	1.75
3	90	10	31.50	3.50
4	85	15	29.75	5.25
5	80	20	28.00	7.00

The PVC was stabilised as follows:

- (a) Irgastab (T290), 2.5 grm/100 grm PVC
- (b) Wax E, 0.65 grm/100 grm PVC
- (c) Calcium Stearate, 0.8 grm/100 grm PVC

spectrum by measuring the intensity of bond at 1250 cm^{-1} (due to C-Cl band) after 32 hours of hot extraction ^{in CH_2Cl_2 at} $(40-50^\circ\text{C})$ and expressing this as a function of the absorption measured using a sample containing pure PVC (100% PVC) of the same thickness.

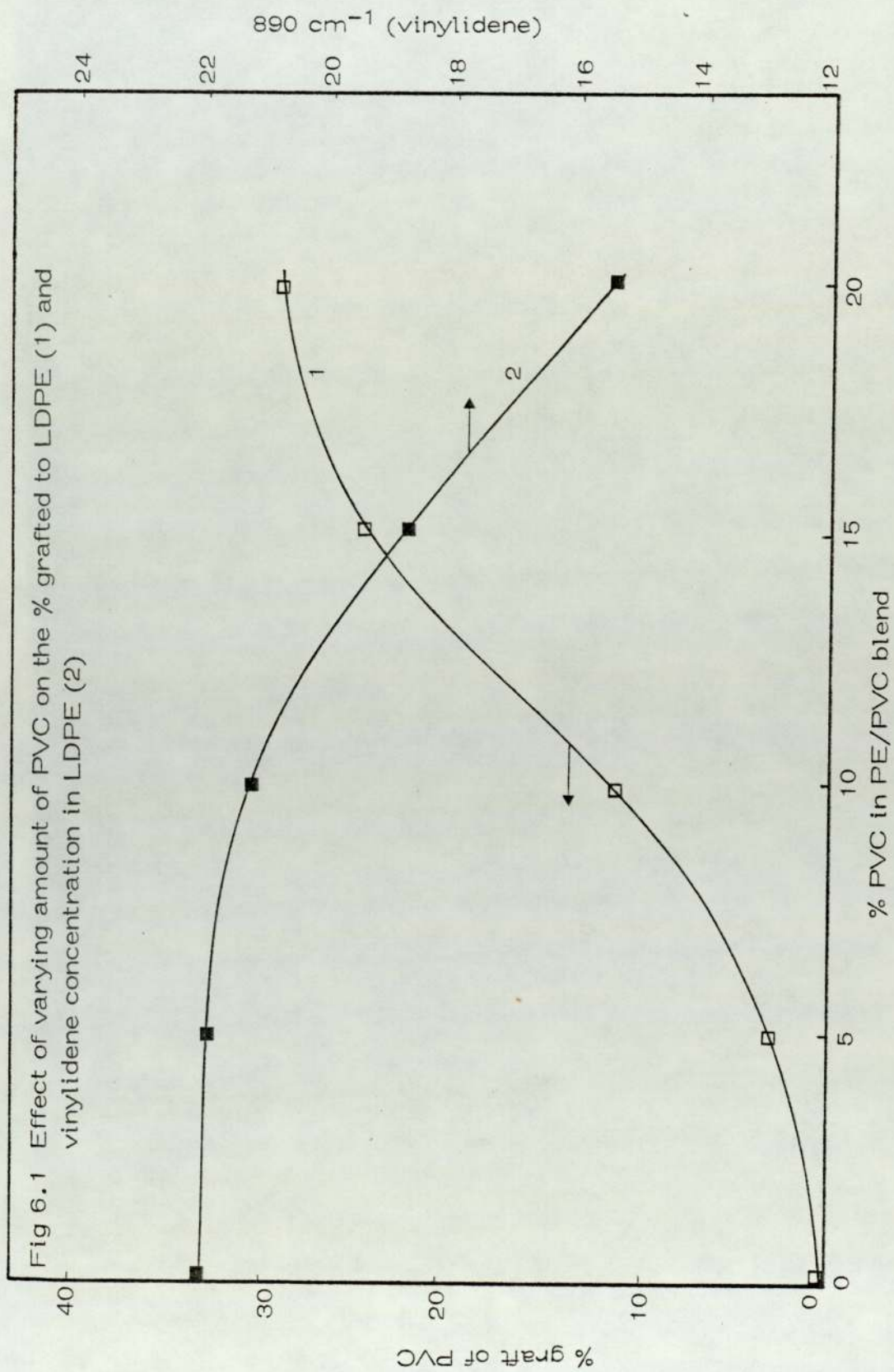
6.A.2 Effect of PVC concentration on mechanical properties of LDPE / PVC blends

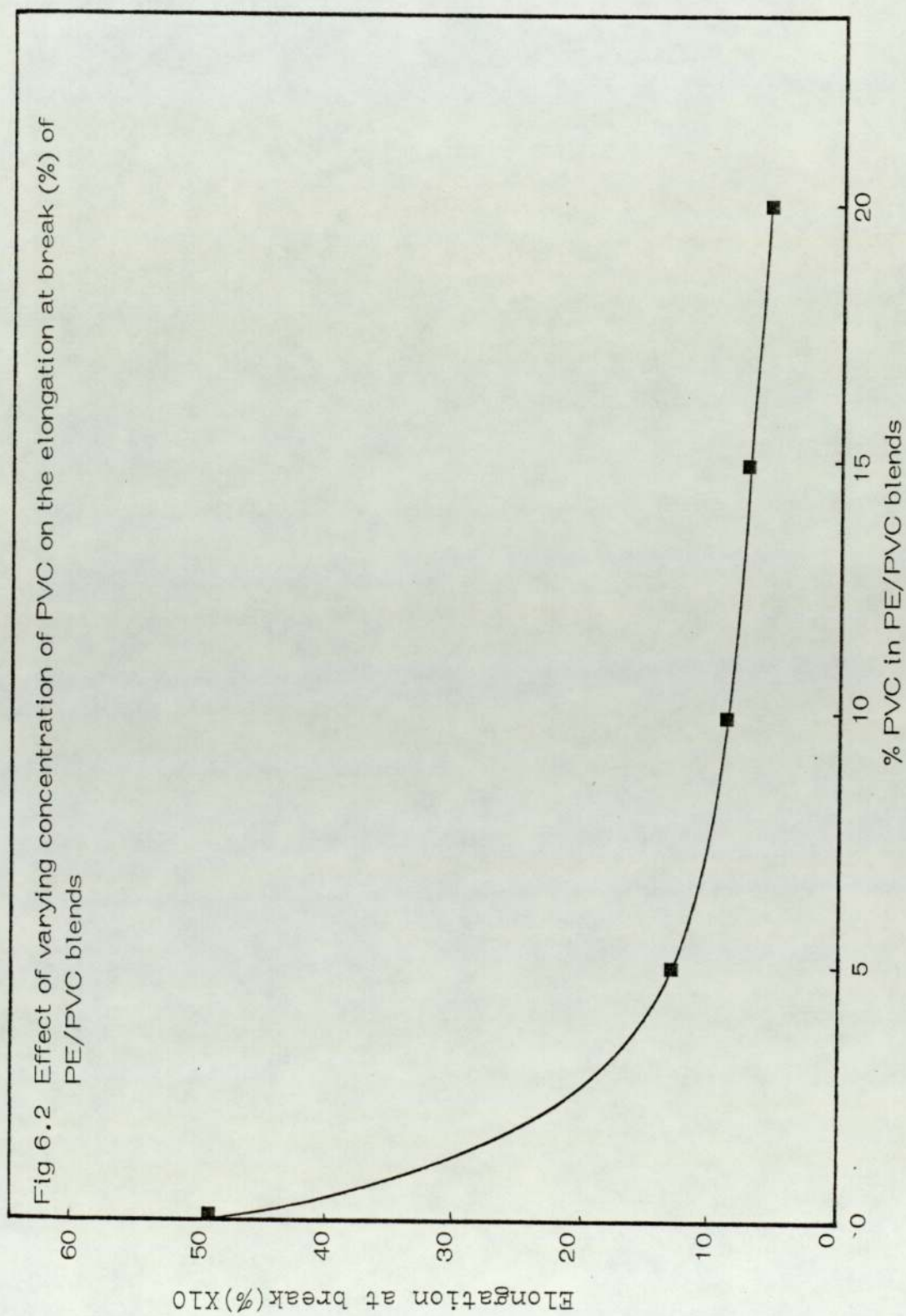
6.A.2.1 Result and discussion

The result obtained from the mixing of 5, 10, 15 and 20% PVC in LDPE at 180°C for 5 minutes indicates some grafting of PVC to LDPE (the % graft was calculated as described in experimental section 6.A.1). The increase in grafting with increase in PVC concentration and a commensurate decay in vinylidene absorption at 890 cm^{-1} was observed (see Fig 6.1, curve 2).

Figs 6.2, 6.3 and 6.4 show that with the addition of PVC to PE, the tensile strength, elongation at break and impact strength dropped with increasing PVC content. These results are in agreement with an experimental study carried out by Han et al⁽²³⁹⁾ who showed that the tensile strength went through a minimum with increasing amount of the weaker component when two incompatible polymers such as PE and PS were blended.

These differences in properties between the compatible and incompatible systems can be explained by two phase morphology of the incompatible blends contrasting with the single homogeneous phase structure of mutually compatible





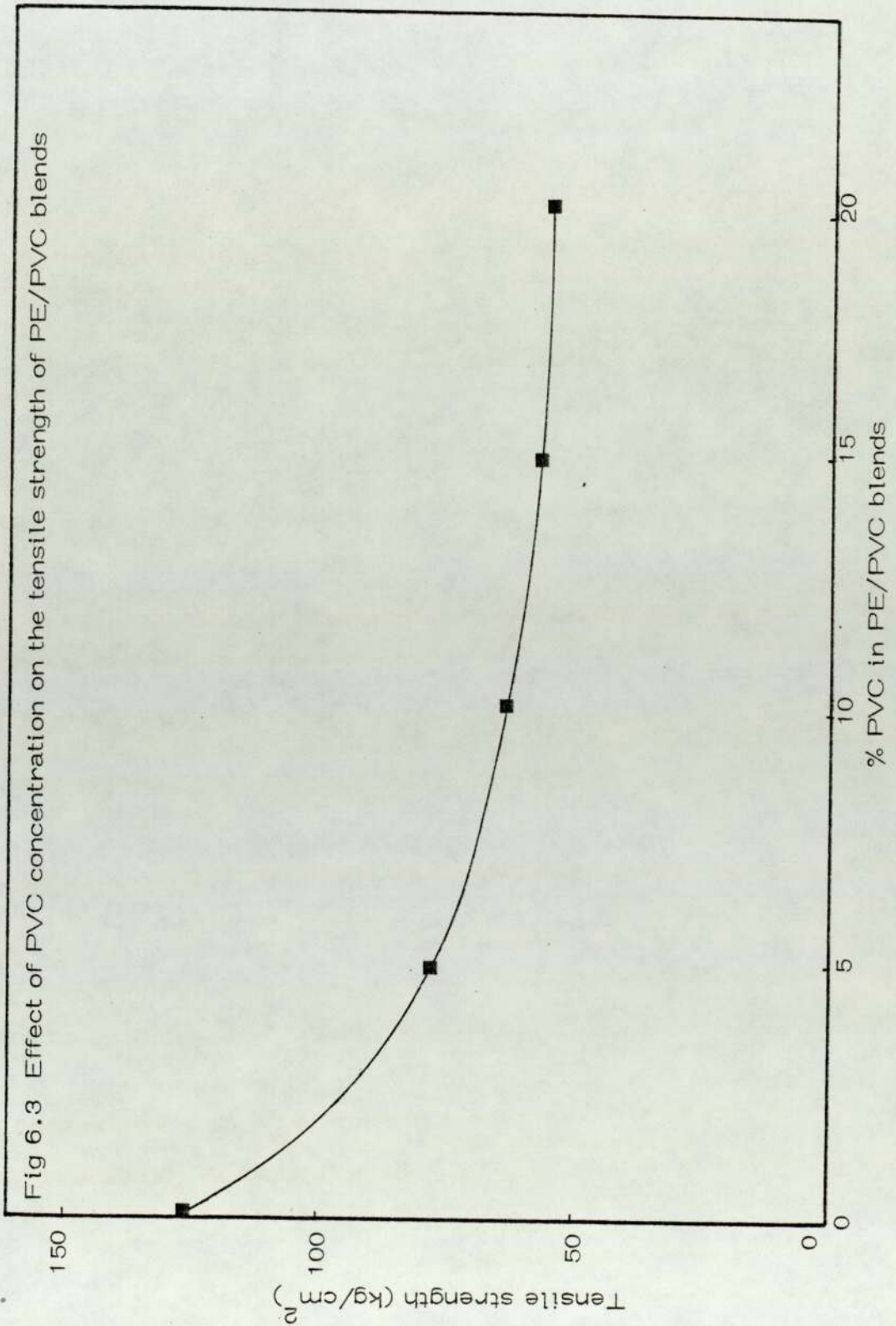


Fig 6.3 Effect of PVC concentration on the tensile strength of PE/PVC blends

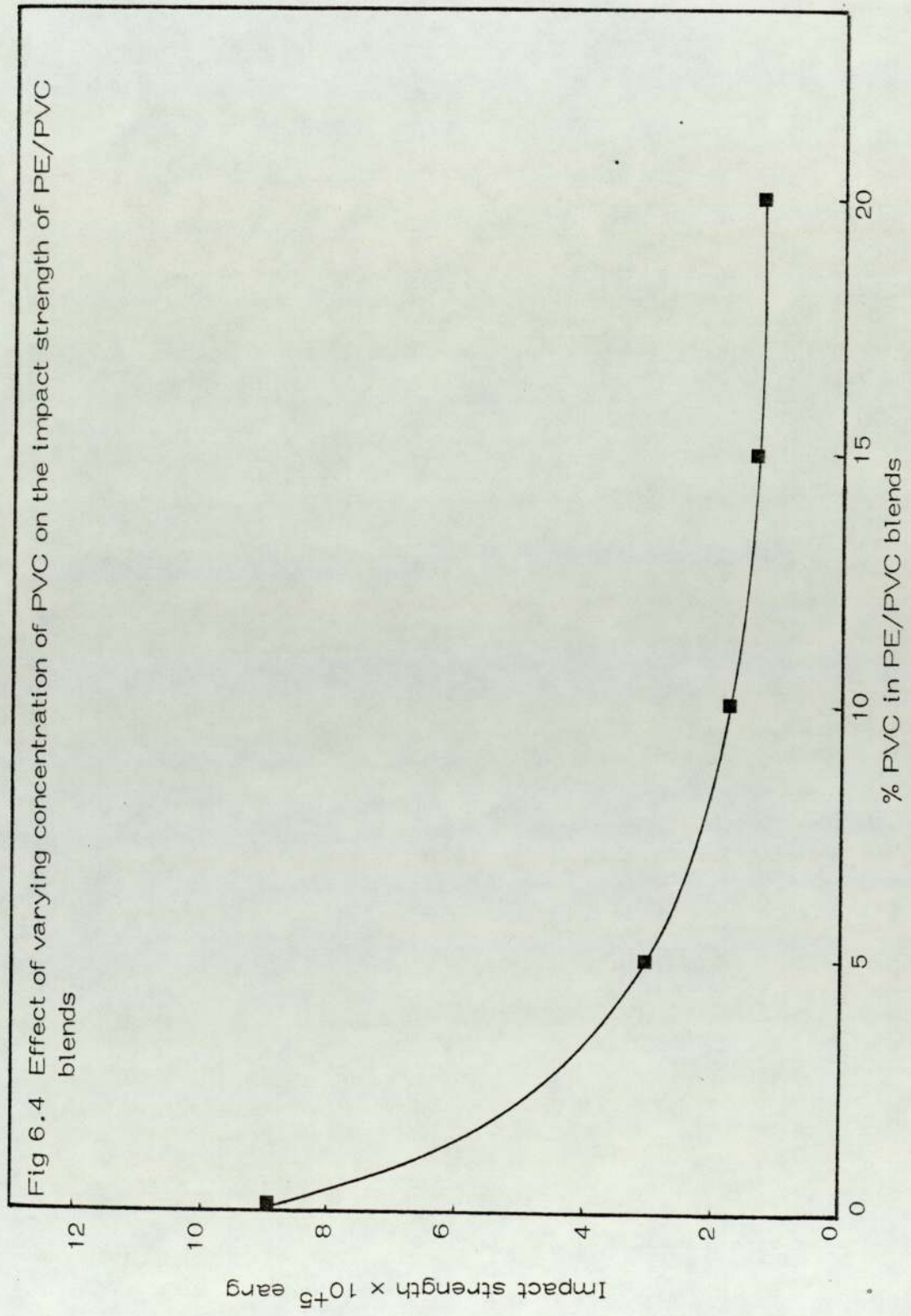


Fig 6.4 Effect of varying concentration of PVC on the impact strength of PE/PVC blends

polymers. It can be seen from the optical micrographs of PE/PVC, plates 1-4, blends that they are heterogeneous blends. The PVC exists as domains which are dispersed in the PE matrix. McGill and Fousie⁽²³⁵⁾ blended 55 parts of PE with 45 parts of PVC and found that PE formed the continuous phase and PVC the dispersed phase. This was so as PE had the lower melt viscosity at the temperature of blending and moulding. This structure is also consistent with the findings of Han and YU⁽²³⁶⁾ and J L Work⁽²⁴⁰⁾ who both showed that in any incompatible mixture, the component having the lower melt viscosity at the temperature of processing tended to form a continuous phase in the mixture. The greater the viscosity difference, the greater was this tendency. The viscosity of one component relative to the other could be changed by changing the molecular weight of the components and or the temperature of mixing.

The PVC domain can be seen to increase in amount and size with increasing PVC content in the blends. The PVC particles tend to exist in spherical shape. In contrast to the blend, the polyethylene optical micrograph showed a single continuous phase (plate 1).

The production of continuous film by the use of an extruder (18 mm, Betol with barrel zone 3 at 180°C, barrel zone 2 at 170°C, barrel zone 1 at 160°C, die zone 1 and 2 at 180°C) did not show improved mixing over the torque rheometer. Plates 5 and 6 show the particle size of PVC on the surface of extruded film. This can be related to insufficient mixing in the extruder.



Plate 1 100 % LDPE (OPTICAL)
Mn x 200

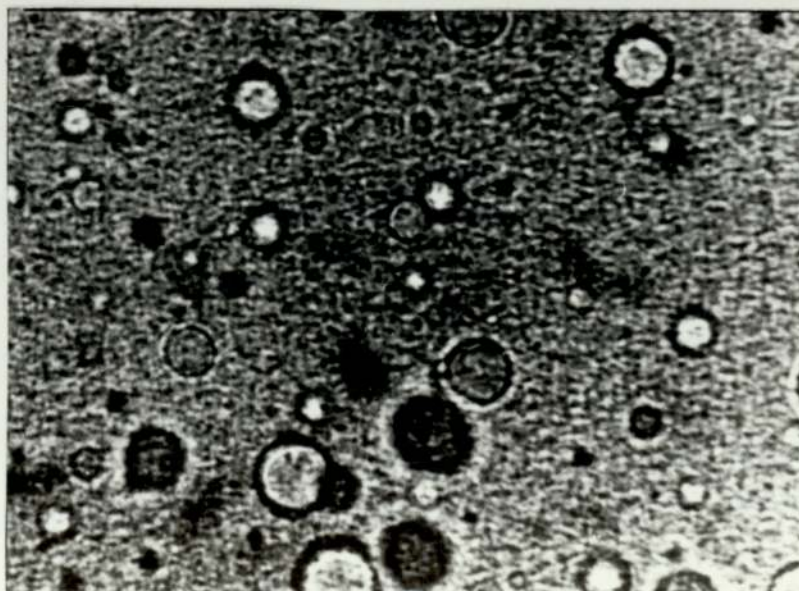


Plate 2 (PE+5% PVC) (OPTICAL)
Mn x 400

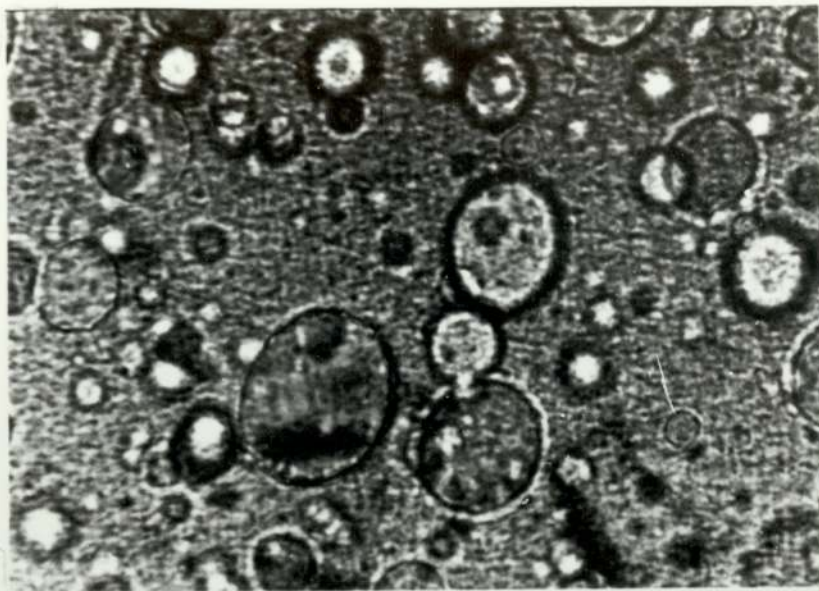


Plate 3 (PE + 10% PVC) (OPTICAL)
Mn x 400

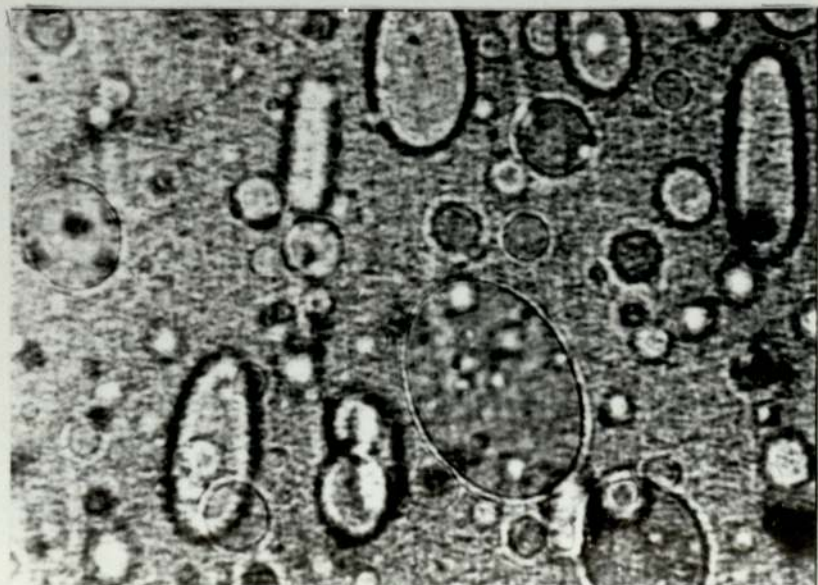


Plate 4 (PE + 20% PVC) (OPTICAL)
Mn x 400

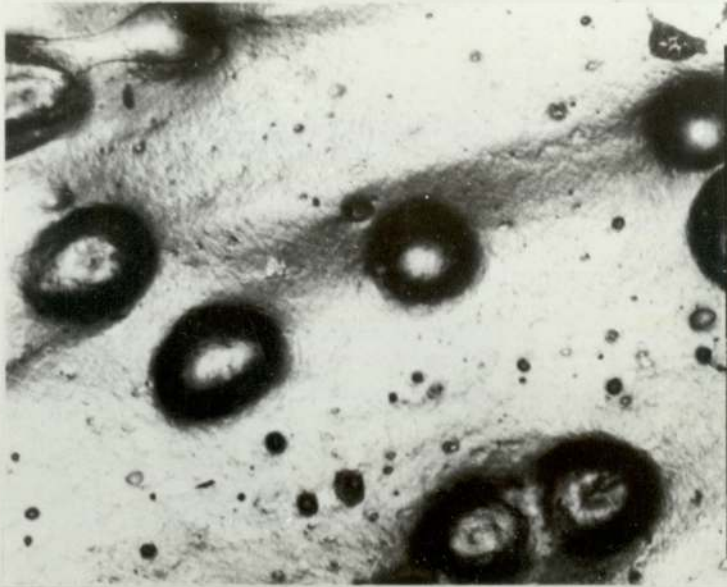


Plate 5 (PE + 10%PVC) (Optical)
Mn x 100

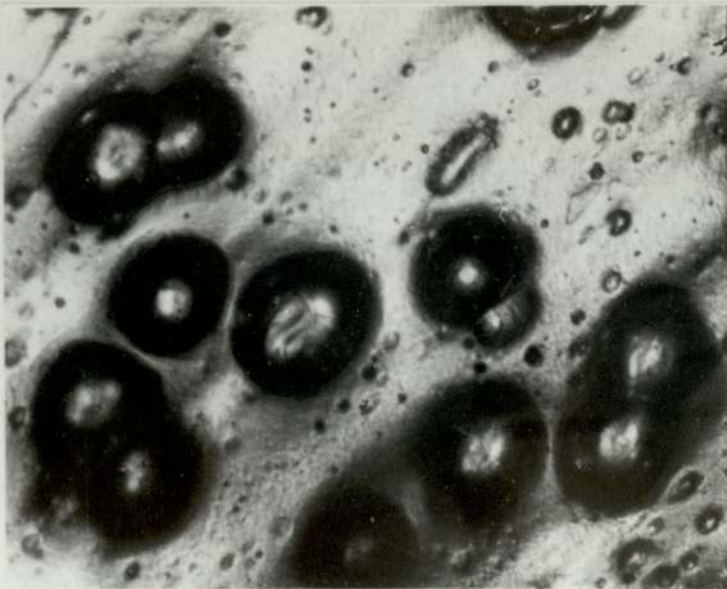


Plate 6 (PE + 20%PVC) (Optical)
Mn x 100

Plates 7-10 show scanning electron microscope photographs of specimens cut directly from the torque rheometer samples; these demonstrate the distribution of the particles throughout the matrix. The white bands could be due to surface cracking on cooling, *due to* contraction of the sample. All the photographs show nodules of PE coated PVC particles and give a good representation of the random distribution of the PVC phase. These results are in agreement with a study by Scott and co-workers⁽²⁴¹⁾ in which it was shown that the PVC exists as domain in the continuous phase of PE under microscope examination. The PVC domains do not adhere well to the surrounding PE matrix due to their incompatibility. Kerner⁽²⁴²⁾ predicted that if there were mutual adhesion the two phases of a blend, the tensile strength versus composition curve would be an 'S' shaped relationship. Since the result obtained for PE/PVC blend is not 'S' shaped, it can be assumed that adhesion between the dispersed and continuous phase is poor.

When a blended sample is subjected to the tensile force, the domains detach themselves partially or completely from the continuous phase and voids are created between the two phases. This explanation is supported by results obtained by Scott and co-workers⁽²⁴¹⁾ who studied the morphology and mechanical behaviour of a similar system. Plates 11 and 12 show the fracture surface of 10% PVC sample. This photograph clearly shows the 'wells' which have contained the particles although no large voids can be seen, probably due to the recovery of the sample after fracture. The diagram of the photograph (Plate 12) indicates some important features of the fracture surface⁽²⁴¹⁾.



Plate 7 (PE + 15%PVC) X 500 (S.E.M)

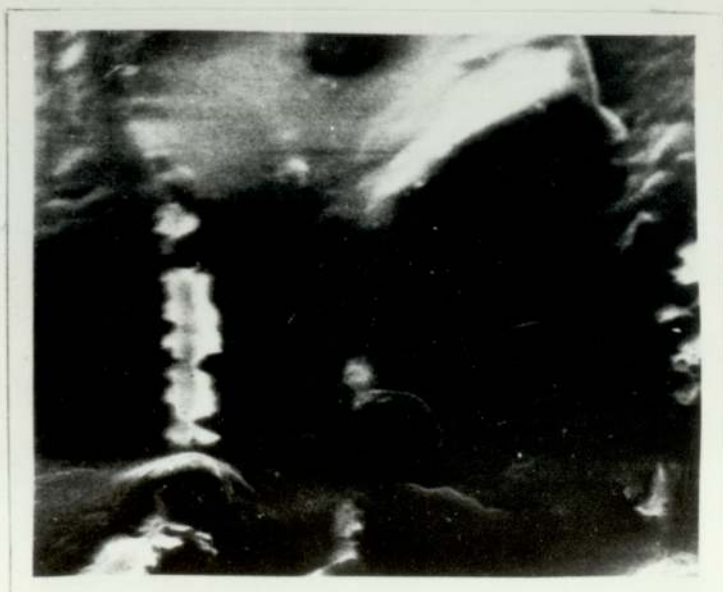


Plate 8 (PE + 15% PVC)X 2,000 (S.E.M)

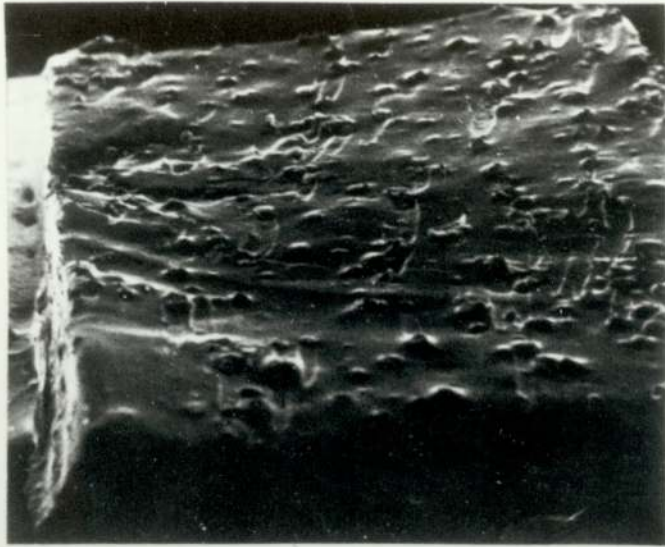


Plate 9 (PE + 20% PVC)X200 (S.E.M)



Plate 10 (PE + 20% PVC)X1000 (S.E.M)

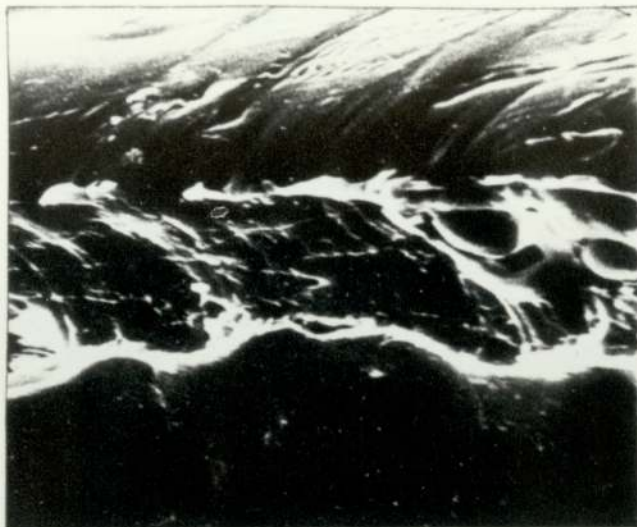


Plate 11 Fracture surface of a
10% P.V.C sample X1,000

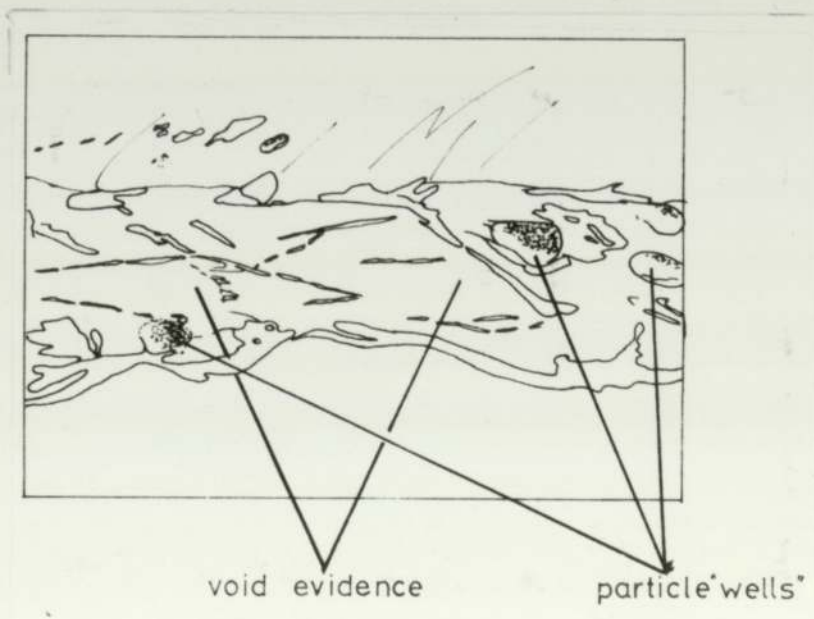


Plate 12 Diagram of above

Optical microscopic examination was used to observe the changes in morphology of samples under tensile stress. Initially, elastic deformation occurs equally within the matrix and particles. At the point of plastic deformation, the weak adhesion between the particle and the matrix is broken, and the matrix begins to deform. As PVC is much stronger than LDPE, the PVC particle is still within its elastic region and at this point the PVC particle will revert to its original unstressed form. The matrix and particle are parted at right angles to the applied stress. A void is thus formed between the matrix and particle. This break between the matrix and particle occurs at the point of highest stress concentration within the specimen. As further stress is applied, separation between other particles and the matrix occurs leading to a gradual spread into the particle region (see Fig 6.A.2.1).

As deformation continues, the more plastic LDPE is caused to flow around the particle in the general direction of the applied stress creating extended voids with the particles suspended at their centres. At an advanced state of deformation, the voids around the particle are highly extended along the stress direction. Failure occurs when the number of coalescing voids reduces the particle cross-sectional area to a limit where the stress cannot be sustained and fracture of the specimen occurs.

The tensile forces are mainly borne by the continuous phase and the tensile strength of the film decreases with increasing amount and size of the discrete PVC particles. McGill and Fourie⁽²³⁵⁾ reported that the physical properties of PE/PVC blend improved considerably with decreasing domain size. This explains why increasing PVC content from 0 to 20% increases the amount and

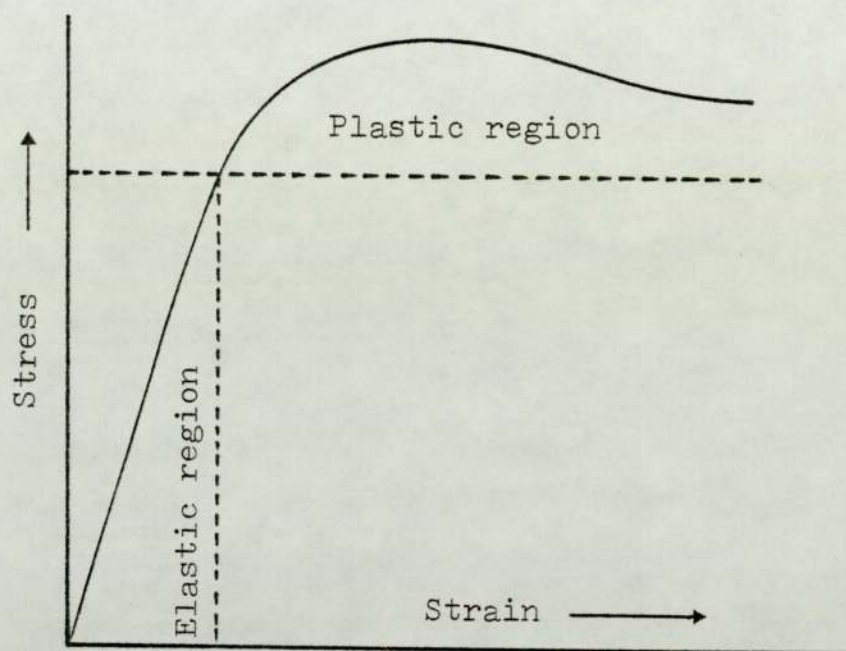


Fig 6.A.2.1 Graphical representation of the stress/strain curve produced by the blends.

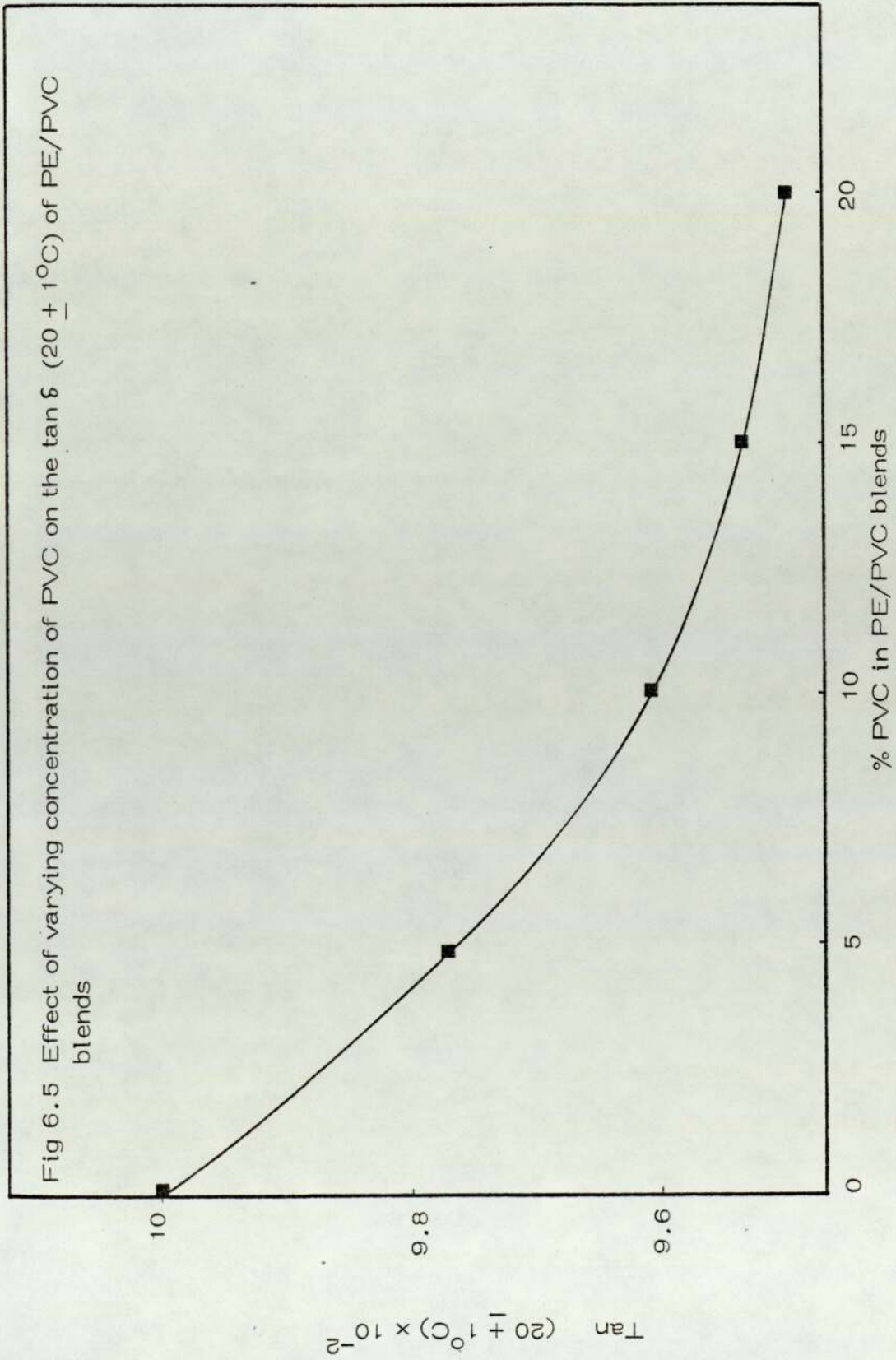
size of domain and decreases the tensile strength of the blends.

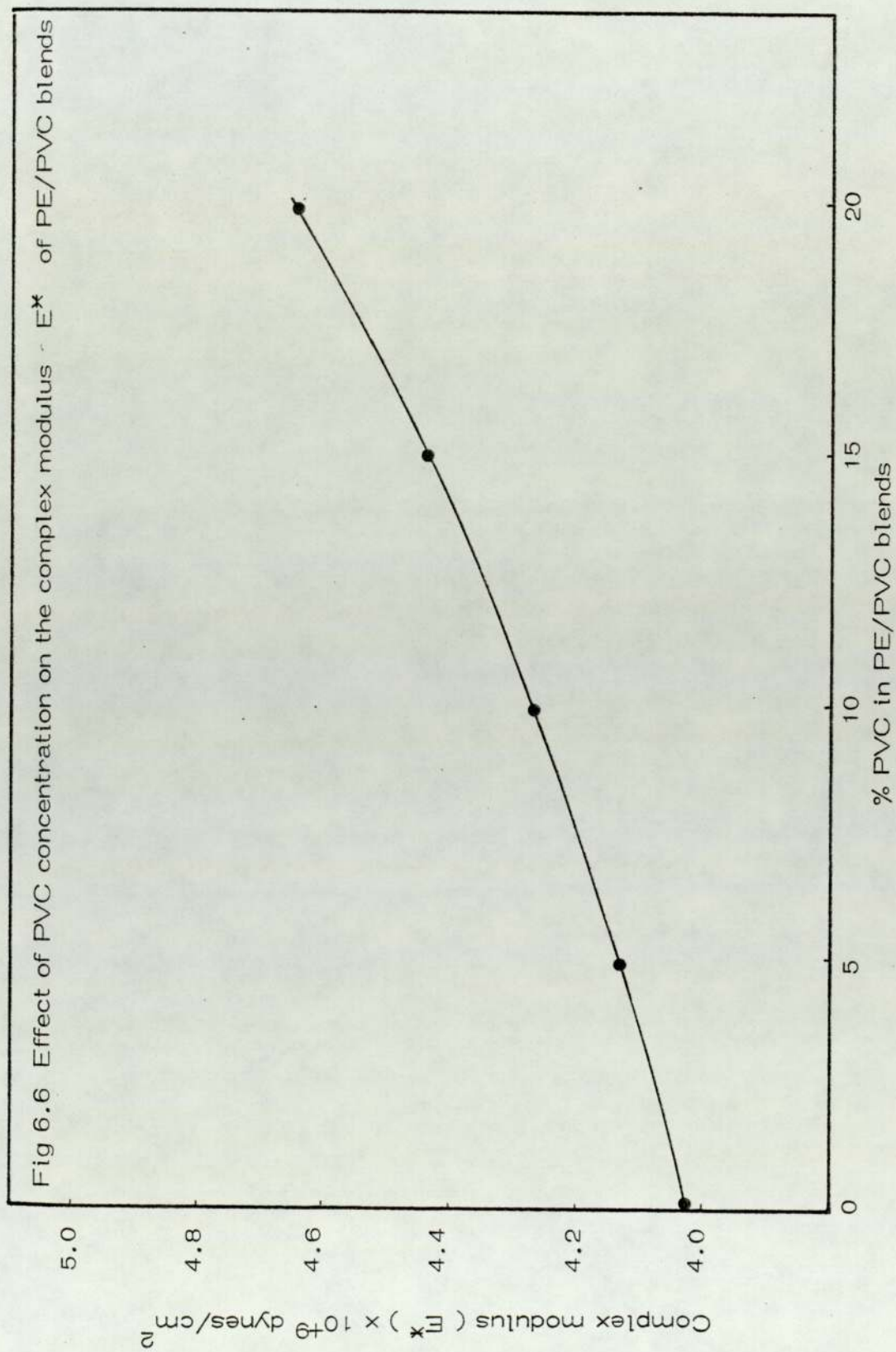
The impact strength follows a similar decrease to the elongation curve (Fig 6.4). This is again due to the increased viscoelasticity (Fig 6.4) as a result of the addition of polyvinyl chloride (PVC). Impact energy is dissipated by relaxation mechanisms, ie chain rotation.

Fig 6.5 shows the decrease in $\tan \delta$ at room temperature ($20 \pm 1^\circ\text{C}$) -vs- PE/PVC blend compositions. There is often a good correlation between the impact strength and the dynamic mechanical properties of polyblends⁽²⁴³⁻²⁴⁸⁾. Impact strength generally increases as the size of the damping peak due to the rubber phase increases⁽²⁴⁵⁻²⁴⁷⁾ (see Figs 6.4 and 6.5). Boehme et al⁽²⁴⁹⁾ studied the effect of fillers on dynamic mechanical properties of polyethylene. They found that fillers often decrease the damping as expressed by G''/G' ; in which case the damping can generally be approximated by^(250,251) (see Chapters 1 and 4 for fuller discussion):

$$G''/G' = (G''/G')_1 Q_1 + (G''/G')_2 Q_2$$

(Q_1 and Q_2 refer to the matrix phase and dispersed phase respectively) The damping of most rigid fillers is very low compared to that of the polymer, so $(G''/G')_2$ is nearly zero and can be neglected. So it might be expected that $\tan \delta$ (at room temperature, $20 \pm 1^\circ\text{C}$) will decrease as the PVC content increases. Fig 6.6 shows an increase in complex modulus with increase of PVC content. This is supported by Nielsen⁽²⁵¹⁾ and Boehme⁽²⁴⁹⁾ who found that fillers often increase the modulus.





6.A.3 Effect of PVC Concentration on Thermal Oxidation of PE/PVC Blends

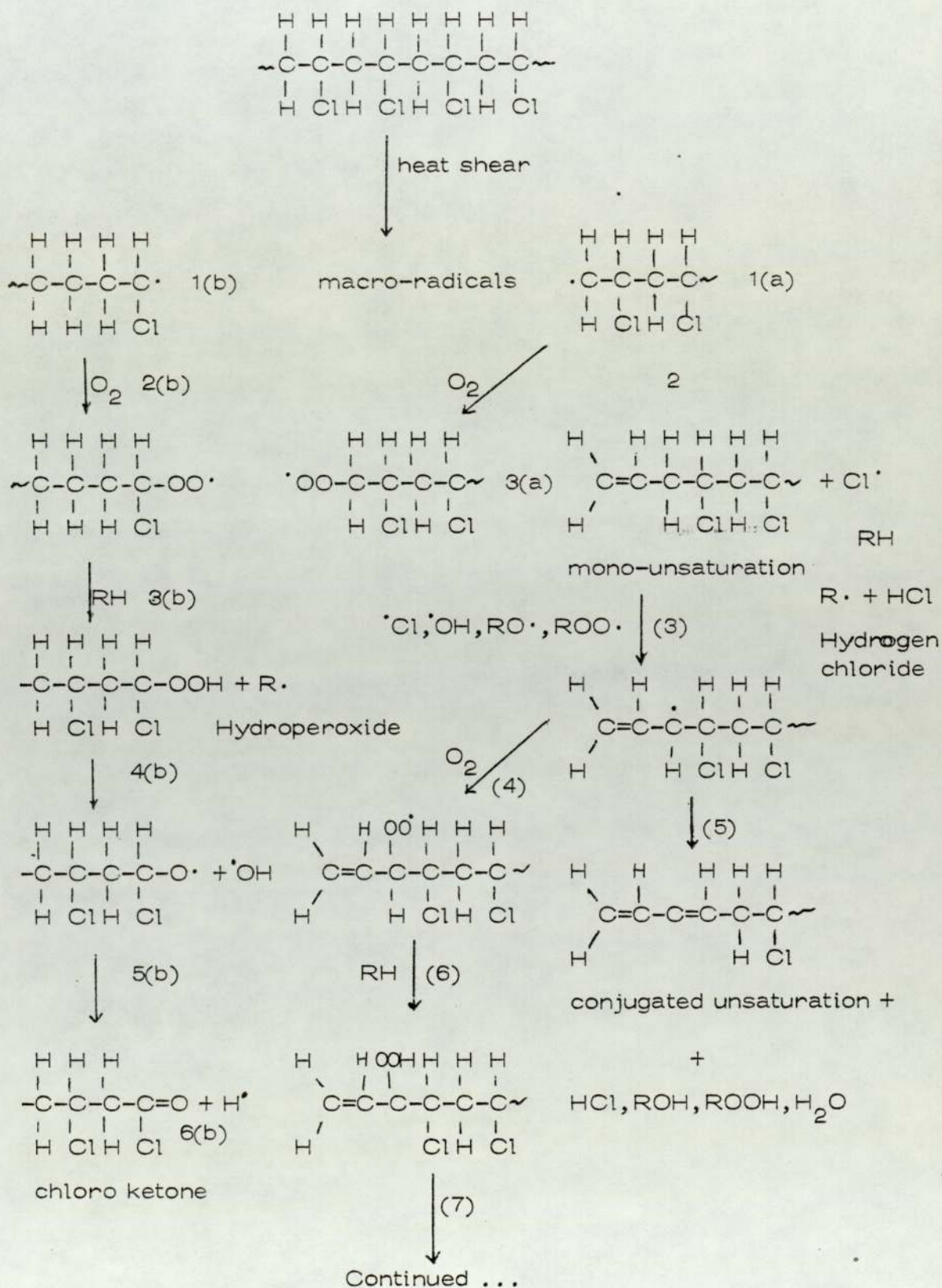
6.A.3.1 Introduction

The degradation of polyethylene and polyvinyl chloride as pure polymers have been extensively studied^(291,252,292). Little work has been previously reported on degradation of blends. Before discussing this, it is useful to consider briefly the degradation of each polymer contained in the blends.

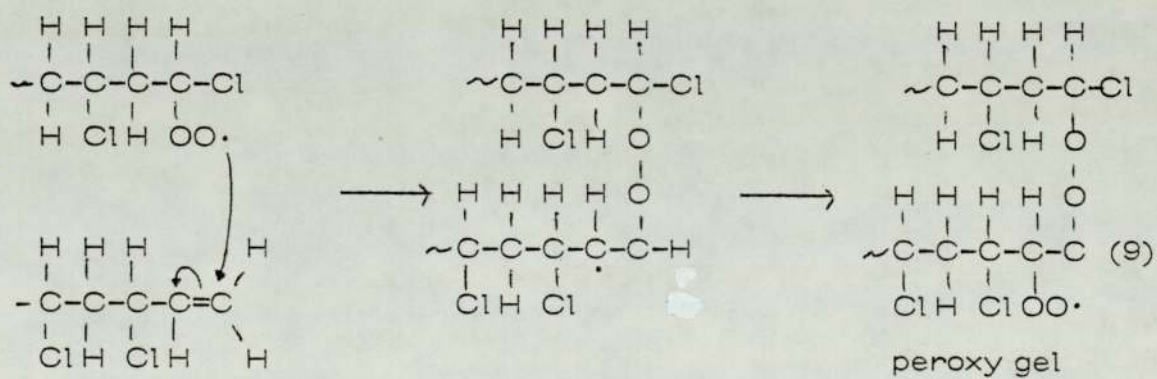
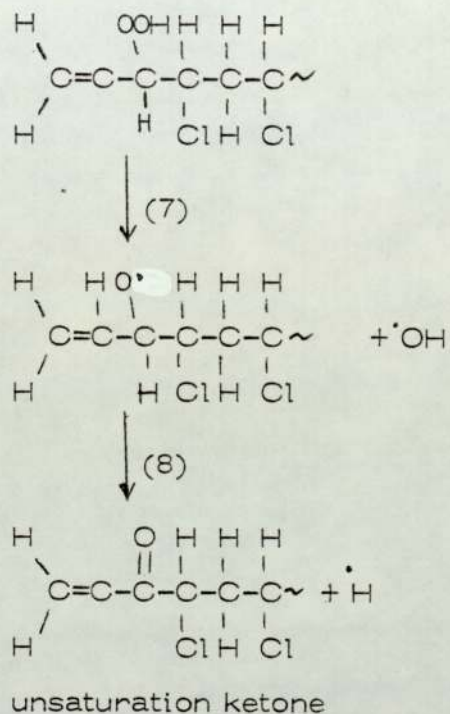
The thermal and uv degradation of LDPE has been discussed in Chapter 4. Photochemical degradation of polyvinyl chloride can be discussed in relation to thermal and high energy degradation because these processes are well known and several fundamental reactions occur in a similar way^(210,291,292,252).

Although the access of air is restricted in the torque rheometer, it has previously been shown that oxygen is always present⁽¹⁴⁸⁾. It has been suggested^(148,198) that the effect of oxygen during processing may have a significant effect. Scott and Vyvoda^(291,292,210) after a systematic and detailed study of the degradation of rigid polyvinyl chloride during processing in the RAPRA torque rheometer have suggested the following fundamental reaction sequence to account for the chemical modification undergone by the polymer:

Scheme



Scheme Continued



During commercial processing operations, the solid polymer is subjected to high temperature and high mechanical shear in order to cause melting and mixing. The melt is moulded, extruded or fabricated by a variety of suitable means. The solid polymer initially passes through the rubbery phase during which macroradical formation occurs by chain scission. The rubbery phase is most susceptible to scission due to its limited deformability on application of shear. When the rubbery phase fuses to the melt phase (liquid), the polymer is more readily deformed by applied shear and macroradical formation would be less favoured. The macroradicals formed by the scission process (see Scheme 1(a) and 1(b)) undergo rapid chemical reaction to produce peroxides and unsaturation (Scheme 2(b), 3(a) and 2). Peroxide formation is facilitated by the presence of entrapped oxygen in the polymer. The formation of unsaturation is accompanied by liberation of hydrogen chloride and the production of allylic sites in the polymer. The allylic hydrogen atoms are most susceptible to abstraction by free radicals and this leads to the formation of further peroxides and conjugated unsaturation in the polymer. Conjugated unsaturation in turn leads to colour formation during processing.

The thermal decomposition of hydroperoxides produces alkoxy and alkylperoxy free radicals (Scheme 4(b)). The alkoxy radicals may be terminated by ketone formation and the alkylperoxy radicals may abstract labile hydrogen atoms from the polymer to produce more hydroperoxide and/or react with unsaturation generated to form peroxy cross-links (Scheme 9).

Polymers and random copolymers are homogeneous materials.

Any discussion of the degradation of polymer blends must begin with the observation that, with very few exceptions, blends of two polymers are heterogeneous. This is seen most clearly when a film is cast from a solution. If the solution contains one polymer, the film will be transparent, if it contains two polymers, the resulting film will usually be opaque, due to phase separation and light diffraction between the two phases. This phase separation has an important bearing on the type of reaction which can occur in the degrading blend.

Optical and scanning electron microscopic examination of a heterogeneous polymer blend is shown in Plates 1-12. There exists a continuous phase of PE and a dispersed phase of PVC, so that we have domains consisting of a single pure polymer, separated by a phase boundary from the domains of the other polymer.

Because of the two-phase nature of polymer blends, degradation can be grouped into two categories⁽²⁵³⁾ comprising reactions occurring in the bulk of one or other or both domains, and reactions occurring at phase boundaries. Since the effective interfacial volumes involved are small in relation to the bulk volume of the sample, bulk reactions within a phase are much more probable than reactions across a boundary surface⁽²⁵³⁾. McNeill has suggested that six processes appear feasible⁽²⁵³⁾:

in bulk:	small molecule + macromolecule
	small radical + macromolecule
	small molecule + macroradical

at phase boundaries	2 small molecules (product interaction)
	2 macromolecules
	macromolecule + macroradical

In some situations, product interaction might also occur in the gas phase or after condensation⁽²⁵³⁾.

6.A.3.2 Results and Discussion

Figs 6.7 to 6.10 show infra-red spectra of processed LDPE and blend compositions (LDPE/PVC, 10, 15 and 20% PVC) which were thermally oxidised in an oven for various lengths of time at $100 \pm 2^\circ\text{C}$ in the presence of air. The three regions in the spectra viz $3600\text{--}3000\text{ cm}^{-1}$, $1850\text{--}1600\text{ cm}^{-1}$ and $1200\text{--}850\text{ cm}^{-1}$ where the most pronounced changes are found correspond to the absorption frequencies associated with O-H stretching mode⁽¹⁸²⁾ in various hydroxyl containing compounds, C=O stretching vibration in carbonyl oxidative products⁽¹⁸²⁾ and C-H bending or deformation modes in olefinic double bonded compounds respectively.

As mentioned in Chapter 4, during the thermal oxidation of low density polyethylene at 110°C in air the infra-red absorption band at 3555 cm^{-1} became more intense as the oxidation proceeded. This absorption was attributed to hydroperoxide groups. The wavelength of this band is identical to the wavelength of the band due to O-H stretching vibration in t-butyl hydroperoxide, cumene hydroperoxide and cyclohexene hydroperoxide⁽²⁵⁴⁾. It was indicated that the 3555 cm^{-1} band denotes the presence of a free hydroperoxide group, whereas 3400 cm^{-1} band denotes an associated

Fig 6.7 Change in hydroxyl hydroperoxide ($3600-3000\text{ cm}^{-1}$) and carbonyl ($1800-1600\text{ cm}^{-1}$) absorption during thermal oxidation of 100% LDPE film (numbers on curves are heating time in hours)

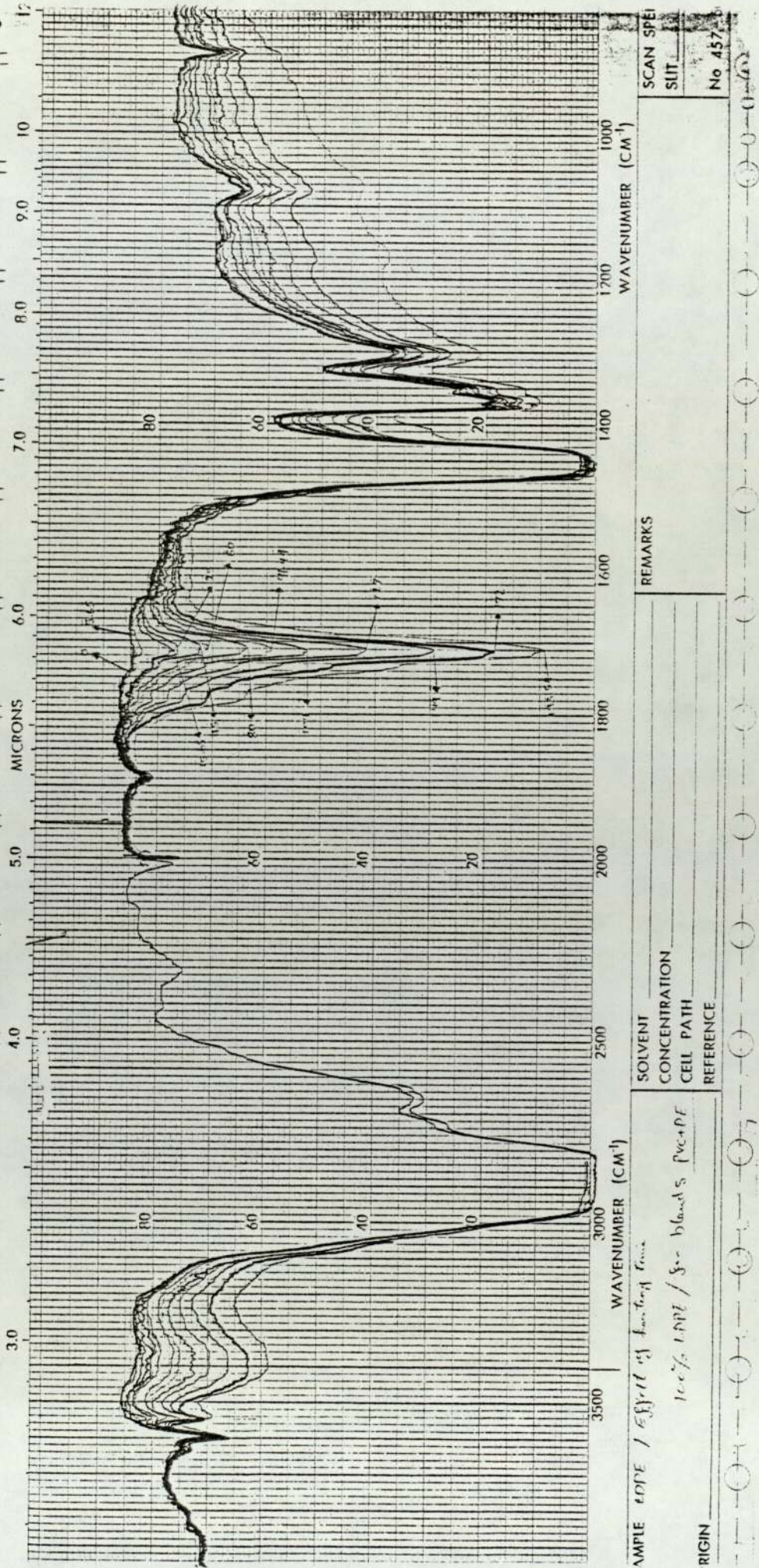
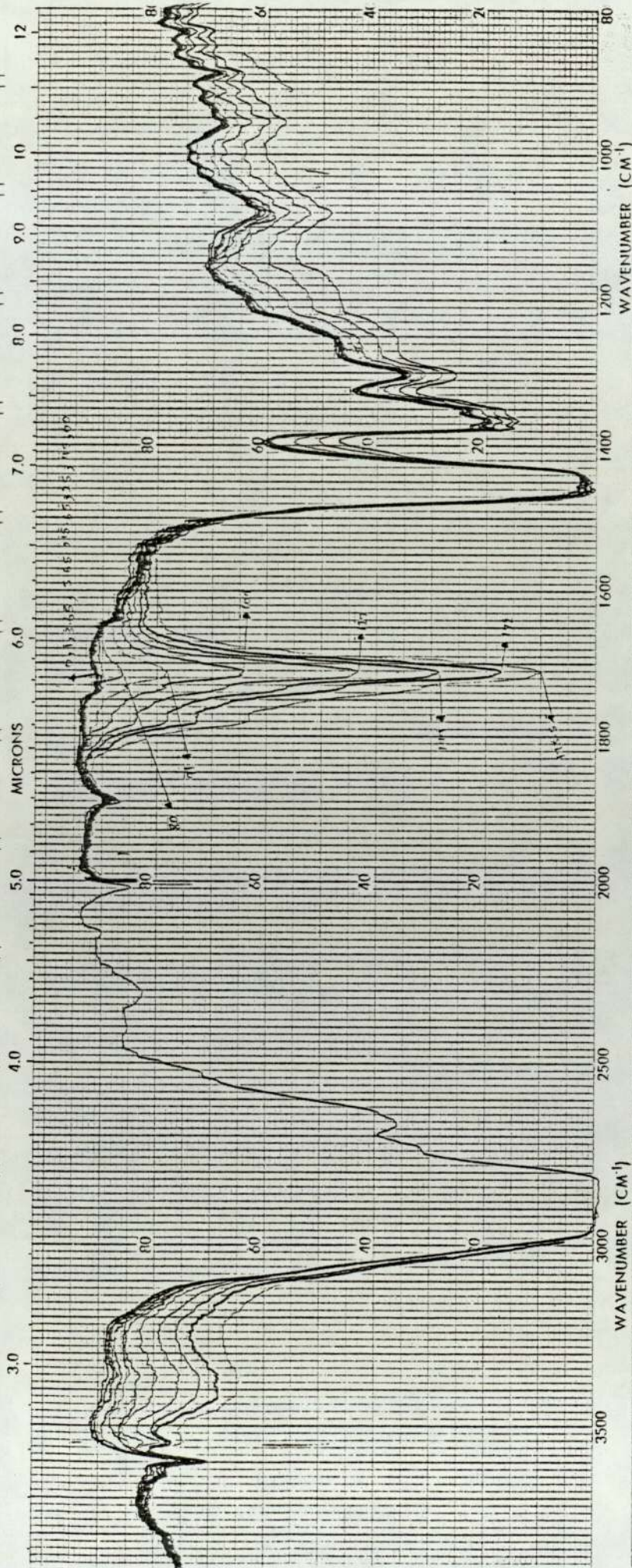
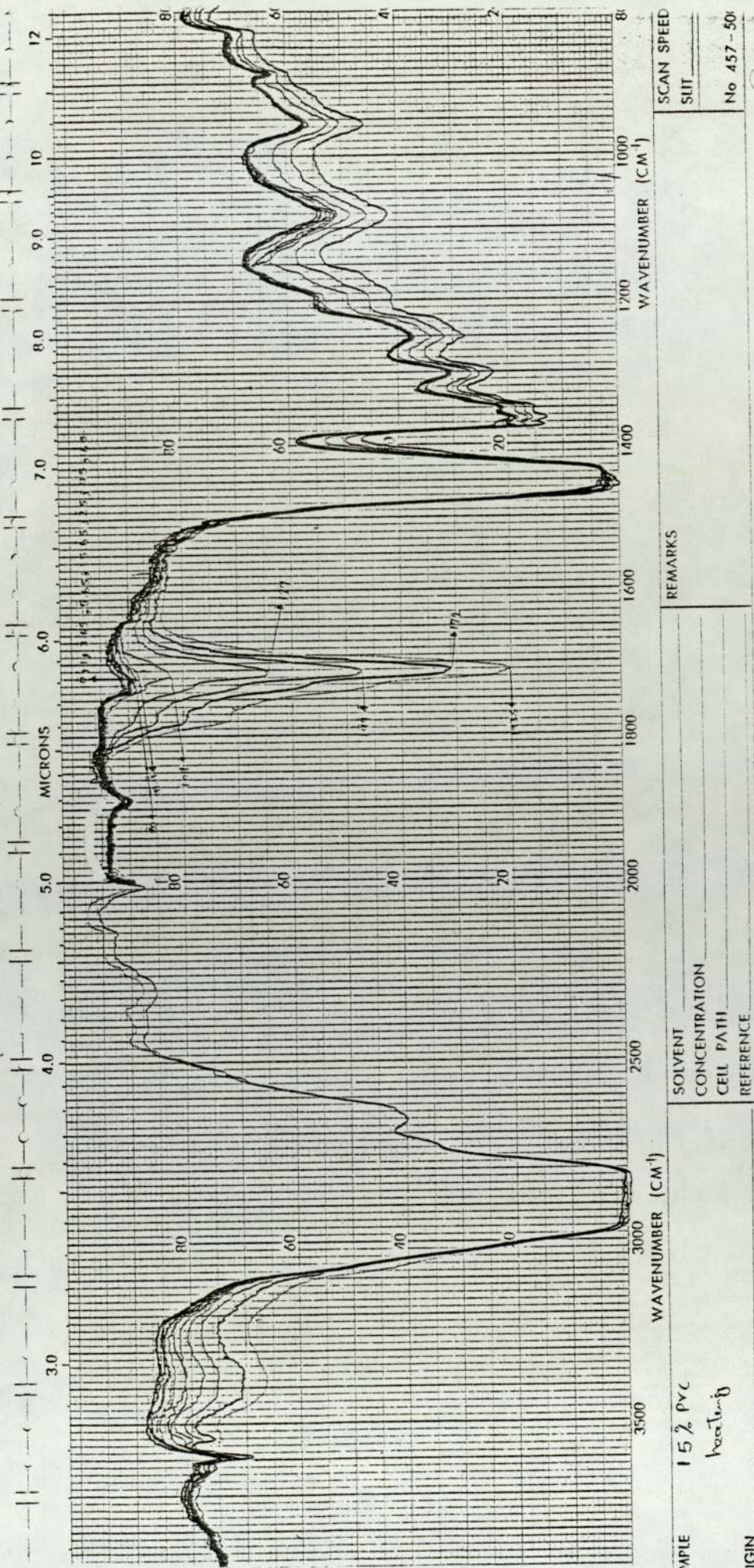


Fig 6.8 Change in hydroxyl hydroperoxide ($3600-3000\text{ cm}^{-1}$) and carbonyl ($1800-1600\text{ cm}^{-1}$) absorption during thermal oxidation of LDPE + 10% PVC film (numbers on curves are heating time in hours)



FILE	10% PVC	SOLVENT		REMARKS	SCAN SPEED
	Non-oxid	CONCENTRATION			SLIT
		CELL PATH			
		REFERENCE			No. 457-5001
3IN					

Fig 6.9 Change in hydroxyl hydroperoxide ($3600-3000\text{ cm}^{-1}$) and carbonyl ($1800-1600\text{ cm}^{-1}$) absorption during thermal oxidation of LDPE + 15% PVC film (numbers on curves are heating time in hours)



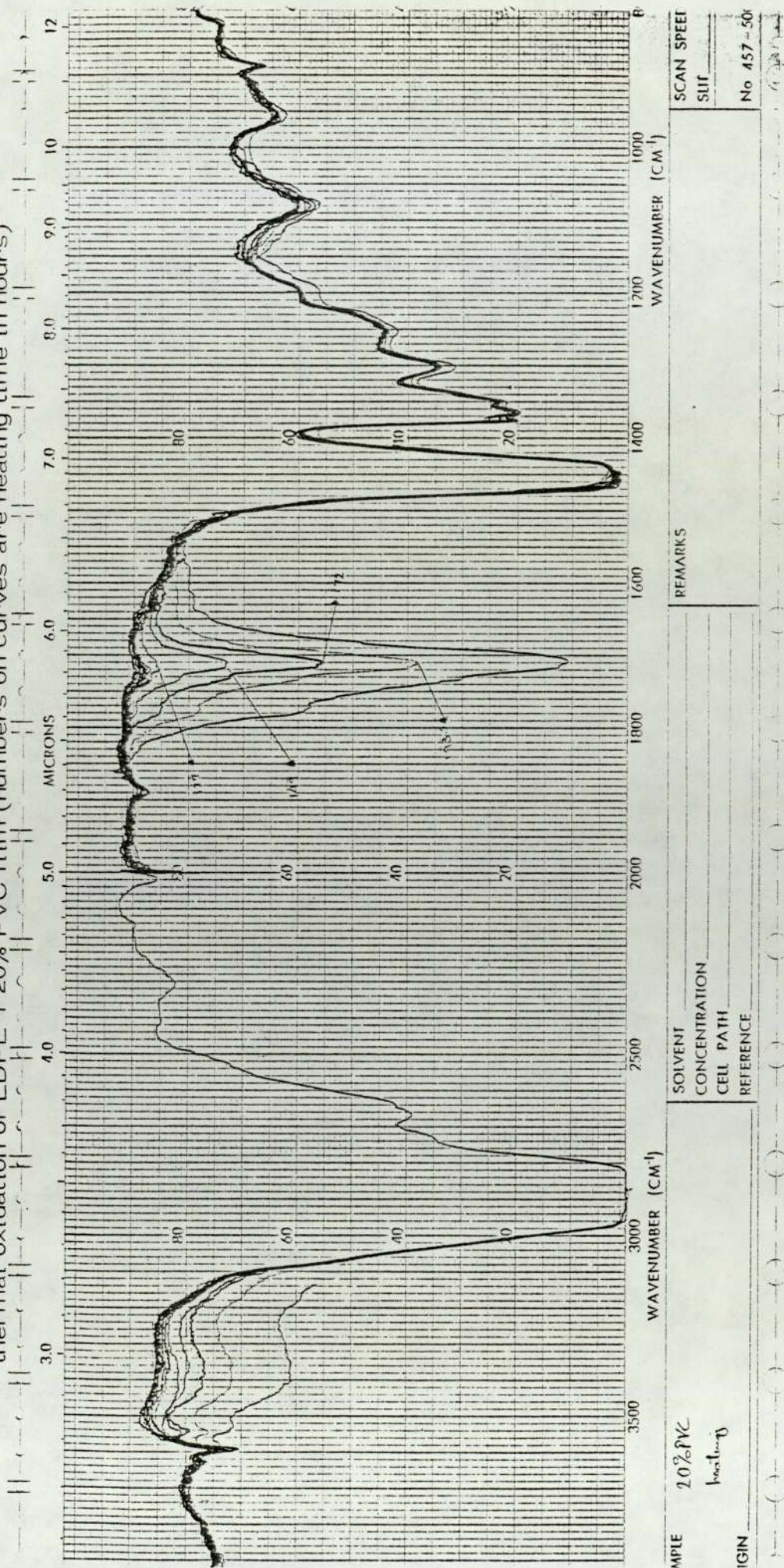
WAVENUMBER (CM ⁻¹)	REMARKS	SCAN SPEED
3500		SUIT
3000		No 457-50
2500		
2000		
1800		
1600		
1400		
1200		
1000		
800		
MICRONS		
3.0		
4.0		
5.0		
6.0		
7.0		
8.0		
9.0		
10		
12		

SAMPLE 15% PVC heating

SOLVENT _____
 CONCENTRATION _____
 CELL PATH _____
 REFERENCE _____

WAVENUMBER (CM⁻¹)

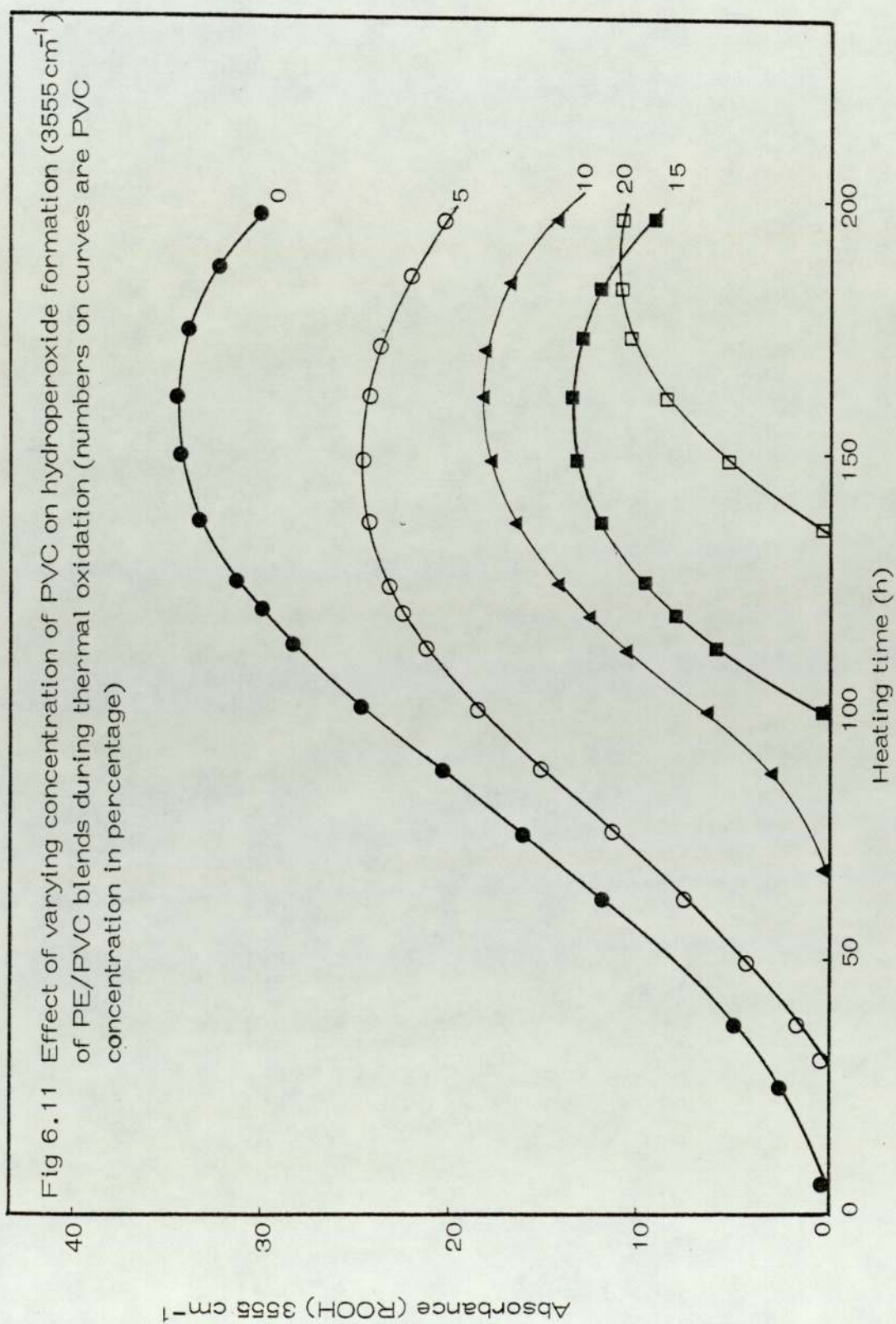
Fig 6.10 Change in hydroxyl hydroperoxide (3600-3000 cm^{-1}) and carbonyl (1800-1600 cm^{-1}) absorption during thermal oxidation of LDPE + 20% PVC film (numbers on curves are heating time in hours)



hydroperoxide group.

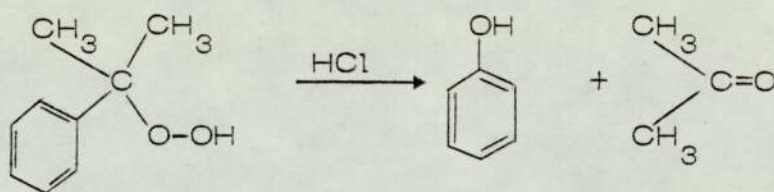
Fig 6.11 presents curves showing the change in hydroperoxide concentration with heating time at $100 \pm 2^\circ\text{C}$ in processed blends (5, 10, 15 and 20% PVC). Hydroperoxide shows an induction period that increased with the percentage of PVC in the blends. This could be due to the decomposition of hydroperoxide in the system by hydrogen chloride formed from degraded PVC. The dehydrochlorination of PVC under a variety of thermal and processing conditions has been well documented⁽²⁵⁵⁾. The effect of hydrogen chloride on the degrading polymer has not been clearly explained in the literature. Under most conditions and especially in the presence of oxygen, hydrogen chloride has been reported to exhibit dehydrochlorination catalysis⁽²⁵⁶⁻²⁵⁸⁾, though under certain experimental conditions it has also been found to inhibit dehydrochlorination⁽²⁵⁹⁾. The mechanism by which dehydrochlorination reactions are influenced by hydrogen chloride has been described in terms of ionic⁽²⁵⁶⁻²⁵⁸⁾, free radical⁽²⁶⁰⁻²⁶²⁾, molecular (concerted)⁽²⁶³⁾ and dual⁽²⁶⁴⁾ mechanisms.

Recently, it has been shown that in addition to dehydrochlorination, peroxide formation⁽²⁶⁵⁾ is a significant chemical modification occurring during the degradation of the polymer under processing conditions and the interaction of peroxides and hydrogen chloride is thought to be responsible for the rapid HCl elimination from the polymer during processing. (Though such a reaction has been previously reported⁽²⁶⁶⁾). Thus the effects of hydrogen chloride on the thermal decomposition of peroxides may be central to the understanding

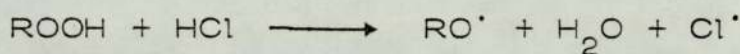


of PVC degradation.

Scott and co-workers⁽²⁵⁷⁾ recently studied the effect of hydrogen chloride on decomposition of hydroperoxide. They found that the mechanism of the peroxide decomposing reaction is predominantly ionic at low hydrogen chloride to peroxide molar ratios whilst at relatively high (> 1) molar ratios, a free radical mechanism is favoured.



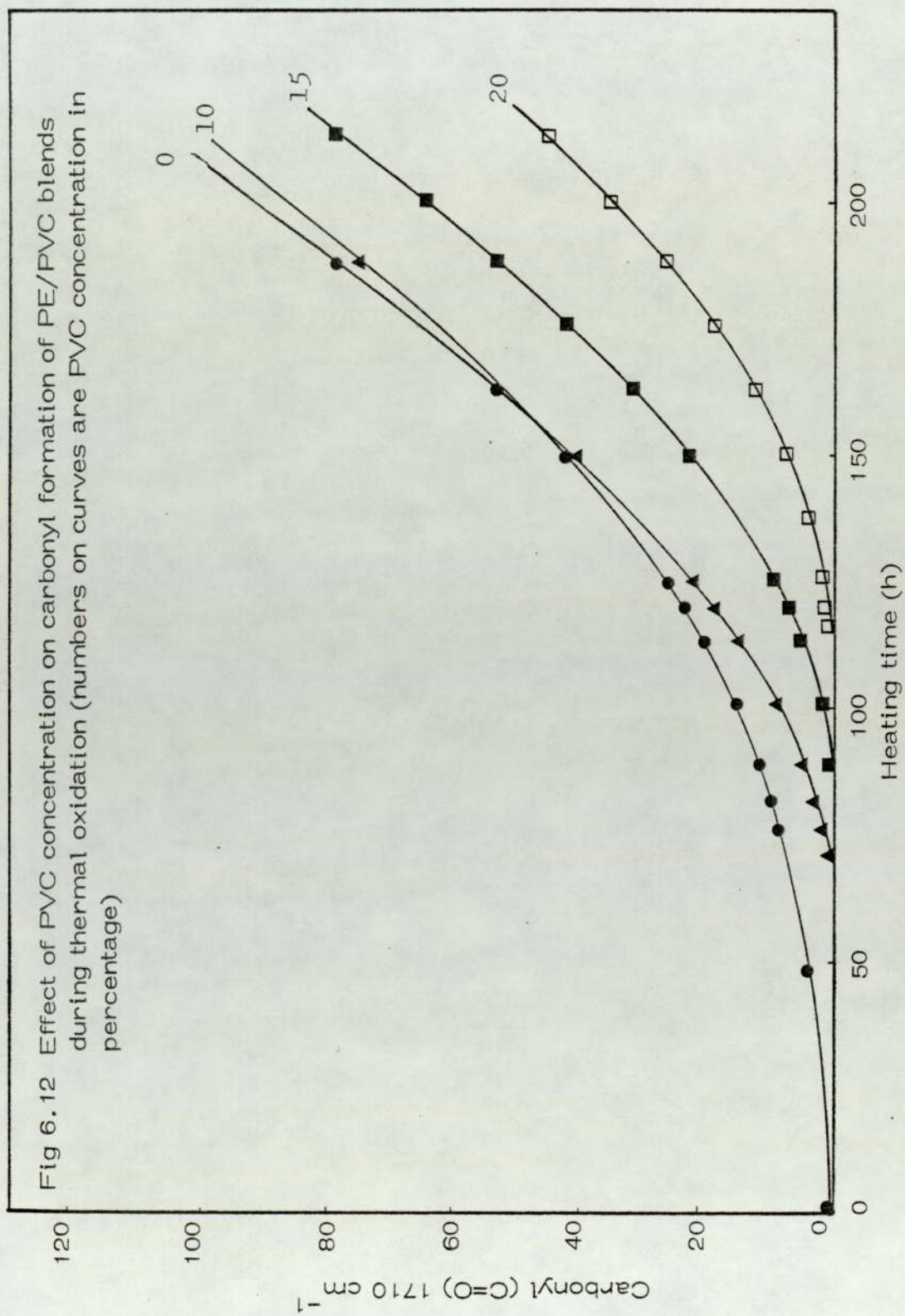
ionic decomposition



free radical decomposition

The inhibition of oxygen absorption at low hydrogen chloride concentration and the enhanced pro-oxidant effect observed at higher hydrogen chloride concentrations are entirely consistent with these mechanisms⁽²⁶⁷⁾.

During processing of blends (5, 10, 15 and 20% PVC in LDPE) and a further thermal oxidation, it seems that (Figs 6.11, 6.12) hydrogen chloride formed from degraded PVC can act as an antioxidant. This effect can also be observed in the carbonyl and hydroperoxide absorptions at 1710 and 3555 cm^{-1} respectively, which gave a longer induction period with increase in PVC concentration in the blend. A plot of induction period



of hydroperoxide against PVC concentration showed a linear relationship (Fig 6.13).

The results in Figs 6.11, 6.12 and 6.13 suggest that hydrogen chloride undergoes an ionic reaction with hydroperoxide formed in LDPE. Moreover, reduction of hydrogen chloride concentration in the presence of PVC stabilisers (T290, dibutyltin maleate) which rely mainly on scavenging hydrogen chloride⁽²⁶⁷⁾ is also evident as a result of the present studies. When the hydrogen chloride concentrations are significantly reduced, a general antioxidant effect is observed due to ionic destruction of peroxides by a deficiency of hydrogen chloride. In the absence of HCl scavenging stabiliser (T290) the induction period to hydroperoxide and carbonyl formation in a PE/PVC blend containing 20% PVC was found to be eliminated (Figs 6.10, 6.14, 6.15 and 6.16). This can be attributed to the pro-oxidant reaction between peroxides and high HCl concentration leads to free radical processes and hence peroxide accumulation⁽²⁶⁷⁾. Fig 6.17 indicates the effect of dibutyltin maleate (T290) concentration on the induction period of hydroperoxide.

An optical microscopic study of thermally oxidised PVC and blends with LDPE (Plates 13-18) indicate the formation of colour around the boundaries of the polymer phases. This colour is due to the formation of polyconjugated unsaturation in PVC.

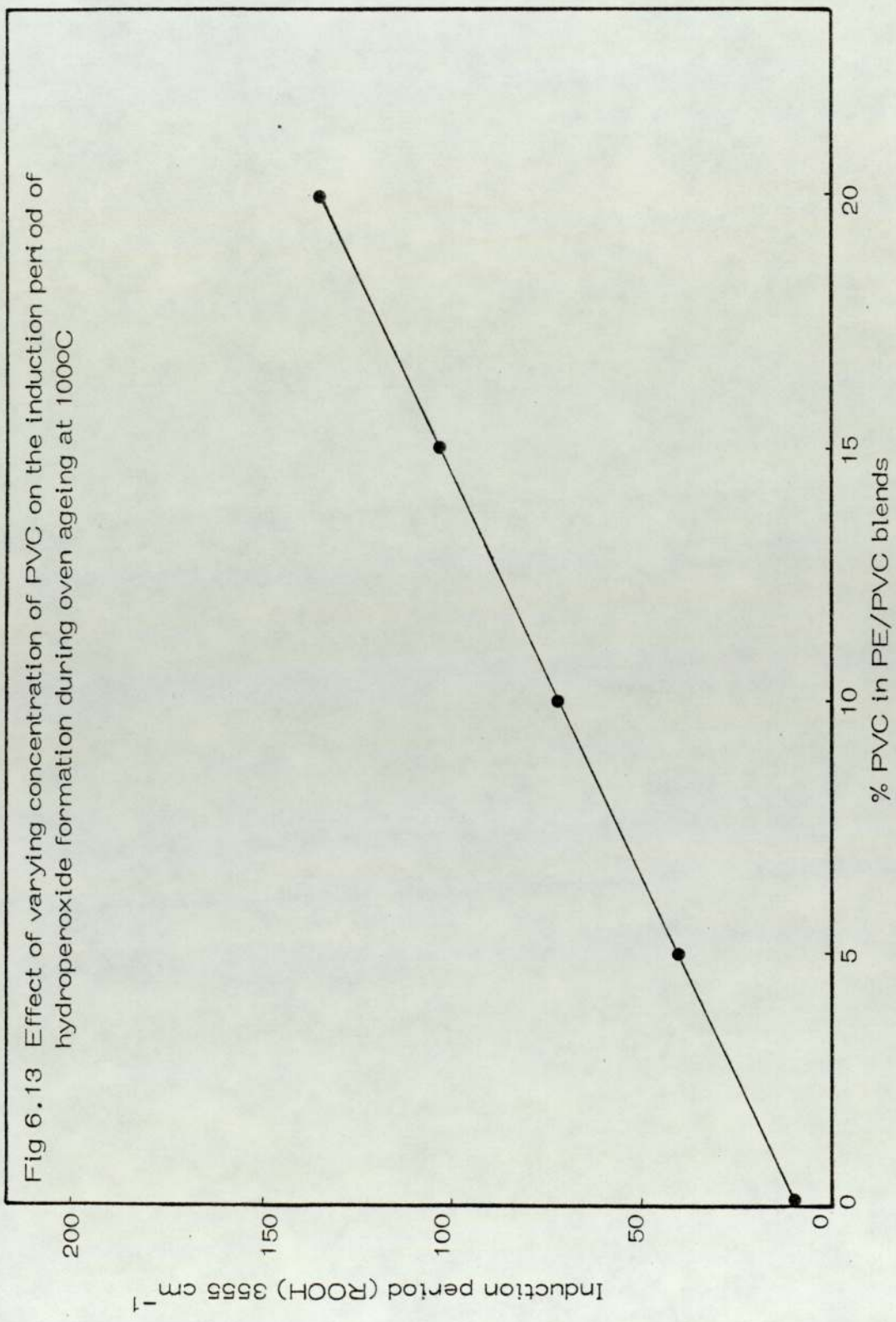
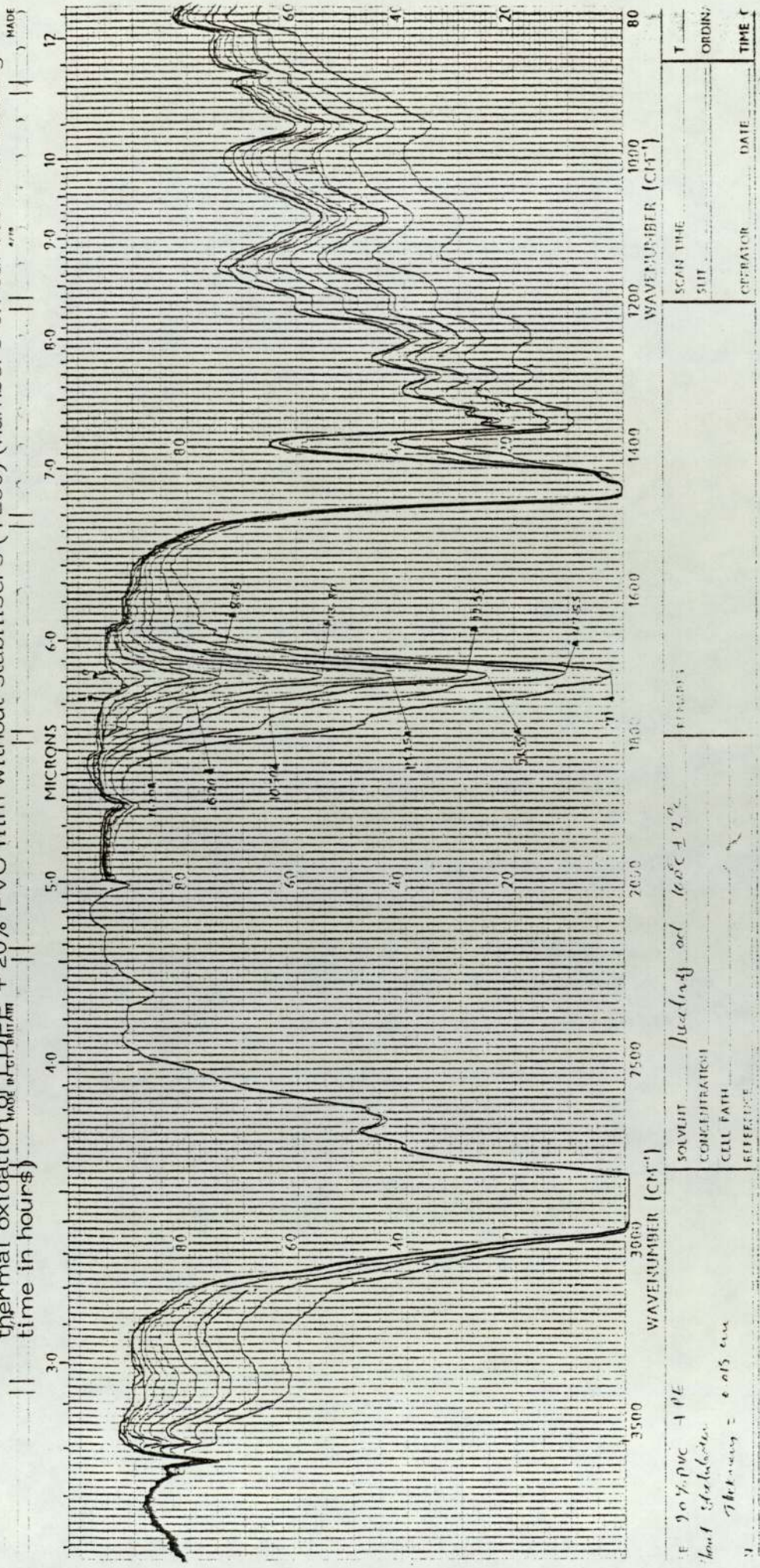


Fig 6.13 Effect of varying concentration of PVC on the induction period of hydroperoxide formation during oven ageing at 100°C

Fig 6.14 Change in hydroxyl hydroperoxide (3600-3000 cm^{-1}) and carbonyl (1800-1600 cm^{-1}) absorption during thermal oxidation of LDPE + 20% PVC film without stabilisers (T290) (numbers on curves are heating time in hours)

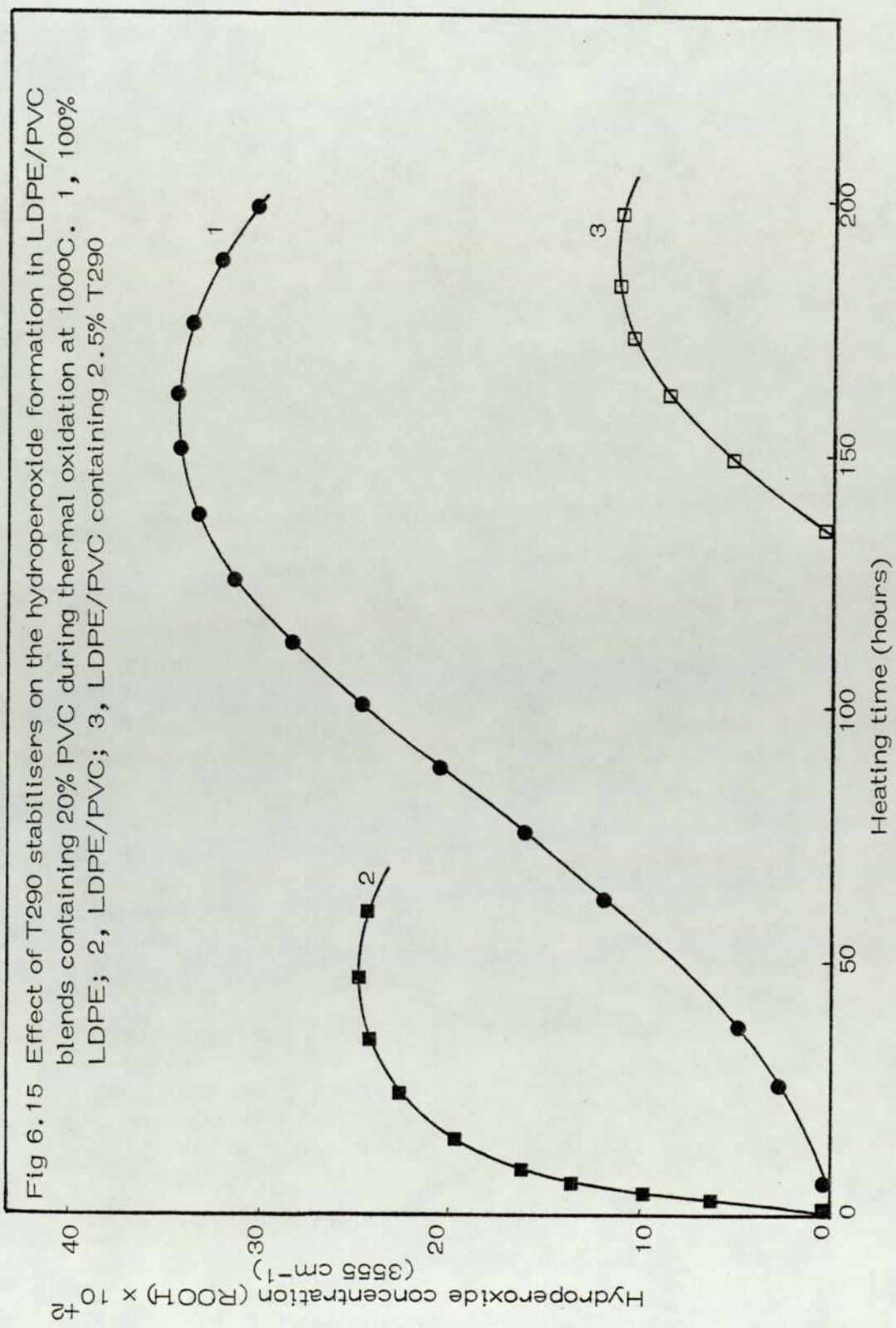


SOLVENT: *None* HEATING: *100°C ± 2°*
 CONCENTRATION: _____
 CELL PATH: _____
 REFERENCE: _____

T: _____ SCAN TIME: _____
 ORDIN: _____ SIFT: _____
 OPERATOR: _____ DATE: _____
 TIME: _____

E 90% PVC + 10%
 heat stabiliser
 Thickness = 0.015 cm

Fig 6.15 Effect of T290 stabilisers on the hydroperoxide formation in LDPE/PVC blends containing 20% PVC during thermal oxidation at 100°C. 1, 100% LDPE; 2, LDPE/PVC; 3, LDPE/PVC containing 2.5% T290



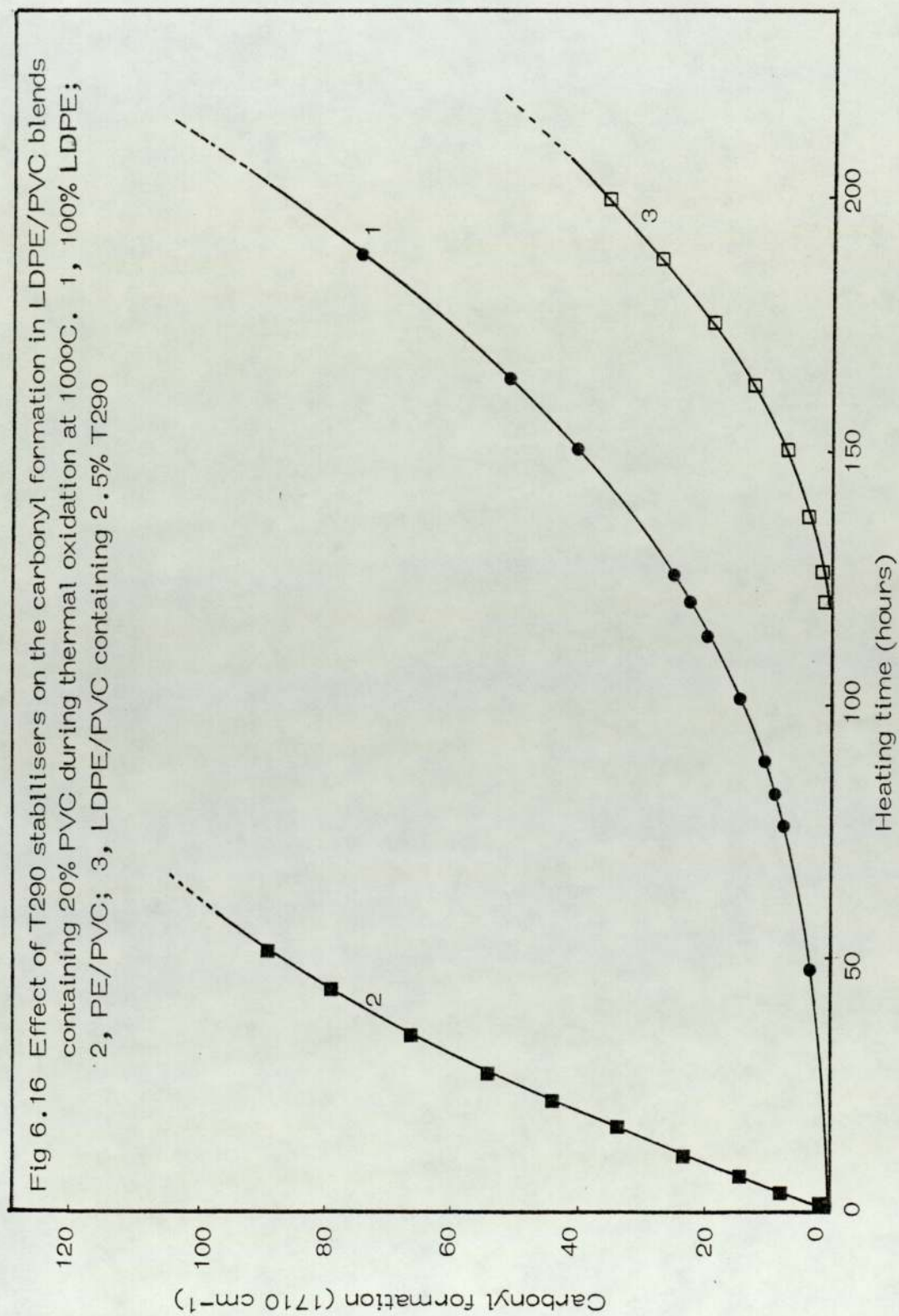


Fig 6.17 Effect of T290 concentration on the induction period of hydroperoxide formation during thermal oxidation of PE/PVC blends. 1, 2.5 mol/100 g PVC; 2, 1.25 mol/100 g PVC

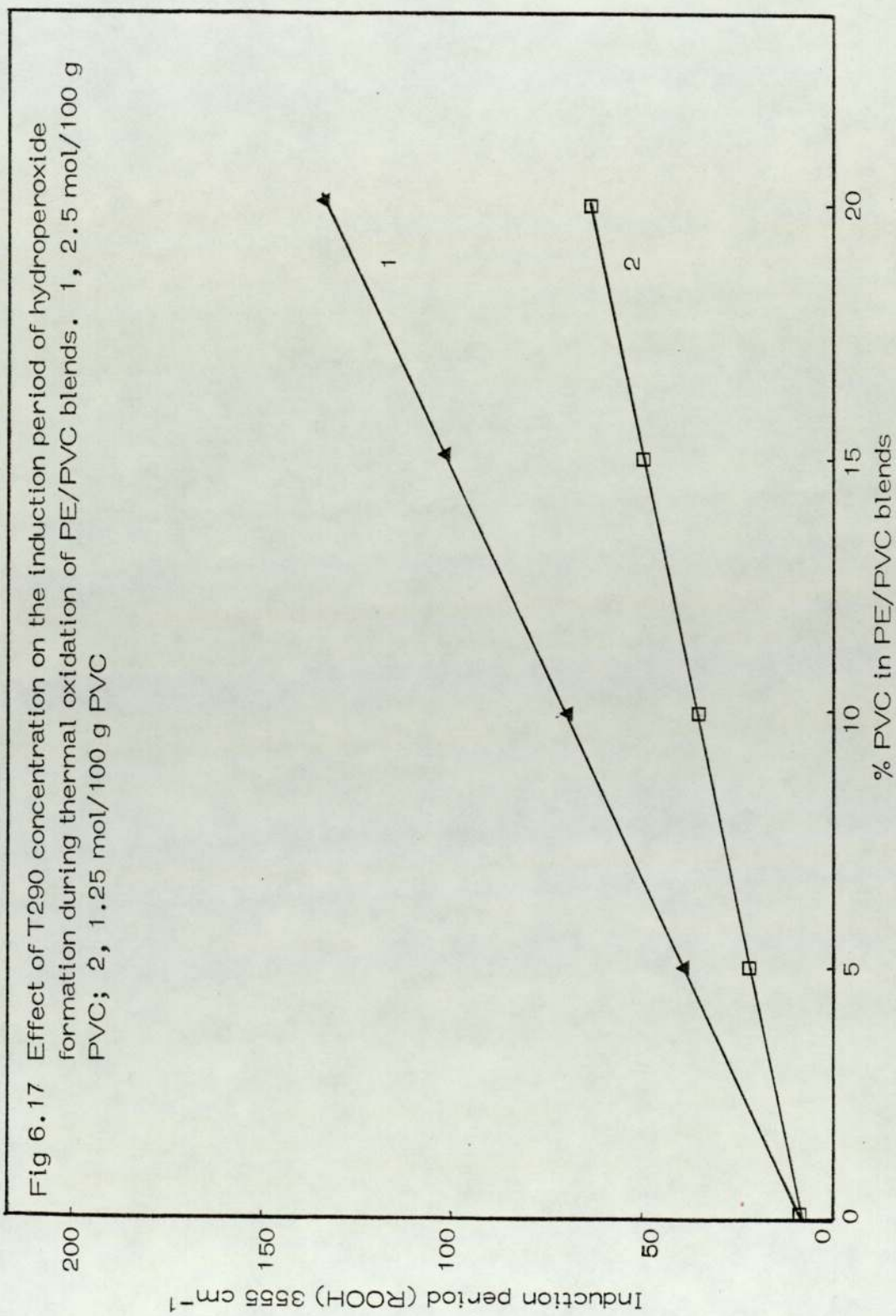




Plate 13 (100%PVC) Sample without heating (heating time= 0)



Plate 14 (100%PVC) Sample during 200 hours heating time at 100° C



Plate 15 (100%PVC) Sample during 450 hours heating time at 100° C



Plate 16 (PE + 20%PVC) Sample during
150 hours heating time at 100°C , $M_n=100$



Plate 17 (PE + 20%PVC) Sample during
330 hours heating time at 100°C , $M_n=100$

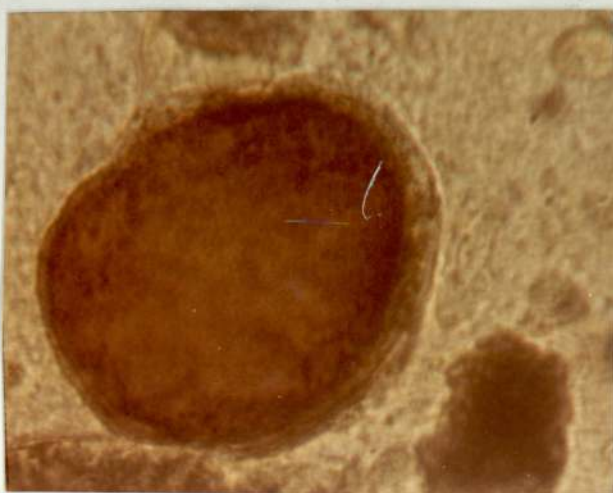


Plate 18 (PE + 20%PVC) Sample during
650 hours heating time at 100°C , $M_n=100$

6.A.4 Effect of PVC Concentration on the Photo-oxidation of LDPE/PVC Blends

6.A.4.1 Results and Discussion

Figs 6.18 - 6.21 show the change with uv irradiation in the different regions in the infra-red spectrum of film containing different blends. Differences were observed between the spectra of thermally oxidised (Figs 6.7 - 6.10) and photo-oxidised (Figs 6.18 - 6.21) blends film.

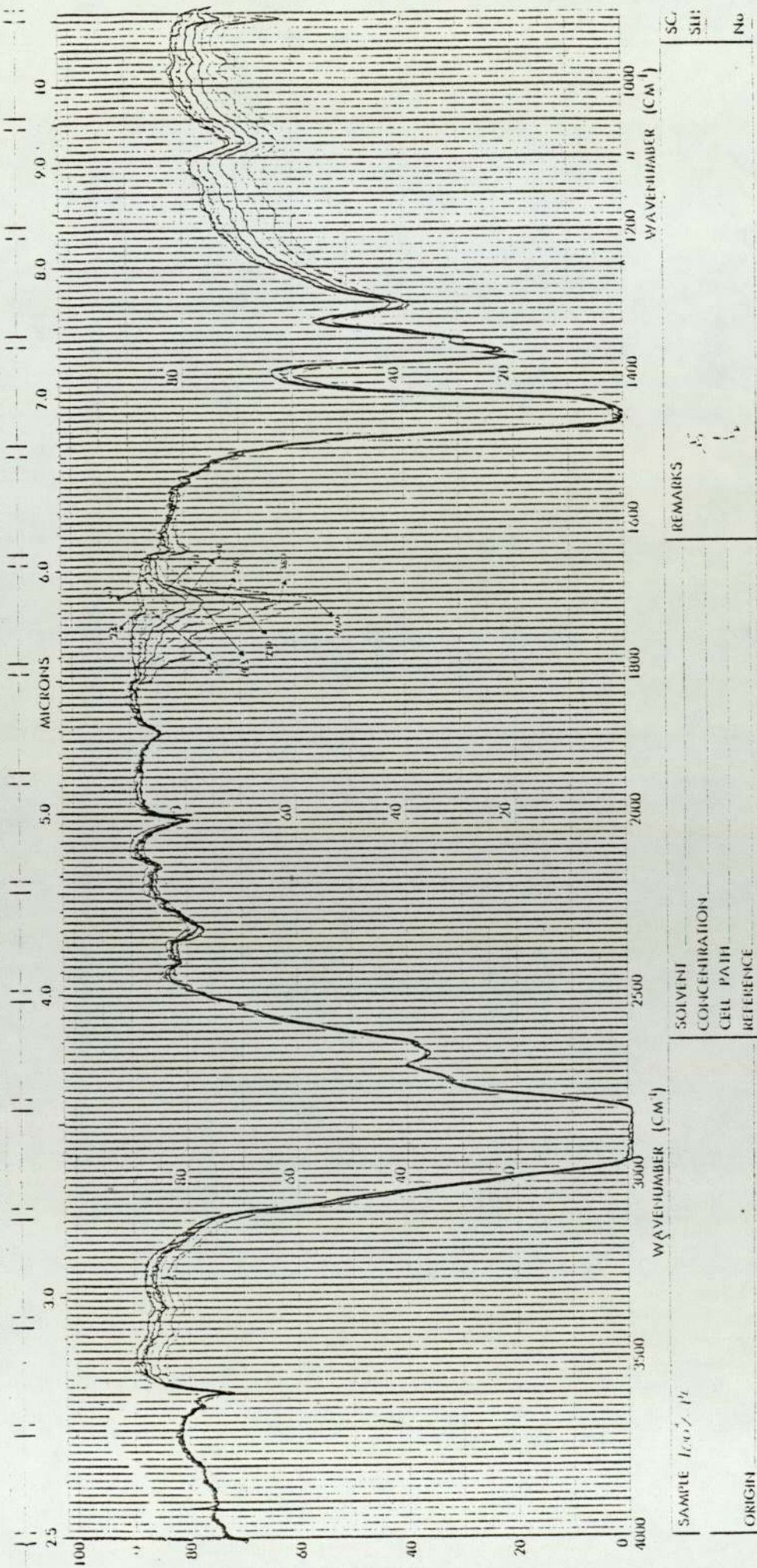
In the carbonyl region ($1800 - 1650 \text{ cm}^{-1}$) photo-oxidised blend films, like thermally oxidised films (Figs 6.7 - 6.10) showed a complex absorption with a large number of bands, the intensity of which increased with exposure time.

Fig 6.22 shows the effect of PVC concentration on the photo-oxidative stability of the blends and indicates that with increasing PVC concentration the rate of oxidation increased.

The deterioration of the physical properties was followed by stress-strain measurements, change in dynamic mechanical properties and impact strength as a function of exposure time (Figs 6.23 and 6.24). In the case of 100% LDPE, the tensile strength, elongation at break and impact strength were found to decrease with increasing uv exposure time. This is expected as the average molecular weight of polyethylene chains is reduced with photo-oxidation (more details in Chapter 4)⁽¹⁹⁷⁾.

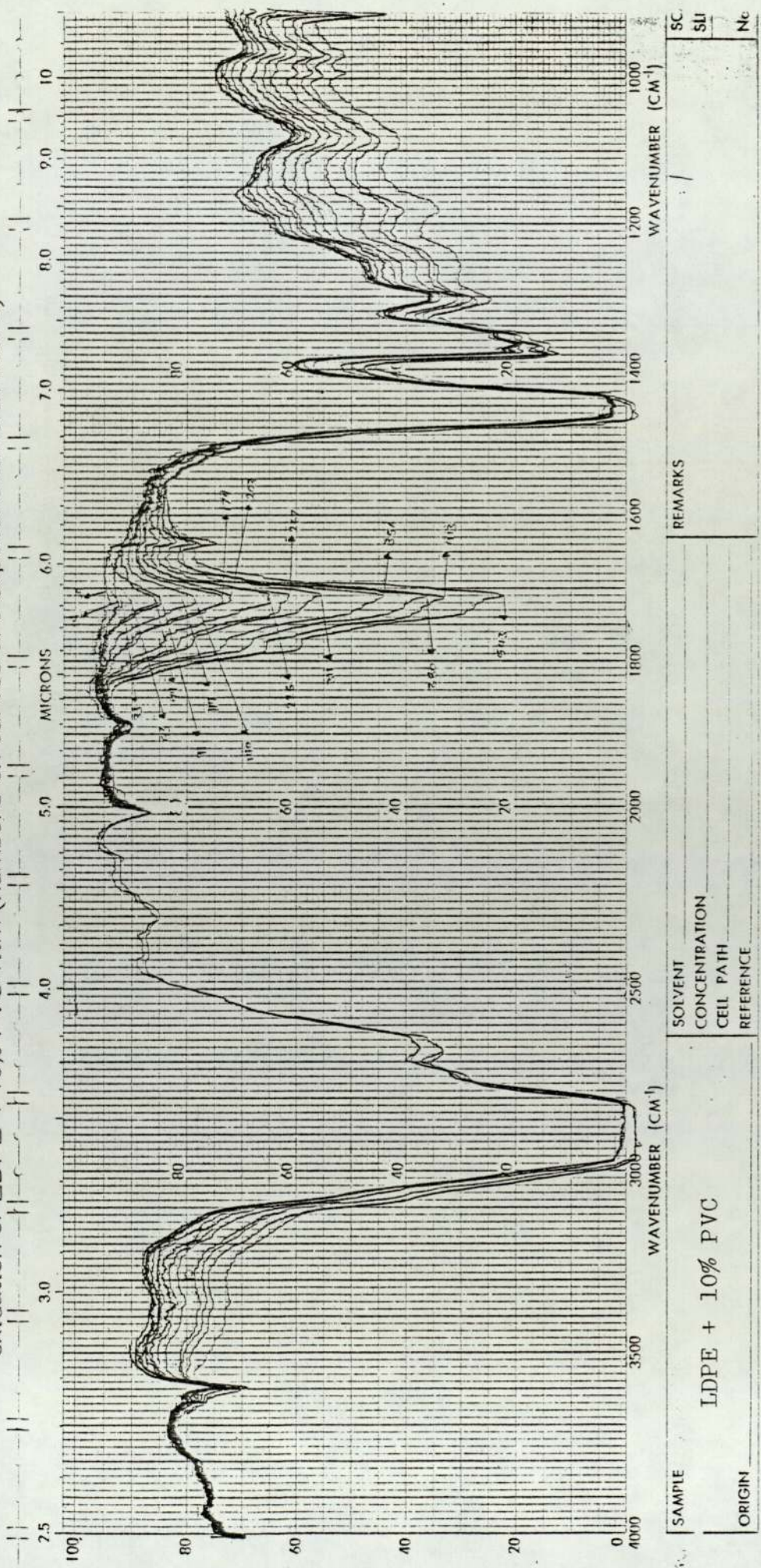
PE/PVC blends which were subjected to uv irradiation behave

Fig 6.18 Change in hydroxyl (3500-3000 cm^{-1}) and carbonyl (1800-1600 cm^{-1}) absorption during photo-oxidation of LDPE film (numbers on curves are exposure time in hours)



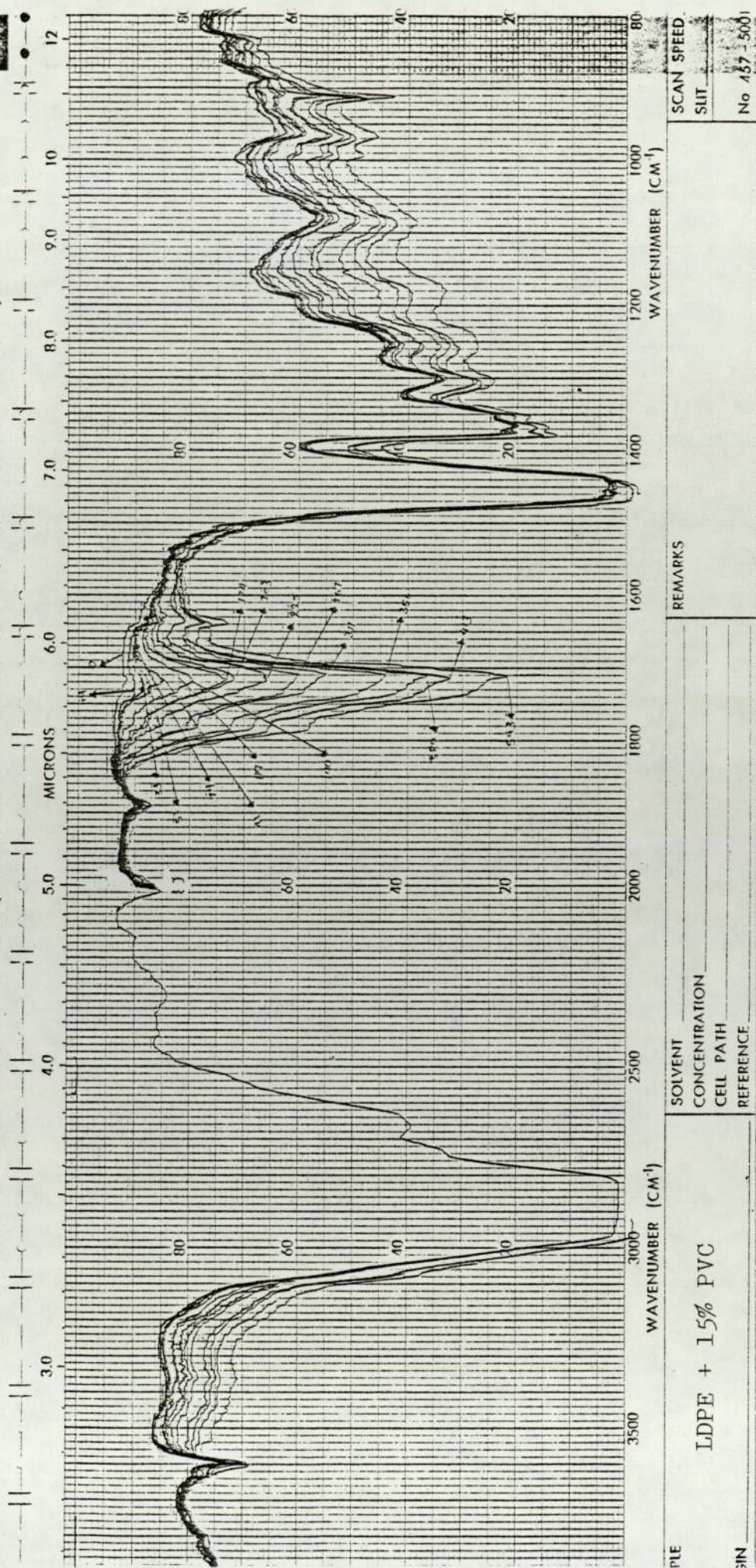
SAMPLE		SOLVENT		SC
10007-12				SU
		CONCENTRATION		No
		CELL PATH		
		REFERENCE		
ORIGIN		REMARKS		
				

Fig 6.19 Change in hydroxyl ($3500-3000\text{ cm}^{-1}$) and carbonyl ($1800-1600\text{ cm}^{-1}$) absorption during photo-oxidation of LDPE + 10% PVC film (numbers on curves are exposure time in hours)



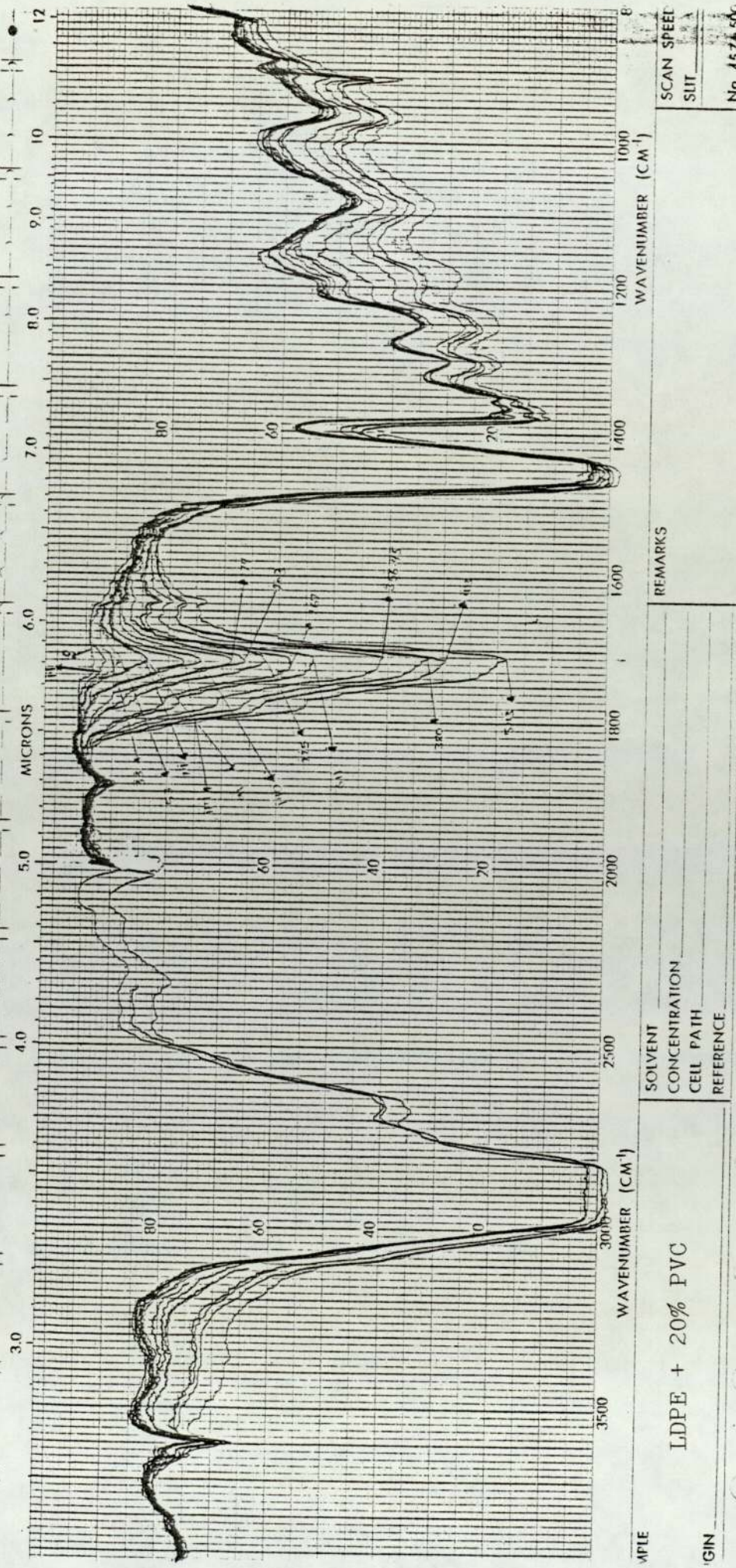
SAMPLE	SOLVENT	REMARKS	SC
	LDPE + 10% PVC		SU
ORIGIN	CONCENTRATION		Nc
	CELL PATH		
	REFERENCE		

Fig 6.20 Change in hydroxyl (3500-3000 cm^{-1}) and carbonyl (1800-1600 cm^{-1}) absorption during photo-oxidation of LDPE + 15% PVC film (numbers on curves are exposure time in hours)



FILE	SOLVENT	REMARKS
	CONCENTRATION	
	CELL PATH	
	REFERENCE	
LDPE + 15% PVC		
SCAN SPEED		
SLIT		
No 457, 5001		

Fig 6.21 Change in hydroxyl ($3500-3000\text{ cm}^{-1}$) and carbonyl ($1800-1600\text{ cm}^{-1}$) absorptions during photo-oxidation of LDPE + 20% PVC film (numbers on curves are exposure time in hours)



FILE _____

SAMPLE _____

LDPE + 20% PVC

SOLVENT _____

CONCENTRATION _____

CELL PATH _____

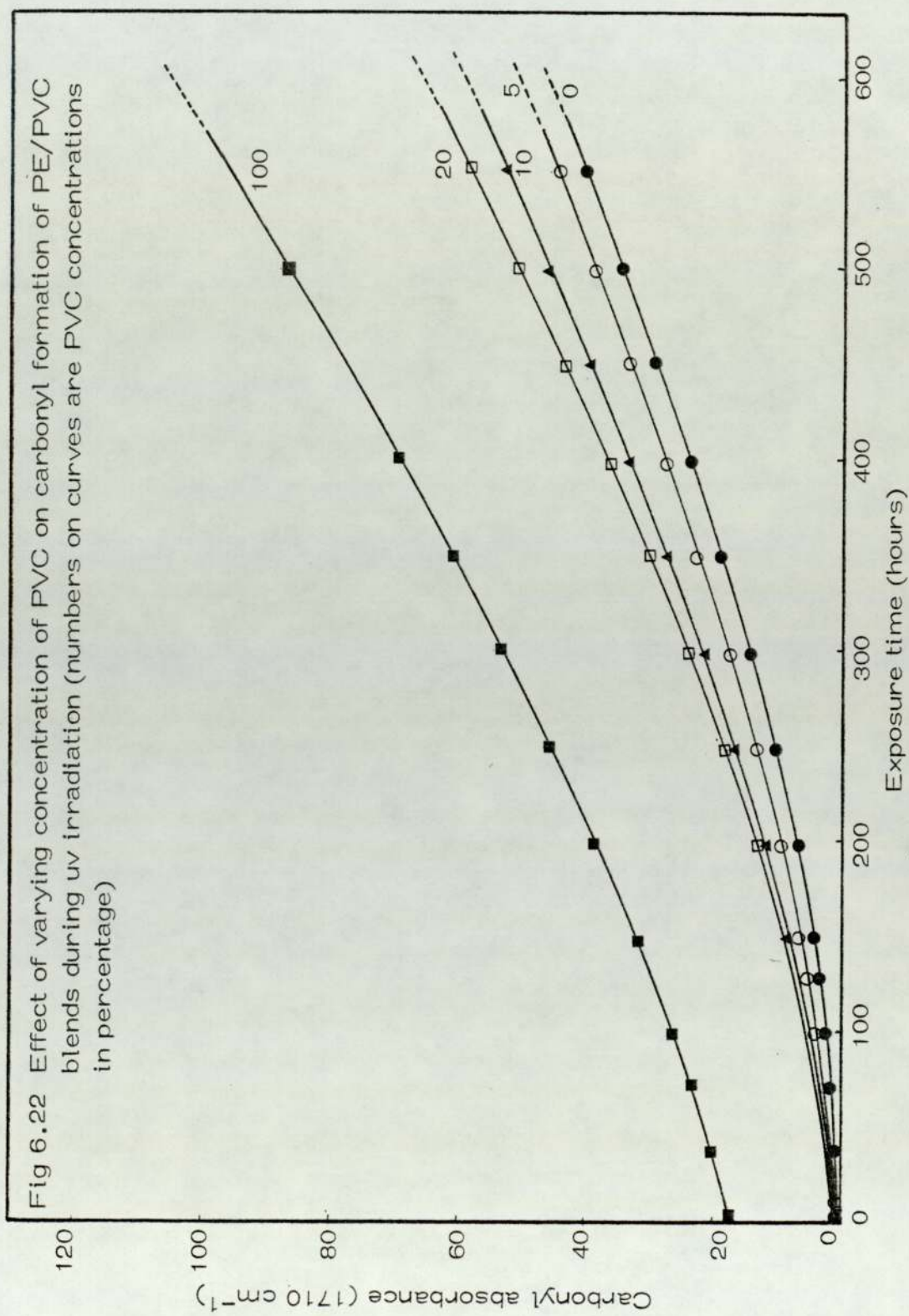
REFERENCE _____

REMARKS _____

SCAN SPEED _____

SUIT _____

No 457-500



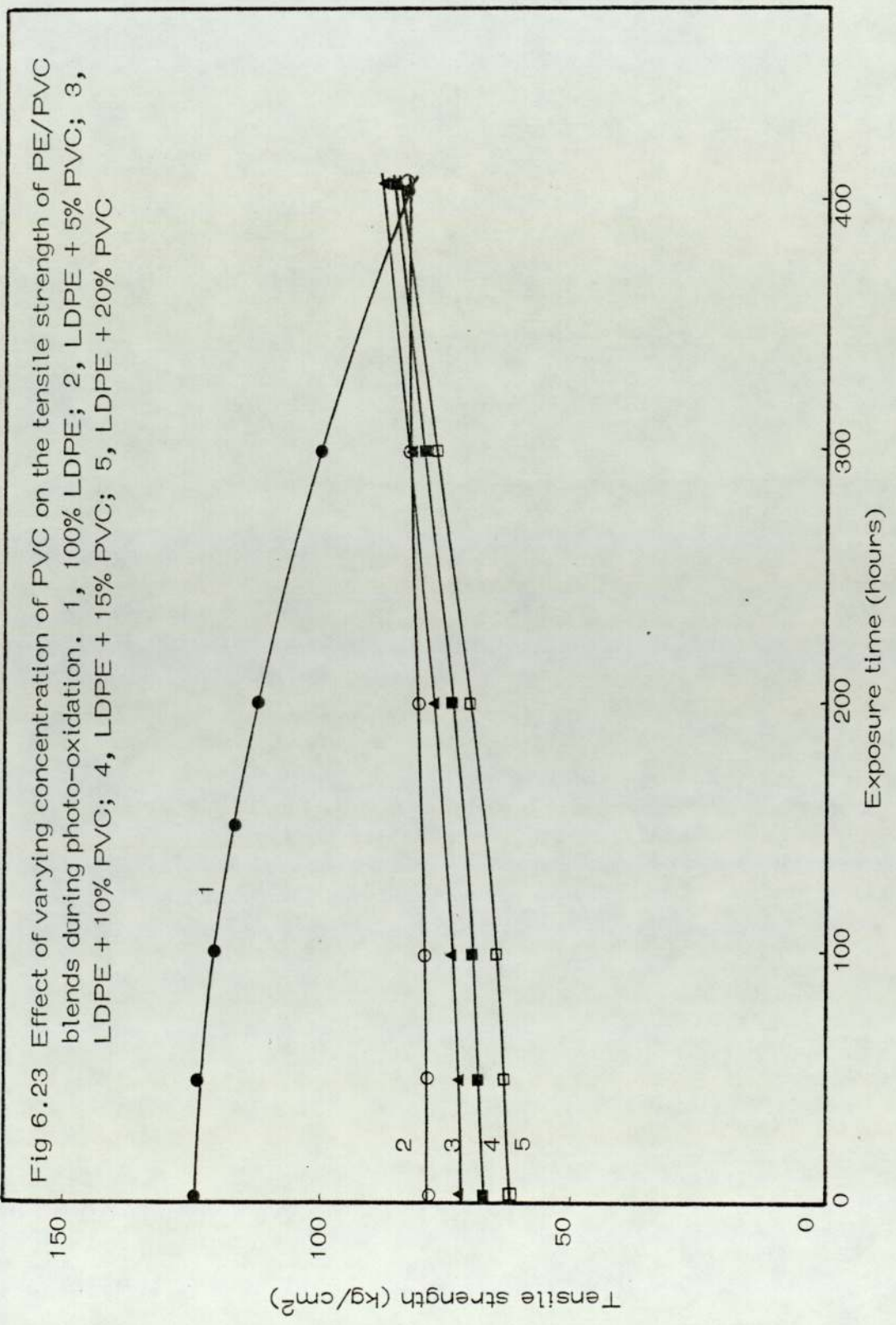
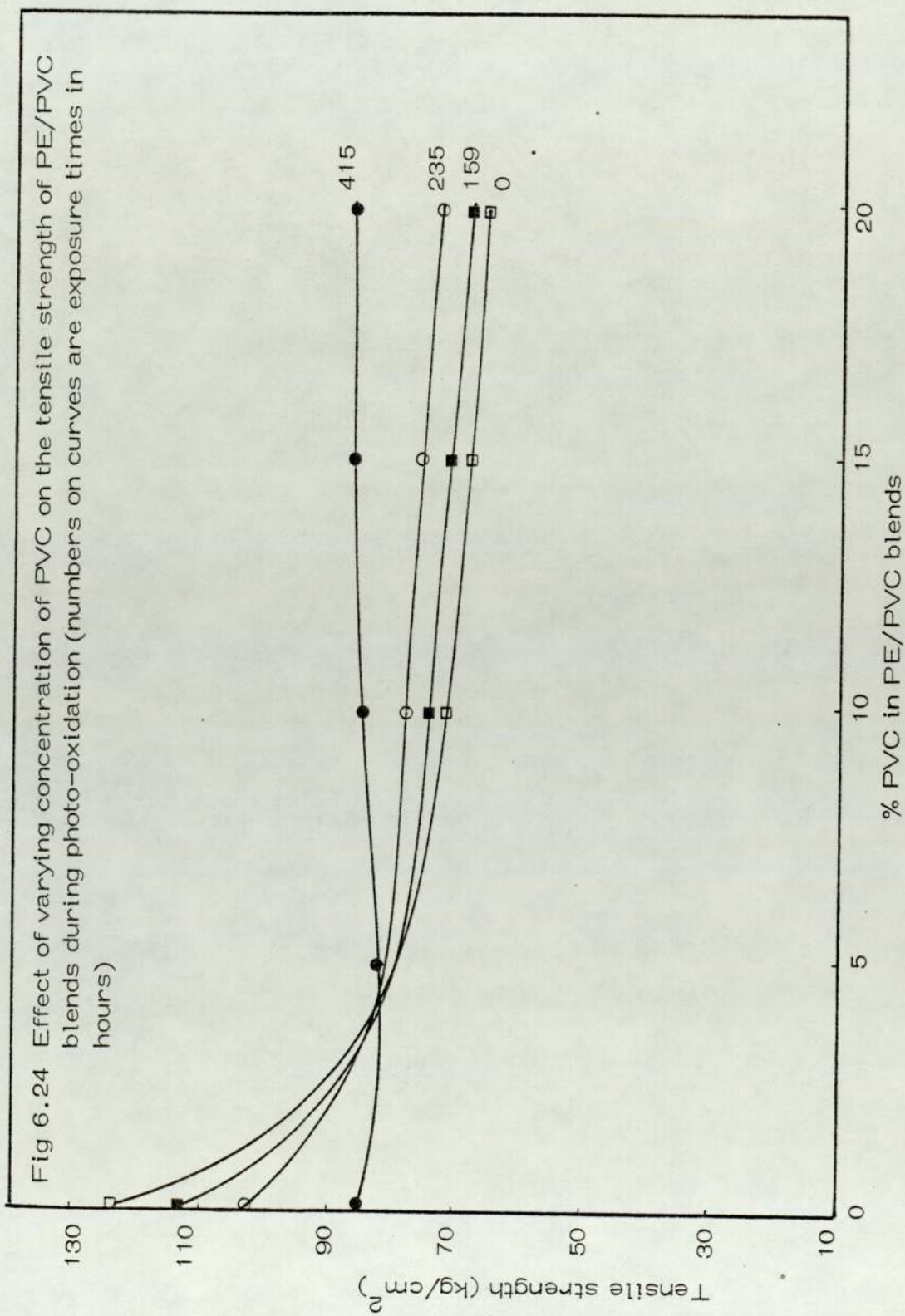


Fig 6.23 Effect of varying concentration of PVC on the tensile strength of PE/PVC blends during photo-oxidation. 1, 100% LDPE; 2, LDPE + 5% PVC; 3, LDPE + 10% PVC; 4, LDPE + 15% PVC; 5, LDPE + 20% PVC



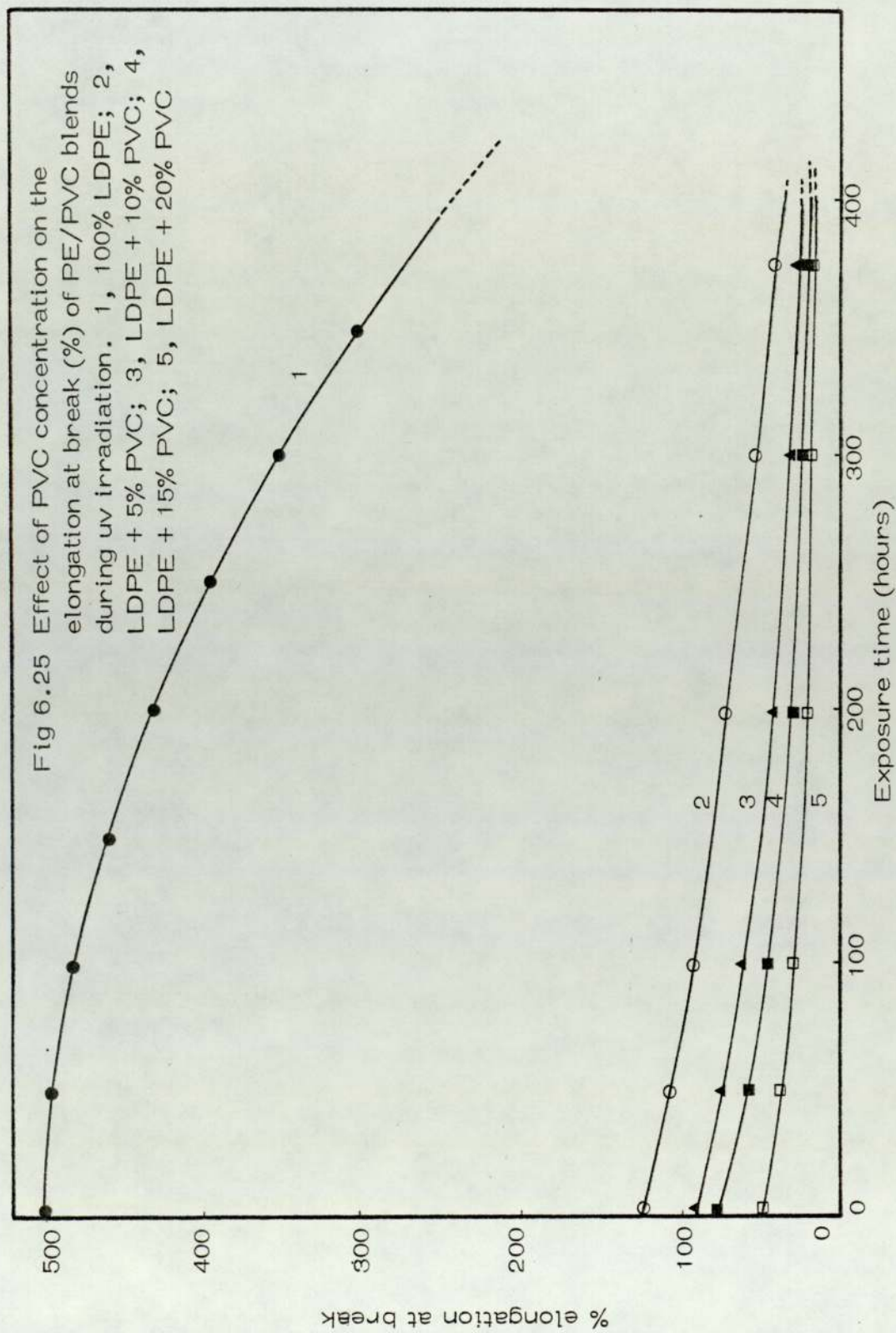
rather differently from low density polyethylene. The tensile strength of the blends increased during uv irradiation as a function of exposure time (Figs 6.23 and 6.24). The elongation at break and impact strength of the blends decreased with irradiation time (Figs 6.25 - 6.27).

It is believed that there are three main factors contributing to the mechanical strength of the incompatible polymer blends:

- (1) the nature and proportion of the continuous phase,
- (2) the occurrence of interaction at the interface, and
- (3) the nature and proportion of the dispersed phase (this is an important factor which increases in importance in the presence of additives).

When the PE/PVC blends are exposed to uv irradiation, two main processes take place at the same time. The first is the degradation of the PE continuous phase and in the PVC dispersed phase resulting in weaker and lower tensile strength of the blend. The other is the interaction at the interface of the domains and matrix. The product of interaction between PE and PVC has been shown in section 6.A.2.1 to be partially grafted and acts effectively as a solid phase dispersant (SPD) and holds the two phases together. This will contribute to an increase in the tensile strength of the blend. The overall tensile strength of the blends will then depend on the net effect of the two degradation processes.

In the case of blends which contain the highest PVC concentration



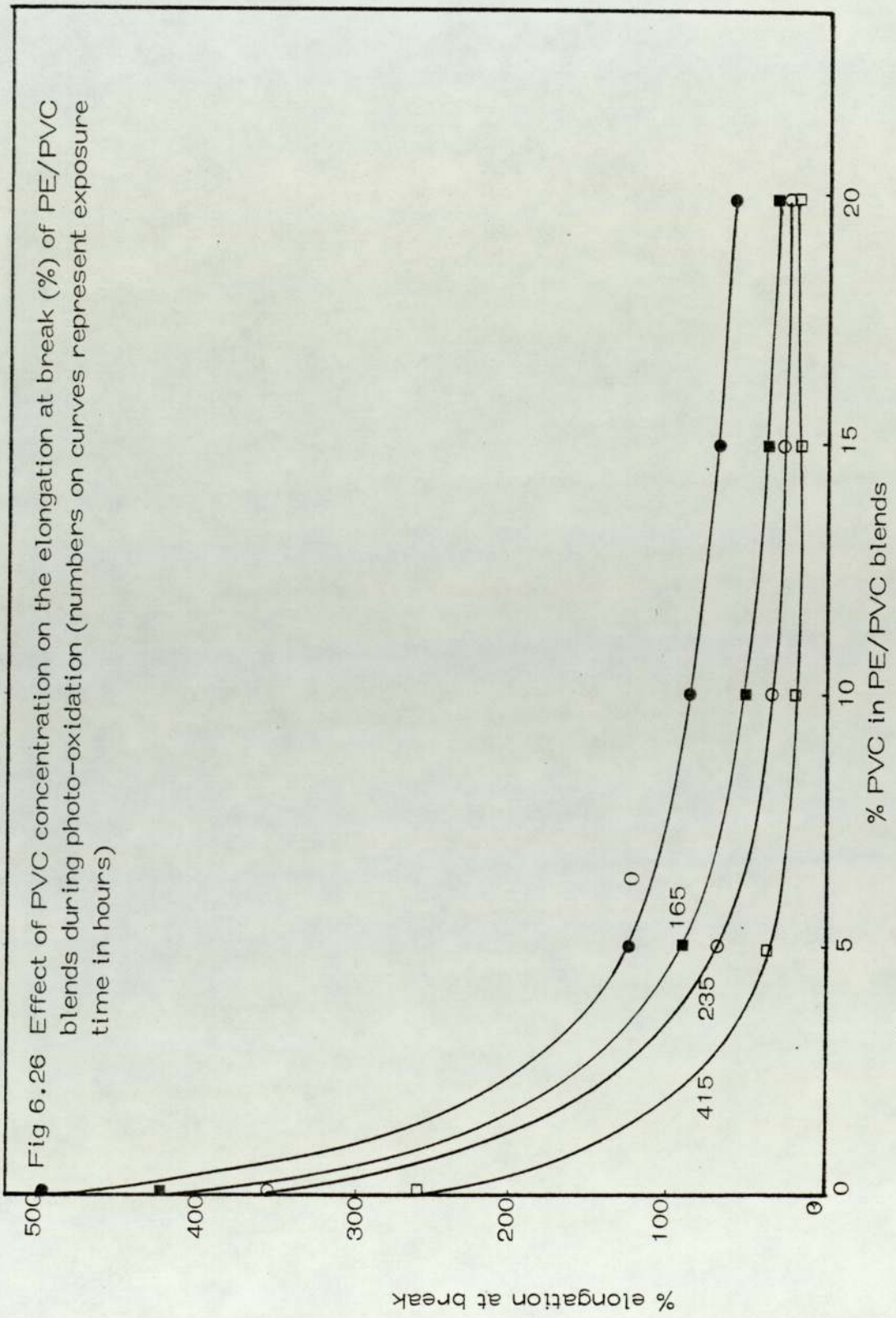
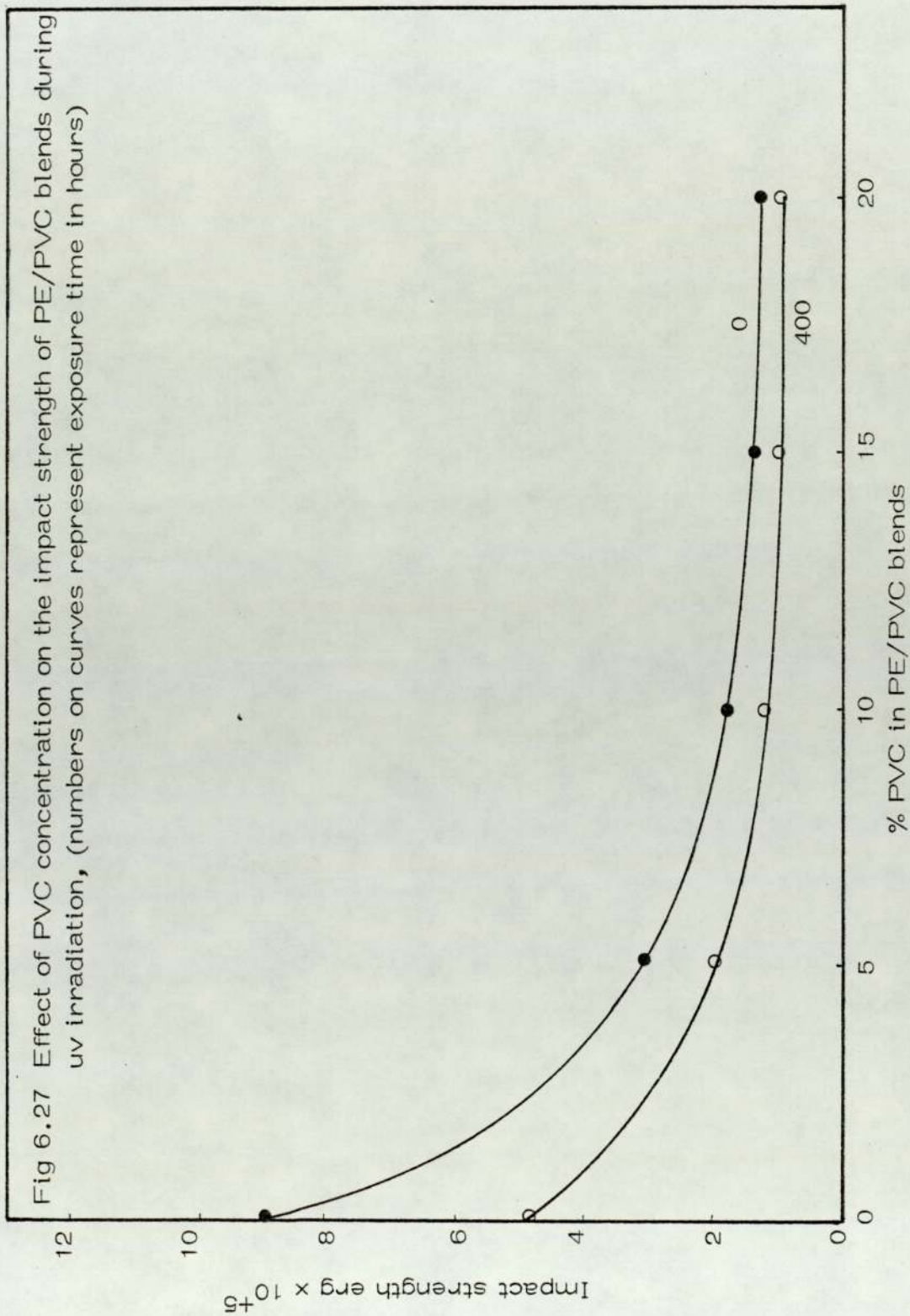


Fig 6.27 Effect of PVC concentration on the impact strength of PE/PVC blends during uv irradiation, (numbers on curves represent exposure time in hours)



(eg, 20%), there is the greatest increase in tensile strength with irradiation time (Figs 6.23 and 6.24). This seems to be associated with a higher photo-oxidation rate of 20% PVC blends (Fig 6.22).

The deterioration of impact strength as irradiation is increased may be due to the degradation of phases which reduce their ability to respond noticeably to deformation (Fig 6.27).

The elongation at break of blends depends mainly on the continuous PE phase and is seen to decrease with irradiation time due to the reduction in molecular weight of the matrix (Figs 6.25 and 6.26).

As mentioned previously, dynamic mechanical properties are extremely sensitive to all kinds of relaxation processes which in turn depend on structural heterogeneity and the morphology of multiphase systems^(60,268,269). Blends of PE/PVC show a decrease in $\tan \delta$ (at room temperature, $20 \pm 1^\circ\text{C}$) with increasing concentration of PVC (Fig 6.5). It might be expected that because polyvinyl chloride has a lower $\tan \delta$ ($20 \pm 1^\circ\text{C}$) and higher modulus than PE (see Chapter 1), when blends are subjected to uv irradiation, $\tan \delta$ and complex modulus will increase with exposure time (Figs 6.28 and 6.29) due to the increasing crystallinity of the blends during uv irradiation (see arguments in Chapters 1, 4 and 5). It has been shown⁽²⁰⁶⁾ that crystallinity in polyethylene greatly depends on chain-branching. Since the presence of bulky side groups prevent the close packing of molecules, they thereby reduce the density and crystallinity in the polymer (see Chapters 1 and 4).

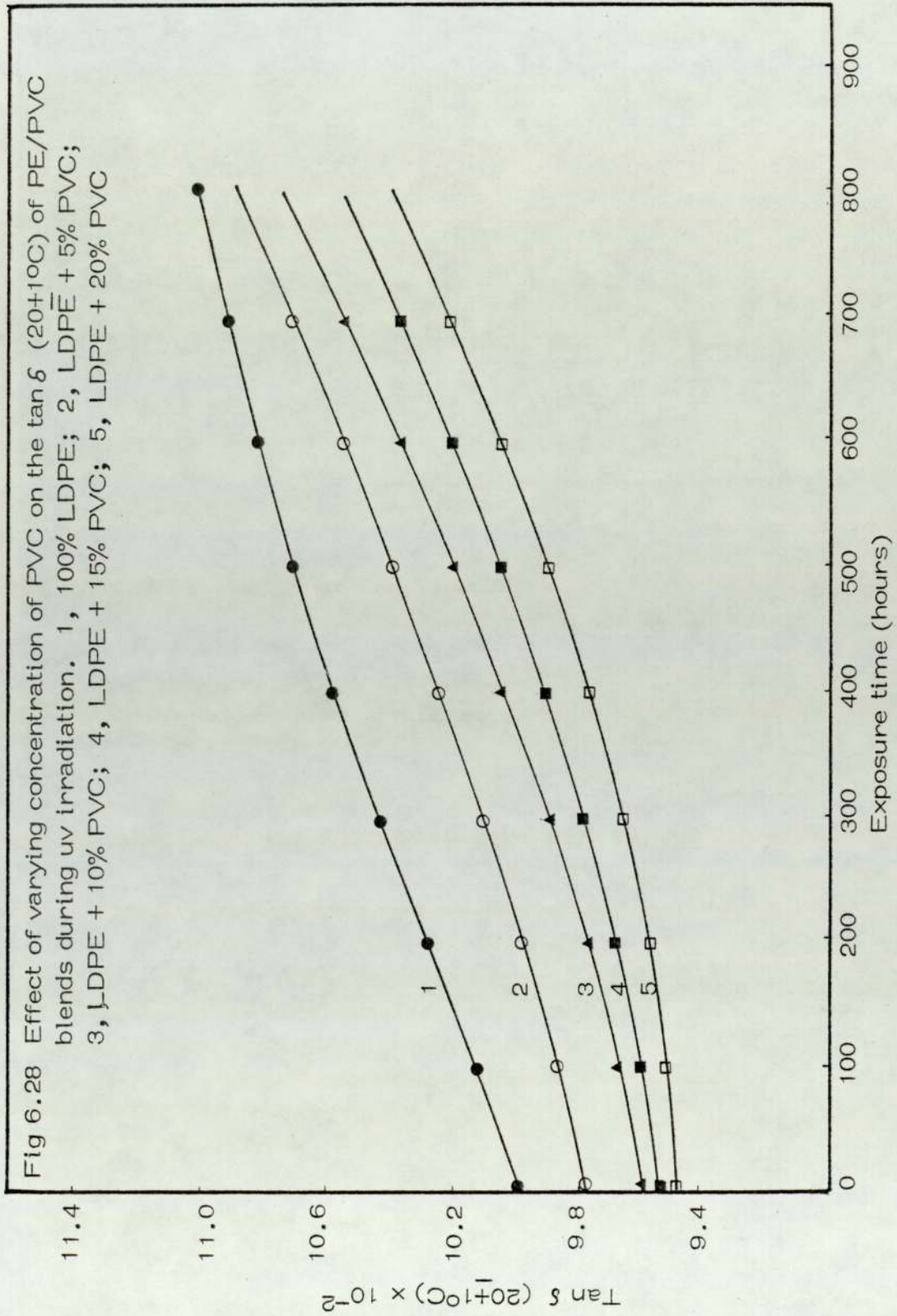
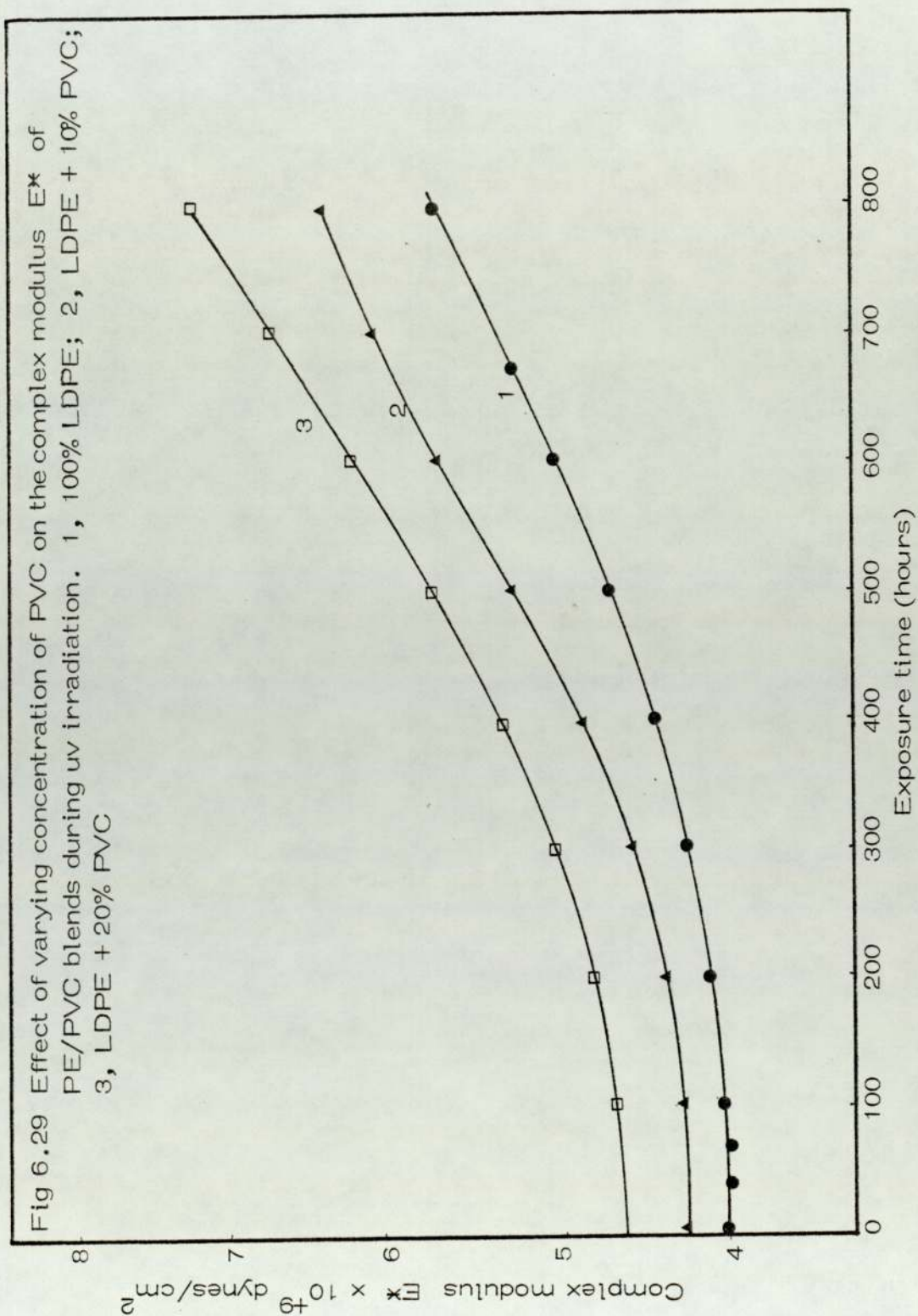


Fig 6.29 Effect of varying concentration of PVC on the complex modulus E^* of PE/PVC blends during uv irradiation. 1, 100% LDPE; 2, LDPE + 10% PVC; 3, LDPE + 20% PVC



6.A.5 The Effect of Some Transition Metal Ions on Thermal and uv Oxidation of PE/PVC Blends

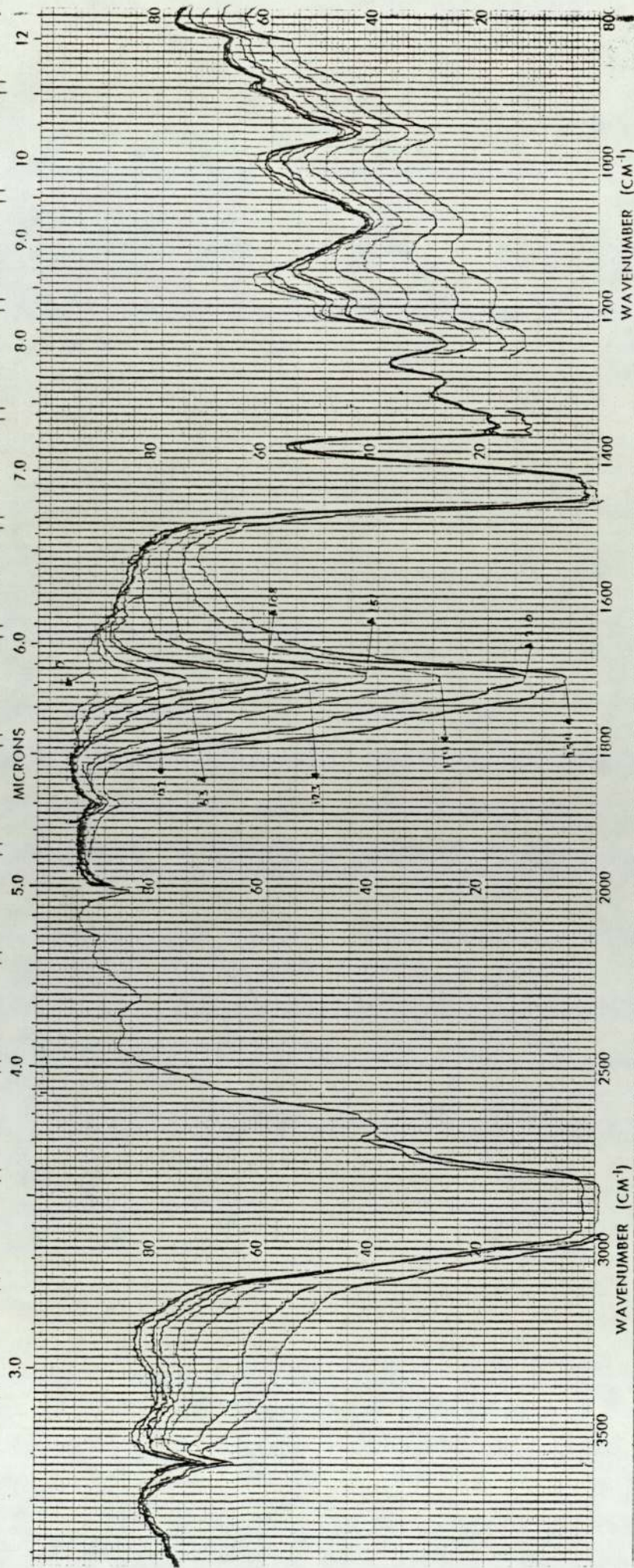
The common transition metal ions are particularly likely to be contaminants during the reprocessing of PVC due to attack of HCl on machinery. The effect of a typical pro-oxidant transition metal ion, ferric stearate (FeSt) on the uv stability of blends are shown in Figs 6.19, 6.20, 6.30 and 6.31 (for 100% PE see Chapter 4, Figs 4.17-4.19). It is clear that as measured by carbonyl absorption, FeSt has a catastrophic effect on the uv stability of LDPE/PVC blends (Fig 6.32). This supports the conclusion of Scott and co-workers⁽¹²³⁾. The stability of the blends compared to the LDPE might be due to interaction of the PE and PVC. The interaction between the two polymer phases (or boundaries) can play a retarding role which prevent the oxidation of both polymeric components from the formation of the main products of oxidation (eg, C=O at 1710 cm^{-1}) (Fig 6.32). The appreciable change in carbonyl absorption during exposure time (Fig 6.32) has an effect on the mechanical properties of the blends (Figs 6.33-6.36). The mechanical damping, complex modulus, percentage elongation and tensile strength at break show appreciable change during exposure time with different concentrations of FeSt (Figs 6.33-6.36) (discussion of these changes are given in Chapters 2, 4 and 5).

6.A.6 Introduction of Some Solid Phase Dispersants (SPD's) to Improve the Toughness of Blends

6.A.6.1 Introduction

Blends of incompatible polymers such as PE and PVC possess poor mechanical properties and cannot be considered for many applications. Additives which modify the blend to give it ductility may provide a solution to this problem.

Fig 6.30 Change in hydroxyl (3500-3000 cm^{-1}) and carbonyl (1800-1600 cm^{-1}) absorption during photo-oxidation of LDPE + 10% PVC + 2×10^{-4} mole/100 gm FeSt film (numbers on curves are exposure time in hours)



FILE	SOLVENT	REMARKS	SCAN SPEED
	CONCENTRATION		SPLIT
:IN	CELL PATH		No 457-5001
	REFERENCE		

7 μm^{-1} 11 vol/100 gm
10 % PVC

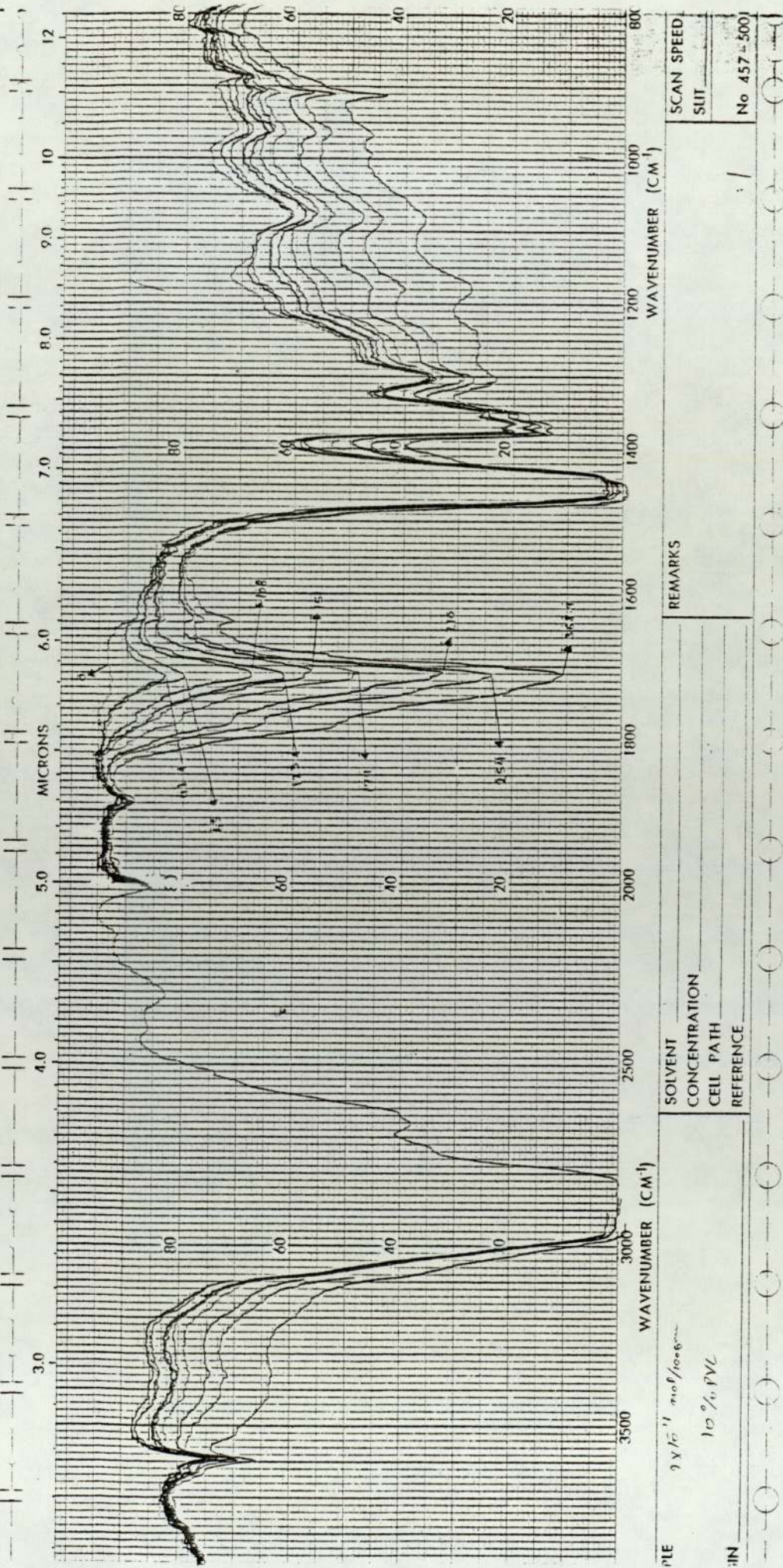
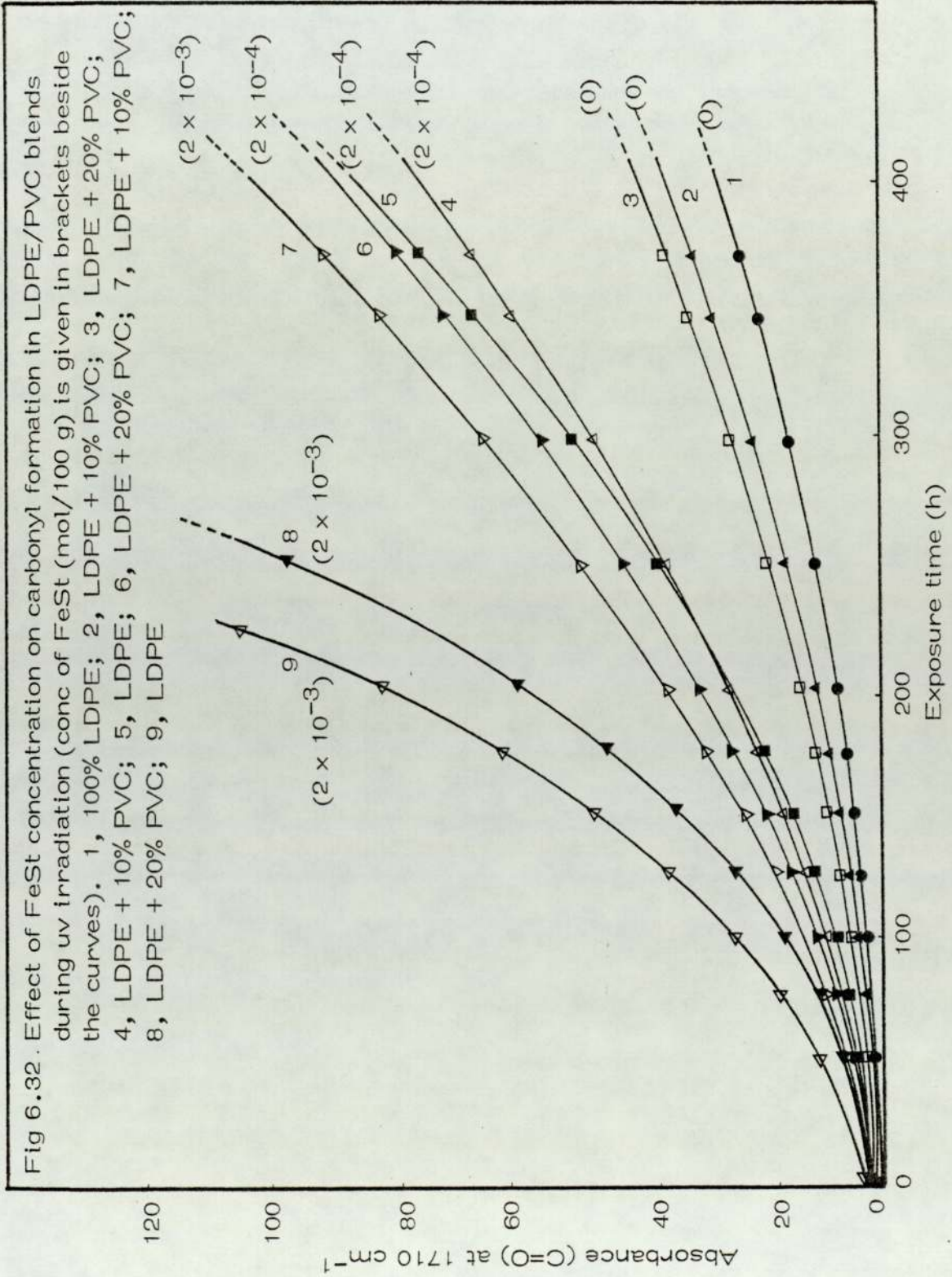


Fig 6.3 Change in hydroxyl ($3500-3000\text{ cm}^{-1}$) and carbonyl ($1800-1600\text{ cm}^{-1}$) absorption during photo-oxidation of LDPE + 20% PVC + 2×10^{-4} mol/100 gm FeSt film (numbers on curves are exposure time in hours)

FILE	1×10^{-1} mol/100 gm	SOLVENT		REMARKS		SCAN SPEED	
IN	10% PVC	CONCENTRATION				SPLIT	
		CELL PATH					No 457-500
		REFERENCE					



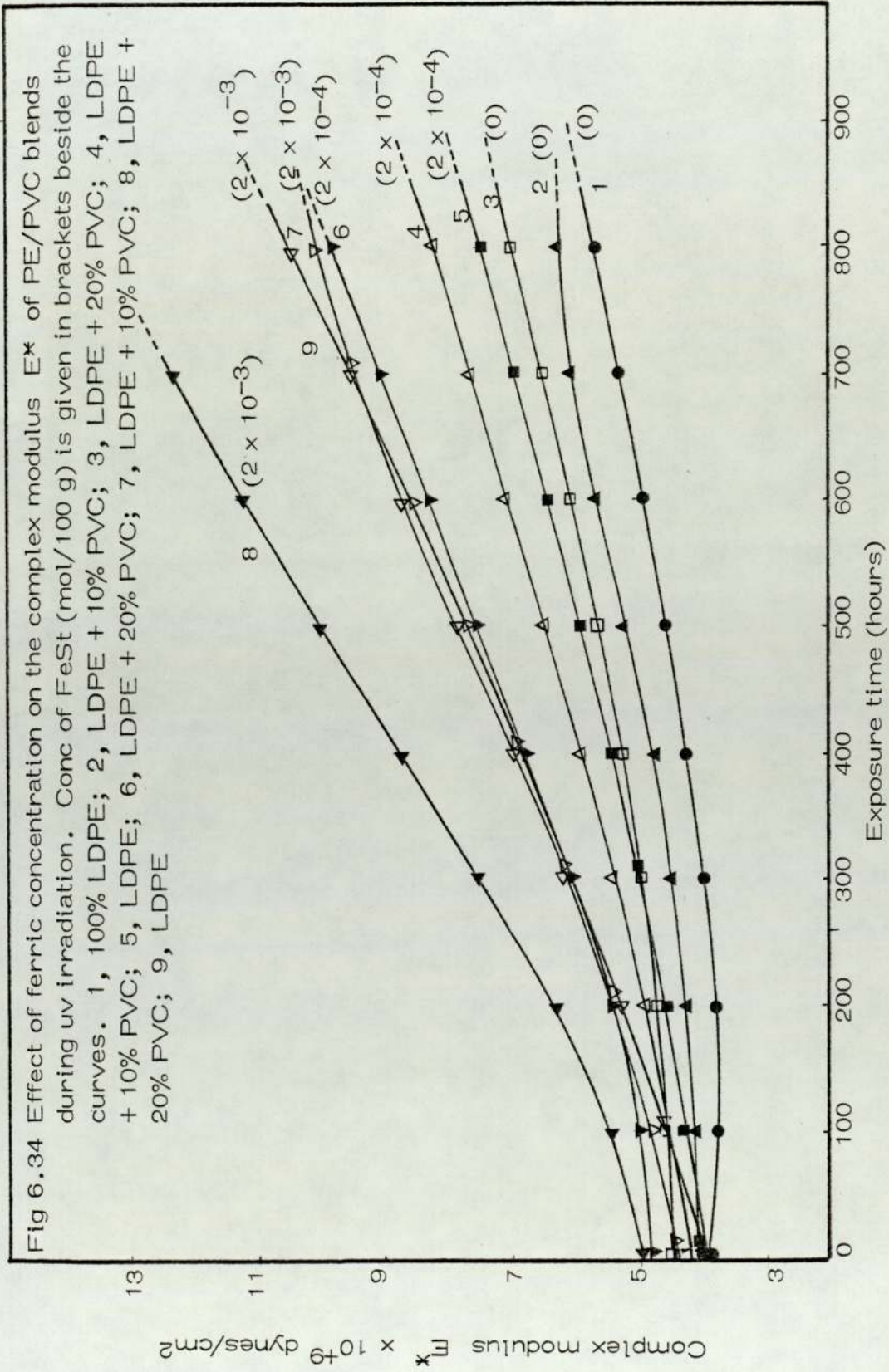
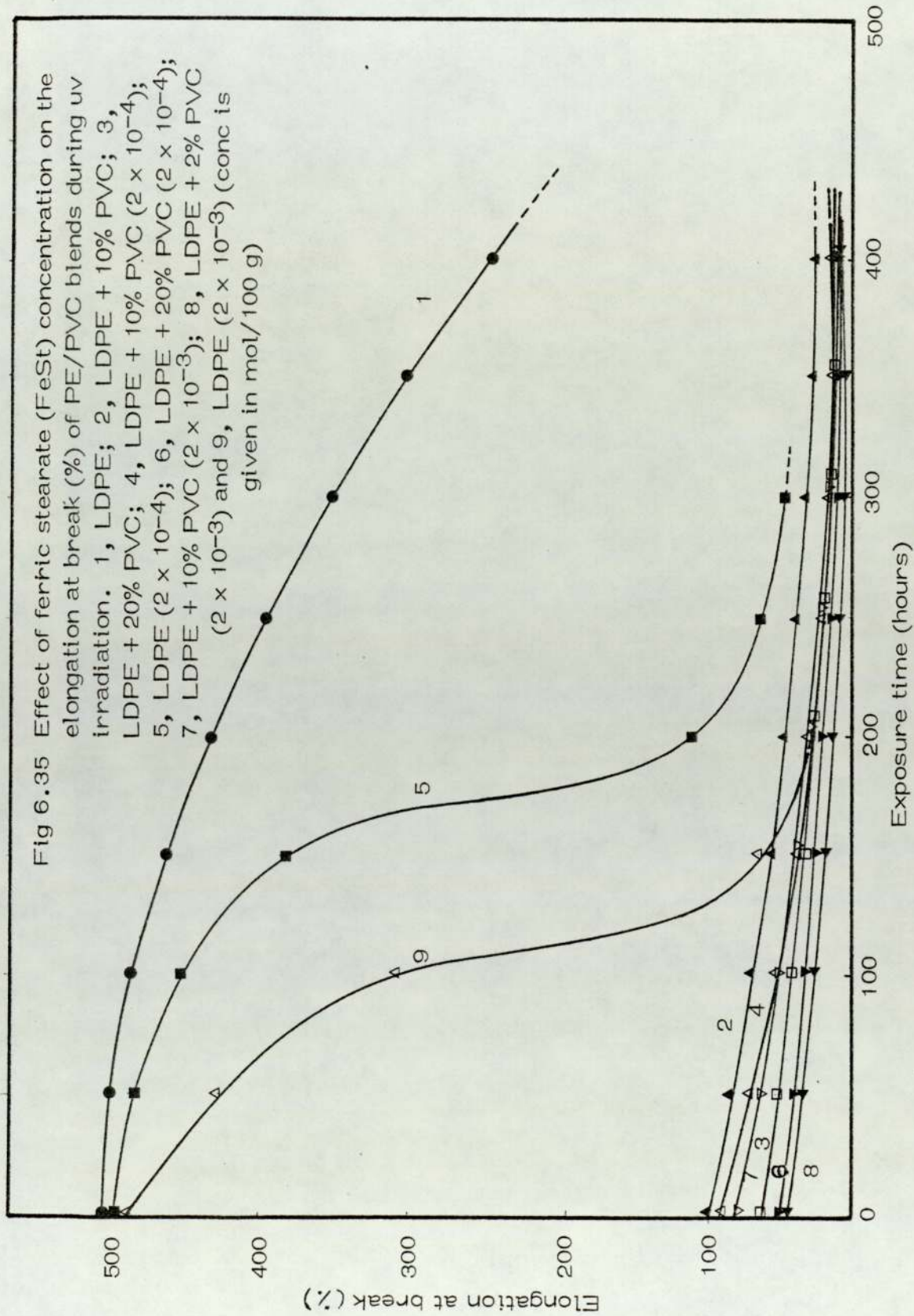
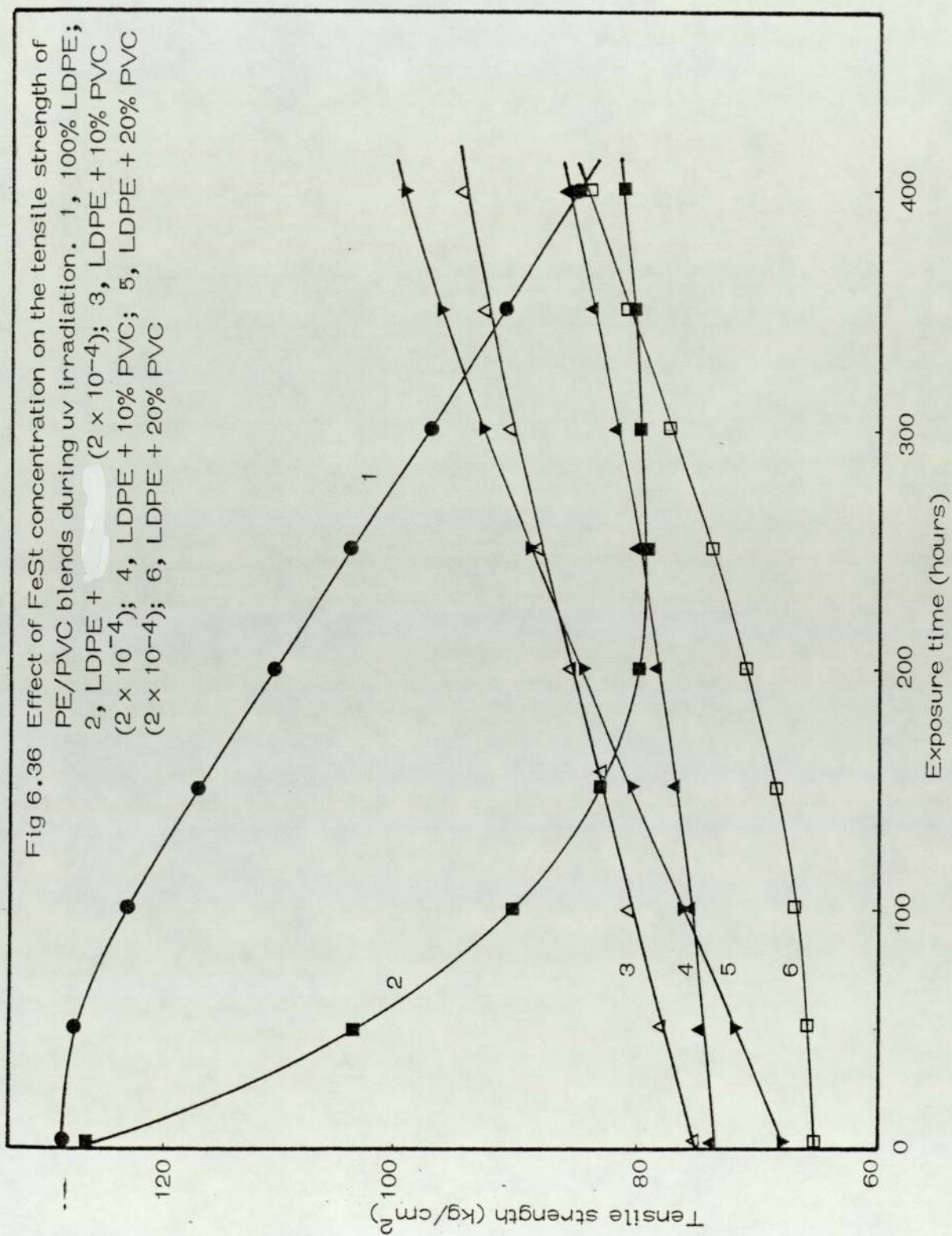


Fig 6.35 Effect of ferric stearate (FeSt) concentration on the elongation at break (%) of PE/PVC blends during uv irradiation. 1, LDPE; 2, LDPE + 10% PVC; 3, LDPE + 20% PVC; 4, LDPE + 10% PVC (2×10^{-4}); 5, LDPE (2×10^{-4}); 6, LDPE + 20% PVC (2×10^{-4}); 7, LDPE + 10% PVC (2×10^{-3}); 8, LDPE + 2% PVC (2×10^{-3}) and 9, LDPE (2×10^{-3}) (conc is given in mol/100 g)





Introduction of some selected additives, termed solid phase dispersant (SPD) was tried in attempting to improve the performance of these blends by enhancing their strength and toughness.

The use of solid phase dispersants in polymer blends has been extensively studied. Paul and co-workers⁽²³⁷⁾ have shown that the stress-strain behaviour, especially ductility, of some incompatible polymer blends is greatly improved by the addition of chlorinated polyethylene (CPE). This improvement is greatest for blends containing polyethylene and PVC. The most effective CPE's have some residual polyethylene crystallinity and may be described as black-like polymers with ethylene sequences and chlorine containing sequences. It is postulated that CPE addition improves the blend properties by increasing the adhesion between domains in the blend via interactions with the blend components. This hypothesis was explored by thermal analysis, dynamic mechanical testing, adhesion studies and microscopy⁽²³⁷⁾. It is concluded that the interaction of CPE with polyethylene derives from compatibility of rather long methylene sequences in CPE with the polyethylene which results in good adhesion bonding. The interaction of CPE may not be owing to segmental compatibility but simply good mutual adhesion between similar polar materials. They have not observed any interaction or adhesion between CPE and polystyrene as would be expected⁽²³⁷⁾. CPE addition to blends is accompanied by a decrease in component domain size.

6.A.6.2 Experimental

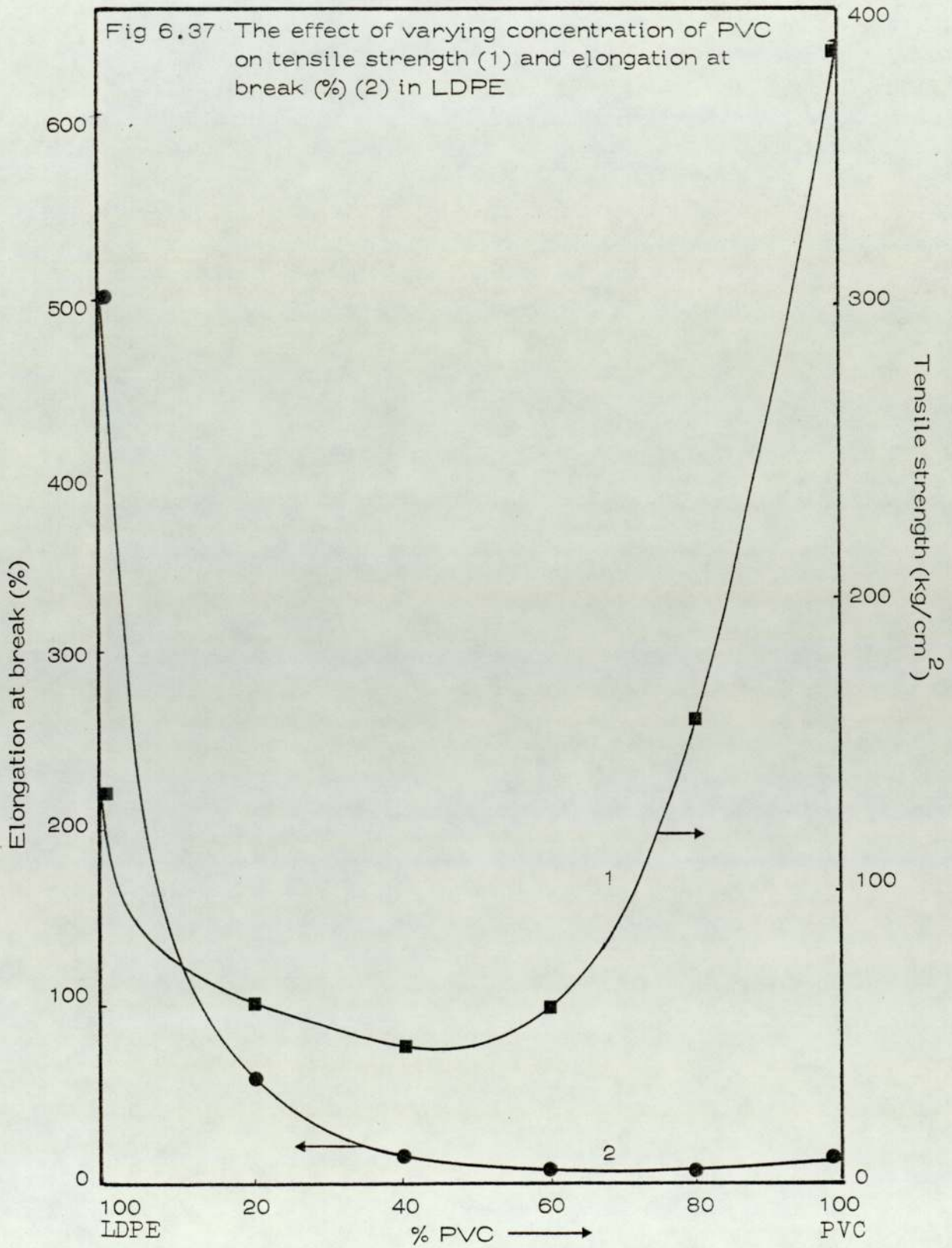
The blends were carried out at 180°C in the RAPRA torque rheometer for 5 minutes in closed chamber. The processed blends were compression moulded at 180°C for 2 minutes into sheets as described in the main experimental Chapter 3.

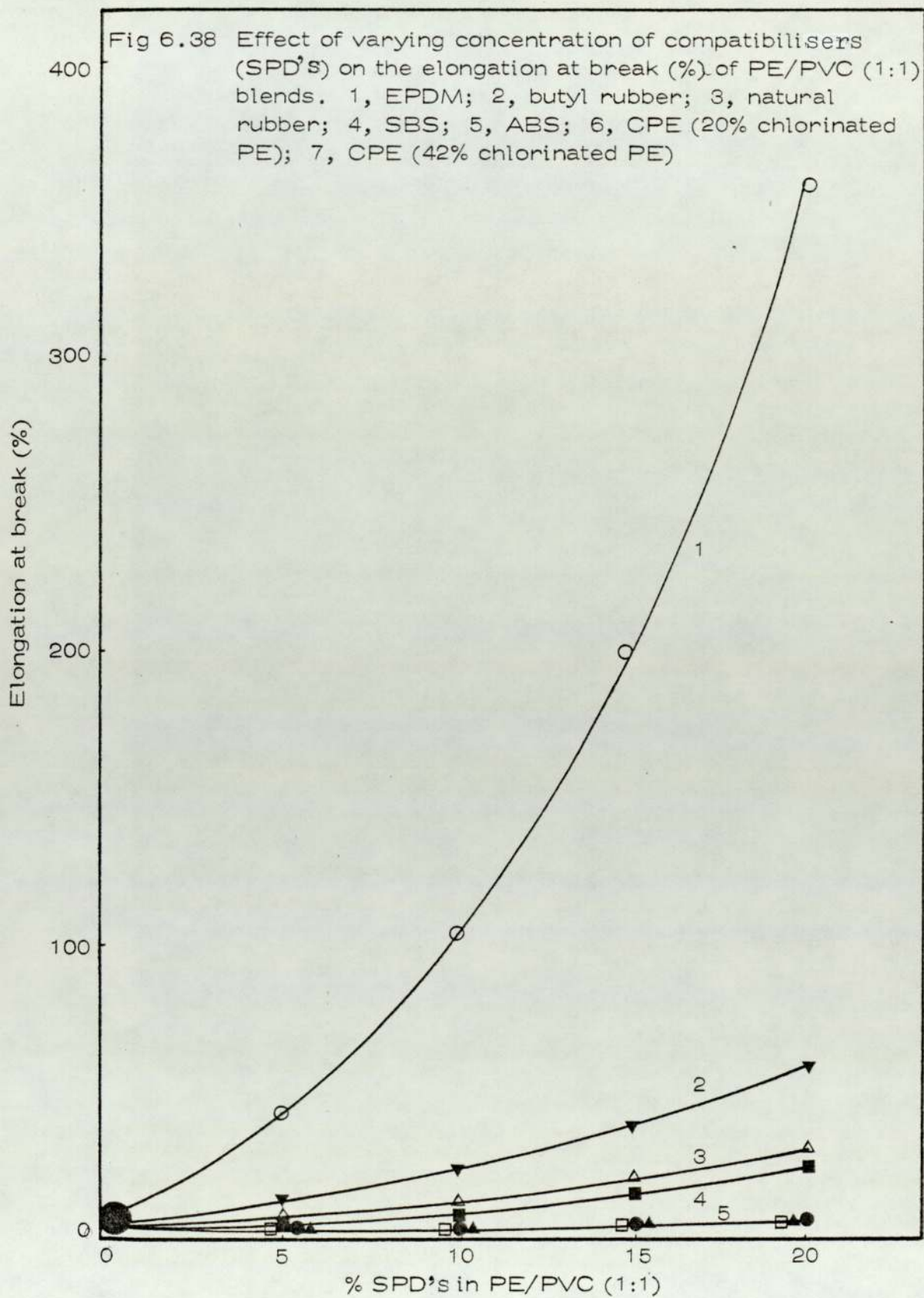
The additives consisting of EPDM, ABS, ACS, NR, SBS, and CPE (20% and 42% chlorinated polyethylene) (see Table 6.1, Chapter 6, Section 6.A.1) were used to improve the toughness of the blends.

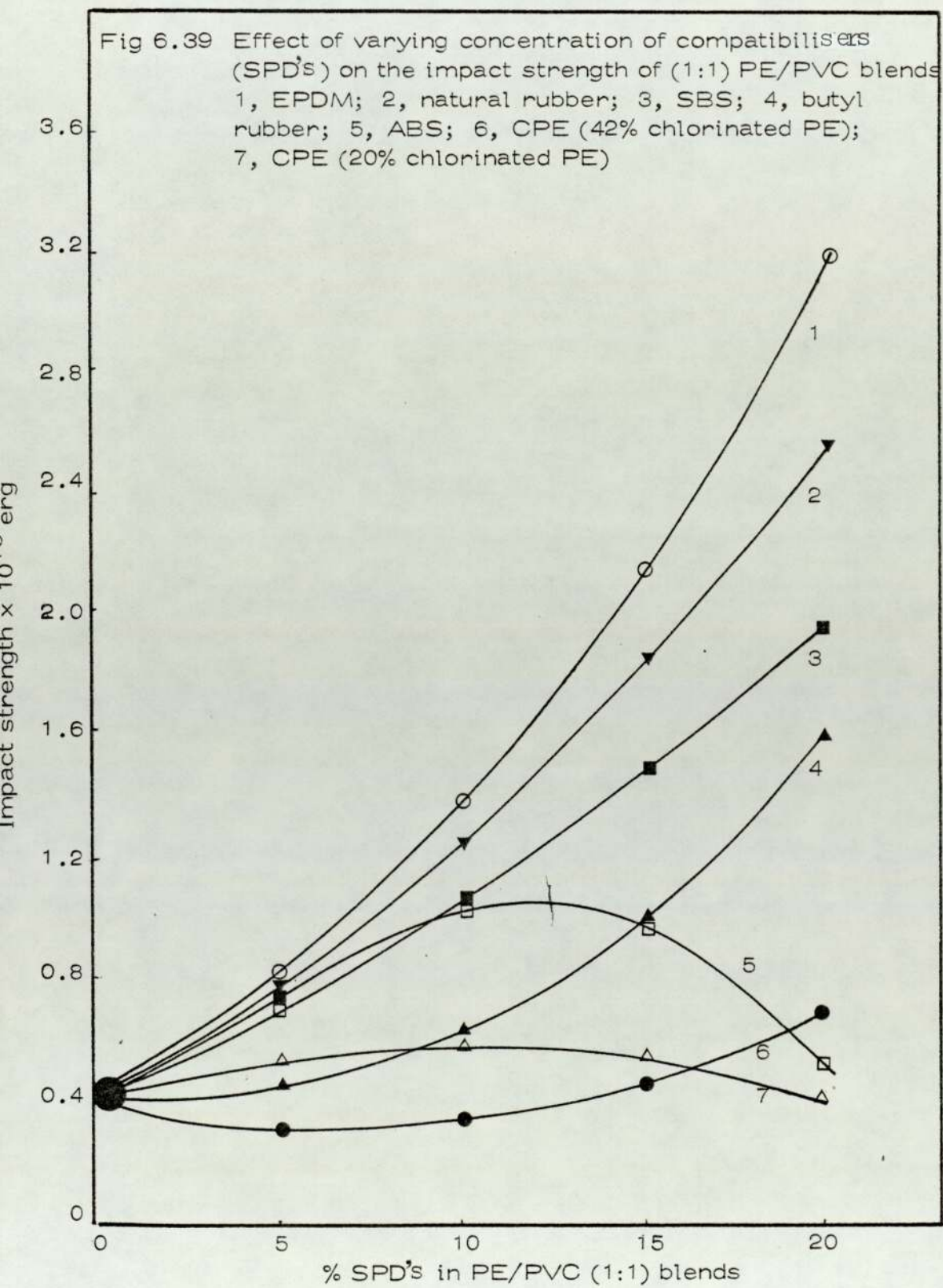
6.A.6.3 Results and Discussion

The tensile strength measurements indicate minimal strength in the range 30–50% of either polymer (eg PVC in PE, Fig 6.37). This is believed to represent the worst concentration as far as mechanical properties are concerned, probably due to phase separation in an incompatible system and for this reason this blend was chosen for the study of SPD's.

The mechanical properties of PE/PVC without SPD has been discussed previously (see Section 6.A.2). Table 6.A.2 and Figs 6.38, 6.39 and 6.40) show the effect of seven additives on 1:1 or 50/50 LDPE/PVC blends. EPDM is more effective in improving % elongation at break (from 5.0 to 370) and impact strength (from 0.35 to 3.15) than other additives and this effect increases sharply with concentration (eg 20% EPDM, Figs 6.38 and 6.39). Tensile strength decreases from 46 to 36 kg/cm² due to the lower tensile strength of EPDM compared with PVC (Fig 6.40). EPDM appears therefore to be a







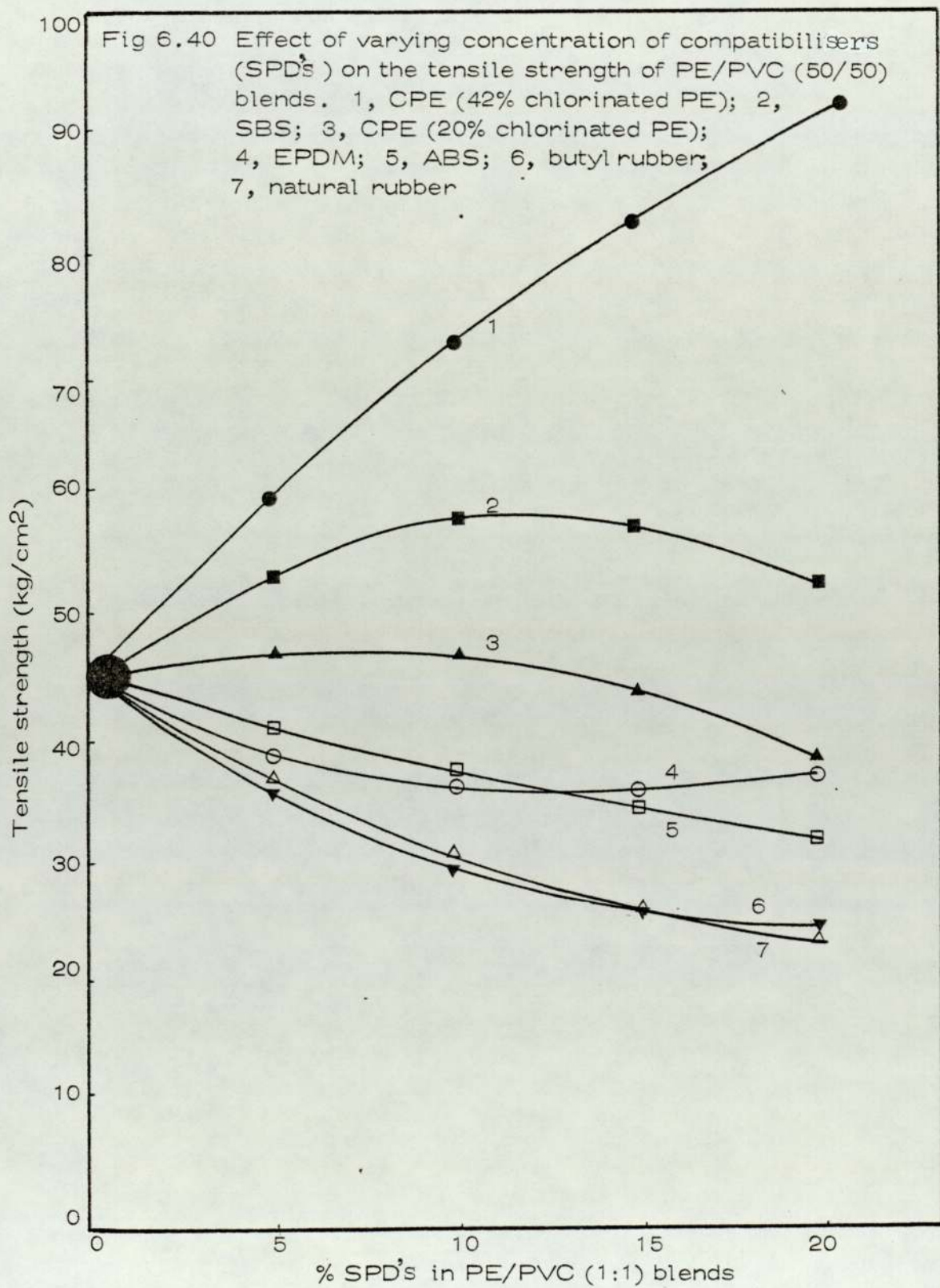


Table 6.A.2 The effect of varying concentration of SPD's on the mechanical properties of PE/PVC (50/50) blends

No.	Formulation	Elongation at break (%)	Tensile strength (kg/cm ²)	Impact strength (x 10 ⁺⁵) ergs
	PE + PVC + additives (%)			
1	PE	480-500	128	8.5-9.0
2	50 + 50 + 0	5	45	0.35-0.4
3	45 + 45 + 10 EPDM	100	37.5	1.35
4	40 + 40 + 20 EPDM	370	38.0	3.15
5	45 + 45 + 10 SBS	8.0	58.0	1.1
6	40 + 40 + 20 SBS	30.0	53.0	2.0
7	45 + 45 + 10 BR	25.0	32.0	0.62
8	40 + 40 + 20 BR	60.0	26.0	1.6
9	45 + 45 + 10 NR	12.5	31.0	1.25
10	40 + 40 + 20 NR	32.0	24.0	2.6
11	45 + 45 + 10 ABS	-	38.0	1.05
12	40 + 40 + 20 ABS	-	34.0	0.5
13	45 + 45 + 10 CPE(20%)	-	46.5	0.6
14	40 + 40 + 20 CPE(20%)	-	38.0	0.4
15	45 + 45 + 10 CPE(42%)	-	72.0	0.35
16	40 + 40 + 20 CPE(42%)	-	94.0	0.75

most effective phase dispersant (SPD) for the PE and PVC blends to enable them to be used in some specific application. The reasons for this improvement are not well understood and require further work (see Chapter 7).

6.B The Effect of Polypropylene Concentration on Mechanical Properties of LDPE-PP Blends

6.B.1 Introduction

Almost from the time that polypropylene was introduced as a commercial resin, there has been interest in its blends with its sister polymer in the polyolefin family, polyethylene. During the period from 1962 to 1969 some 34 patents were issued on this subject, 11 of them United States patents, and all assigned to resin manufacture. They are mostly concerned with improving the low temperature properties and impact resistance of polypropylene but do not provide much quantitative evidence as to what has actually been accomplished. Of the published papers dealing with the physical, chemical and rheological properties of blends of these two polyolefins, about half are by Plockocki and co-workers⁽²⁷⁰⁻²⁷⁴⁾, and published in journals unavailable to us and our knowledge of their contents is limited to what can be gleaned from abstracts and citations by other authors. Plockocki carried out melt-blending of the two polymers. Most of the other investigations have been concerned with blending by coprecipitation of the polymers from solution or from suspension. For example, Kulezner and co-workers⁽²⁷⁵⁾ prepared blends of Ziegler and Phillips type linear polyethylenes with isotactic polypropylene by vacuum drying

methanol suspension of the polymers. In addition to studying the rheological properties of these blends in a rotational viscometer, they also measured⁽²⁷⁵⁾ tensile strength and concluded that their results indicated mutual solubility of the components in the molten state.

Recently, Oscar and James⁽²⁷⁶⁾ investigated the properties of high density polyethylene (HDPE) and isotactic polypropylene blends. They⁽²⁷⁶⁾ melt-blended HDPE in the following percentage by weight: 0, 10, 33.3, 40, 50, 66.6, 90 and 100 on the PP. Their blends showed similar two phase character to those of Slonimskii⁽²⁷⁷⁾ and Plockocki⁽²⁷⁰⁻²⁷⁴⁾.

6.B.2 Experimental

Materials: Low density polyethylene and unstabilised polypropylene were used as described in Chapters 3, 4 and 5.

Processing: The blends were processed at 180°C in the RAPRA torque rheometer for 5 minutes in a full chamber. The blends were then compression moulded at 180°C for 2 minutes into sheets as described in Chapter 3.

Table 6.B.1 shows the formulation with varying proportions of PP (0, 5, 10, 15 and 20%). All formulations were based on 35 gram of polymer (in a full mixer chamber).

Tensile strength, % elongation and Young's modulus were calculated at the cross-head speed of 2 cm/min at room temperature ($21 \pm 1^\circ\text{C}$) (details are given in Chapter 3).

Table 6.B.1

Compositions (%)		Change weight to mixer (g)	
LDPE	PP	LDPE	PP
100	0	35	0
95	5	33.25	1.75
90	10	31.50	3.50
85	15	29.75	5.25
80	20	28.00	7.00

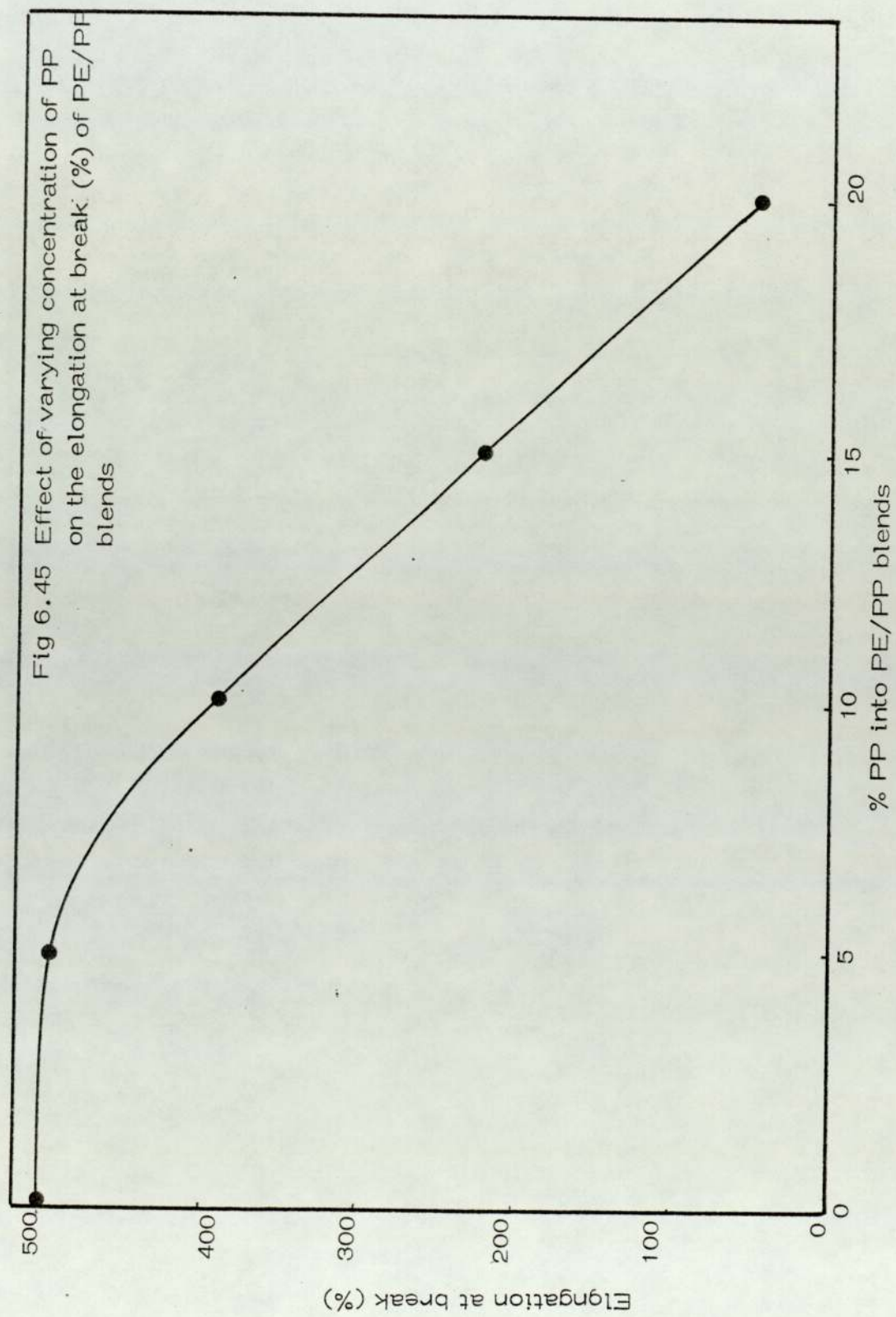
Dynamic mechanical property measurements and optical microscopy examination were carried out as described in the main Experimental Chapter 3.

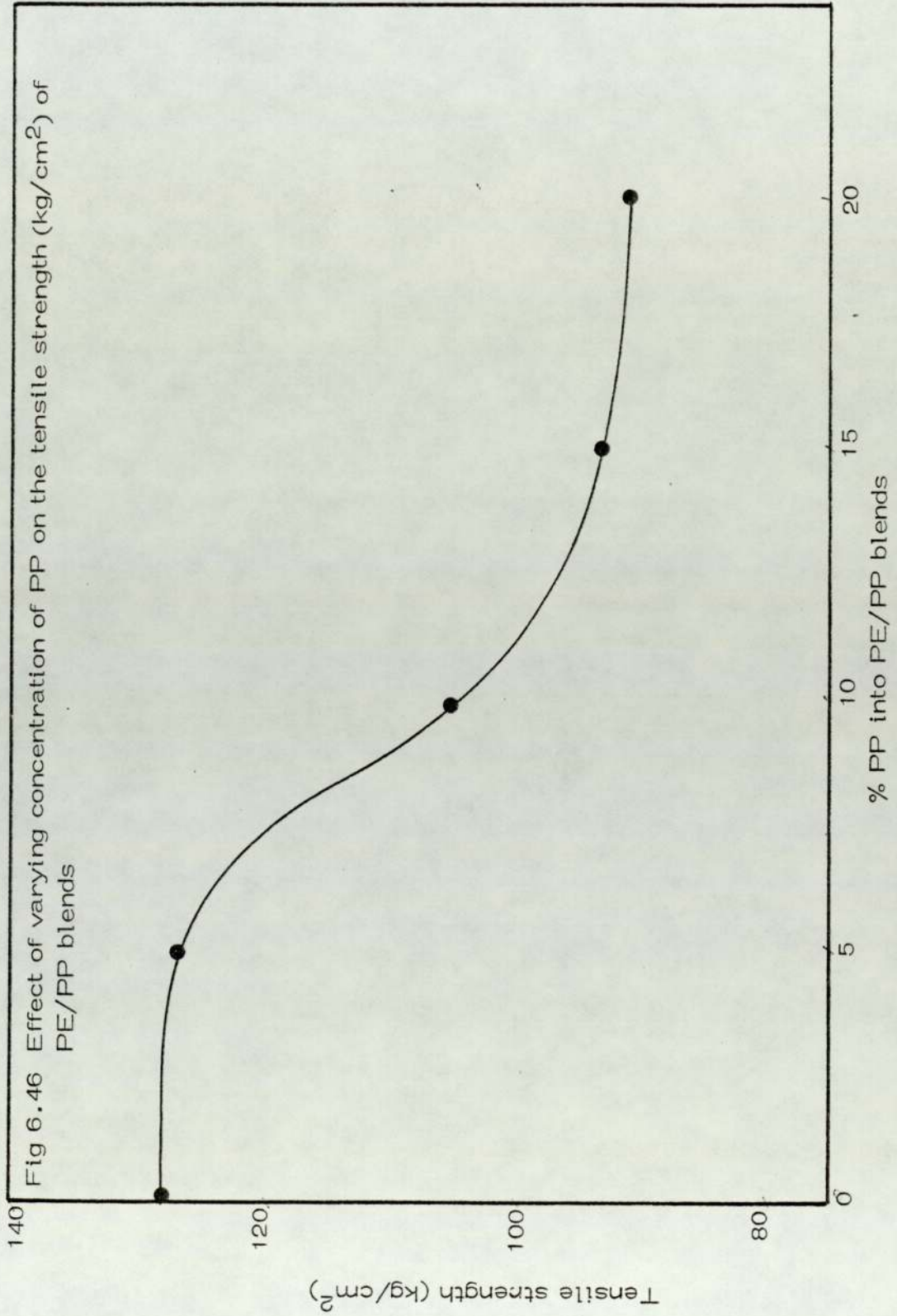
6.B.3 Results and Discussion

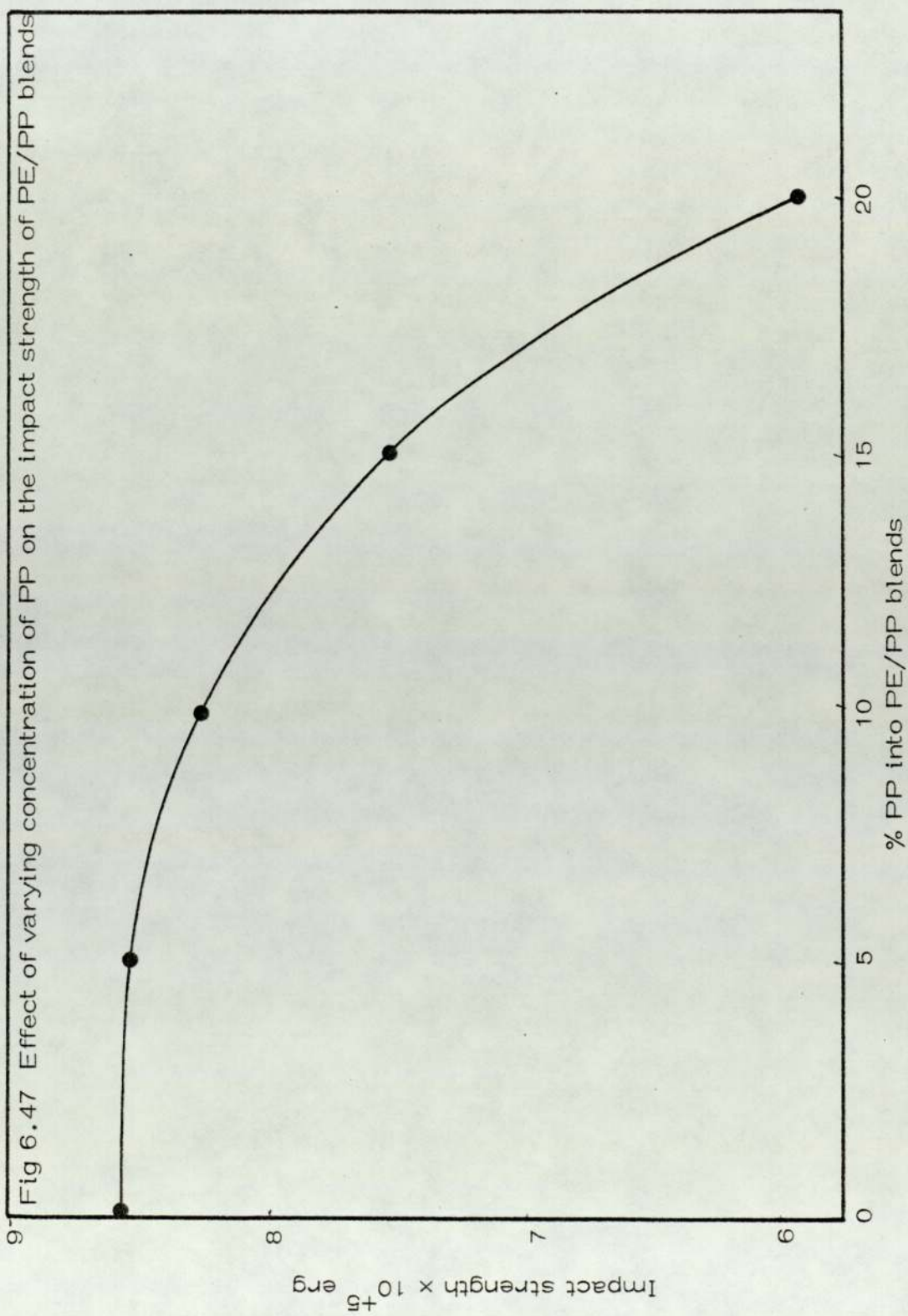
Fig 6.45 shows the % elongation at break plotted against blend composition. This decrease of % elongation at break for 5% polypropylene is not significant and 5% blend shows similar % elongation at break as LDPE. The tensile strength also appears to decrease up to 20% PP in to blend (Fig 6.46). Impact strength follows a similar curve to elongation at break (Fig 6.47).

From Figs 6.45 - 6.47 it appears that above 5% polypropylene acts as a rigid filler which increases the modulus as measured from the initial slope of the stress-strain curve. Generally fillers cause a decrease in elongation to break and also often decrease the tensile strength of a material⁽²⁷⁸⁾. There are important exceptions, especially with such fillers as carbon black in rubber⁽²⁷⁸⁾. This increase in visco-elasticity can be explained in terms of decreased chain rotation in polyethylene by which elongation occurs, hence the blend becomes more brittle^(278, 60).

Impact strength also decreases with elongation at break (Fig 6.47) which is again due to the increased visco-elasticity as a result of the addition of polypropylene. Impact energy is dissipated by relaxation mechanism (chain rotation) similar to those operating during elongation, which accounts for the similarity of curves. The decrease in impact strength was







expected as little relaxation of chain can occur within the polypropylene phases and the impact energy is transferred to the polyethylene matrix thus magnifying the effect of impact.

Optical micrographs of LDPE/PP blends are shown in Plates 1B-4B. Micrographs (Plates 1B and 2B) showed a single phase comparable to LDPE for 5% PP in LDPE indicating complete compatibility. Optical microscopy of the 20% blend (Plate 3B) indicates a different morphology from the 5% blend due to the incompatibility of PP at this concentration relative to 100% PE (Plate 4B).

A study of the dynamic mechanical properties of the blends indicates that $\tan \delta$ ($20 \pm 1^\circ\text{C}$) decreases as the polypropylene concentration is increased (Fig 6.48). As described in Chapter 5, polypropylene has a lower $\tan \delta$ (20°C) and higher complex modulus than LDPE⁽⁶⁰⁾. The decrease in $\tan \delta$ (20°C) and increase in complex modulus (Figs 6.48 and 6.49) may be due to rigidity of polypropylene than polyethylene.

6.B.4 Effect of Polypropylene (PP) Concentration on the Photo-oxidation of LDPE Blends

6.B.4.1 Introduction

Polypropylene is known to be much less stable than polyethylene. Polypropylene present in mixed waste expected to increase photo-sensitivity (for more details see Chapters 4 and 5).



Plate 1B 100% LDPE (OPTical)
Mn = 200



Plate 2B (PE + 5% PP) (Optical)
Mn x 400

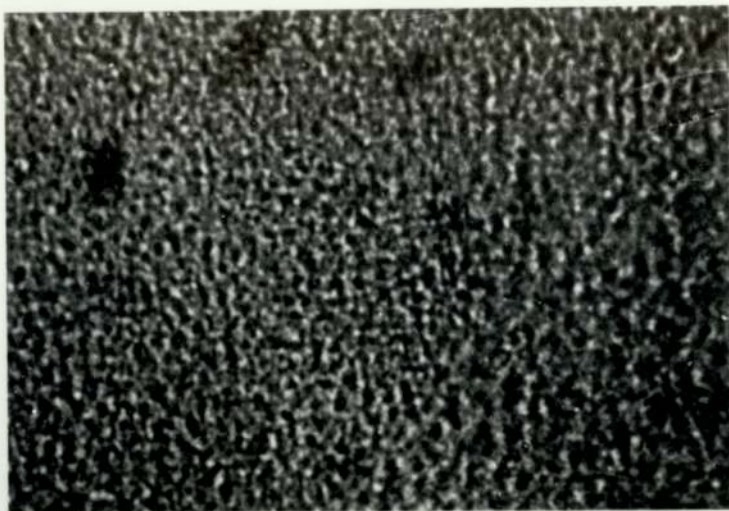


Plate 3B (PE + 20% PP) (Optical)
Mn = 400

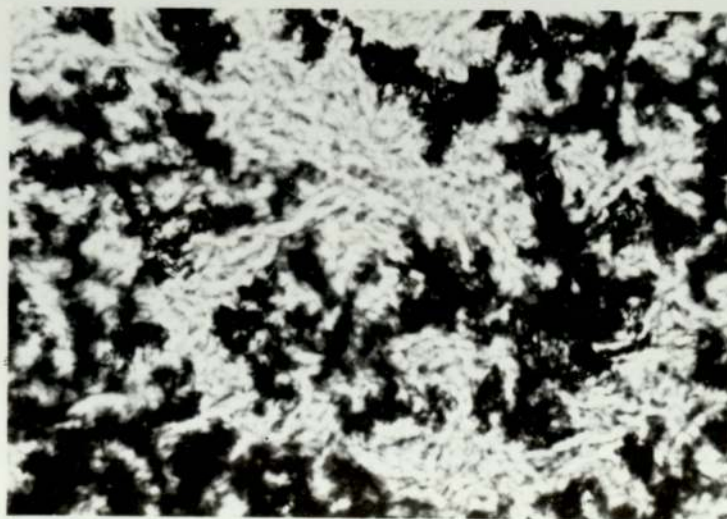
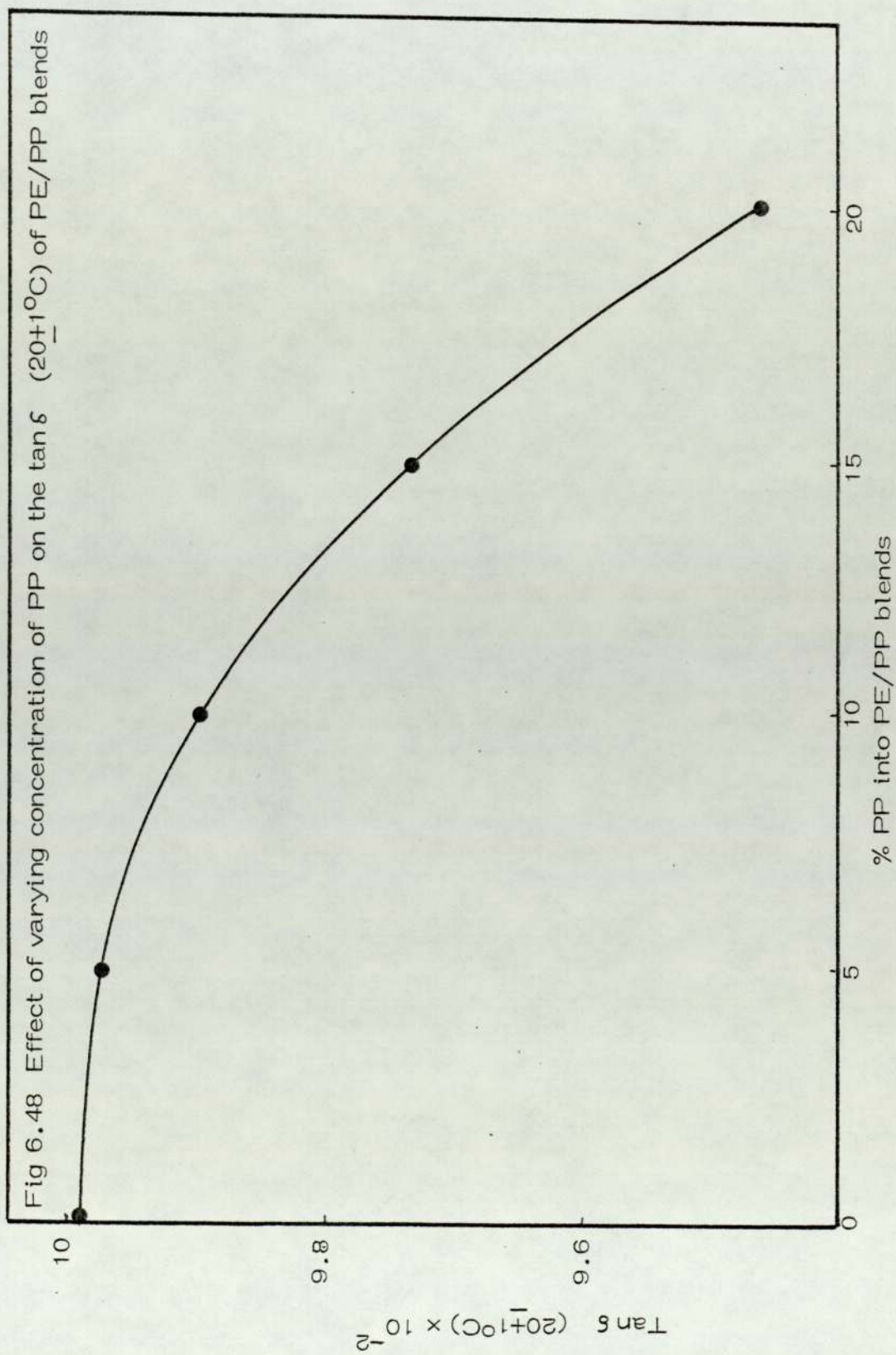


Plate 4B 100%pp (Optical)
Mn = 400



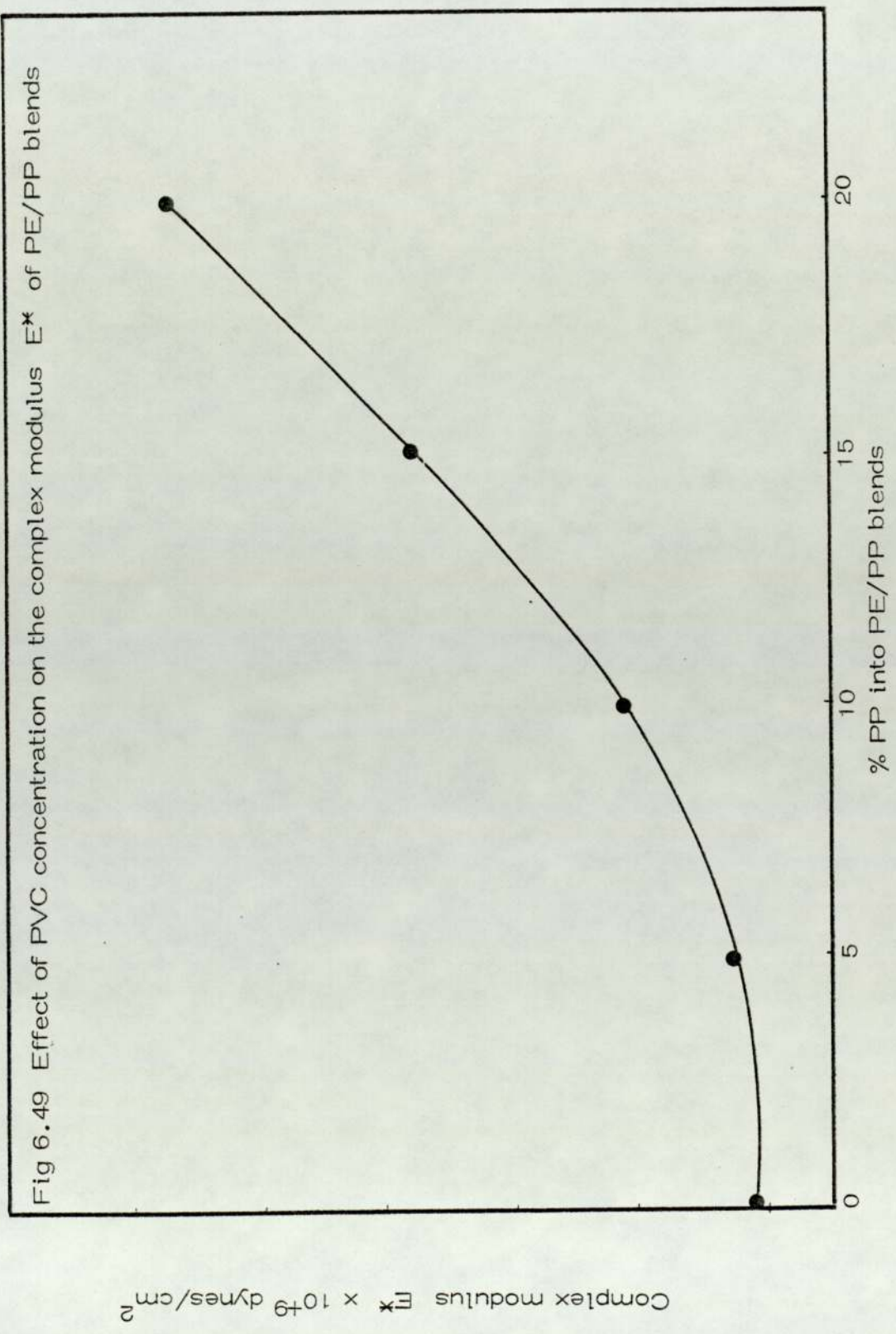


Fig 6.49 Effect of PVC concentration on the complex modulus E^* of PE/PP blends

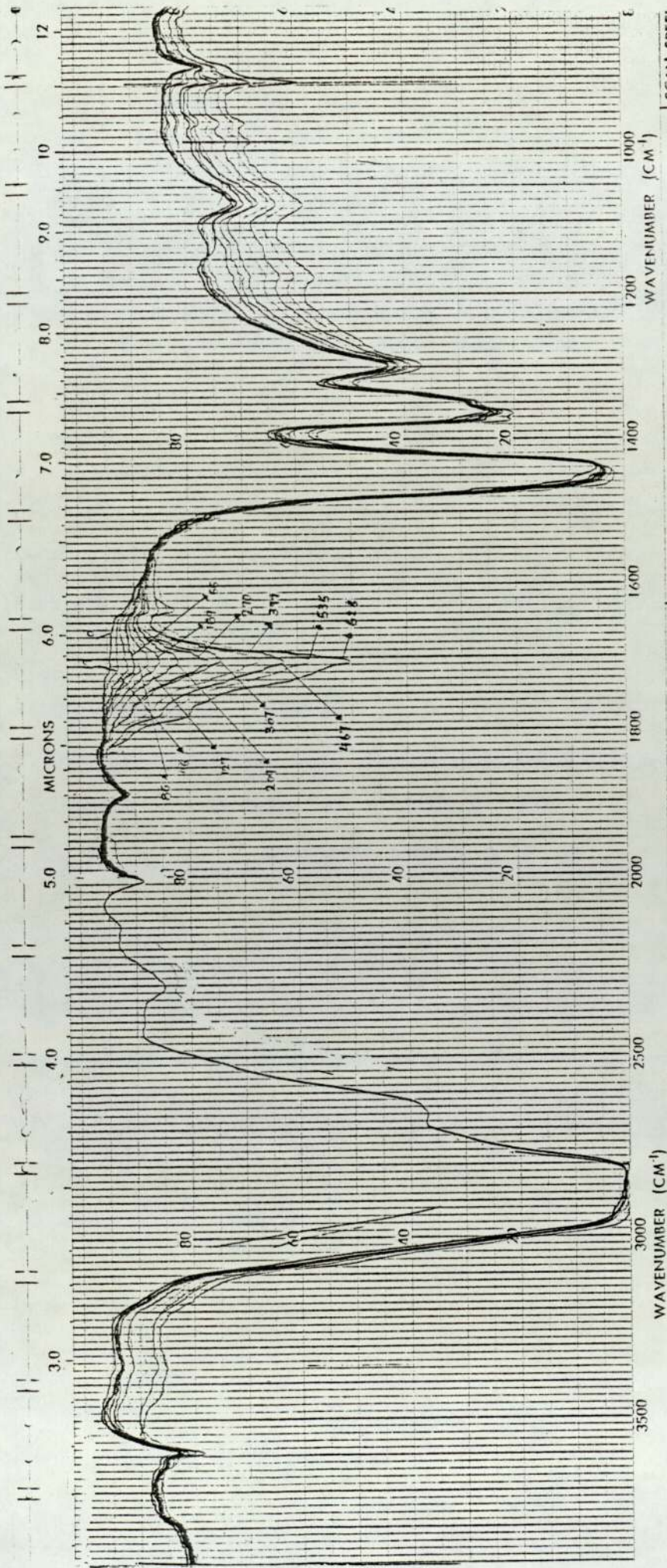
6.B.4.2 Results and Discussion

Infra-red examination of the LDPE/PP blends during uv irradiation shows the effect of polypropylene concentration on the rate of some growing functional groups in the region of $3000 - 3500 \text{ cm}^{-1}$ (OH) and $1700 - 1715 \text{ cm}^{-1}$ (C=O) respectively, (Figs 6.50 - 6.54). Examination of Figs 6.50 to 6.54 shows that as the concentration of the polypropylene (PP) is increased, the polyblends show greater susceptibility to ultraviolet light degradation (Fig 6.55). This lower photo-oxidative stability of the polyblends can be attributed to the presence of a labile hydrogen on the tertiary carbon in the polypropylene (See Chapter 5). Moreover, the melt processing operation involves a temperature (180°C) under which thermal oxidation of the polypropylene would be expected to give hydroperoxides and carbonyl groups which are believed to be the main photo-initiators (see Chapter 5).

The difference in the rate of photo-oxidation of the polyblends is also reflected in the change in mechanical properties. Fig 6.56 shows that elongation at break decreases more rapidly as the polypropylene concentration is increased. On prolonged exposure, this decrease in % elongation at break for the blends is only small (Figs 6.56 and 6.57). This is consistent with the fact discussed earlier (section 6.A.4) that chain scission predominates in PP.

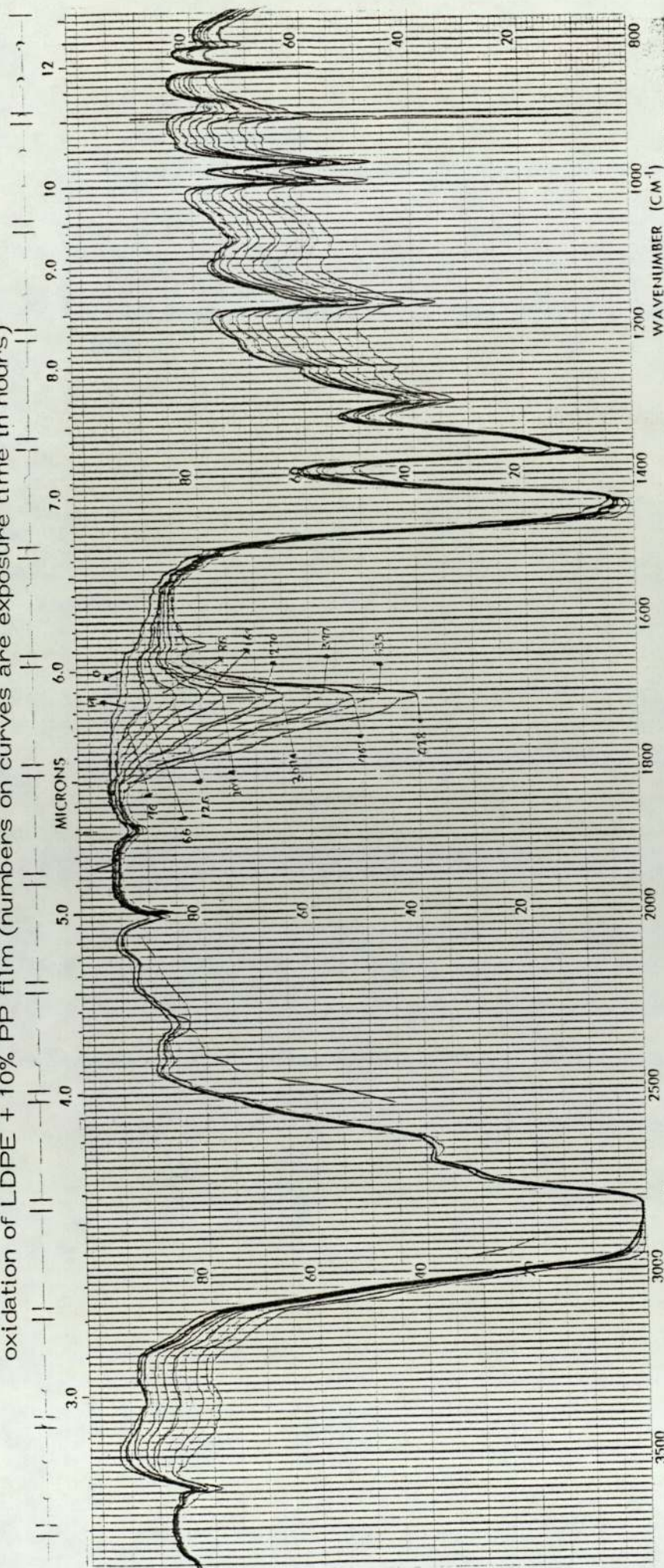
Tensile strength for the 10% and 20% polypropylene decreases during the early stages of uv irradiation but on further exposure the blends show an increase (Figs 6.58 and 6.59). Moreover, the increase for the 20% polypropylene blend is

Fig 6.50 Infra-red spectra of photo-oxidised LDPE film (numbers on curves are exposure time in hours)



SAMPLE 100% PE for the PET PP blends	SOLVENT CONCENTRATION CELL PATH REFERENCE	REMARKS	SCAN SPEED SLIT No 457-50
WAVENUMBER (CM ⁻¹)	WAVENUMBER (CM ⁻¹)	WAVENUMBER (CM ⁻¹)	WAVENUMBER (CM ⁻¹)

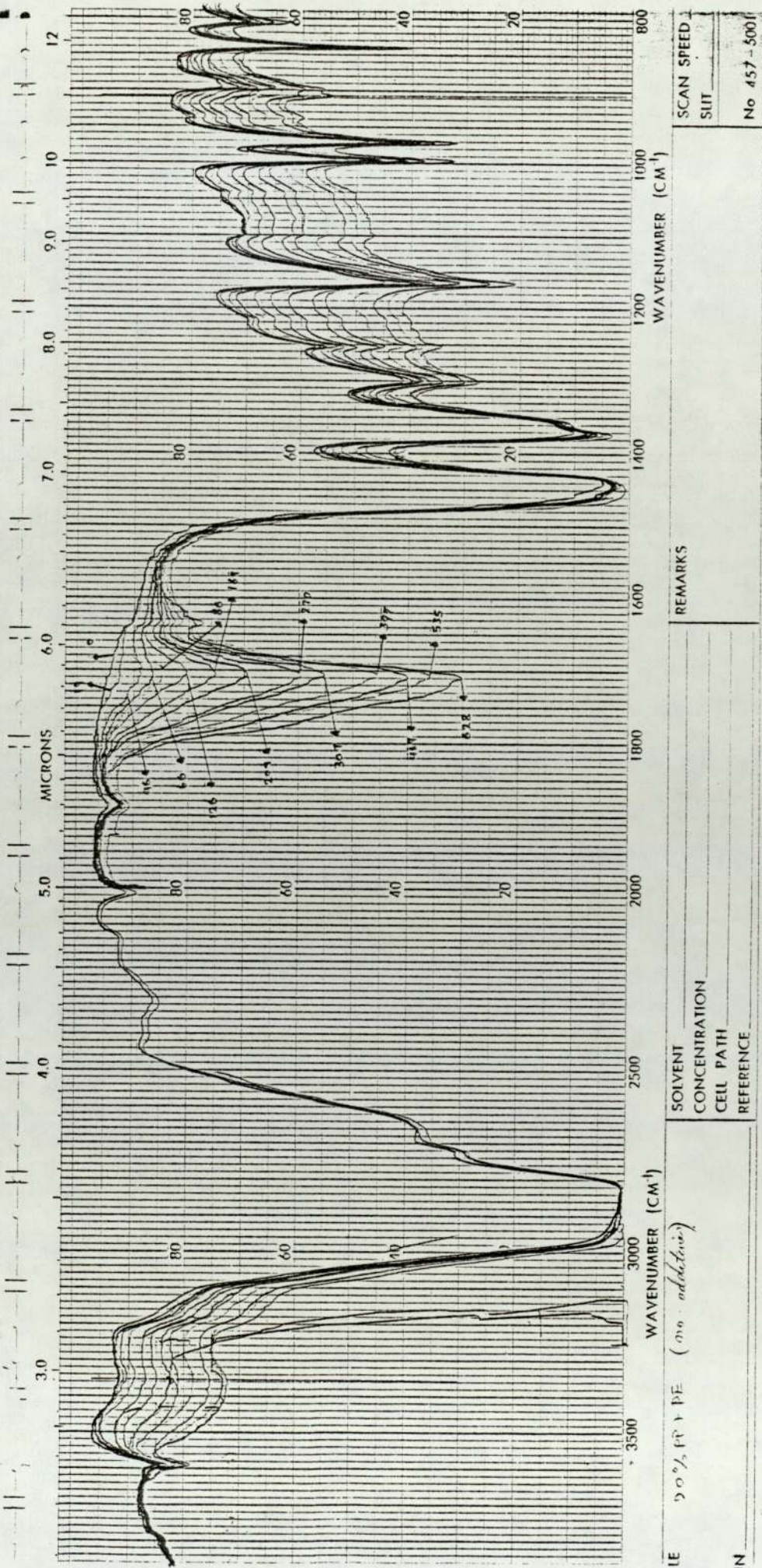
Fig 6.51 Change in hydroxyl (3500-3000 cm^{-1}) and carbonyl (1800-1600 cm^{-1}) absorption during photo-oxidation of LDPE + 10% PP film (numbers on curves are exposure time in hours)



REMARKS	SCAN SPEED
	SUIT
No 457-5001	
SOLVENT	
CONCENTRATION	
CELL PATH	
REFERENCE	

E (10/100-4PE) / 166000
 η_{sp}/c (15-15.5) : 0.115-0.185

Fig 6.52 Change in hydroxyl (3600-3000 cm^{-1}) and carbonyl (1800-1600 cm^{-1}) absorption during photo-oxidation of LDPE + 20% PP film (numbers on curves are exposure time in hours)



LE 20% PP + PE (no additive)

WAVENUMBER (CM^{-1})

WAVENUMBER (CM^{-1})

SCAN SPEED

SPLIT

No 457-500

REMARKS

SOLVENT

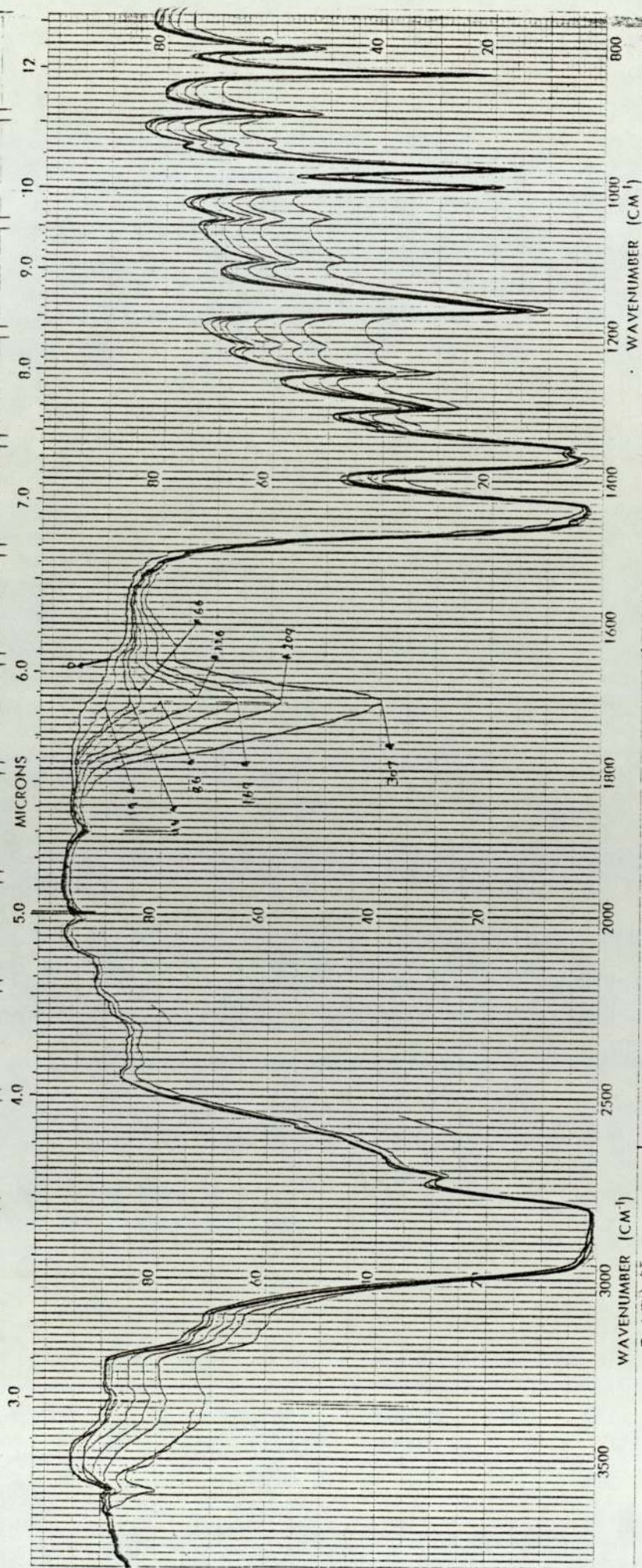
CONCENTRATION

CELL PATH

REFERENCE

IN

Fig 6.53 Change in hydroxyl ($3600-3000\text{ cm}^{-1}$) and carbonyl ($1800-1600\text{ cm}^{-1}$) absorption during photo-oxidation of LDPE + 50% PP film (numbers on curves are exposure time in hours)



SCAN SPEED
SLIT
No 457-5001

REMARKS

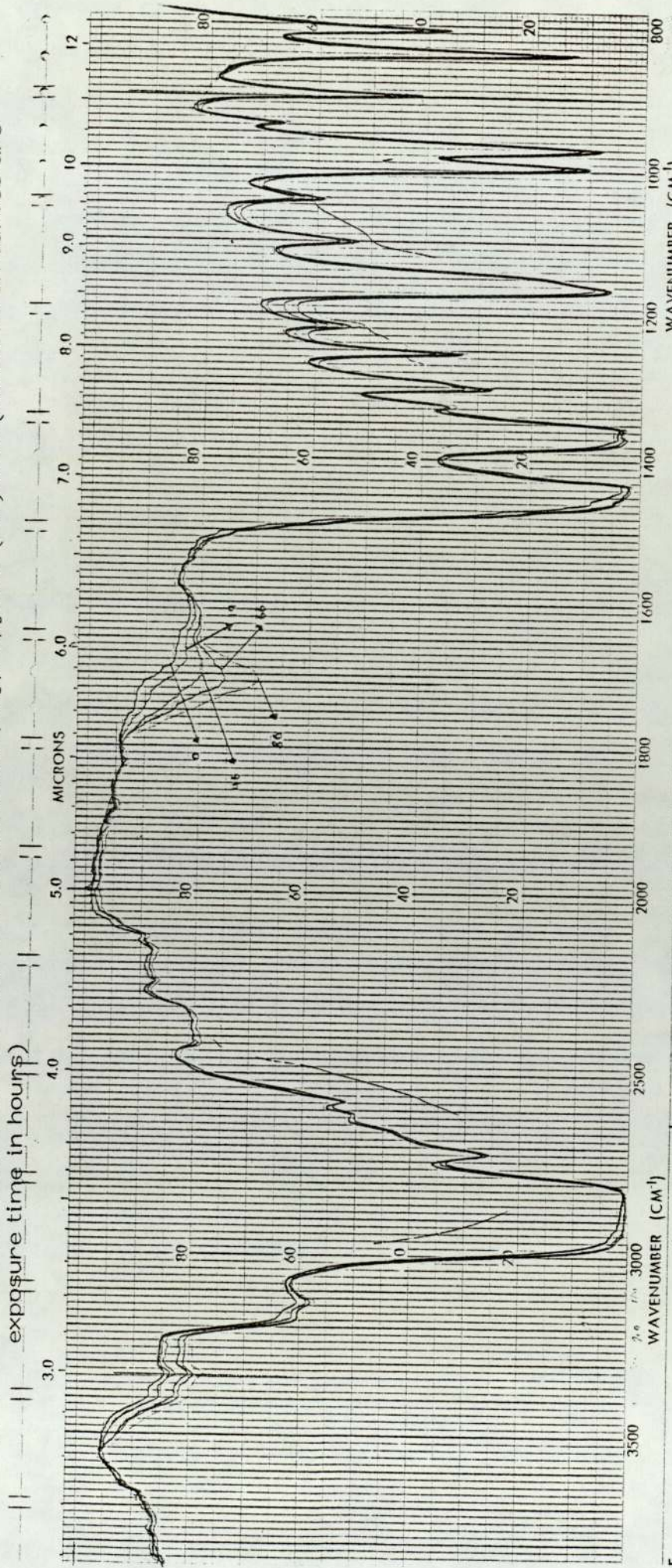
SOLVENT
CONCENTRATION
CELL PATH
REFERENCE

5.0% PP/1 PE

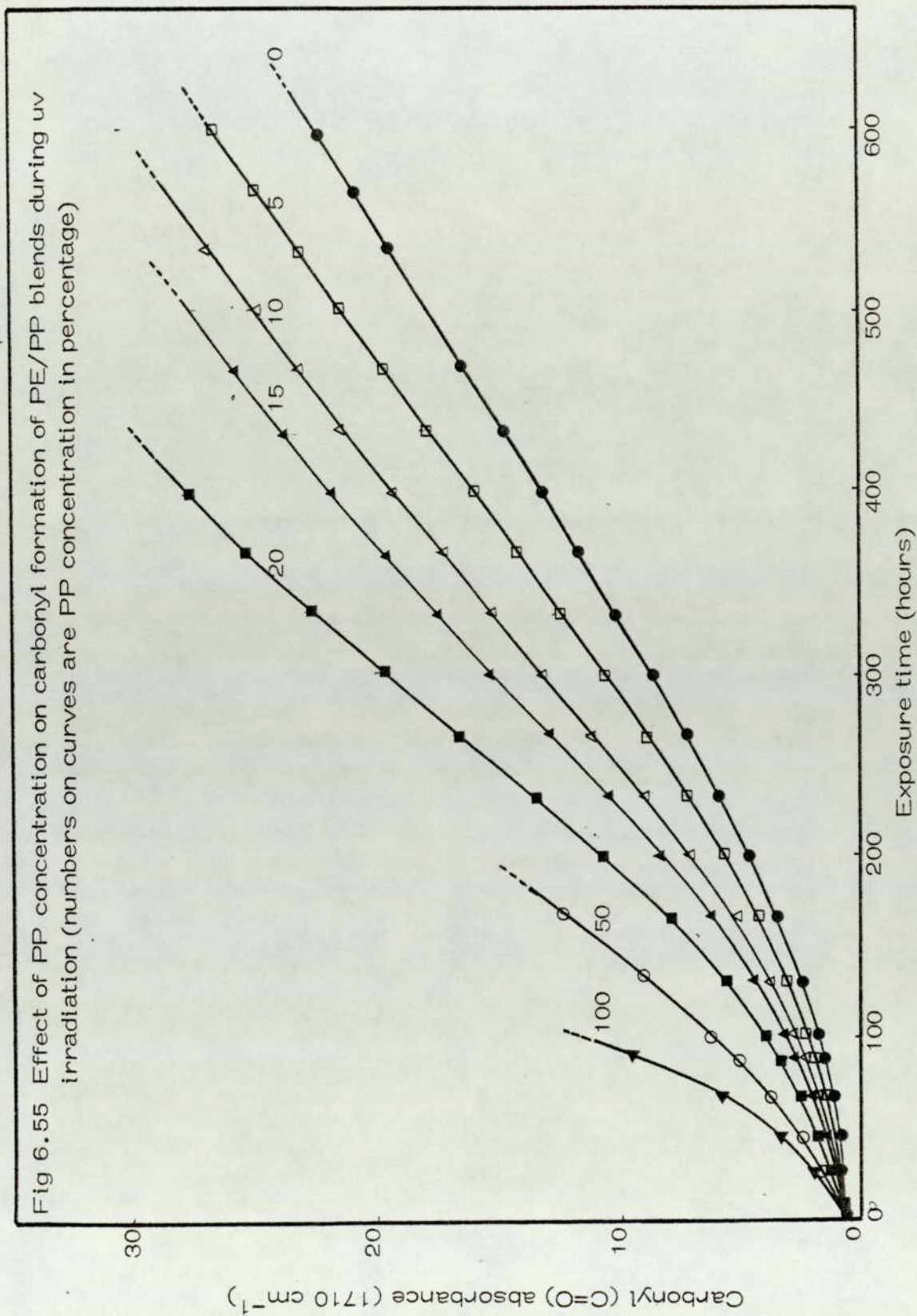
add. 1.0%
Thickness = 0.05 - 0.075

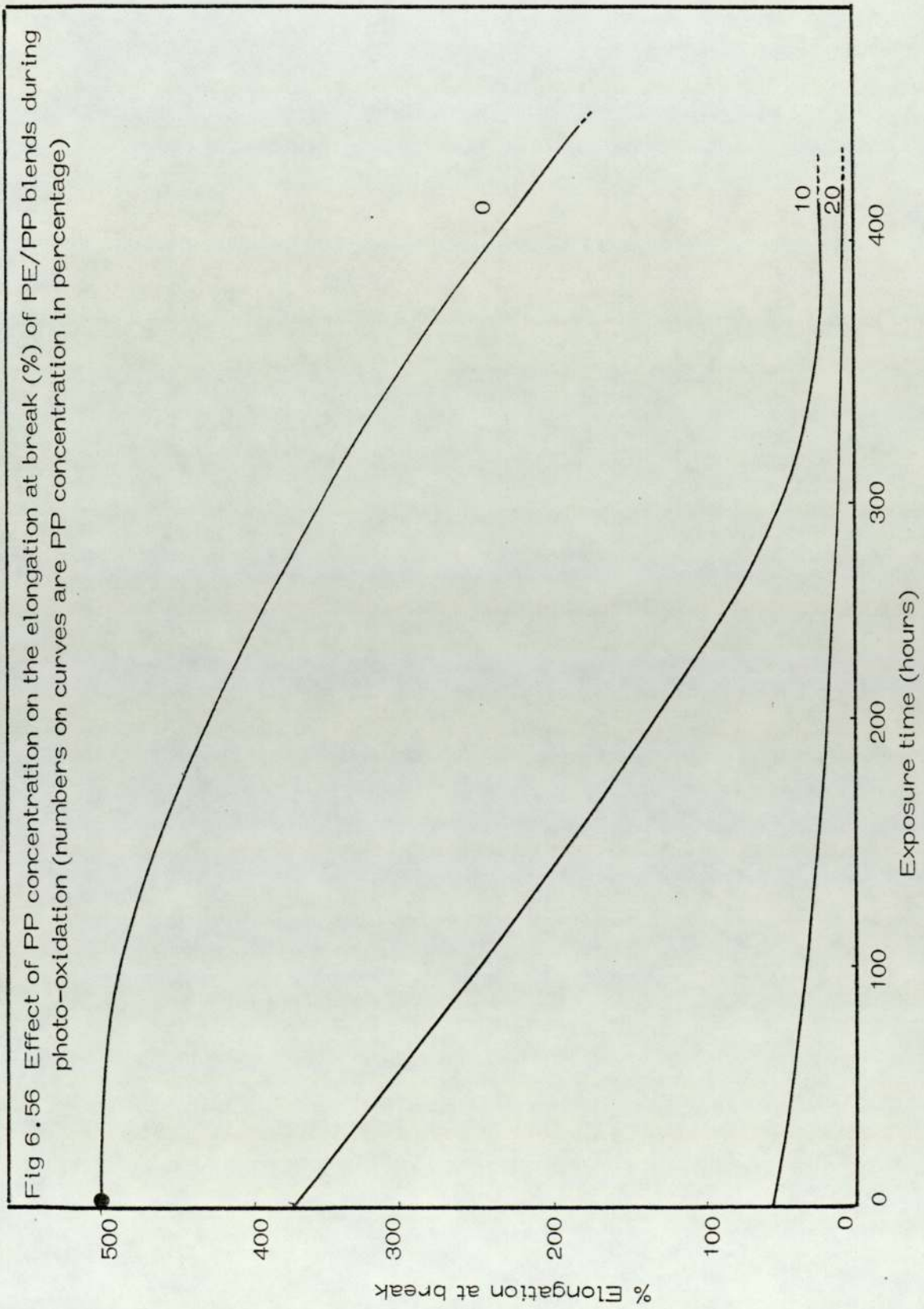


Fig 6.54 Infra-red spectra of photo-oxidised unstabilised polypropylene (PP) film (numbers on curves are exposure time in hours)



E	WAVENUMBER (CM ⁻¹)	SCAN SPEED
	SOLVENT	SUIT
	CONCENTRATION	No. 457-5001
	CELL PATH	
	REFERENCE	
REMARKS		
2 PP (for the head) (0.015 - 0.0155)		





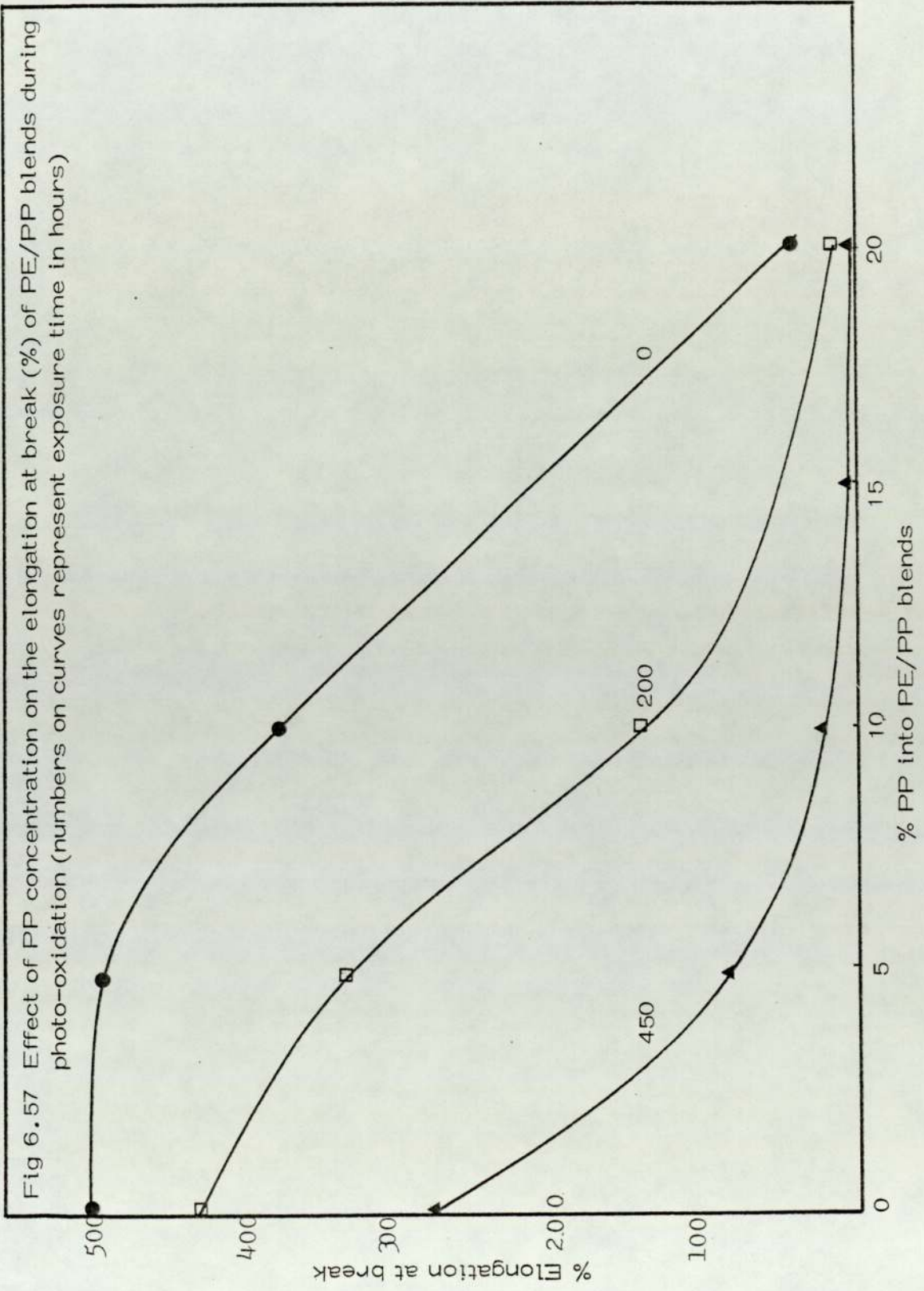


Fig 6.58 Effect of varying concentration of PP on the tensile strength of PE/PP blends during photo-oxidation (numbers on curves are PP concentration in percentage)

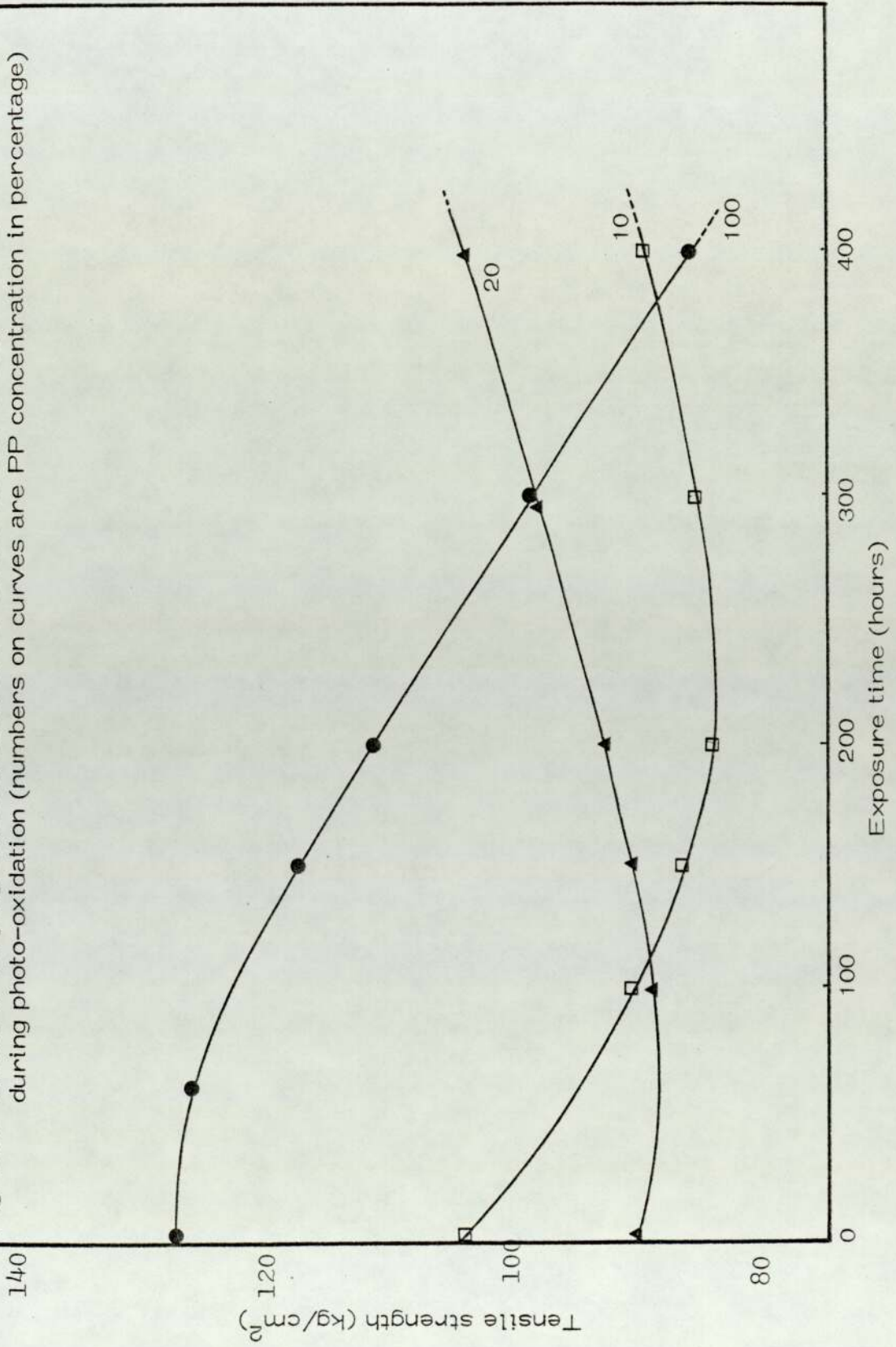
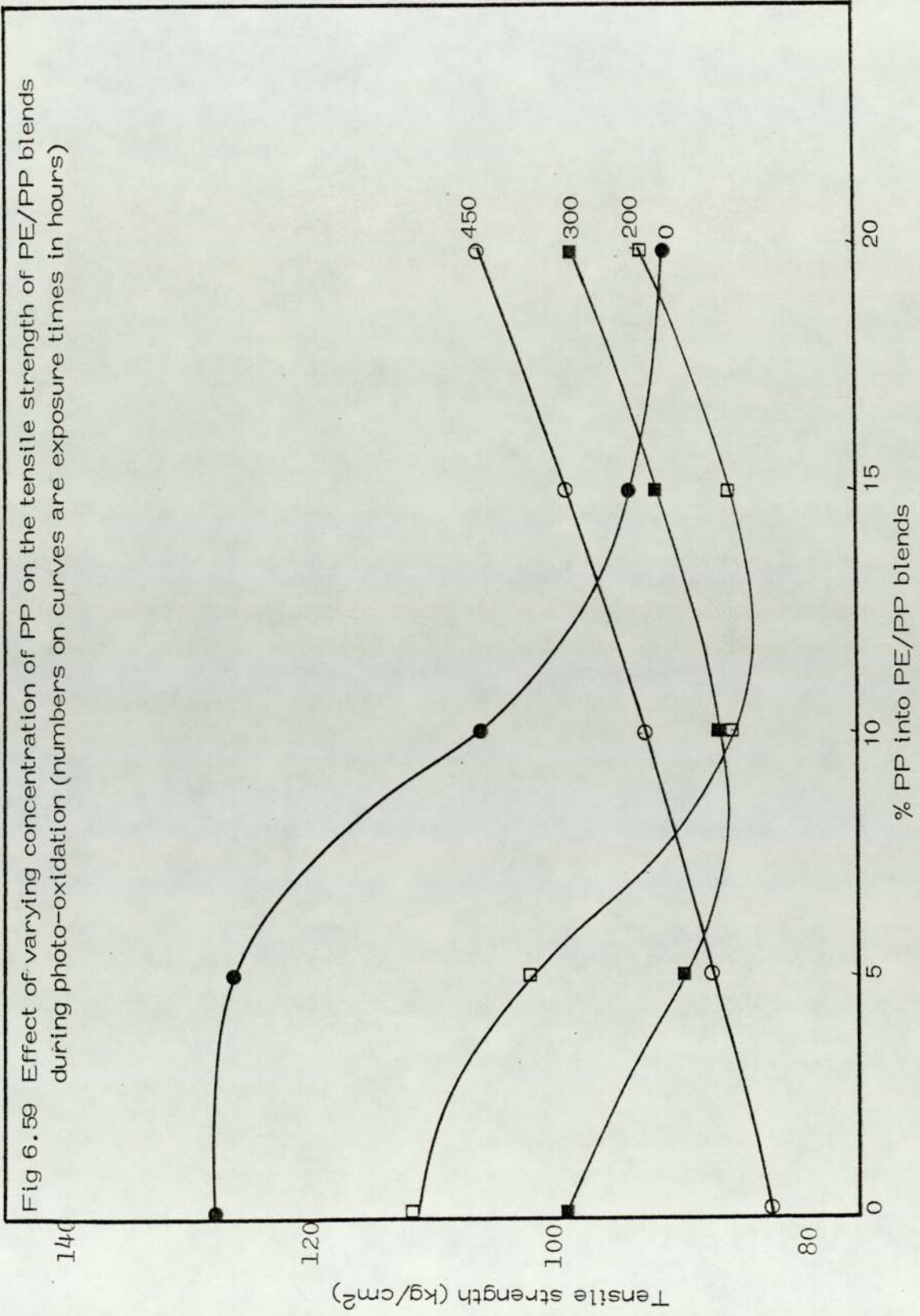
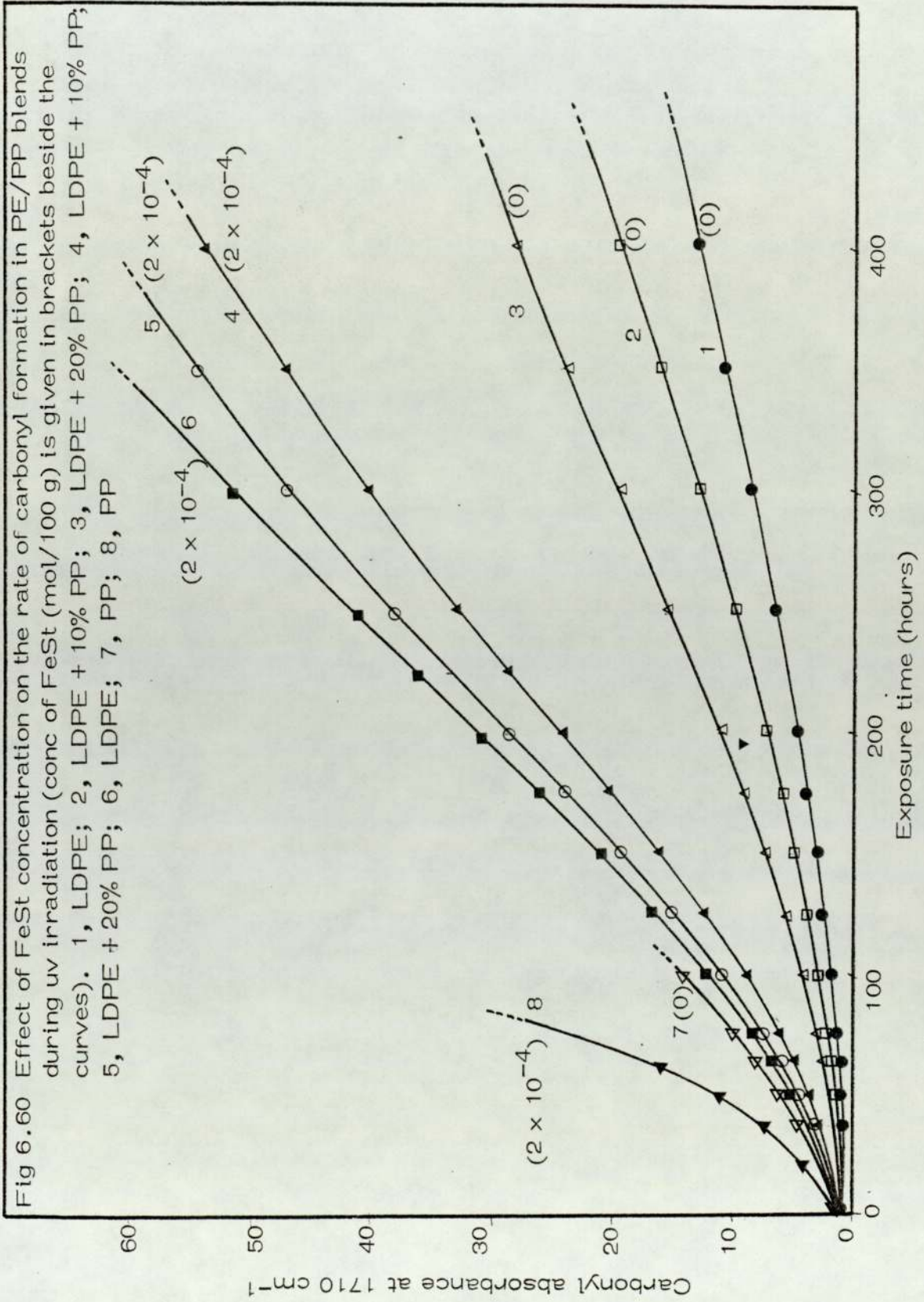


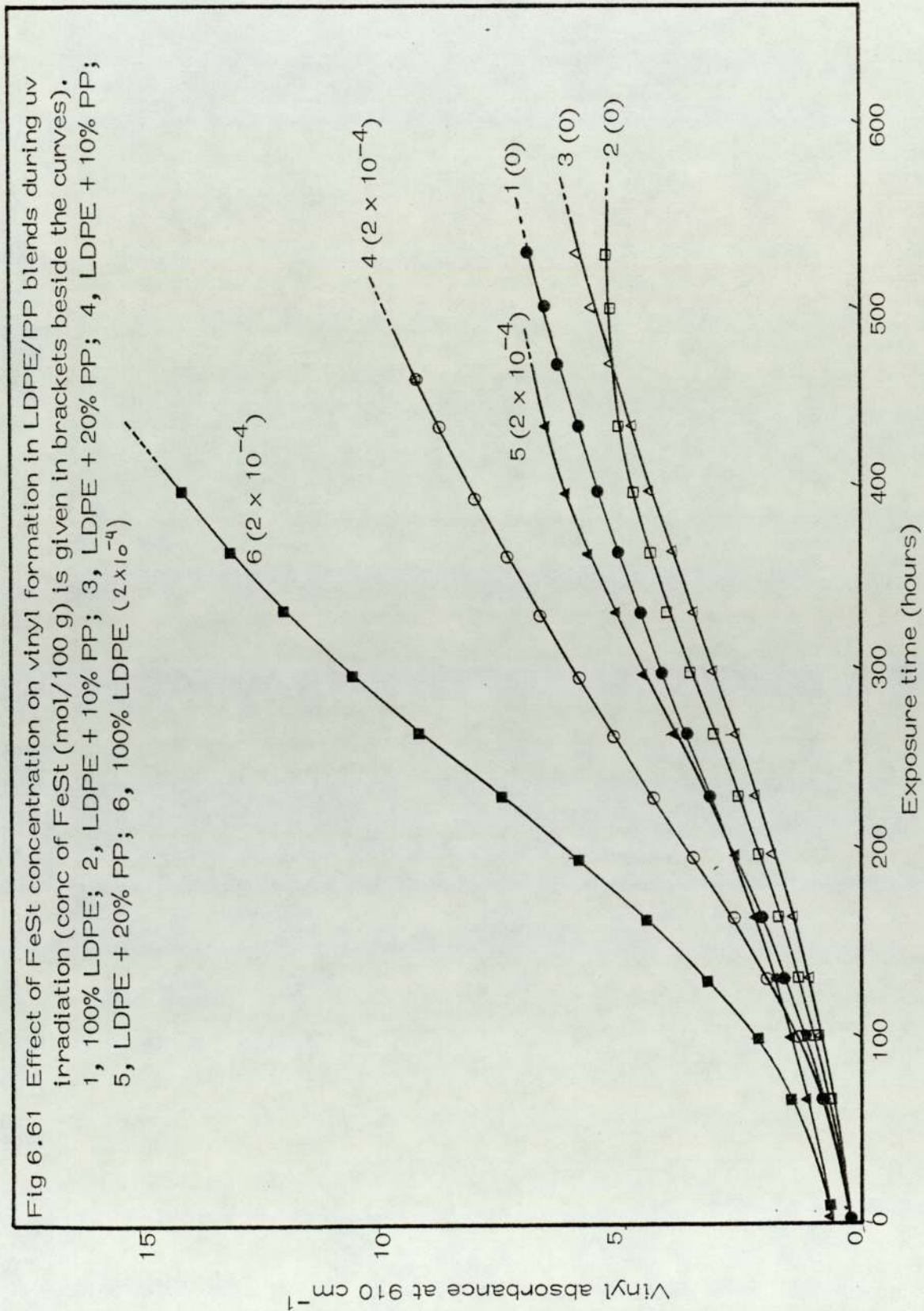
Fig 6.59 Effect of varying concentration of PP on the tensile strength of PE/PP blends during photo-oxidation (numbers on curves are exposure times in hours)



higher and started at an earlier stage of uv irradiation than did the 10% polypropylene blend (Fig 6.58). The increase in tensile strength is probably similar in origin to that for the PE/PVC blends and again is probably caused by some interaction at the boundaries of the two phases of the polymers. The probability of such interaction is higher for 20% than 10% polypropylene blends due to the rate of oxidation during uv irradiation (Fig 6.55).

The common transition metal ions are likely contaminants during processing and are not adequately removed from waste plastics. Transition metal ions have been shown previously (in Chapters 4 and 5) and also in section 6.A.5 to have a powerful pro-oxidant effect on the polymers and polyblends. Fig 6.60 shows the effect of ferric stearate (FeSt) on the photo-oxidation of PE/PP blends: It appears that in the presence of FeSt LDPE has lower stability than 10% and 20% polypropylene when subjected to uv light. This stability of the blends compared to the LDPE again might be due to some interaction between the PE and the PP phases (PE is the continuous phase and PP is the dispersed phase in the system)⁽²³⁵⁾. This interaction between the two polymer phases (or boundaries) can play a retarding role which prevents the oxidation of both polymeric components. The formation of the main products of oxidation (C=O at 1710 cm^{-1} , Figs 6.60 and vinyl at 910 cm^{-1} , Fig 6.61) show a significant reduction for the blends (10% and 20% PP) compared with the pure components.





6.B.5 Introduction of Some Solid Phase Dispersants (SPD's) to Improve the Toughness of Blends

6.B.5.1 Introduction

Many commercially produced grades of high impact strength polypropylene are physical blends of polypropylene and EPDM (ethylene propylene–diene terpolymer) and a recent paper by Speri and Patrick⁽²⁷⁹⁾ describes one such system. Their results indicate that the optimum particle size is near $0.5\ \mu\text{m}$ but they point out that this is achievable only under conditions of high shear and when bulk viscosities of the continuous and disperse phases are closely matched. Because the bulk viscosities of EPDM is so high, these conditions can only be met with those polypropylenes whose molecular weights and bulk viscosities are too high for convenient injection moulding. Addition of high density polyethylene (HDPE) increases the dispersibility of EPDM and helps to maintain high flexural modulus in the toughened polypropylene and hardens it sufficiently for application in typical thermoplastic processing techniques.

Polypropylene toughened by addition of 15 – 25 wt % EPDM or EPDM–HDPE is used principally in injection moulding applications. Because the EPDM is neither cross-linked nor grafted to the matrix (in contrast to high impact polystyrene or ABS resins) injection moulded articles have a complex phase morphology which is unusually sensitive to melt flow patterns. As a result, such blends often exhibit especially weak knit lines, formed in multiplygated injection mouldings.

6.B.5.2 Experimental

In order to improve mechanical properties such as elongation at break and impact strength at break, selected additives (eg EPDM, ACS, ABS, SBS, PU and BR, see section 6.A.2) were blended with PE/PP (50/50) blends as described in section 6.A.6.2.

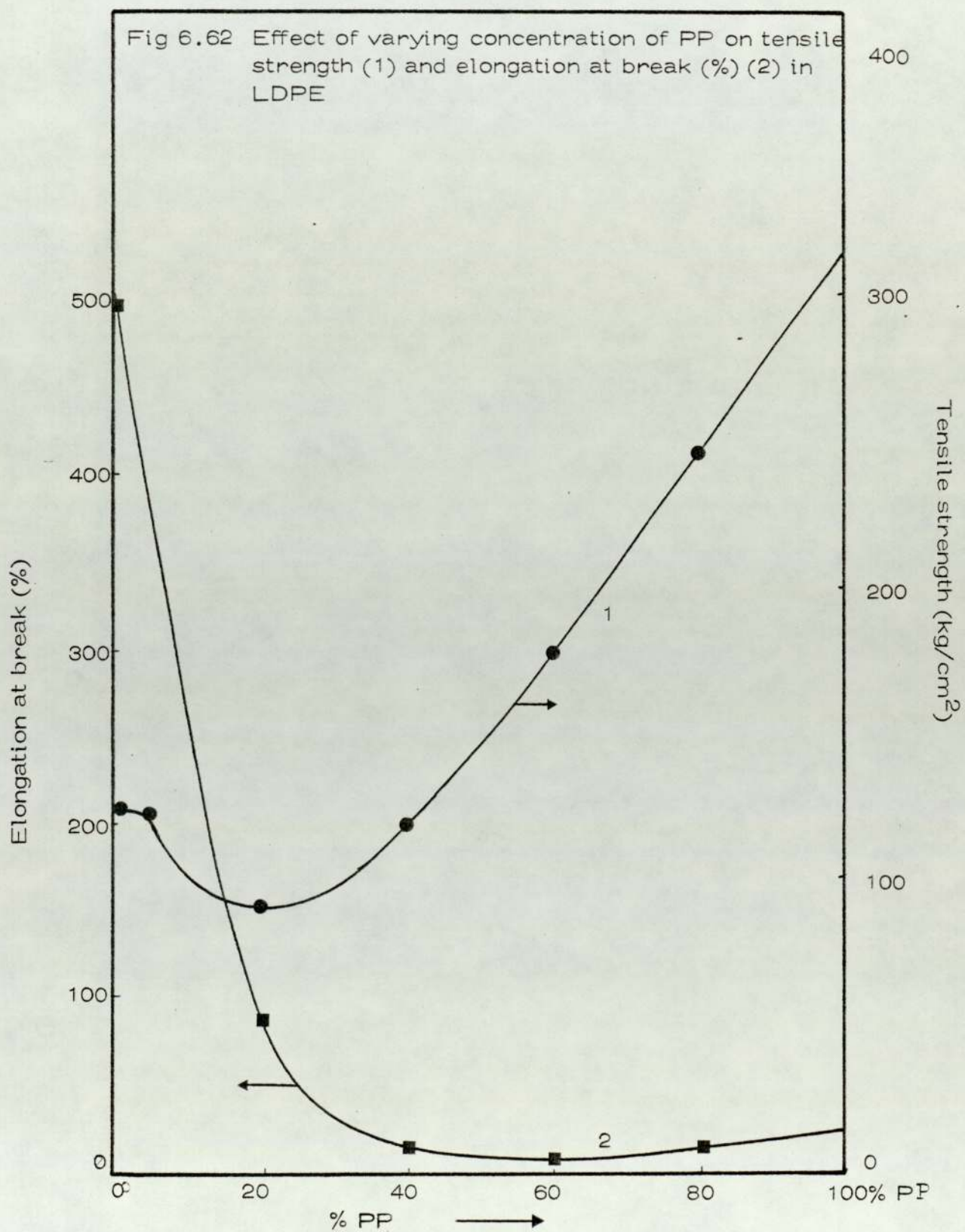
6.B.5.3 Results and Discussion

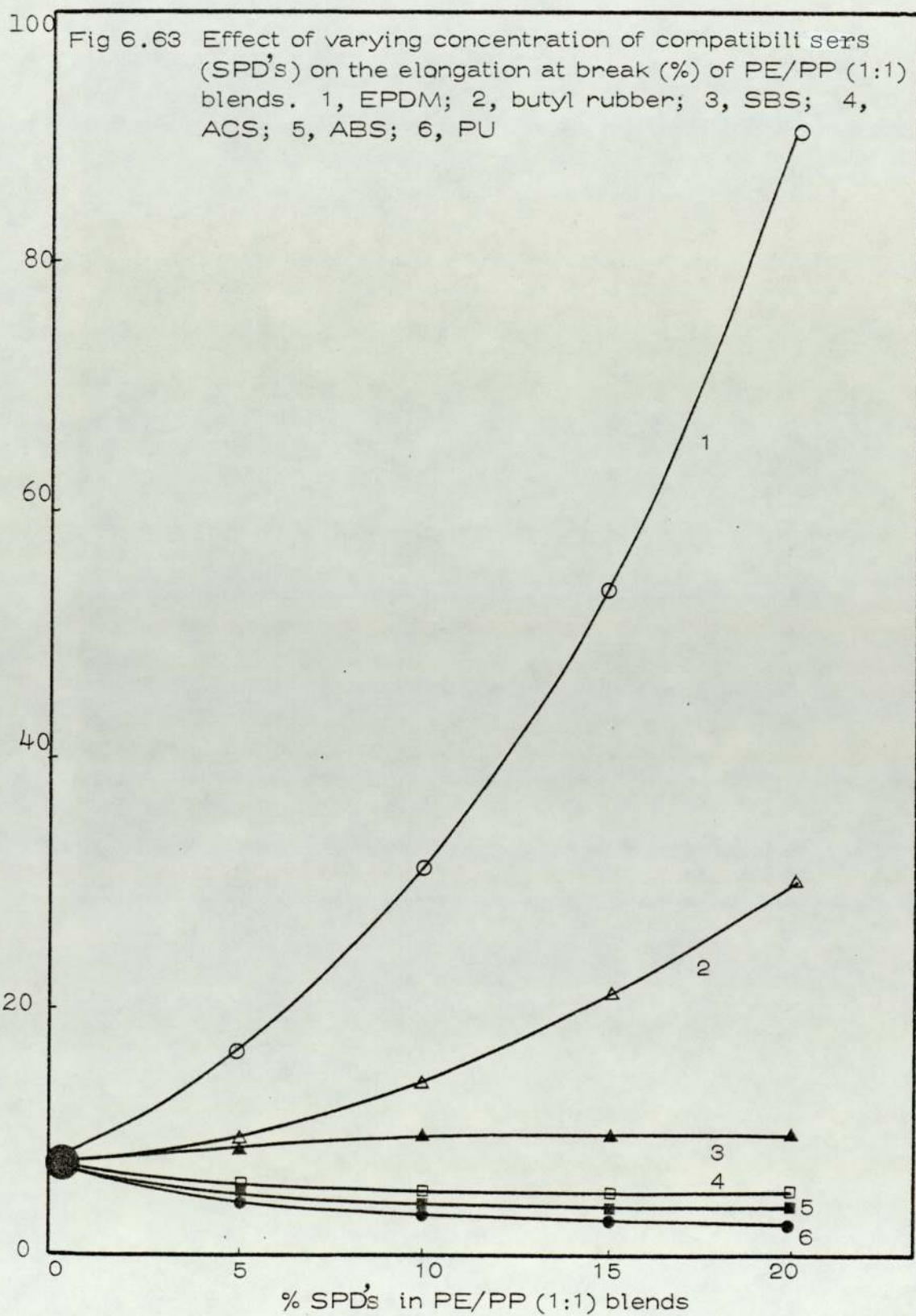
The tensile strength and % elongation at break indicate a minimal in the range of 30–50 percent of PP into PE (Fig 6.62). Table 6.B.2 and Figs 6.63–6.65 show the effect of the above additives on the 50/50 PE and PP blends. Figs 6.63 and 6.65 indicate that EPDM causes a significantly better improvement in elongation at break (%) and impact strength of (50/50) PP/PE blends than other additives. This is most evident at higher concentrations of EPDM (eg 20% EPDM). In PE/PP blends, the reason for the improvement in % elongation at break and impact strength is not well understood and would require further investigation (see Chapter 7).

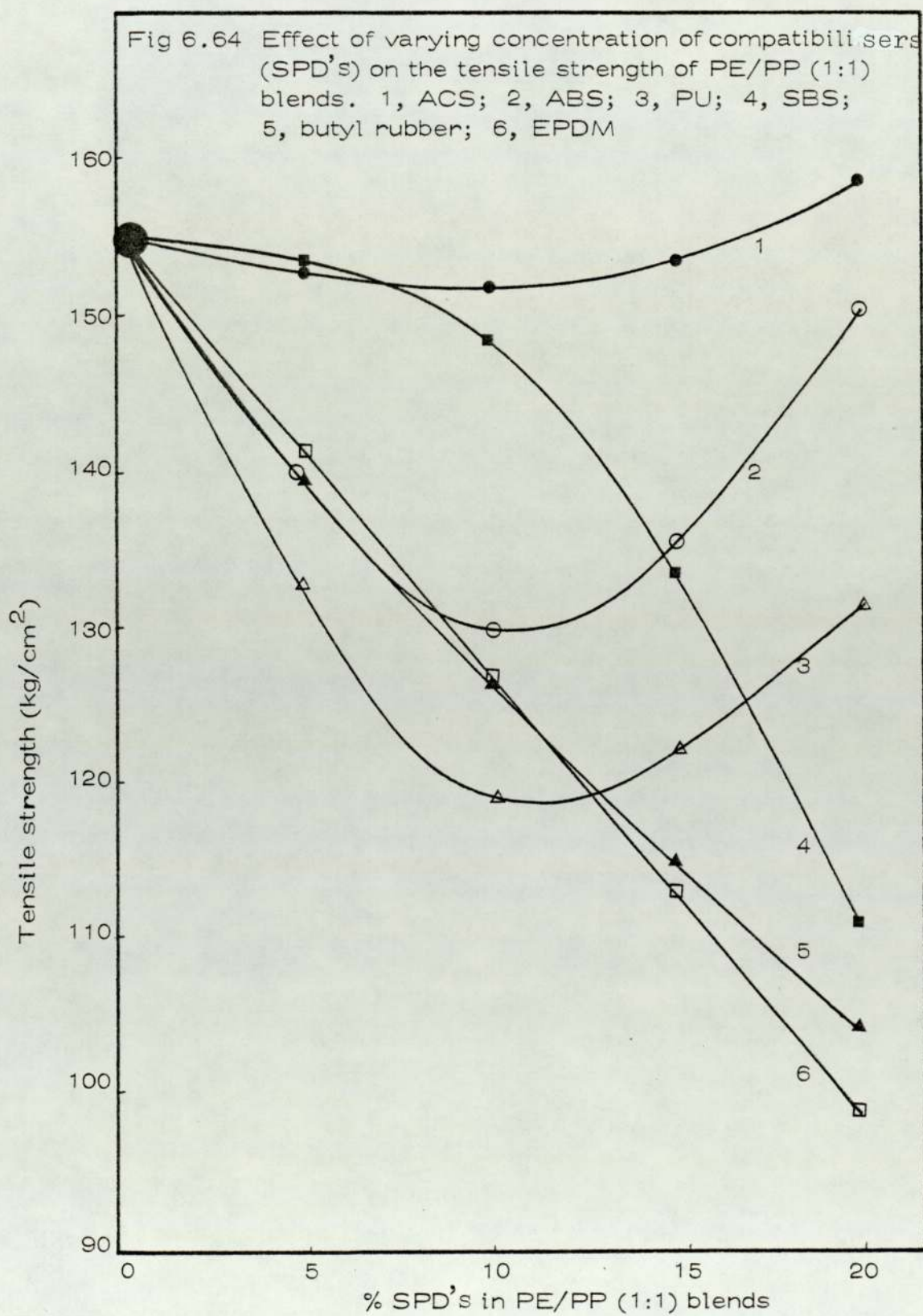
6.C Effect of Polystyrene (PS) Concentration on Mechanical Properties of LDPE Blends

6.C.1 Introduction

Blends that contain roughly equal properties of PE and PS have the strength of PE and the brittleness of PS⁽²⁸³⁾. This combination of properties is very poor and consequently such blends have little value as structural materials. PE and PS







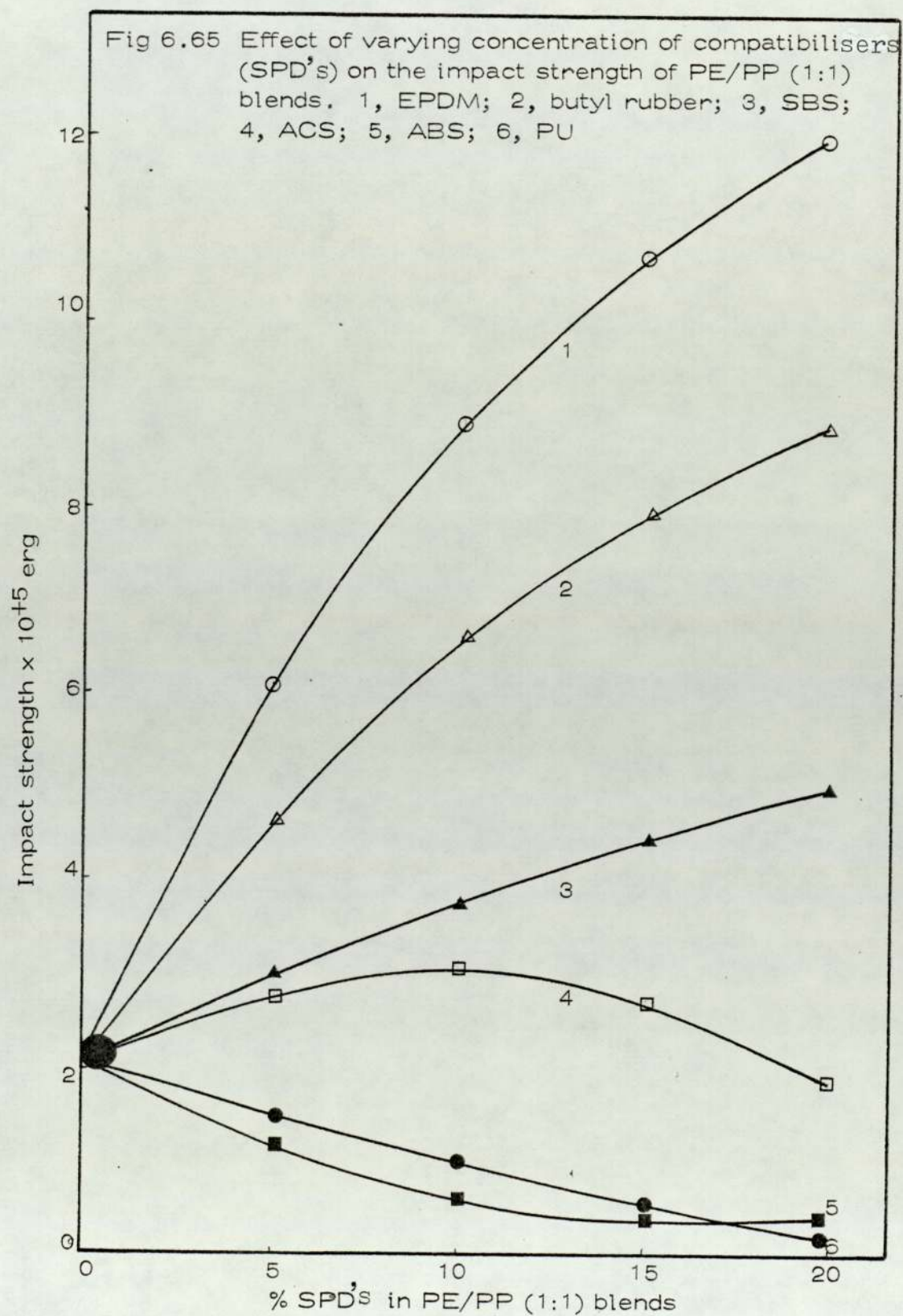


Table 6.B.2 Effect of varying concentration of SPD's on the mechanical properties of PE/PP (50/50) blends

No	Formulation	Elongation at break (%)	Tensile strength (kg/cm ²)	Impact strength (x 10 ⁺⁵) ergs
	PE + PP + additives (%)			
1	100 % LDPE	480-500	128	8.5-9.0
2	50 + 50 + 0	7.33	156.0	1.96
3	45 + 45 + 10 EPDM	32.0	126.0	9.01
4	40 + 40 + 20 EPDM	90.5	98.0	11.7
5	45 + 45 + 10 BR	13.5	126.5	6.7
6	40 + 40 + 20 BR	31.0	106.0	8.8
7	45 + 45 + 10 SBS	9.50	149.0	3.75
8	40 + 40 + 20 SBS	10.50	110.0	5.05
9	45 + 45 + 10 ABS	4.50	130.0	0.55
10	40 + 40 + 20 ABS	4.66	151.0	0.35
11	45 + 45 + 10 ACS	7.0	152.0	3.2
12	40 + 40 + 20 ACS	6.0	157.0	1.6
13	45 + 45 + 10 PU	3.3	119.0	0.95
14	40 + 40 + 20 PU	2.98	131.0	0.195

are quite immiscible and microscopic examination reveals rather large domain structures⁽²⁸⁰⁻²⁸²⁾. D Heikens and Barensten⁽²⁸²⁾ have studied the particle size and domains in polystyrene/polyethylene blends as a function of their melt viscosity. A potential approach to this problem is to incorporate additives into the blend which will bind together the incompatible polymers. Suitably chosen block or graft copolymers are attractive candidates for this role since they are likely to be located at domain boundaries and provide adhesion between the phases⁽²⁸⁰⁻²⁸³⁾.

It was postulated that the properties of melt blends of polystyrene and polyethylene might be improved by the additives of a graft copolymer of styrene onto a polyethylene backbone^(237,281). Such grafts have been studied extensively but no commercial source exists. The use of high energy radiation for forming PE-g-PS were studied by C E Locke and coworkers.⁽²³⁷⁾ Grafting of styrene onto polyethylene was accomplished by the direct method using a cobalt⁶⁰ source of γ -rays. They used⁽²³⁷⁾ graft copolymers of styrene onto polyethylene as additives to improve the mechanical properties of PE/PS blends. Blends containing equal properties of low density polyethylene and polystyrene were selected for their study since composition represents the poorest balance of properties in this system. The addition of graft copolymers generally increased both the yield strength and the elongation at break of the blend.

Barensten, Heikens and Piet⁽²⁸⁰⁻²⁸²⁾ concluded from microscopic examination that if the content of one of the polymers in PS/PE blends is less than 40%, this polymer

forms a dispersed phase.

6.C.2 Experimental

Polystyrene (PS) containing external lubricant was supplied by Shell under the name of 'Shell Carinex general purpose' and low density polyethylene (LDPE) which is explained in section 6.A and Chapter 4 were used in this experiment.

Blends of PS and LDPE were processed at 180°C in the RAPRA torque rheometer for 5 minutes in closed chamber and also continuous film of even thickness was extruded using an 18 mm Betol (Betol Machinery Ltd., Luton, Bedfordshire). Fixed temperature settings were used throughout all operations. These were as follows: barrel zone 3 at 180°C, barrel zone 2 at 170°C, barrel zone 1 at 160°C, die zones 1 and 2 at 180°C. The blends which processed from the torque rheometer then compression moulded at 180°C for 2 minutes into sheets as described in Chapter 3.

Table 6.C.1 shows the formulation with varying properties of PS (0, 2, 4, 6, 8 and 10% PS). All formulations were based on 35 gm of polymer.

Tensile strength, % elongation and Young's modulus were calculated at the cross-head speed of 2 cm/minutes at room temperature ($21 \pm 1^\circ\text{C}$) (more details are given in Chapter 3).

Dynamic mechanical property measurements and optical microscopy examination were carried out as described in the main experimental Chapter 3.

Table 6.C.1

	Composition (%)		Charge weight to mixer	
	LDPE	PS	LDPE	PS
100	0	35	0	
98	2	34.28	0.72	
96	4	33.56	1.44	
94	6	32.84	2.16	
92	8	32.12	2.88	
90	10	31.4	3.6	

6.C.3 Results and Discussion

Optical micrographs of low density polyethylene alone and in presence of 2, 4 and 10% polystyrene are shown respectively in Plates 1C-4C. It is seen from the optical micrographs that polyethylene alone showed a fine texture (Plate 1C) whereas no texture is observed in presence of polystyrene (Plates 2C-4C).

Figs 6.70 - 6.73 show the changes in modulus, tensile strength, elongation at break and impact strength of pure LDPE and in presence of PS. Modulus in the blend increases with increasing PS concentration and other mechanical properties decrease compared to LDPE alone.

It can be observed from all the optical micrographs (Plates 1C-4C) that the blends have a two phase structure. Polyethylene forms a continuous phase, while polystyrene forms domains which are embedded in polyethylene matrix⁽²⁸⁰⁾. This clearly shows that the two polymers are incompatible. As the amount of polystyrene in the blends increases the domain size increases and it is an indication of increased incompatibility. This incompatibility of PE/PS is supported by the work of Paul and co-workers⁽²³⁷⁾ on the dynamic mechanical properties of blends. They found that⁽²³⁷⁾ there is two distinct transitions (T_g) corresponding to the PE and PS. They also compared the melt blends of PE/PS with the graft (LDPE-g-PS).

It is possible, as observed earlier from PE/PVC and PE/PP, the increased incompatibility might be reflected in the mechanical properties of the blends which would deteriorate



Plate 1C 100% LDPE (Optical)
Mn = 200

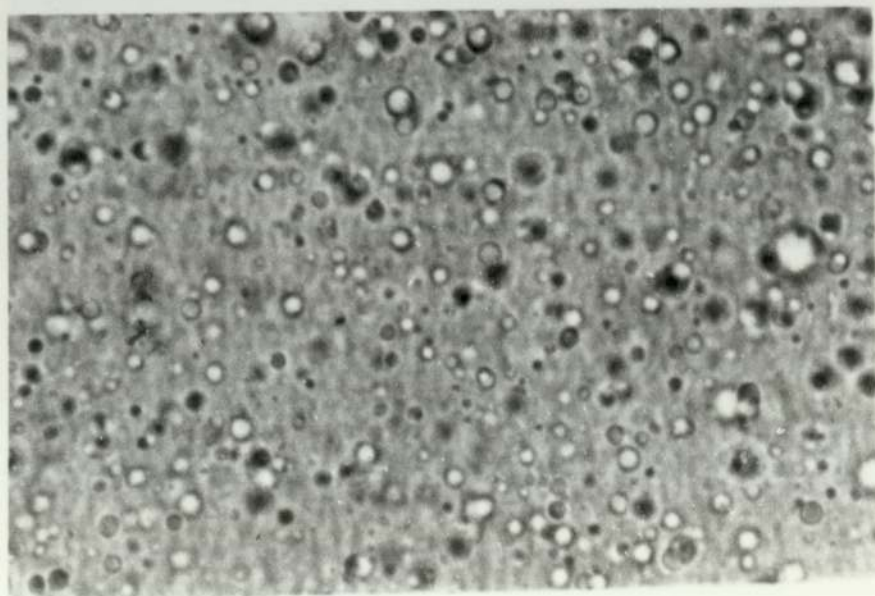


Plate 2C (PE+2%PS) (Optical)
Mn = 400

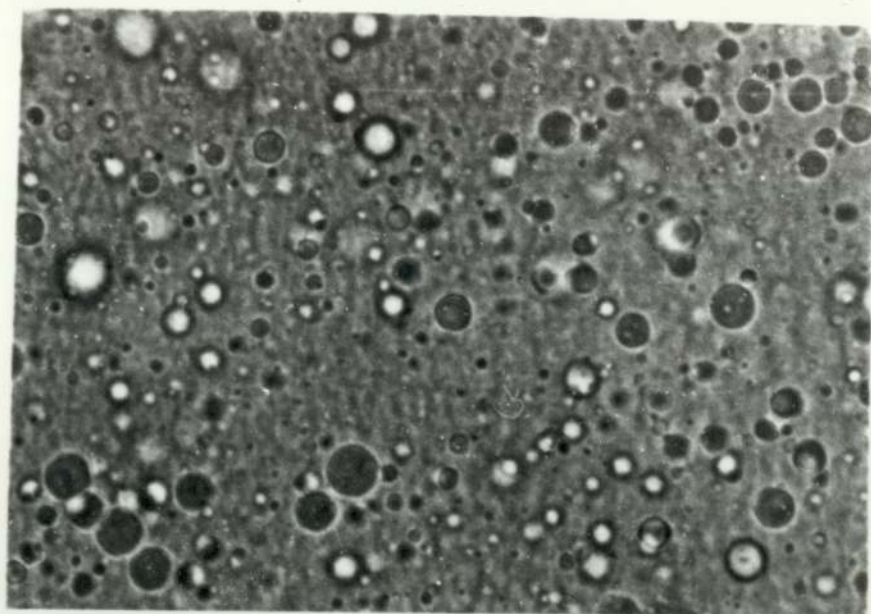


Plate 3C (PE + 4% PS) (Optical)

$M_n = 400$

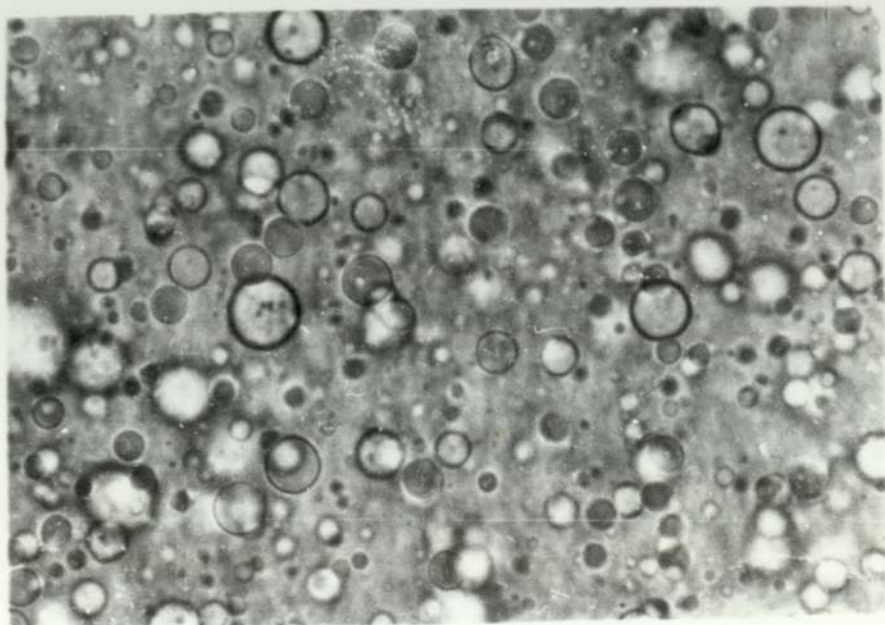
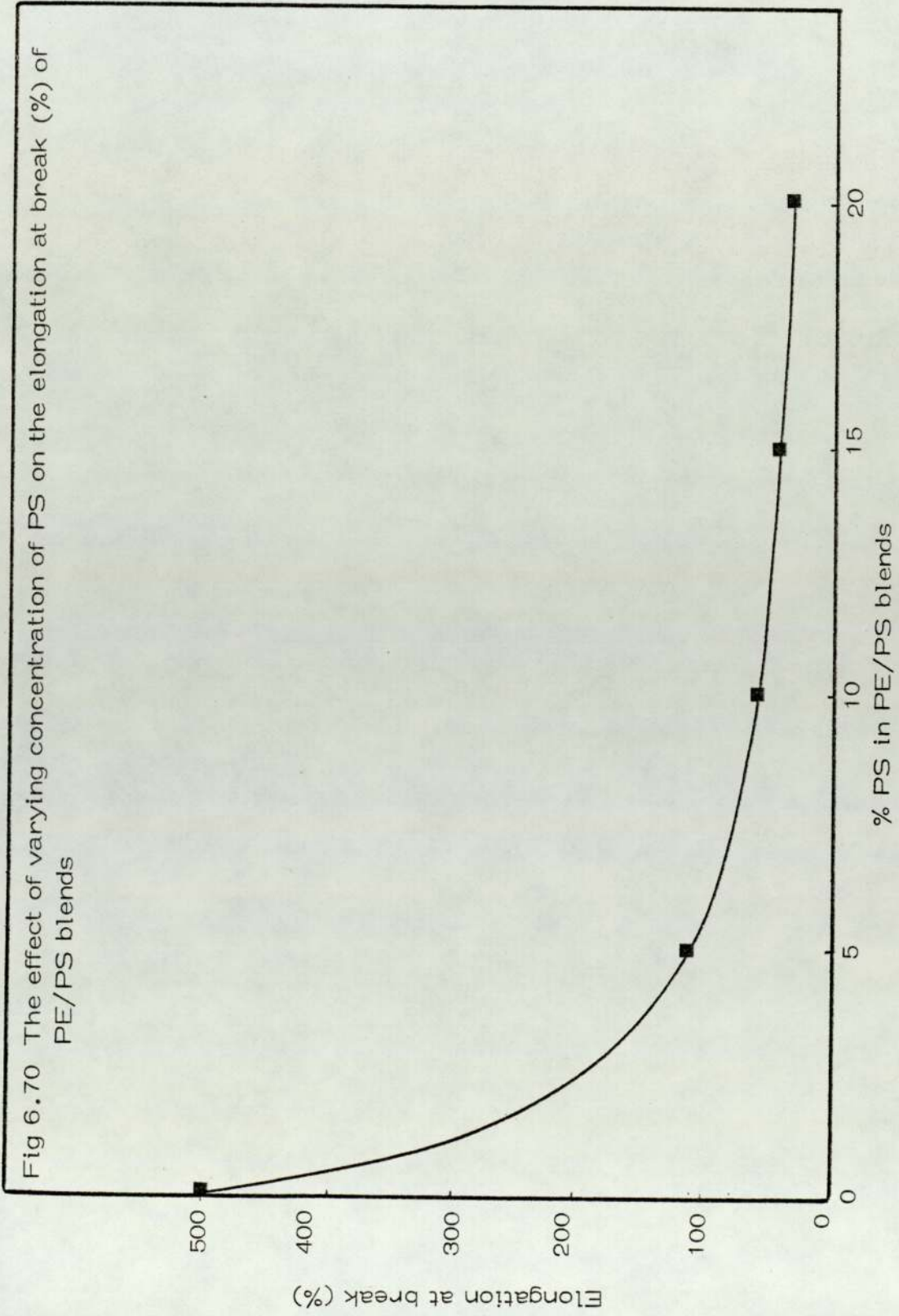
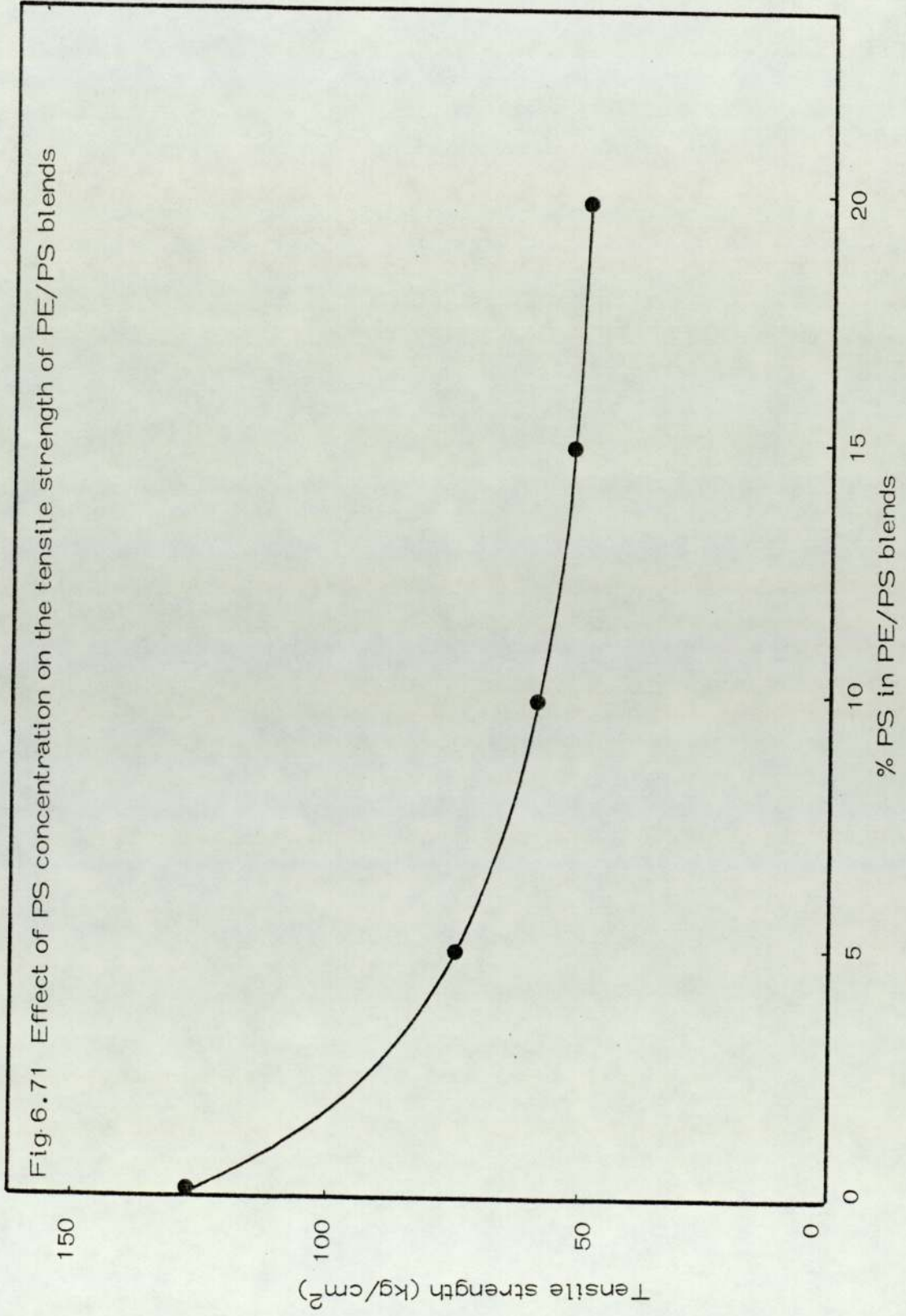


Plate 4C (PE + 10% PS) (Optical)

$M_n = 400$





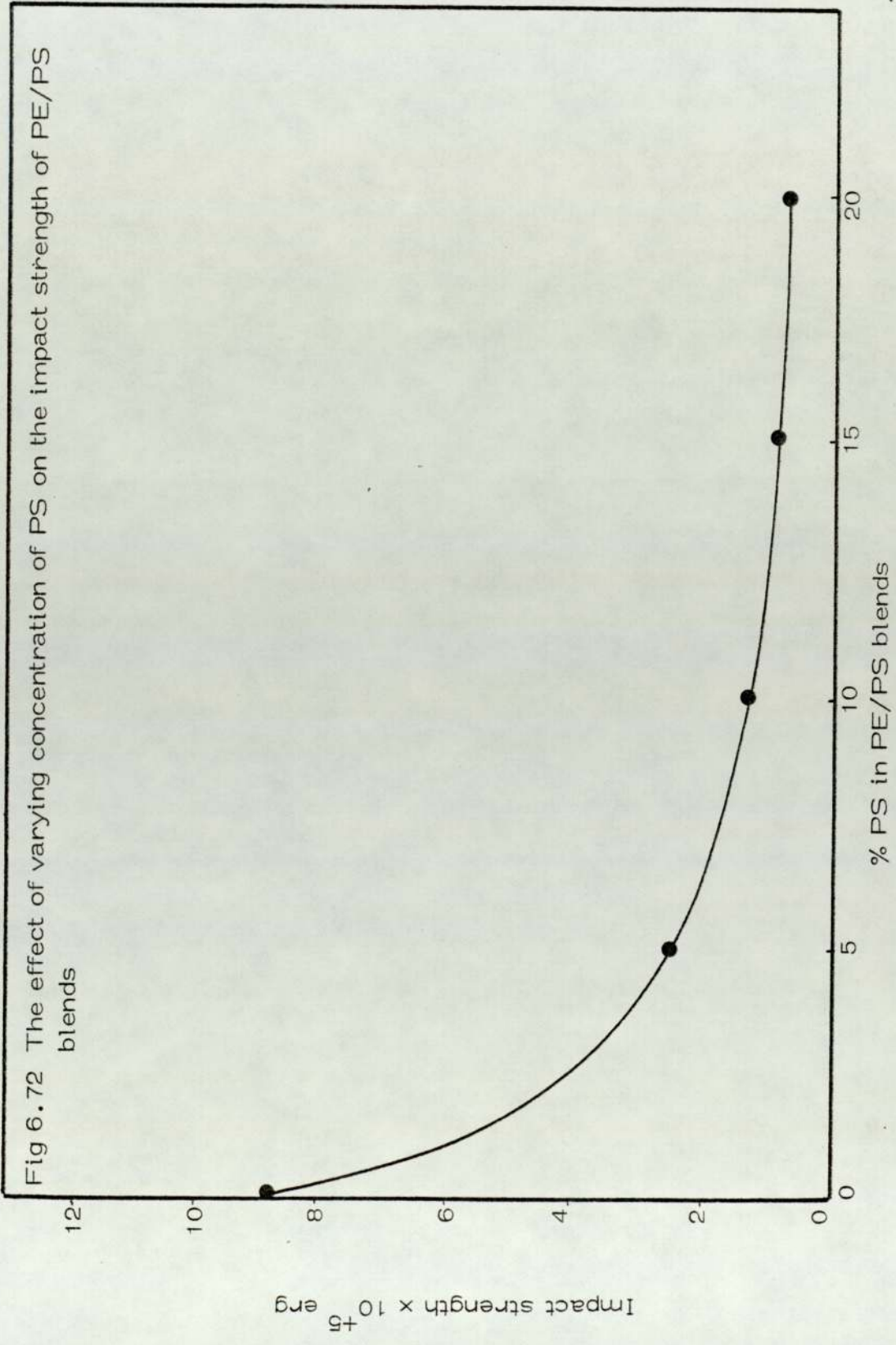
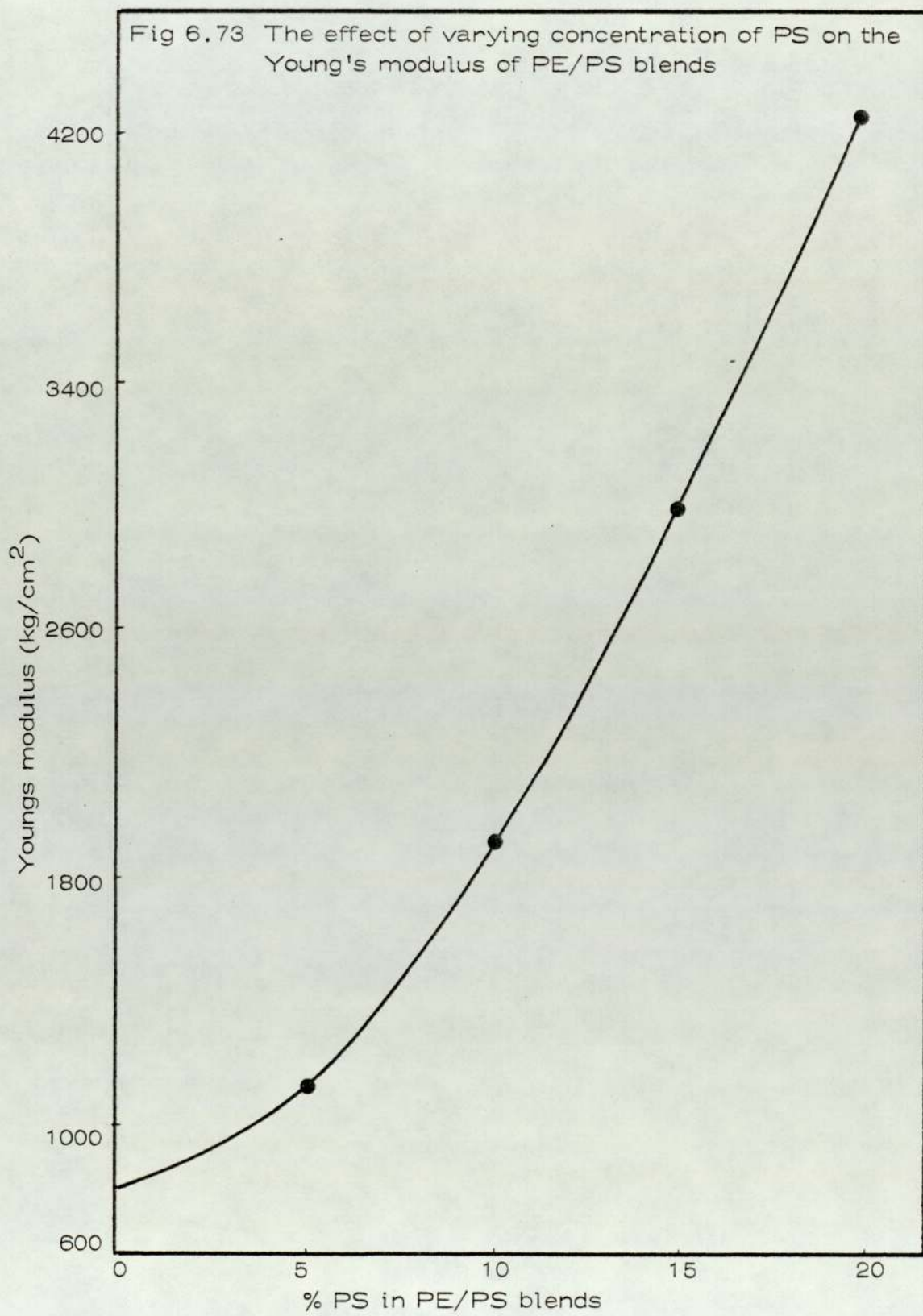


Fig 6.72 The effect of varying concentration of PS on the impact strength of PE/PS blends



as the amount of polystyrene in the blends is increased (Figs 6.70 - 6.72).

The increasing proportions of PS, lead to increase in ^{the} modulus of blends (Fig 6.73) in agreement with the work done by Ziegel and Romanoff^(284a). They prepared blends with high modulus by the use of polymers such as polystyrene, polyamide and poly(methyl methacrylate) in fillers dispersed in a low modulus matrix of ethylene/vinyl acetate copolymer. It is believed⁽²⁷⁸⁾ that elongation at break is ^avery sensitive indicator of compatibility, interactions and morphology in blends. Decrease in elongation at break, tensile strength and impact (Figs 6.70 - 6.72) may be attributed to increase in incompatibility (Plates 1C-4C) (see more discussion in PE/PVC and PE/PP sections).

6.C.4 Effect of PS Concentration on the Photo-oxidation of LDPE Blends

6.C.4.1 Introduction

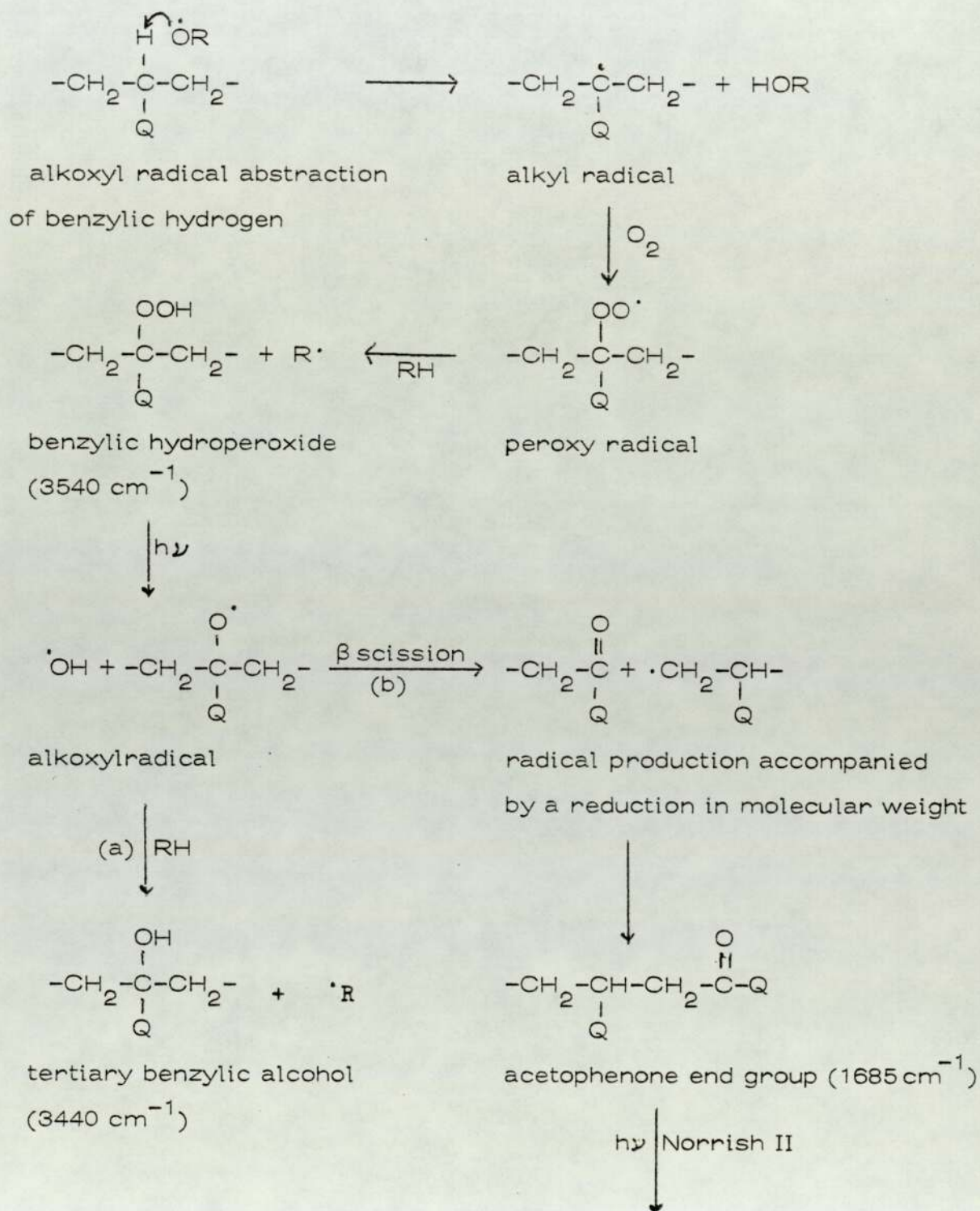
The photo-oxidation of LDPE has been discussed in Chapter 4. Polystyrene is known to be less photo-stable than PE⁽¹⁴⁸⁾. Consequently ^{the} presence of PS in PE is expected to increase ^{the} photo-sensitivity of blends. Scott and co-workers^(201,285,33) have studied the photo-oxidation of polystyrene and believed that hydrogen abstraction by an alkoxy radical derived from the decomposition of hydroperoxides produced during thermal processing may occur at either the benzylic or methylenic centre. The bond dissociation energy of a benzylic carbon-hydrogen bond is approximately 355 k J mol^{-1} while that of

a methylenic bond is about 397 k J mol^{-1} ^(284b). Consequently two principal mechanistic schemes (2 and 3) have been suggested by Scott and co-workers^(285).

Hydrogen abstraction by an alkoxy (or peroxy) radical from the tertiary benzylic centre (see scheme 2) will predominate producing an alkyl radical whose stability may be increased by resonance with the aryl substituent⁽²⁸⁶⁾. Nevertheless combination with atmospheric oxygen will occur rapidly with the formation of a peroxy radical capable of hydrogen abstraction from another polystyrene chain to produce hydroperoxide. Homolysis of tertiary benzylic hydroperoxide will result in an alkoxy radical which will either undergo β -scission (b) with the production of radicals or abstract a hydrogen (a) to form benzylic alcohol (3440 cm^{-1}). Acetophenone-type end group formed via β -scission may undergo Norrish type II photolysis with molecular product formation (acetophenone) and formation of an (unsaturated) styrene end group. Norrish type I photolysis of acetophenone type end group (or acetophenone) will result in further chain cleavage with formation of alkyl and acyl radicals. The acyl radical will combine with (diradical) oxygen producing peracid via hydrogen abstraction from the polymer hydrocarbon (RH). Breakdown of the peracid may lead to benzoic acid with further hydrogen abstraction. An important termination reaction involving alkoxy and alkyl radicals derived in scheme 2 may be postulated to account for the gel formation observed⁽²⁸⁵⁾ during the latter stages of photo-oxidation. This has been attributed to tertiary aryl ether ($1105 - 1000 \text{ cm}^{-1}$).

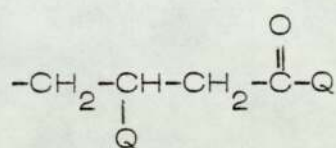
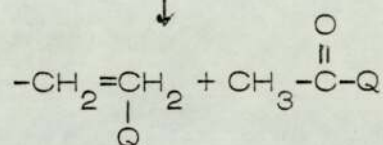
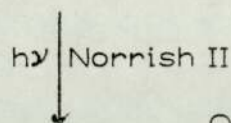
Alkyl (or peroxy) radical abstraction of the methylenic hydrogen

Scheme 2

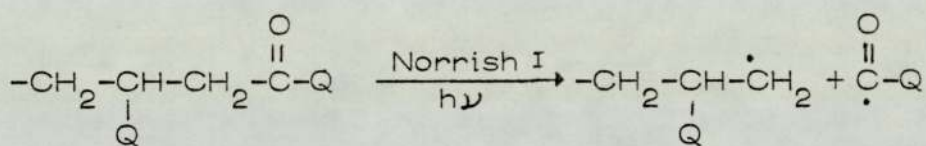


Continued

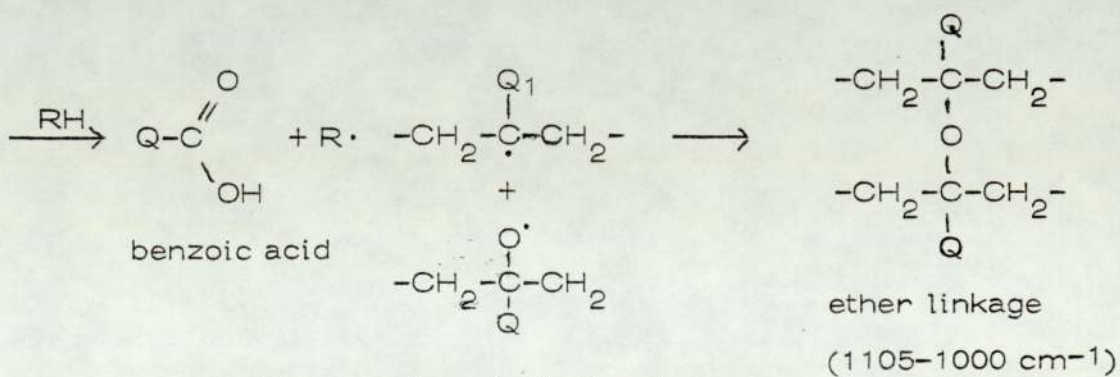
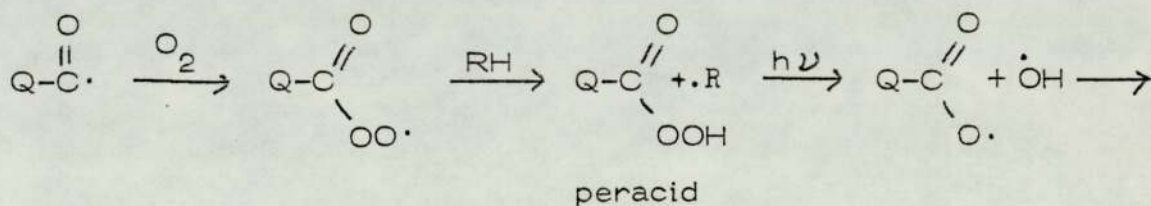
Scheme 2 Continued

acetophenone end group (1685 cm^{-1})

acetophenone + unsaturated chain end

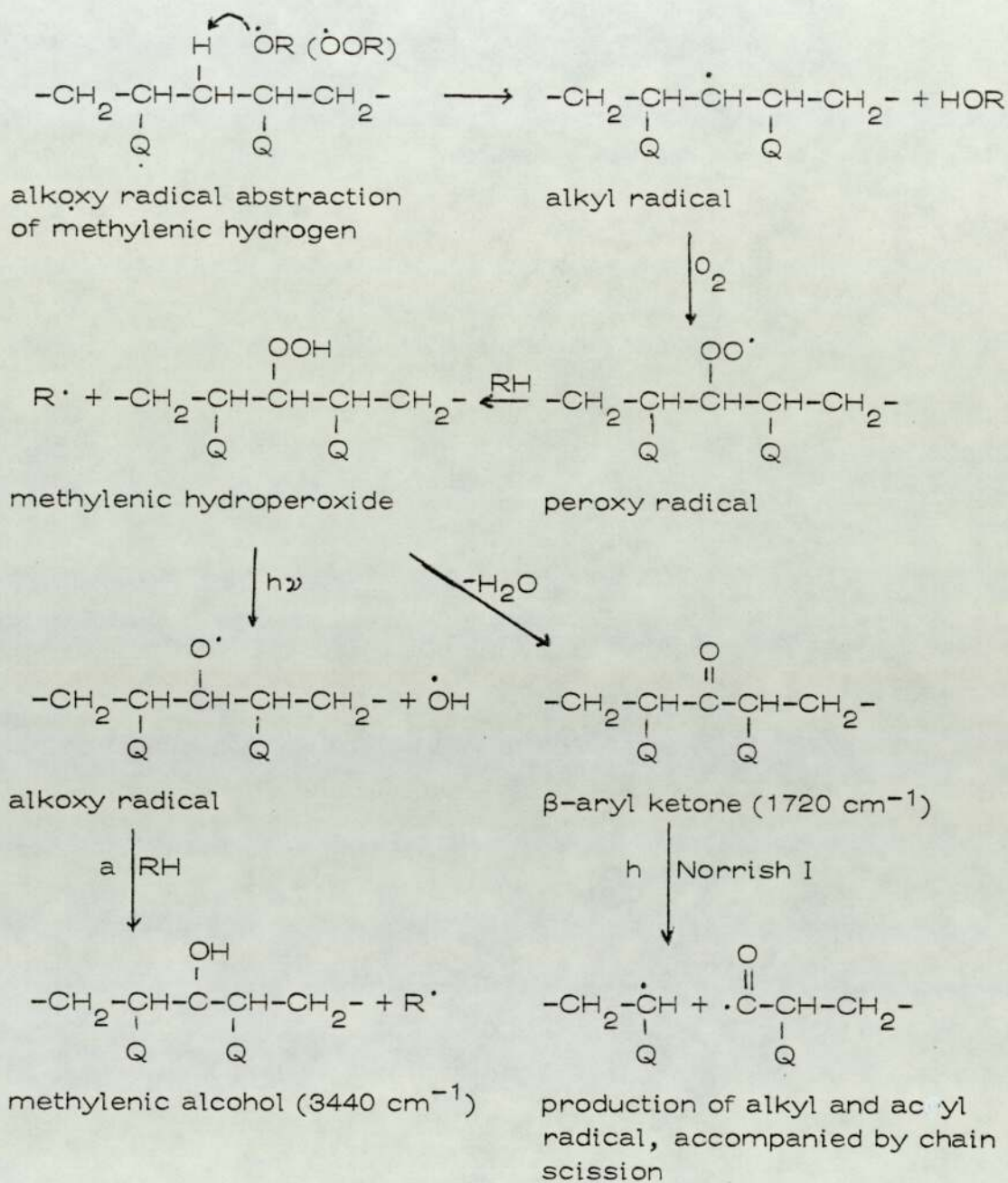


alkyl and acyl radicals

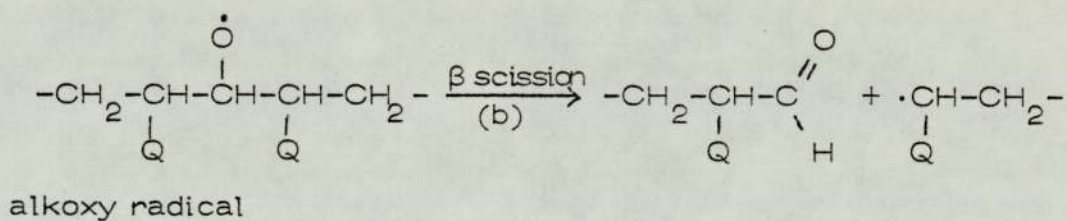
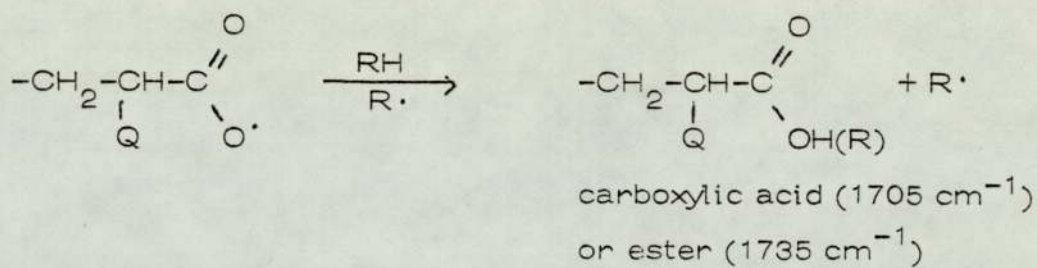
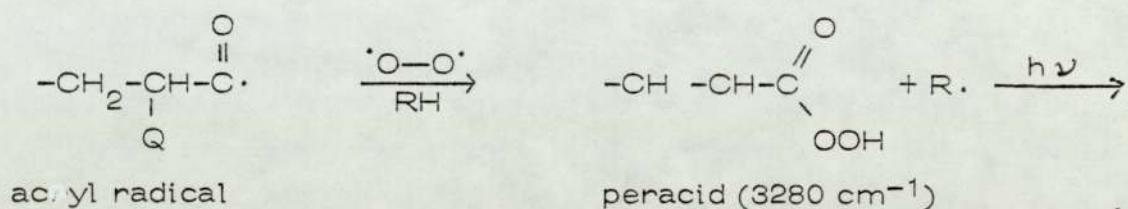


Termination of alkyl and alkoxy radicals

Scheme 3



Continued

Scheme 3-Continued

Formation of aldehyde (1720 cm^{-1}) and alkyl radical accompanied by a reduction in molecular weight.

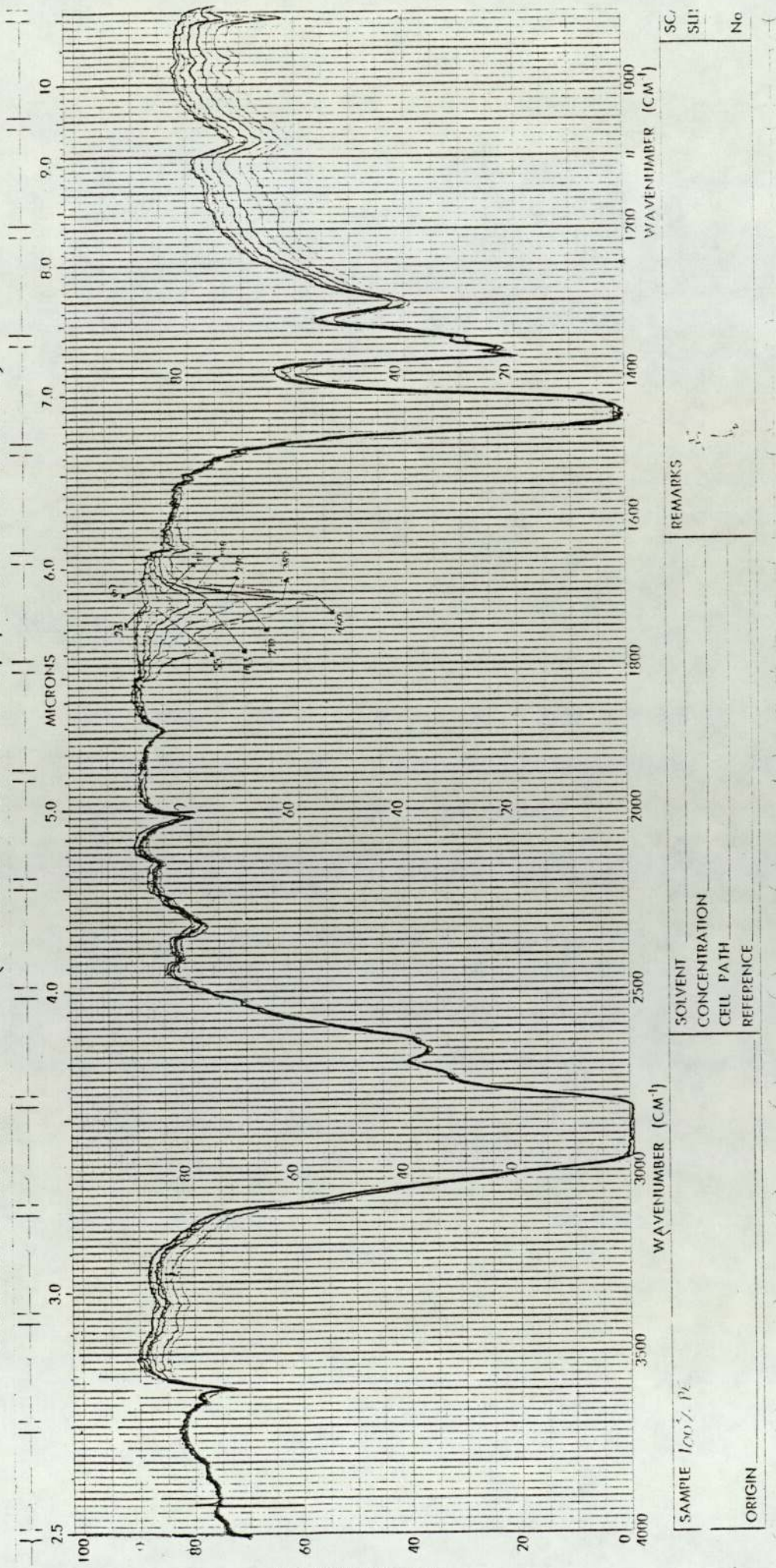
in scheme 3 will similarly lead to formation of an alkyl radical followed by a peroxy radical. However, the hydroperoxide formed by hydrogen abstraction by the peroxy radical may either lose water to form main chain ketone (1720 cm^{-1}) or undergo homolysis resulting in an alkoxy radical. This will in turn hydrogen abstract (a) to form methylenic alcohol (3440 cm^{-1}). Norrish type I photolysis of β -aryl ketone (1685 cm^{-1}) will result in production of alkyl and acyl radicals accompanied by chain scission. The acyl radical will subsequently combine with (diradical) oxygen followed by hydrogen abstraction to form peracid (3280 cm^{-1}). Cleavage of the oxygen-oxygen bond of peracid will produce an alkoxy radical capable of either abstracting a hydrogen or combining with an alkyl radical to form carboxylic acid (1705 cm^{-1}) or ester (1735 cm^{-1}).

An alternative reaction to hydrogen abstraction by the methylenic alkoxy radical produced in scheme 3 is β -scission (b) resulting in formation of aldehyde (1720 cm^{-1}) and an alkyl radical accompanied by a reduction in molecular weight⁽²⁸⁵⁾.

6.C.4.2 Results and Discussion

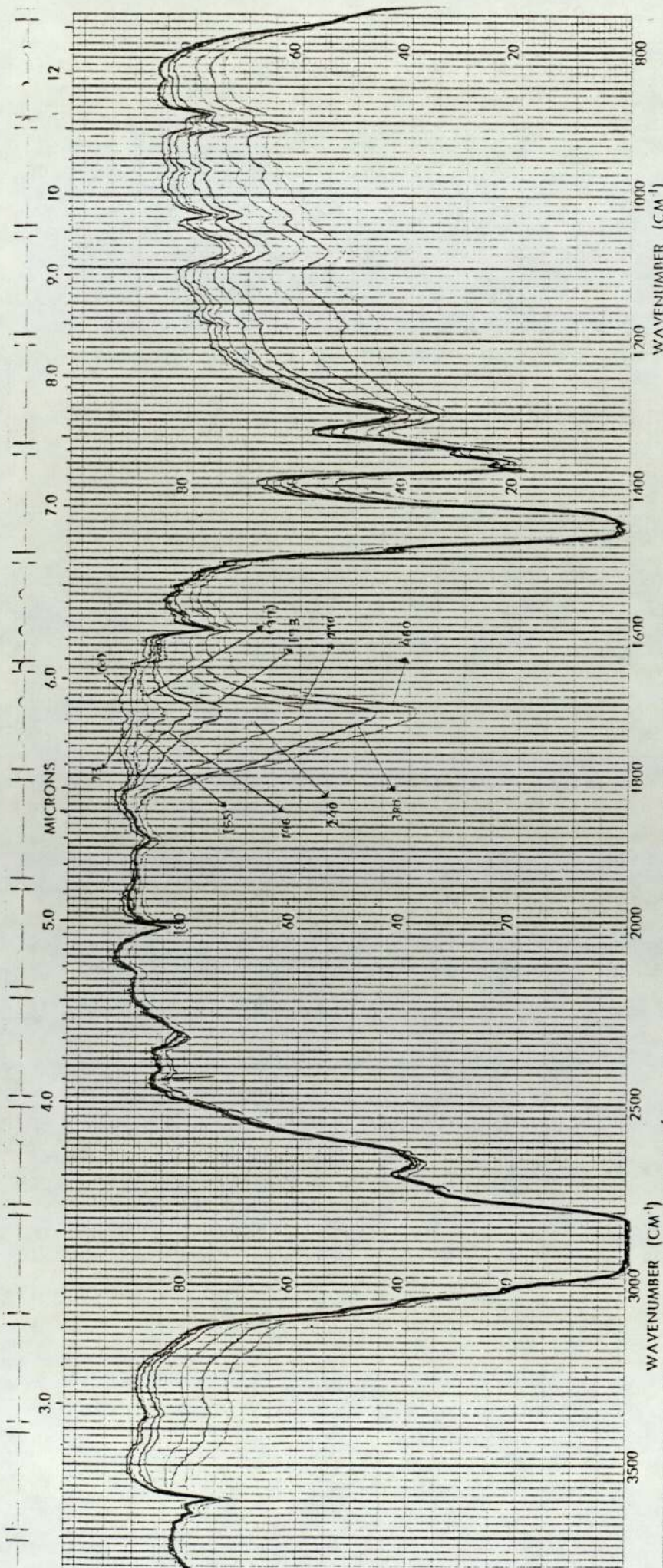
Infra-red studies of uv irradiation films of PE and PE/PS blends are shown in Figs 6.74 - 6.79. Figs 6.74 - 6.79 clearly show the effect of PS in the blends on the rate of formation of functional groups in the regions of $3000 - 3500\text{ cm}^{-1}$ (OH) and $1700 - 1725\text{ cm}^{-1}$ (C=O) respectively. Fig 6.80 shows that as the concentration of the PS is increased, the polyblends show greater susceptibility to ultra-violet light degradation. This lower photo-oxidative stability of the blends

Fig 6.74 Change in hydroxyl (3500-3000 cm⁻¹) and carbonyl (1800-1600 cm⁻¹) absorption during photo-oxidation of LDPE film (numbers on curves are exposure time in hours)



SAMPLE 100% P2		REMARKS		SC:
ORIGIN				SUI:
SOLVENT				No
CONCENTRATION				
CELL PATH				
REFERENCE				

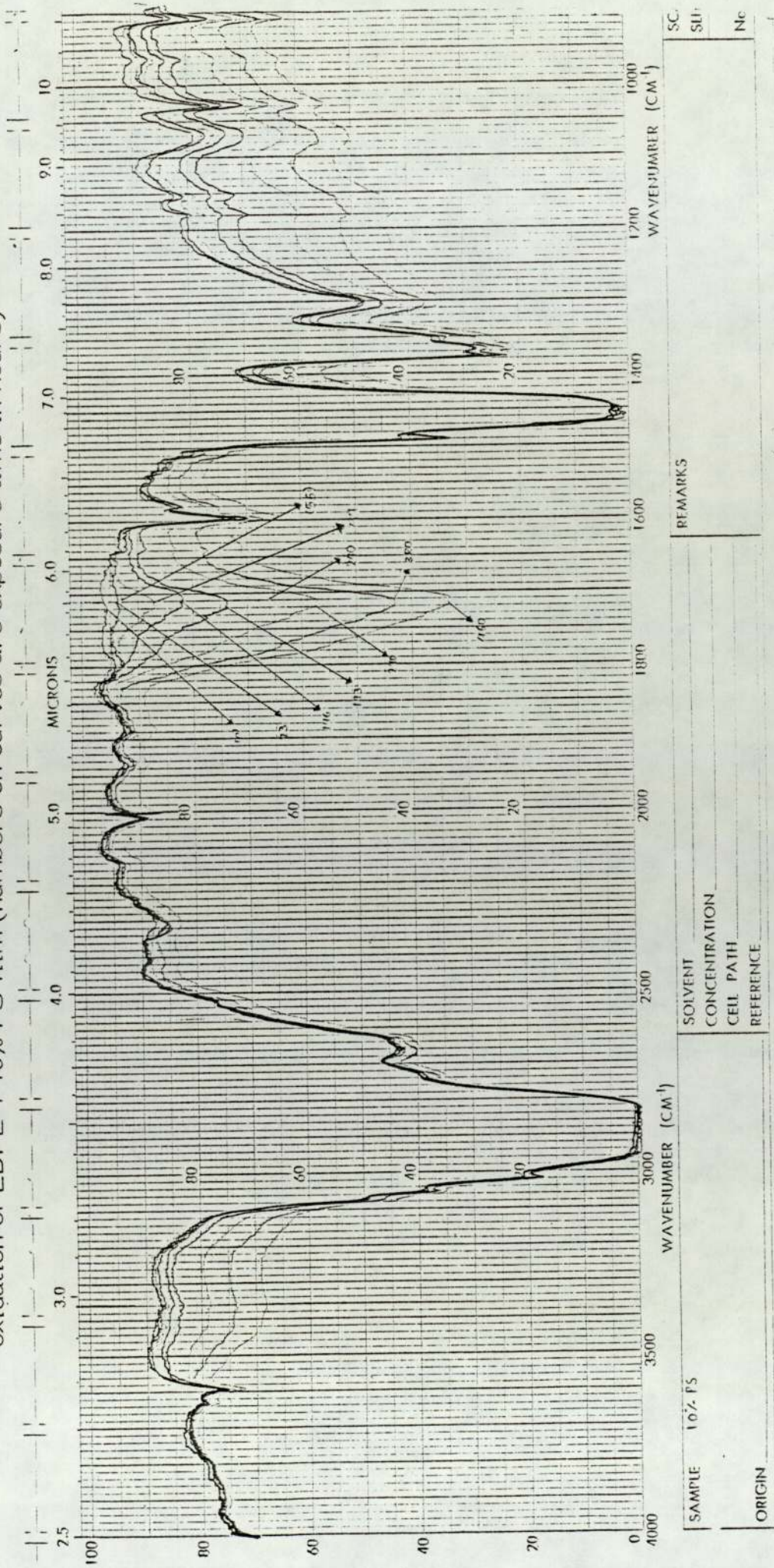
Fig 6.75 Change in hydroxyl (3500-3000 cm^{-1}) and carbonyl (1800-1600 cm^{-1}) absorptions during photo-oxidation of LDPE + 4% PS films (numbers on curves are exposure time in hours)



47.15

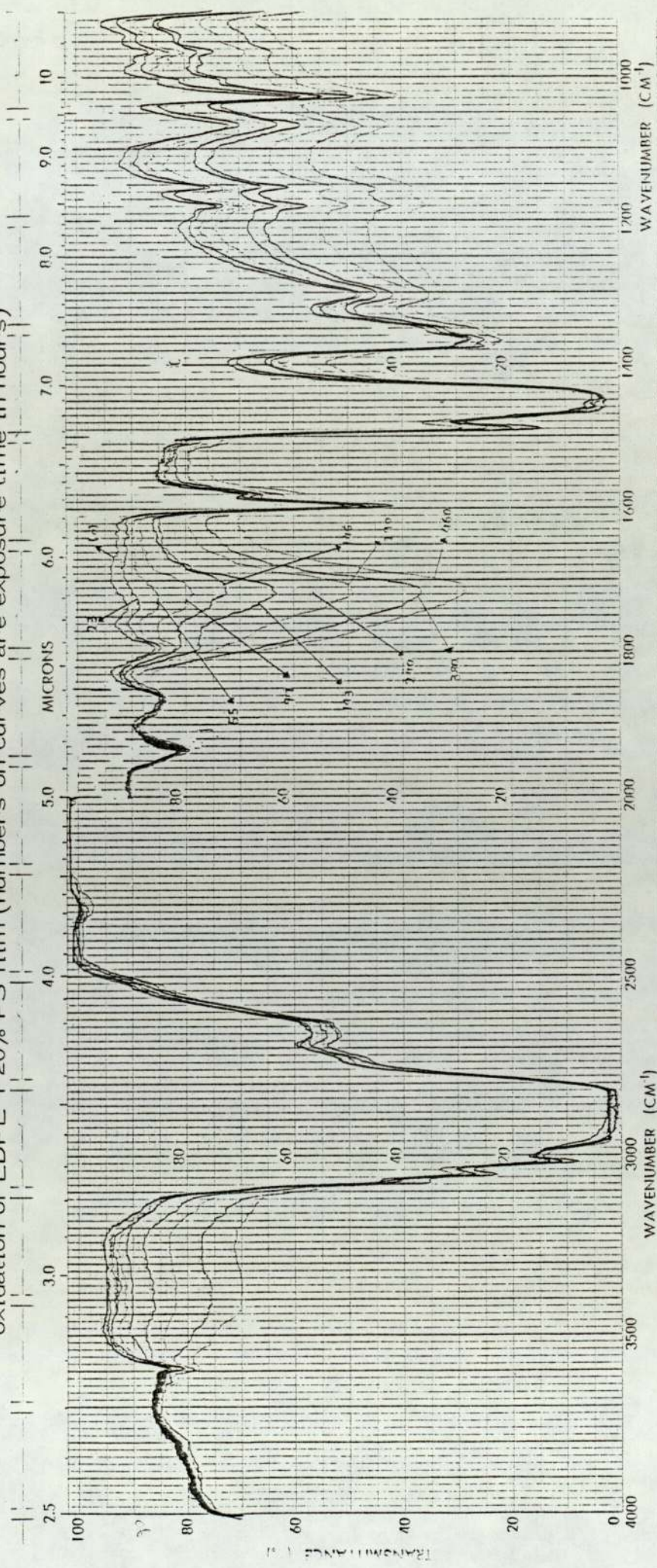
WAVENUMBER (CM^{-1})	3500	3000	2500	2000	1800	1600	1400	1200	1000	800	
MICRONS	2.86	3.33	4.00	5.00	5.56	6.25	7.14	8.33	10.00	12.50	
REMARKS	SOLVENT _____ CONCENTRATION _____ CELL PATH _____ REFERENCE _____										
SCAN SPEED	SUIT										
No	457-5001										

Fig 6.76 Change in hydroxyl (3500-3000 cm^{-1}) and carbonyl (1800-1600 cm^{-1}) absorption during photo-oxidation of LDPE + 10% PS film (numbers on curves are exposure time in hours)



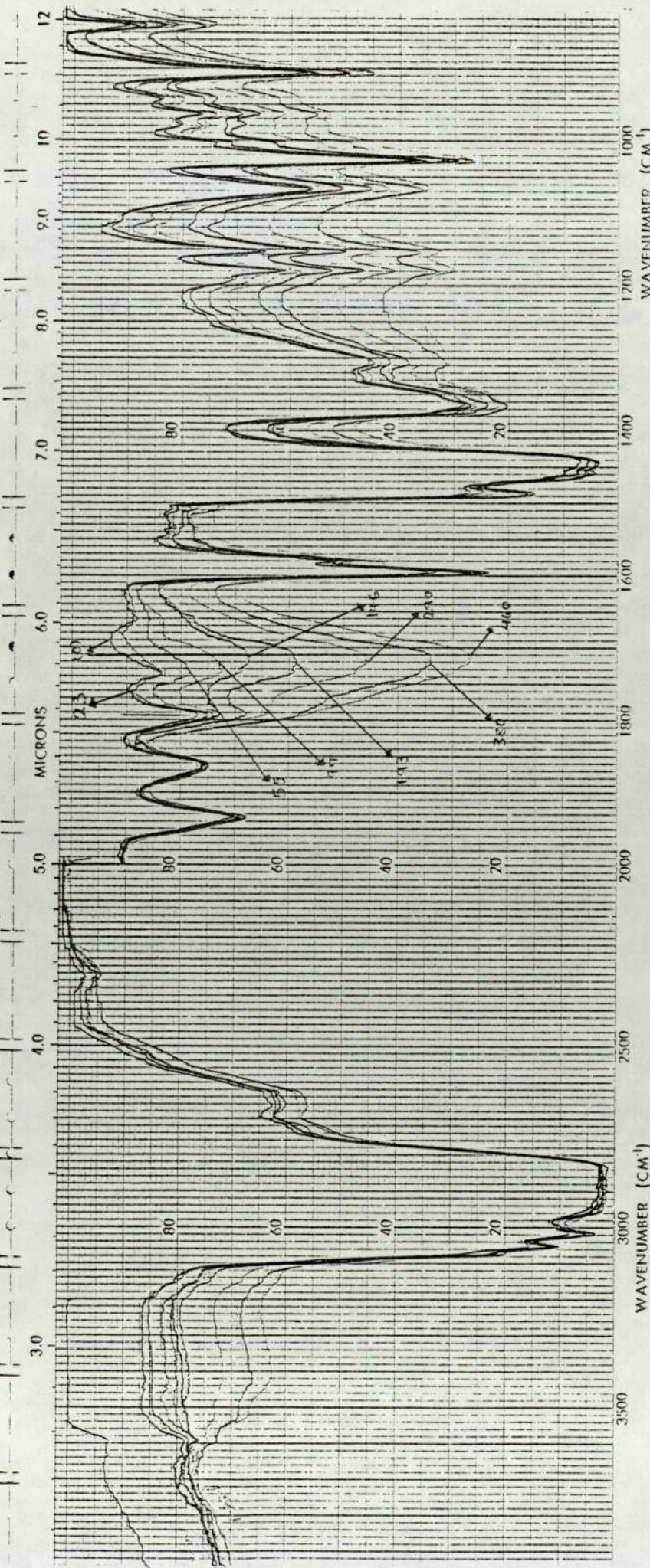
SAMPLE	10% PS	REMARKS	SC:
			SU:
ORIGIN			NC:
	SOLVENT		
	CONCENTRATION		
	CELL PATH		
	REFERENCE		

Fig 6.77 Change in hydroxyl (3500-3000 cm^{-1}) and carbonyl (1800-1600 cm^{-1}) absorption during photo oxidation of LDPE + 20% PS film (numbers on curves are exposure time in hours)



SAMPLE $\text{LDPE} + \text{PS}$	SOLVENT	REMARKS	SC
	CONCENTRATION		
ORIGIN	CELL PATH	/	SI
	REFERENCE		

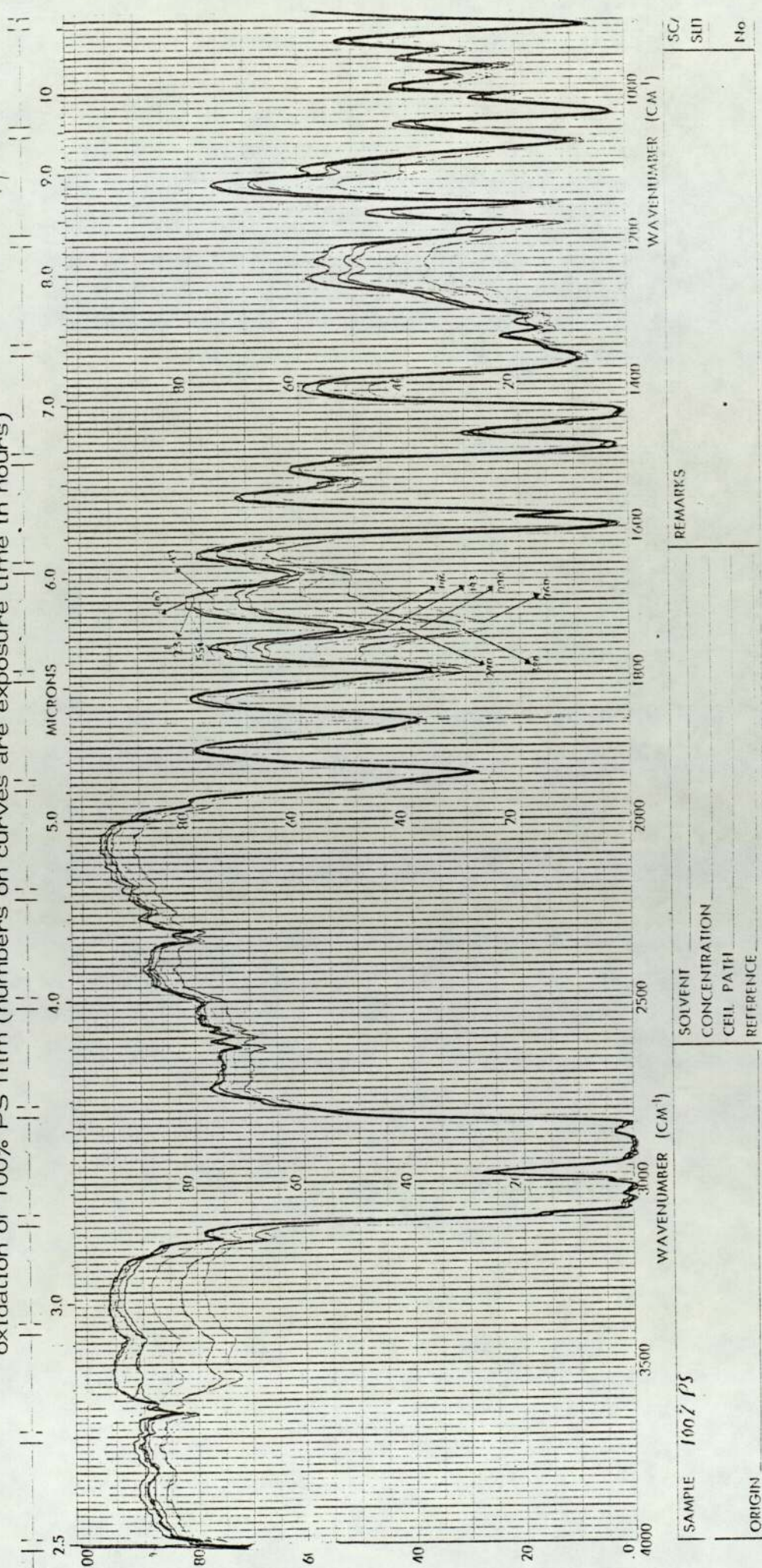
Fig 6.78 Change in hydroxyl (3500-3000 cm^{-1}) and carbonyl (1800-1600 cm^{-1}) absorption during photo-oxidation of LDPE + 40% PS film (numbers on curves are exposure time in hours)

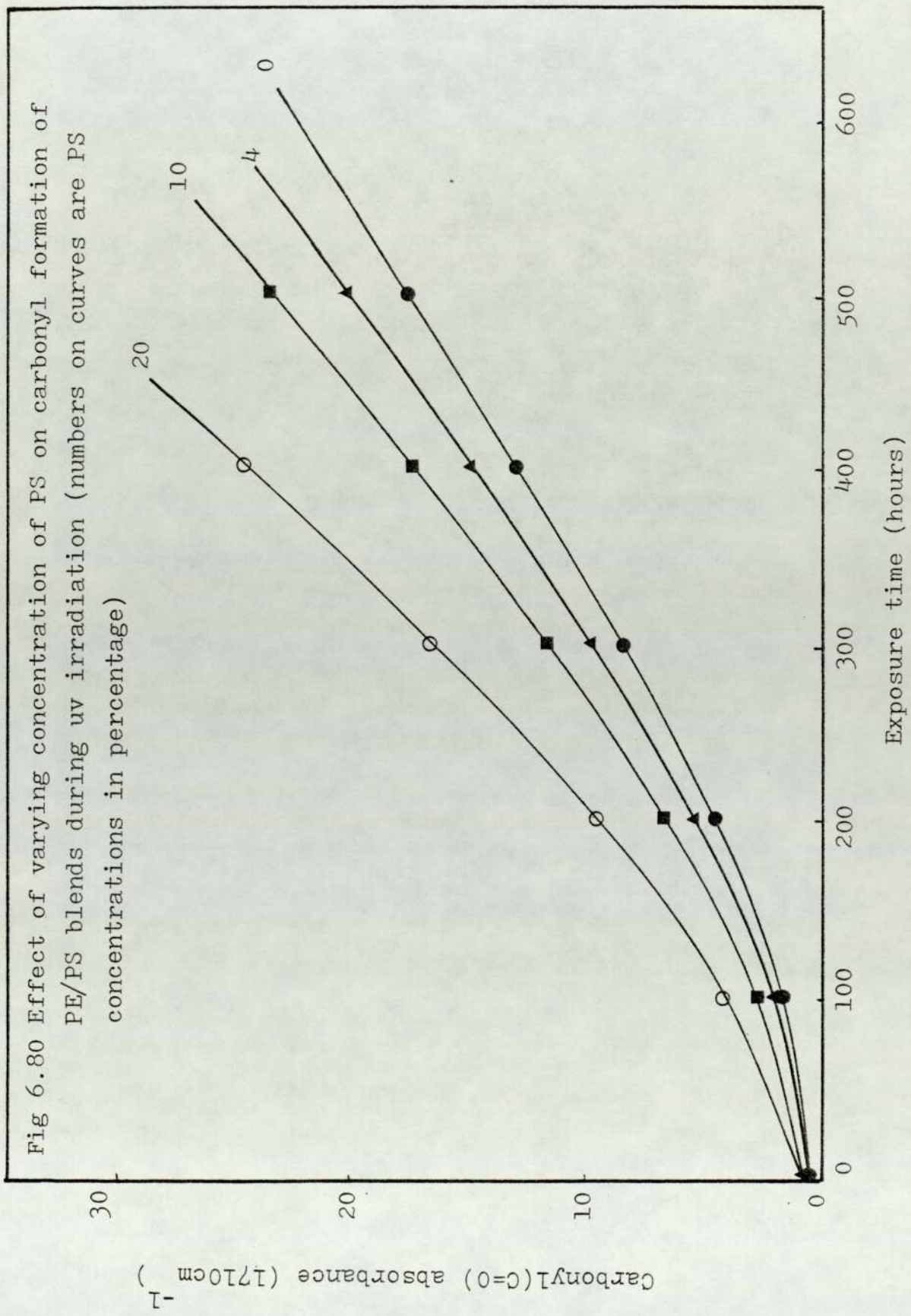


SAMPLE <i>LDPE/PS</i>	SOLVENT	REMARKS	SCAN SPEED
	CONCENTRATION		SPLIT
	CELL PATH		No 457-51
	REFERENCE		

ORIGIN

Fig 6.79 Change in hydroxyl (3500-3000 cm^{-1}) and carbonyl (1800-1600 cm^{-1}) absorption during photo-oxidation of 100% PS film (numbers on curves are exposure time in hours)





can be attributed to the presence of a labile hydrogen on the tertiary carbon in the polystyrene (see schemes 2 and 3 for mechanisms).

The deterioration of the physical properties was followed by stress-strain measurements as a function of exposure time (Figs 6.81 - 6.84). In the case of 100% PE the tensile strength and elongation at break were found to decrease with increasing exposure time. However, PE/PS blends behave rather differently when subjected to uv light. The tensile strength of the blends increased during uv irradiation (Figs 6.83 and 6.84). This increase in tensile strength at the later stage of photo-oxidation may be explained as due to the interaction at the interface of domain and matrix (Sections 6.A.4 and 6.B.4). The product of interaction between PE and PS can act effectively as a solid phase dispersant (SPD) and holds the two phases together. This will contribute to an increase in the tensile strength of the blend. The overall tensile strength of the blends will then depend on the net effect of the degradation processes. In this case, blends which contain higher concentration of PS (eg 20% PS) indicates the greatest increase in tensile strength with irradiation time (Figs 6.83 and 6.84).

6.C.5 Introduction of some Solid Phase Dispersants (SPD's) to Improve the Toughness of Blends

6.C.5.1 Introduction

Locke and co-workers⁽²³⁷⁾ recently investigated to improve the toughness of PE/PS blends. They tried to use graft copolymers of styrene onto polyethylene as additives to improve the

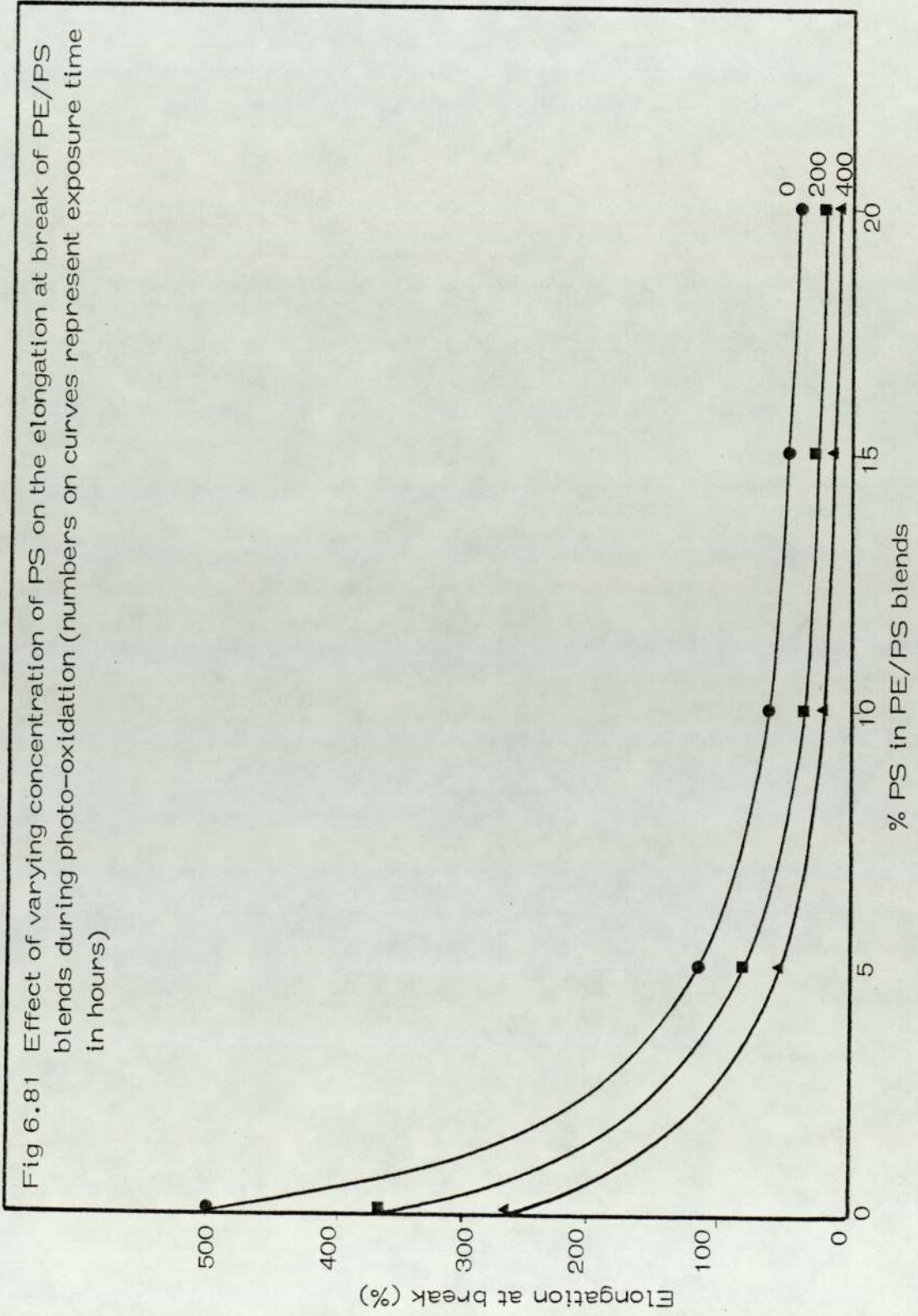
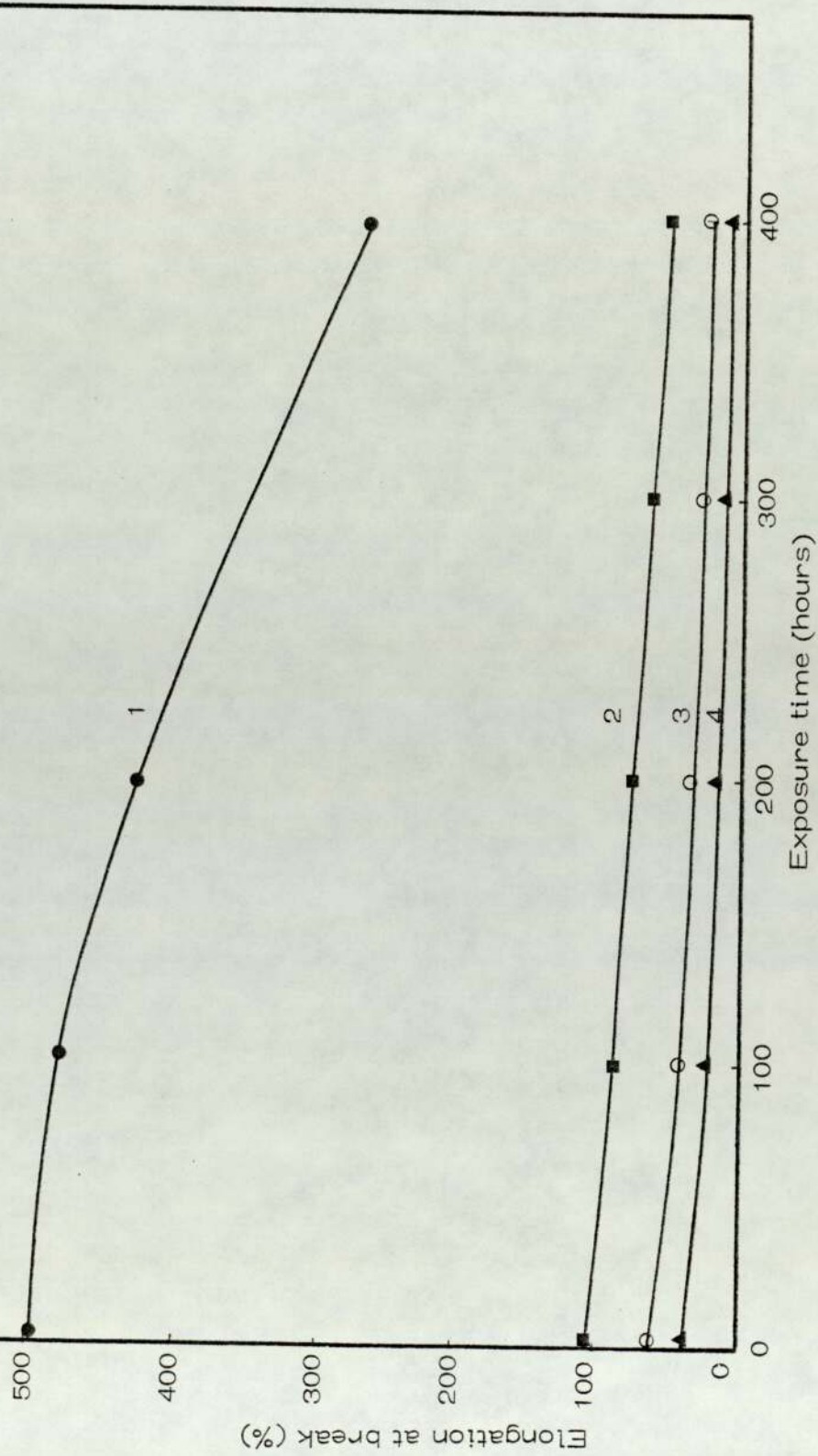


Fig 6.82 Effect of PS concentration on the elongation at break (%) of PE/PS blends during uv irradiation. 1, 100% LDPE; 2, LDPE + 5% PS; 3, LDPE + 10% PS; 4, LDPE + 20% PS



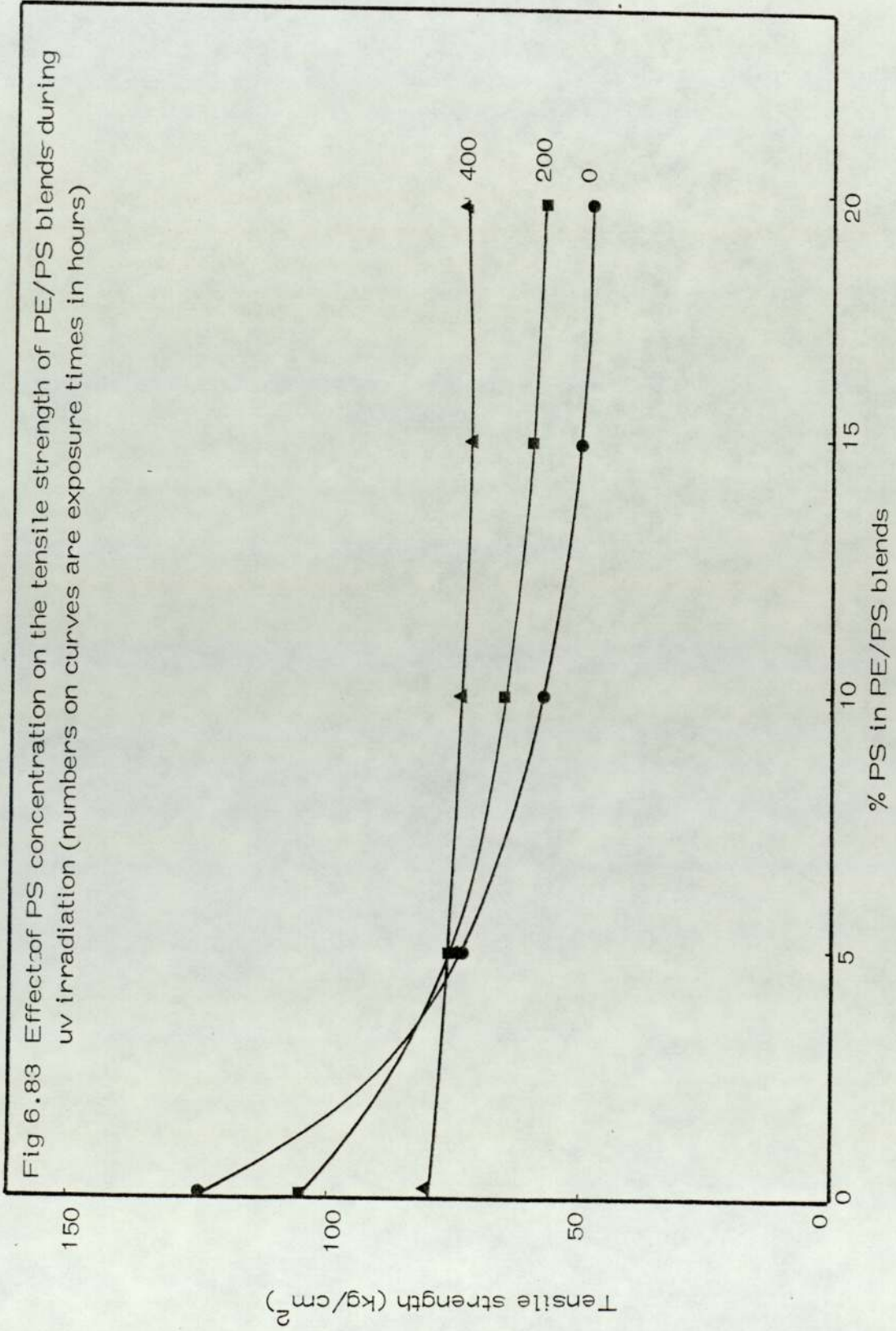
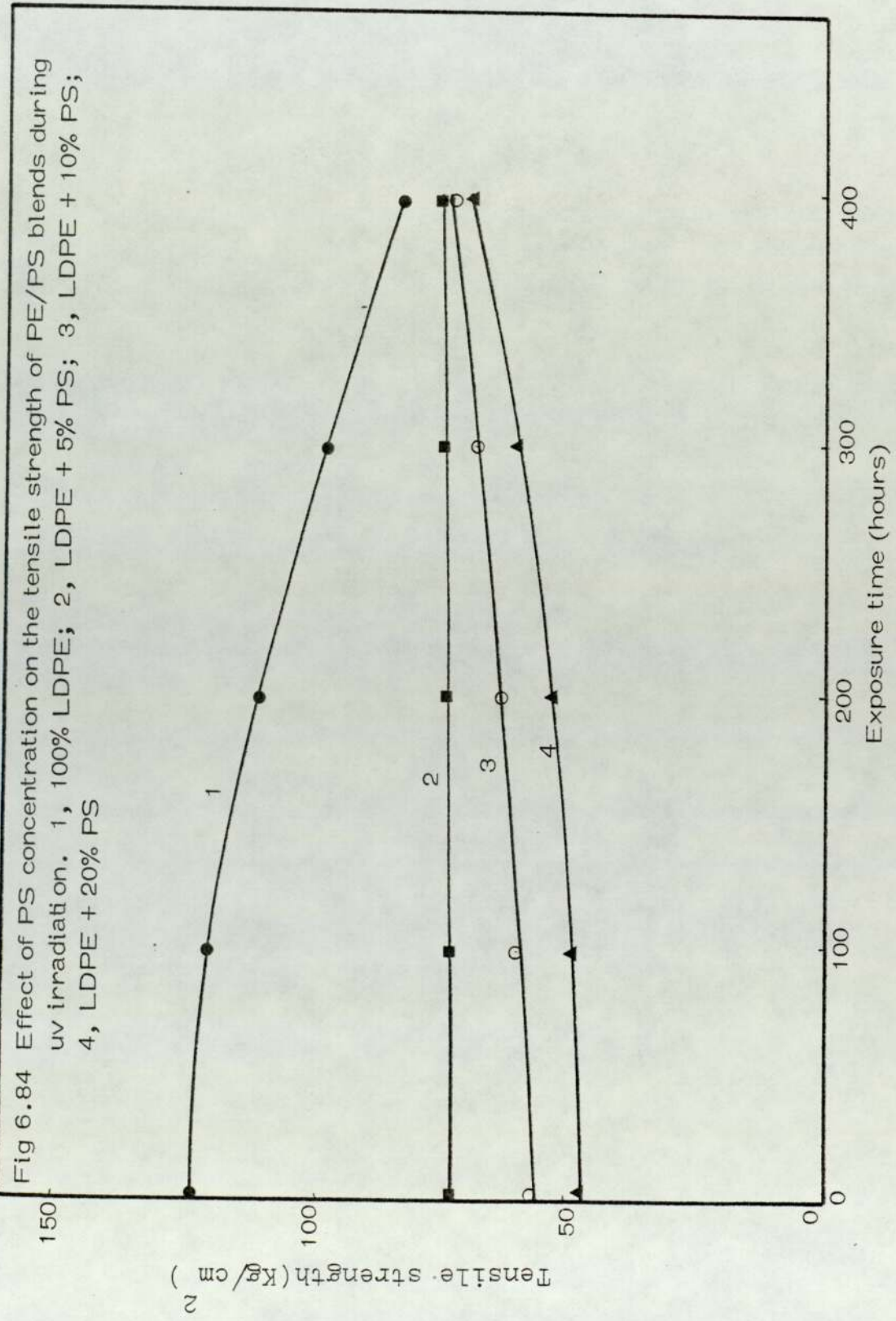


Fig 6.84 Effect of PS concentration on the tensile strength of PE/PS blends during uv irradiati on. 1, 100% LDPE; 2, LDPE + 5% PS; 3, LDPE + 10% PS; 4, LDPE + 20% PS



mechanical properties of polyethylene-polystyrene blends. It is believed that⁽²³⁷⁾ grafting provides adhesion at the interface since the two chain types can be expected to penetrate the phase of their own type in much the way of a surfactant functions. Addition of polyethylene-g-polystyrene to blends of polyethylene and polystyrene should improve adhesion at the domain interface of these very incompatible polymers^(278,280). This improved adhesion should in turn improve the mechanical properties of the blends.

6.C.5.2 Experimental

In order to improve mechanical properties of PE/PS blends such as impact strength, tensile strength and elongation at break, selected additives (eg ABS, ACS, EPDM, NR, BR, HIPS and SBS) were blended with PE/PS (50/50) blends as described in Sections 6.A.6.2 and 6.A.2).

6.C.5.3 Results and Discussion

Fig 6.85 shows the minimal tensile strength and elongation at break of the PE/PS blends containing 30-50% PS. Table 6.C.2 and Figs 6.86 - 6.88 show the effect of varying amounts of seven additives on 50/50 PE/PS blends. SBS shows the highest improved effect on impact strength (Fig 6.86) and tensile strength (Fig 6.87) and elongation at break (Fig 6.88). This is most evident at higher concentrations of SBS (eg 20% SBS). The tensile strength and impact strength are very similar to the unmodified LDPE (Table 6.C.2). The percentage elongation at break also increased from the low value of 2.5% to the 65%. These improvements in mechanical properties

Fig 6.85 The effect of varying concentration of PS on tensile strength (1) and elongation at break (%) (2) in LDPE

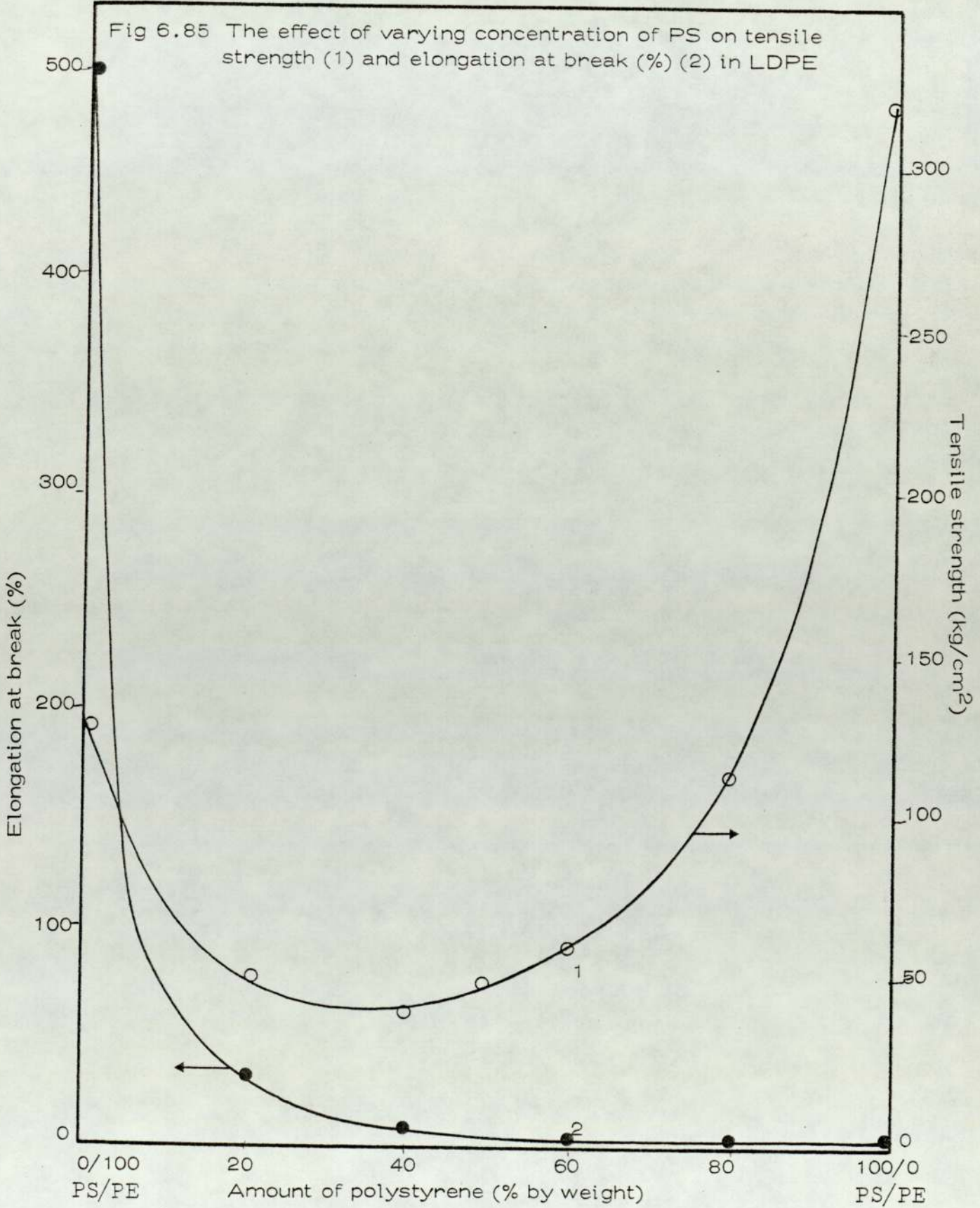


Fig 6.86 Effect of varying concentration of compatibilisers (SPD's) on the impact strength of PE/PS (50/50) blends. 1, SBS; 2, NR; 3, EPDM; 4, BR; 5, HIPS; 6, ACS; 7, ABS

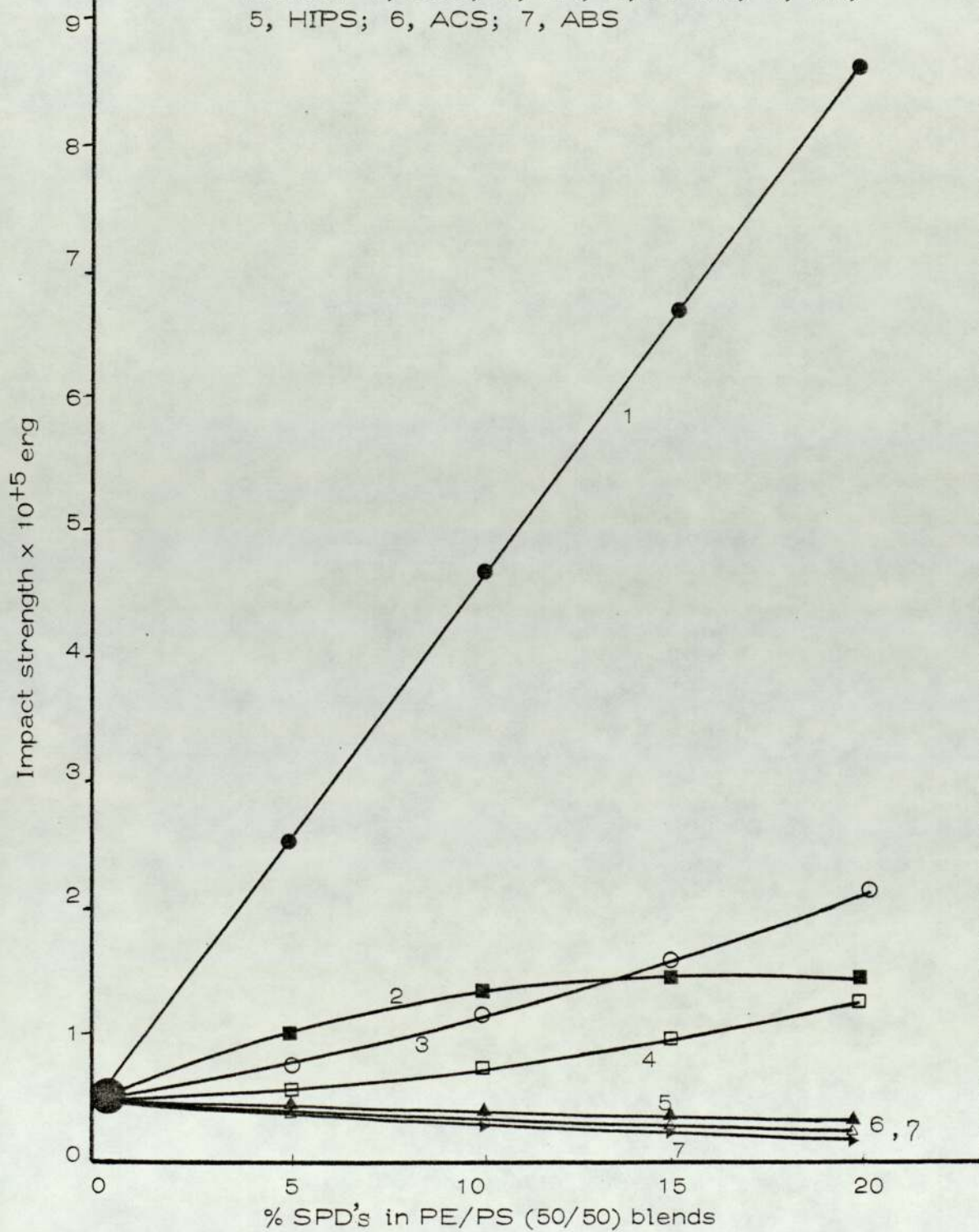


Fig 6.87 Effect of varying concentration of compatibilisers (SPD's) on the tensile strength of PE/PVC (50/50) blends. 1, SBS; 2, HIPS; 3, EPDM; 4, BR; 5, ABS; 6, ACS; 7, NR

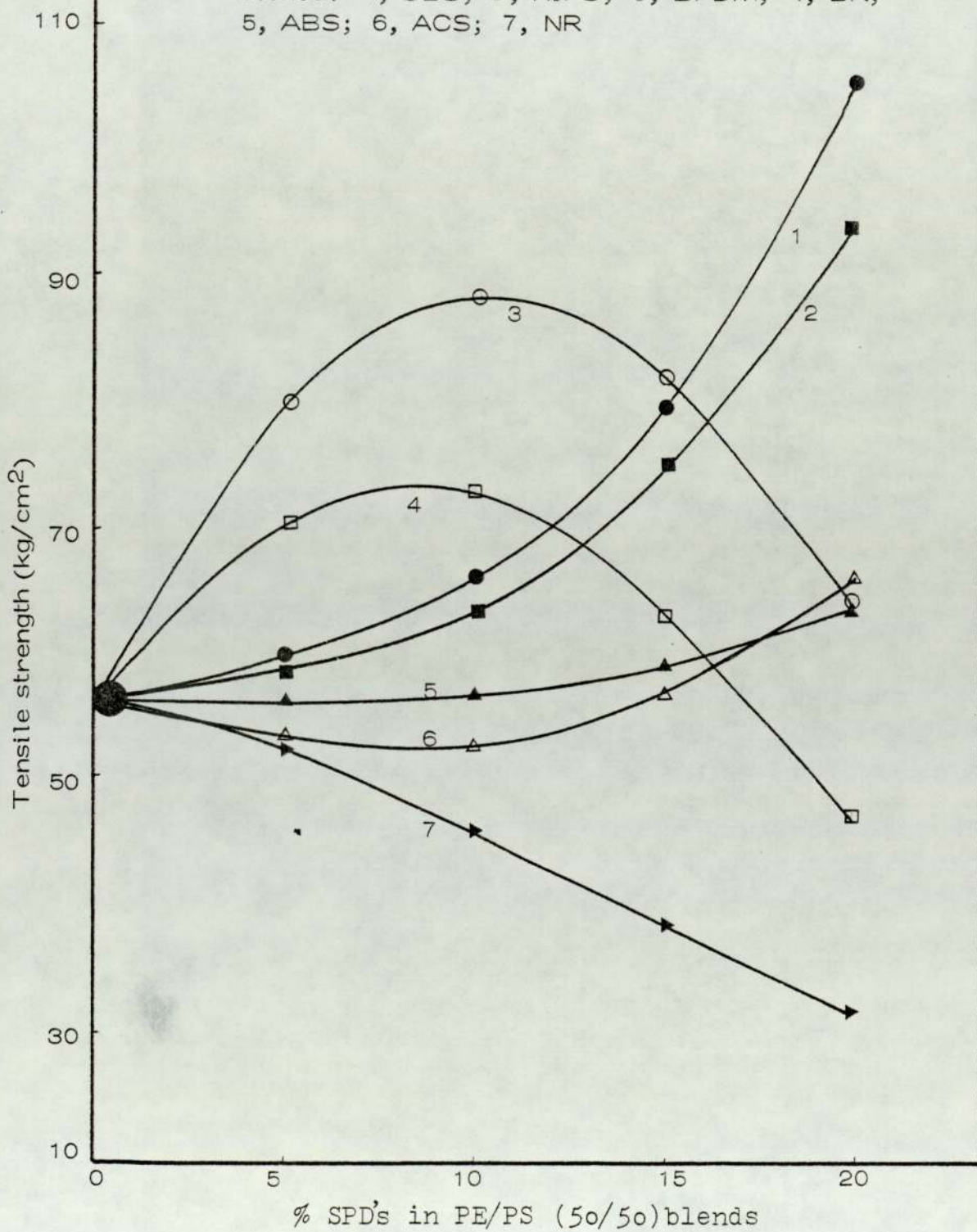


Fig 6.88 Effect of varying concentration of compatibilisers (SPD's) on the elongation at break (%) of PE/PVC blends. 1, SBS; 2, NR; 3, EPDM; 4, BR; 5, HIPS; 6, ACS; 7, ABS

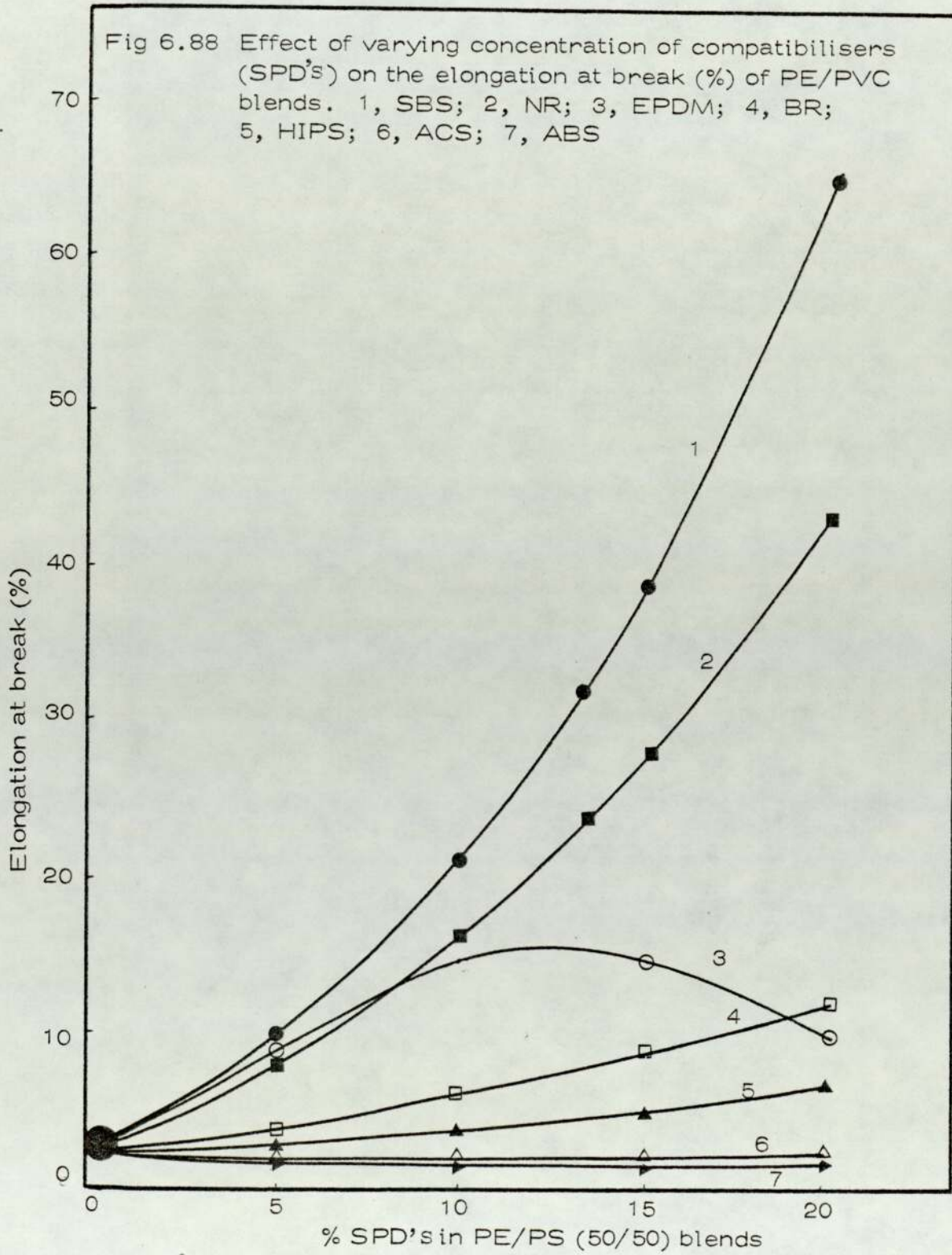


Table 6.C.2. The effect of varying concentration of SPD's on the mechanical properties of PE/PS (50/50) blends

No	Formulation	Elongation at break (%)	Tensile strength (kg/cm ²)	Impact strength (x 10 ⁺⁵) ergs
	LDPE + PS + additives (%)			
1	LDPE	480-500	128.0	8.5-9
2	PS	1.5-2.0	300-320	< 0.6
3	50 + 50 + 0	1-2	60	≈ 0.5
4	45 + 45 + 10 SBS	21	66	4.7
5	40 + 40 + 20 SBS	65	105	9.0
6	45 + 45 + 10 EPDM	15	88	1.2
7	40 + 40 + 20 EPDM	10	64	2.2
8	45 + 45 + 10 HIPS	4	64	< 0.6
9	40 + 40 + 20 HIPS	7	94	< 0.6
10	45 + 45 + 10 ABS	2.0	57	< 0.6
11	40 + 40 + 20 ABS	1.5	64	< 0.6
12	45 + 45 + 10 BR	6.5	73	0.7
13	40 + 40 + 20 BR	12.0	47	1.4
14	45 + 45 + 10 ACS	2.0	53	0.6
15	40 + 40 + 20 ACS	2.5	66	0.6
16	45 + 45 + 10 NR	17	47	1.4
17	40 + 40 + 20 NR	44	31	1.6

using SBS as SPD for the PE/PS blends to enable them to be used in some specific application. The reason for these improvements in impact strength, tensile strength and % elongation at break is not well understood and would require further investigation (see Chapter 7).

CHAPTER SEVEN

MECHANISTIC CONCLUSIONS

7.1 Effect of processing on the mechanical properties of polymer blends

The study of mechanical properties of incompatible polymer blends (eg PE/PVC, PE/PP and PE/PS) indicates two phase morphology by electron and optical microscopy. In all the blends studied (0-20% PVC, PP, PS in LDPE) PVC, PP and PS exist as domains dispersed in the LDPE matrix (except 5% PP in low density polyethylene which shows a single phase morphology up to this concentration). The amount and average size of the domains increase with increasing PVC, PP and PS content. The tensile strength, elongation at break (%), $\tan \delta$ (at room temperature, $20 \pm 1^\circ\text{C}$) and impact strength of the blends drop with increasing PVC, PS and PP content. The poor mechanical properties of blends can be attributed to the poor adhesion between the continuous and discontinuous phases.

7.2 Photo-oxidation of polymers and polymer blends

PP, PS and PVC are known to be much less photo-stable than polyethylene. PP, PS and PVC present in mixed waste might be expected to increase photo-sensitivity. This lower photostability of the polyblends (eg PE/PP, PE/PVC and PE/PS) is also reflected in the ir change in mechanical properties. During uv irradiation the tensile strength of the blends in all cases decreased initially but began to increase again at a later stage of oxidation. This increase was observed significantly at higher

concentration of PVC, PP and PS in LDPE. All these observations are believed to result from the net effect of two main reactions occurring during uv irradiation of blends: degradation at the interface and the interaction at the interface of the degradation products.

7.3 Thermal Oxidation of Polymer Blends

A study of thermal oxidation of PE/PVC blends indicated a catalytic effect of hydrogen chloride on decomposition of hydroperoxides. It was observed that mechanism of the peroxide decomposition was predominantly ionic at lower hydrogen chloride to peroxide molar ratios (PVC in this stage acting as an antioxidant), whilst at relatively high (> 1) molar ratios, a free radical mechanism is favoured (ie PVC exerts a pro-oxidant effect).

7.4 Modification of polymer blends by solid phase dispersants (SPD's)

The technological usefulness of blends of incompatible polymers such as PE/PVC, PE/PP and PE/PS is in general limited by their poor mechanical properties. Co-blending of some additives (SPDS) caused a significant improvement in the mechanical properties (eg elongation at break (%) and impact strength) for PE/PP, PE/PVC and PE/PS blends. The effectiveness of SPD's appears to be fairly specific to the nature of each component of a two component polymer blend. However, it is found that by selection of copolymers containing blocks with physical affinity for each of the heterophases, an improvement in mechanical properties can be achieved approaching that of the single compounds. Thus for example for PE/PP and PE/PVC, EPDM

appears to be the most effective SPD whereas for PE/PS, SBS is more effective.

7.5 Suggestions for Further Work

- 1 The usage of the recycled plastic blends demands a satisfactory level of mechanical properties (eg tensile strength, impact strength and elongation at break) and this must be capable of being produced reproducibly from mixtures of plastics. A search for suitable solid phase dispersants (SPD's) appears to offer the prospect of producing commercially useful blends from mixed plastics waste.
- 2 On the mechanistic side, further information is required as to how SPD's achieve their effect. Electron and optical microscopy should prove to be useful tools to provide information on molecular interactions at the interface between polymer phases.
- 3 Since photodegradation appears to occur predominantly at the rubbery interphase in SPD modified blends, stabilisation studies should be directed towards the SPD's by specifically stabilising the latter. In particular, the use of antioxidants and uv stabilisers which are chemically attached to the more oxidatively sensitive rubber phase should be examined.

REFERENCES

- 1 A J Warner, C H Parker and B Baun (DeBell and Richardson) 'Solid Waste Management of Plastics', a report to Manufacturing Chemists Association (1971)
- 2 B Baun and C H Parker, SPEJ, 27, 18 (1971)
- 3 M E Fulmer and R F Testin (Battelle) 'The role of plastics in solid waste', a report to the Society of the Plastics Industry (1967)
- 4 A Darnay and W E Franklin (Midwest Research Institute), 'The role of packaging in solid waste management 1966-1976', Public Health Service Pub No 1855 (1969)
- 5 J D Milgren (A D Little) 'Recycling Plastics' presented at the ACS Symp 'Chemical Technology for Resource Recovery' Washington DC, June (1971)
- 6 E R Kaiser 'Composition and Combustion of Refuse', presented at MFCAR Symp on Incineration of Solid Wastes, New York, March (1967)
- 7 M E Banks, W D Lusk and R S Ottinger (TRW) 'New chemical concepts for utilisation of waste plastics' EPA Pub No SW16C (1971)
- 8 N L Drobniq, H E Hull and R F Testin (Battelle) Public Health Pub No 1908 (1971)
- 9 R B Engdahl (Battelle) 'Solid Waste Processing' Public Health Service Pub No 1856 (1969)
- 10 Anon, Chem Eng, 77, 88 (June 15 1970)
- 11 Anon, Mod Plast, 47, 50 (1970)
- 12 L L Scheimer, Plast Technol, 11, 37 (1965)
- 13 J E Raus and H J Fralish, Plast Technol, 12, 51 (1966)
- 14 J L Fergas in 'Polythiène' ed by A Remfrew and P Morigin, Interscience, New York, (1960)

- 15 J L Holman (Bureau of Miners, Rolla Mo) see Chem Eng, News, 49, 7, (May 31 1971)
- 16 Private Communication from D Malloy (Lowel Technological Inst)
- 17 J N Sahramm and R R Blanehand 'The use of GPE as a compatibilizer for reclamation of waste plastics materials' presented at Palisades Section SPE RETEC, Cherry Hall, New Jersey, October (1970), copies available from authors at Dow Corning Chemical Co, Plaquemine La
- 18 W A Mack (Wevner and Pfeleiderer) 'Recycling waste plastics at a profit' presented at National Conference on Waste Recycling Denver, 1971, also see Anon, Chem Eng News, 49, 7 (May 31 1971)
- 19 M Franz, Compost Sci, 11, 4, (1970)
- 20 D G Wilson, Compst Sci, 11, 3 (1970) and S D Senturia, K H Lewis, D G Wilson, H Hibberd and F Winker, Compost Sci, 12, 6 (1971)
- 21 Anon, Plast Technol, 11, 17 (1965)
- 22 Anon, SPEJ, 27, 23 (1971)
- 23 'Packaging Review' (1976) UK
- 24 D R Paul 'Reuse of plastics recovered from solid wastes' progress report to EPA (May 1971)
- 25 M Maramatsu, Int Poly Sci and Tech, vol 2, No 1, p 99 (1975)
- 26 R J Sperker and S L Rosen, Poly Eng And Sci, April (1976) vol 16, no 4
- 27 D R Paul, C E Vinson and C E Locke, Poly Eng Sci, 12, 157 (1972)
- 28 M Matsuo, Japan Plast, 2 July 1968, 6
- 29 G E Malau and H Kestkala, App Polym Symp, 7, 35 (1968)
- 30 V Huelck and M Covitch, (1971) unpublished, Lehigh Univ

- 31 H Keskkula and P A Traylor (1967) *J App Poly Sci*, 11, 2361
- 32 A Ghaffar, A Scott and G Scott, *Int Symp on Degradation and Stabilisation of Polymers*, p 193
- 33 A Ghaffar, A Scott and G Scott, *Eur Poly J*, vol 13, 83 (1977)
- 34 A Ghaffar, A Scott and G Scott, *Eur Poly J*, vol 13, 89 (1977)
- 35 M Bear, (1962) US Pat 3,041,306
- 36 M Bear, (1962) US Pat 3,041,308
- 37 M Bear, (1962) US Pat 3,041,309
- 38 M Bear (1964), *J Pol Sci, A-2*, 2, 417
- 39 F A Voery, I M Kolthoff, A I Medalia and E J Mechan, (1965) *Emulsion Polymerisation (High Polymer Series IX)*, Interscience
- 40 E W Duck (1970), *Br Poly J*, 2, 60
- 41 M R Grancio (1971) *Poly Preprints*, 12, 68, 681
- 42 K Kato (1968) *Japan Plastics* 2 (April) 6
- 43 M Matsuo (1969) *Poly Eng Sci*, 9, 206
- 44 G Scott and M Tahan, *Eur Poly J*, vol 13, 981 (1977)
- 45 R P Petrich (1972) Impact reinforcement of polyvinyl chloride, paper presented at SPE RETEC meeting, Cleveland, Ohio, 7 March (1972) (also presented at *Polymer Conf Series, Mechanical Behaviour of Polymers*, Univ of Utah, June 1974)
- 46 C F Ryan (1972) US Pat 3,678,133
- 47 M Kryorewski and A Galeski, *J App Poly Sci*, vol 15, (1971) 1139
- 48 S Omogi, T Asada and A Tanaka, *J Poly Sci*, vol A-2, no 7, 171 (1969)
- 49 S Omogi, T Asada and A Tanaka, paper A8.10 presented at the *Int Symp on Polymer Chemistry*, Toronto (1968)
- 50 R J Kern, *J Poly Sci*, 21, 19 (1956)
- 51 A D Melstyre, *J App Poly Sci*, 7, 29 (1963)
- 52 G Gee, *Rubb Chem and Tech*, 18 (1943) 71
- 53 P A Small, *J App Chem*, 3, 71 (1953)

- 54 G E Molau, *J Poly Sci*, 34 (1956) 1276
- 55 T R Paxton, *J App Poly Sci*, 7 (1963) 1499
- 56 M Matsuo, G Nozaki and Y Jyo, *Poly Eng Sci*, 9 (3) 197 (1969)
- 56a L Bohn (1966) *Kolloid 22 Polym* 213, 55
- 56b L Bohn (1966), *Rubb Chem Tech*, 41, 495
- 56c S Krause (1972) *J Macromol Sci Rev Macromol Chem*, C7, 251
- 57 M Takajanagi (1963), *Mem Fac Energ, Kyushi Univ* 23, 11
- 58 L E Nielsen (1953), *J Am Chem Soc*, 74, 1435
- 59 W Breuers, W Hild and H Wolff (1954), *Plaste Kautsch*, 1, 170
- 60 L E Nielsen (1962), *Mechanical Properties of Polymers*, Reinhold, 177, (b) 171 (c) 175
- 61 L J Hughes and G L Brown, (1961), *J App Poly Sci*, 5, 580
- 62 L H Sperling, D W Taylor, M L Kirkpatrick, H F George and D R Bardman (1970), *J App Poly Sci*, 14, 73
- 63 M Bear, (1964), *J Poly Sci*, A-2, 2, 417
- 64 E P Cizak (1968) *US Pat* 3,383,435
- 65 J Staelting, F E Karasz and W J Macknight (1969) *Poly Preprints*, 10, 628
- 66 W J Macknight, J Staelting and F E Karasz (1971) in *Multicomponents Polymer Systems (A & V Chem Series No 99)* Platzer, NAJ, ed Chapter 3
- 67 M Bank, J Leffingwell and C Thies (1969), *J Poly Sci*, A-27, 795
- 68 J V Koleske and R D Lundberg (1969) *J Poly Sci*, A-27, 795
- 69 K Schmeider (1962), *Kunststoffe*, 1, 5, 7
- 70 E Jinckel and H V Herwing (1963), *Kolloid-Z*, 148, 57
- 71 M L Dannis (1973), *J App Poly Sci*, 7, 231
- 72 S G Turley (1963), *J Poly Sci*, C-1, 101
- 73 R Buchdhal and L E Nielsen (1950) *J App Poly Pphys*, 21, 482
- 74 A A Movsum-Zade (1964) *Vysokmol, Soedin*, 6, 1340
- 75 V J Shimohara (1959) *J App Poly Sci*, 1, 251
- 76 P V Papero, E Kuba and L Roldan (1967) *Text Res J*, 37, 823

- 77 L H Sperling and O W Friedman (1969) *J Poly Sci*, A-27, 425
- 78 L J Hughes and G L Brown (1963), *J App Poly Sci*, 7, 59
- 79 G Holden, E T Bishop and N R Legge (1969) in the proceedings of the Int Rubb Conf, 1967, MacLaren
- 80 W D Niederhauser and W Bauer Jr (1972), US Pat 3,641,199
- 81 W F Billmeyer Jr, Textbook of Polymer Science
- 82 A M Borders, R D Juve and L D Hess, *Ind Eng Chem*, 38, 955 (1946)
- 83 K Satake, *J App Poly Sci*, 14, 1007 (1970)
- 84 G Holden, E T Bishop and N R Legge, *J Poly Sci*, C26, 37, 1969
- 85 J M Charsier and R J P Ranchoux, *Poly Eng Sci*, 11, 381 (1971)
- 86 C B Bucknall and D Clayton, *J Mat Sci*, 7, 202 (1972)
- 87 S Rabimowitz and P Beardmore, *Critical Rev Macromol Sci*, 1,1,1,(1972)
- 88 C G Bangaw, *Adv Poly Ser*, 99, 86 (1971)
- 89 R G Newberg, D W Young and H C Evans, *Mod Plast*, 26, 119 (Dec 1948)
- 90 D W Young, D J Buckley, R C Newberg and L B Turner, *Ind Eng Chem*, 41, 401 (1949)
- 91 K Fujimoto and N Yoshimura, *Rubb Chem Tech*, 4, 1109 (1968)
- 92 R R Emmeh, *Ind Eng Chem*, 36, 730 (1944)
- 93 D W Young, R G Newberg and R M Howlett, *Ind Eng Chem*, 39, 1446 (1947)
- 94 W Albert, *Kunststoffe*, 53, 86 (1963)
- 95 T J Sharp and J A Ross, *Rubb Chem Tech*, 35, 726 (1962)
- 96 R Buchdahl and L E Nielsen, *J App Phys*, 21, 482(1950)
- 97 *Multicomponent Polymer Systems*, ed Robert.F.Gould 1971
- 98 E H Merz, G C Claver and M Bear, *J Poly Sci*, 22, 325 (1956)
- 99 J A Schmitt and H Heskkula, *J App Poly Sci*, 3, 732 (1960)
- 100 R J Angier and E M Fetters, *Rubb Chem Tech*, 38, 1164 (1965)
- 101 K G Rugeh and R H Beck, Jr, *J Poly Sci*, C30, 447 (1970)

- 102 H Keskkula, App Poly Symp, 15, 51 (1970)
- 103 G M Estes, S L Cooper and A V Tobolsky, J Macromol Sci, C4, 313 (1970)
- 104 S L Aggarwal, ed Block Copolymer, Plenum Press, New York (1975)
- 105 M Morton, J E Magrath and P C Julino, J Poly Sci, C26, 99 (1969)
- 106 H A J Batterd^a and G W Tregear, Graft Polymers, Interscience New York (1967)
- 107 N R Langley, Macromol, 1, 343 (1968)
- 108 N R Langley, and J O Ferry, Macromol, 1, 353 (1968)
- 109 E Jenckel, Kolloid Zeit, 136, 142 (1954)
- 110 L E Nielsen, J App Poly Sci, 8, 511 (1964)
- 111 T Murayama and J P Bell, J Poly Sci, A2, 8, 437 (1970)
- 112 J D Ferry, Viscoelastic Properties of Polymers, John Wiley, New York, 2nd Ed (1969)
- 113 W P Cox, R A Isaksen and E H Morz, J Poly Sci, 44, 149 (1960)
- 114 T P Yim, S E Lovell and J D Ferry, J Phys Chem, 65, 534 (1961)
- 115 G Pezzin, G Ajroldi and C Garbuglis, Rheol Acta, 8, 304 (1968)
- 116a Y Oyanogi and J D Ferry, Proc 4th Int Cong
- 116b R Marzin, Viscoelasticity, Phenomenological Aspects, Chap 2, J T Bergen Ed, Acad Press, New York, (1960)
- 117 L E Nielsen, SPE Journal, 525 (1960)
- 118 M U Amin and G Scott, Eur Poly J, 10, 1019 (1974)
- 119 G Scott and M Tahan, Eur Poly J, 13, 997 (1977)
- 120 G Scott, A Ghaffar and A Scott, Europ Poly J, 13, 83 (1977)
- 121 Gillhane, Poly Eng, and Sci, 225 (1967)
- 122 G Scott and M Tahan, Eur Poly J, 13, 989 (1977)
- 123 G Scott and M U Amin, PhD Thesis, Univ of Aston (1976)
- 124 A Lewis and Gillham, J of App Poly Sci, 6, 422, (1962)
- 125 M Matsuo, C Nozki^a and Y Jyo, Poly Eng Sci, 9 (3) 197 (1969)
- 126 A R Shultz, Am Chem Soc Div, Poly Chem, Preprints, 1455 (Sept 1967)

- 127 G Scott, *Eur Poly J Supp*, 189 (1969)
- 128 W L Hawkins (ed) *Polymer Stabilisation*, Wiley Interscience New York and London (1972) (a) Chap 1 (b) Chaps 2 and 4
- 129 F S Johnson, *J Meteorol*, 2, 431 (1954)
- 130 R E Barker Jr, *Photochem Photobiol*, 7, 275 (1968)
- 131 K L Kolřar, *Ultraviolet Radiation*, Wiley, New York (1965) Chap 4
- 132 R F Gould (ed) *Stabilisation of Polymers and Stabilisation Process*, *Ad Chem Ser*, 85, Am Chem Soc, Washington DC (1968) Chap 19
- 133 R A George, D H Martin and E G Wilson, *J Phys*, C5, 871 (1972)
- 134 R H Partridge, *J Chem Phys*, 45, 1679 (1961)
- 135 F H Winslow and W L Hawkins, *Some Weathering Characteristics of Plastics*, *App Poly Symp*, 4, 29 (1967)
- 136 G Scott, *Chem and Ind*, 7, 271 (1963) and Ref 123
- 137 C S Kujiraj, A Hashiy, K Shibuya and K Nishio, *Photochemistry of polypropylene, I a fundamental react chem High Polymer (Tokyo) 25*, 193 (1968)
- 138 J G Calvert and J N Pitts Jr, *Photochemistry*, 270, New York Wiley and Sons (1966)
- 139 P J Briggs and J F McKellar, *Mechanism of Photostabilisation of polypropylene by nickel oxime chelates*, *J App Poly Sci*, 12, 1825 (1968)
- 140 A Charlesby and R H Partridge, *The identification of luninescence centres in polyethylene and other polymers*, *Proc Roy Soc (London) A288*, 312 (1965); *Thermoeluminescence and phosphorescence in polyethylene under uv radiation*, *Proc Roy Soc (London) A283*, 329 (1965)
- 141 S A Pinner, *Weathering and degradation of plastics*, London Columbia Press, (1966)

- 142 O S Cicchetti, C G Fontani, Gratani, Influence di compositi del Ti^{IV} Sull'Ossidazione di modelli del polipropilene, unpublished results
- 143 A R Burges, Polymer Degradation Mechanisms, Natl Bur St Circ, 525, 149 (1953)
- 144 J G Calvert and J N Pitts, Jr, Photochemistry, 441, NY, Wiley and Sons Inc (1966)
- 145 R C W Norrish and M H Searby, Proc Roy Soc, London, A237, 464 (1956)
- 146 L Bateman and G Gee, Trans Farad Soc, 47, 155 (1951)
- 147 D J Carlsson and D M Wiles, (a) Macromolecules 2 (6) 587 597 (1969), (b) ibid, 7, 259 (1974)
- 148 G Scott, Atmospheric Oxidation and Antioxidants, Elsevier, London and New York (1965) (a) Chap 3, (b) Chap 2, (c) Chap 4 and (d) Chap 5
- 149 M U Amin, G Scott and L M K Tillekeratne, Eur Poly J, 11, 85 (1975)
- 150 D C Mellor, A B Moir and G Scott, Eur Poly J, 9, 219 (1973)
- 151 G V Hutson and G Scott, Chem and Ind, 725 (1972); Eur Poly J, 10, 45 (1974)
- 152 G Scott, Coatings and Plastics Preprints, Am Chem Soc, (Philadelphia) 35, No 1, 163 (1975)
- 153 For reviews of this nomenclature see Noyes W A Jr, G S Hammond and J N Pitts Jr, Ad in Photochem, vol 1, Chap 1, New York, Interscience Pub Inc (1963)
- 154 C H Bamford and R G W Norrish, J Chem Soc, 1504 (1935)
- 155 J E Guillet and R G W Norrish, Proc Roy Soc, 233, 153 (1955)
- 156 P J Wagner and G S Hammond, J Am Chem Soc, 87, 4009 (1965), J Am Chem Soc, 86m 1245 (1966)
- 157 C H Nicol and J E Calvert, J Am Chem Soc, 89, 1790 (1967)
- 158 N C Young and Eu D Feit, J Am Chem Soc, 90, 504 (1968)

- 159 R Srinivasan, *J Am Chem Soc*, 81, 5061 (1969)
- 160 G R McMillan, J G Calvert and J N Pitts, Jr, *J Am Chem Soc*, 86, 3602 (1964)
- 161 F O Rice and E Teller, *J Chem Phys*, 6, 489 (1938)
- 162 W Davis Jr and W A Noyes Jr, *J Am Chem Soc*, 60, 2153 (1947)
- 163 J L Bolland, *Quart Rev (Lond)* 3, 1 (1949)
- 164 G E Franic, *Chem Rev*, 46, 155 (1950)
- 165 L Bateman, *Quart Rev*, 8, 147 (1954)
- 166 O Cicchetti, *Ad Poly Sci*, 7, 70 (1970)
- 167 B D Fesner (1965), *J App Poly Sci*, 9, 3701
- 168 T Hirai (1970) *Japan Plast* 4 (October) 22
- 169 J Shimada and K Kalavki, (1968), *J App Poly Sci*, 12, 671
- 170 N Grassie, I C McNeill and I J Cooke, *J App Poly Sci*, 12 (1968)
- 171 I C McNeill, and D Nell, *Eur Poly J*, 6 (1970) 143
- 172 I C McNeill and D Nell, *Eur Poly J*, 6 (1970) 569
- 173 Y Mizutani, S Matsuoka and K Yamamoto, *Bull Chem Soc, Japan*, 38 (1965) 2045
- 174 A Jamieson and I C McNeill, *J Poly Sci, Part A1*, (1974) 387, 12
- 175 A Jamieson and I C McNeill, *J Poly Sci, Part A1*, (1976) 603, 14 and Ref 174
- 176 A Jamieson and I C McNeill, *J Poly Sci, Part A1*, (1976), 1839, 14
- 177 J L Bolland, *Trans Farad Soc*, 46, 358 (1950)
- 178 K T Paul, *RAPRA Bull*, 2, 29 (1972)
- 179 K T Paul, *RAPRA Members J*, Nov (1963) 273-281
- 180 *Plastics films*, ed J.H.Briston, page 21
- 181 A. Renfrew and ^{P.}/_K Morgan, *Polyethylene (Lond)* (1957), 169
- 182 F M Rugg, J J Smith and R C Bacon, *J Poly Sci*, 13, 535 (1954)
- 183 F H Lohmann, *J Chem Ed*, 32, 155 (1955)
- 184 Ewing, *Instrumental methods of chemical analysis*, McGraw Hill, (1960) 82
- 185 Z Manasek et al, *Rubb Chem Tech*, 36 532 (1963)

- 186 W C Geddes, *Eur Poly J*, 3, 733 (1964)
- 187 J P Luongo, *J Poly Sci*, 42, 139 (1960)
- 188 J C W Chien and C R Boss, *J Poly Sci*, A1, 10, 1579 (1972)
- 189 J A Brydson, *Plast Mat*, Butterworth, 1966, Chap 10, p189
- 190 L H Cross, R B Richard and H A Willis, *Dis Farad Soc*, 9, 235 (1950)
- 191 J J Fox and A E Martin, *Proc Roy Soc*, A175 208 (1940)
- 192 A Elliot, E J Ambrose and R B Temple, *J Chem Phys*, 16, 877 (1948)
- 193 F M Rugg, J J Smith and L H Waterman, *J Poly Sci*, 11, 1 (1953)
- 194 W M Bryant and R C Voter, *J Am Chem Soc*, 75, 6113 (1953)
- 195 C W Bunn, *Trans Farad Soc*, 35, 482 (1939)
- 196 *The Science and Technology of Polymer Fibres*, Book, Chap 2, 131
- 197 K B Chakraborty and G Scott, *Eur Poly J*, 13, 98 (1977)
- 198 K B Chakraborty and G Scott, *Eur Poly J*, 13, 731 (1977)
- 199 K B Chakraborty and G Scott, *Eur Poly J*, 1007, 13 (1977)
- 200 G Scott, Ultraviolet light induced reaction of polymers (ed S S Labana) *ACS Symp Ser*, No 25, 340 (1976)
- 201 A Ghaffar, A Scott and G Scott, *Eur Poly J*, 12, 615 (1976)
- 202 Oaka and Richards, *J Chem Soc*, 2429 (1949)
- 203 B J Baun, *J App Poly Sci*, 2, 281 (1959)
- 204 Aggarwell and Sweeting, *Chem Rev*, 57, 665 (1957)
- 205 Bellamy, *The infra-red spectra of complex molecules* (1957)
- 206 D L Wood and J P Loungo, *Mod Plast* 38, 132, 1961
- 207 Irvin and co-workers, *Chem Phys J*, 25, 549 (1956)
- 208 L E Nielsen (1962) *Mechanical properties of Polymers*, Reinhold, Chaps 2 and 4
- 209 A Ghaffar, A Scott and G Scott, *Europ Poly J*, 11, 271 (1975)
- 210 G Scott, M Tahan and J Vyvoda, *Chem and Ind*, 903 (1976)

- 211 Turi et al, ACS Polymer Preprints, 5, 538 (1964)
- 212 L M Gan and G Scott, unpublished work
- 213 Winslow, Matreyek and Trozzolo, Polymer Preprints, 10(2)
1271 (1969)
- 214 ^{J.} Luongo and ^{R.} Salorey, J App Poly Sci, 7, 2307 (1963)
- 215 ^{Z.} Osawa, ^{m.} Suzuki and ^{y.} Ogierara, J Macromol Sci Chem (1971)
A5(2) 275
- 216 R K Jenkins, J Poly Sci, Poly Lett, 2, 999 (1964)
- 217 J E Bonkowi, Textil Res J, 39, 243 (1969)
- 218 Mod Plast Int, 1972, 2(10), 20
- 219 ^{K.} Abe and ^{K.} Yanagishawa, J Poly Sci, 36 (1959) 536
- 220 C Y Liang, M R Lytton and C J Boone, J Poly Sci, 44, 459 (1969)
- 221 W Heinen, Makromol Chem, 16, 213 (1955)
- 222 G Natta, Makromol Chem, 16, 213 (1955)
- 223 T Miyazawa, J App Poly Sci, 3, 302 (1960)
- 224 J P Lyongo, J Poly Sci, 3, 302 (1960)
- 225 P Blair, D J Carlsson and D M Wiles, J Poly Sci, A1, 10, 1007
(1972)
- 226 G Natta, A Volvassori, G Ciampelli, G Mazzanti, J Poly Sci,
A3, 1965, 1
- 227 R H J Hughes, App Poly Sci, 1959, 13, 417
- 228 J H Adams, J Poly Sci, Part A1, 8, 1279 (1970)
- 229 G Geuskens (ed) Degrad and Stab of Polymers, App Sci Pub,
1975, Chap 5
- 230 D J Carlsson and D M Wiles, Macromolecular, 2, 257 (1969)
- 231 A M Trozzolo and F H Winslow, Macromolecular, 1, 98 (1968)
- 232 N S Allen, R B Cundall, M W Jones and J F McKellar, Chem
and Ind, 110 (1976)
- 233 D J Carlsson, A Garton and D M Wiles, Macromolecules,
9, No 5, 695 (1976)
- 234 N M Emanuel, J Poly Sci, Symp No 51 69 (1975)

- 235 W J McGill and J Fourie, *J App Poly Sci*, 19, 879 (1975)
- 236 C D Han and T C Yu, *App Polym Sci*, 15, 1163 (1971)
- 237 C E Locke and D R Paul, *J App Poly Sci*, 17, 2597 (1973)
- 238 R L Jalbert and J P Smejkal, *Mod Plast Encyc*, 108 (1976)
- 239 C D Han, C A Villamizer and Y W Kim, *J App Poly Sci*, 21, 353 (1971)
- 240 J L Work, *Eng Sci Polym*, 13, 36 (1973)
- 241 A Ghaffar, G Scott and P Crowther, *Eur Poly J*, *Europ. Polym. J.* 14, 631 (1977)
- 242 E H Kerner, *Proc Phys Soc Lond*, 4913, 808 (1956)
- 243 T T Jones, *J Poly Sci*, C16, 3845 (1968)
- 244 M Matsuo, A Ueda and Y Kondo, *Poly Eng Sci*, 10, 253 (1970)
- 245 G C Karas and B Walburton, *Trans Plast Inst*, 30, 198 (1962)
- 246 E R Wagner and L M Robeson, *Rubb Chem Tech*, 43, 1129 (1970)
- 247 H Keskkula, S G Turley and R F Boyer, *J App Poly Sci*, 15, 351 (1971)
- 248 G Cigna, *J App Poly Sci*, 14, 1781 (1970)
- 249 D. Bohme, *J App Poly Sci*, 12, 1097 (1968)
- 250 R W Gray and N G McCrum, *J Poly Sci*, A2, 7, 1329 (1969)
- 251 L E Nielsen, *Trans Soc Rheol*, 13, 141 (1969)
- 252 B Ranby and J E Rabek, *Photodegradation, photo-oxidation and photostabilisation of polymers*, 192
- 253 *Developments in Polymer Degradation -1*, ed N Grassie, Chap 6, 174
- 254 J D Burent, R G J Miller and H A Willis, *J Poly Sci*, 15, 592 (1955)
- 255 F Chevassus and R de Broutelles, *The Stabilisation of PVC*, Arnold, (1963) Chap 1
- 256 G Ayrey, B C Head and R C Poller, *J Poly Sci, Macromol Rev*, 8, 1 (1974)
- 257 Z Mayer, *J Macromol Sci, Rev Macromol Chem*, 10, 263 (1974)
- 258 D Braun, *Degradation and Stabilisation of polymer*, ed G Geuskens, Wiley, New York, (1975) p.23- 41
- 259 M M Zafar and R Mahmood, *Europ Polym J*, 12, 333, (1976)

- 260 V p Gupta and L E St Pierre, J Polym Sci, Polym Chem ed, 11 1841 (1973)
- 261 B Dodson and I C McNeill, J Polym Sci, Polym Chem ed , 14 353 (1976)
- 262 R A Papka and V S Pudov, Polym Sci , USSR, Eng Trans 16, 1636 (1974)
- 263 I K Varma and S S Grover, Makromol Chem, 175, 2515 (1974)
- 264 K P Nolan and J S Shapiro, J Chem Soc, Chem Commun 490 (1975)
- 265 G Scott, M Tahan and J Vyvoda, Chem and Ind 903 (1976)
- 266 J H Raley, F F Rust and W D Vaughan, J Am Chem Soc, 70, 2767, (1948)
- 267 Scott and Cooray, unpublished work
- 268 C B Bucknall, Brit Plast, Nov 1967
- 269 Polymer Blends and composites ,J.A Manson and L H Sperling
- 270 A Plochocki, Polimery,7(6),218 (1962)Cited Zh Khim.1963 abs 24T35
- 271 A Plochocki, Polimery, 10(1),23 (1965)
- 272a A Plochocki,and Z Kohman, Polimery,11(9), 403(1966)
- 272b A Plochocki,and Z KOhman,Polimery, 12 (1),16 (1967) (cited CA67 :5454h)
- 273 A Plochocki, Z Z Kolloid, Polymer,208(2),168(1966) (cited CA65:5549)
- 274 A Plochocki, Plast U Kautschck, 13(2),71(1966)(cited E166-2184-2)
- 275 V N Kulezney, I V Konyukh, G V Vinogradov and I P Dmitrieva, Colloid J USSR,27(4), 259(1965)
- 276 O S Noel and J F Carley, Polym Eng and Sci,1975,No2
- 277 G L Slonimskii, I N Musayelyan, V V Kazantsevi and B M Ozerov, Poly Sci USSR, 6(5)900 (1964)
- 278 Mechanical properties of polymers and composites,vol2, ed E Lawrence, Nielsen, Chap 7, 1962
- 279 W M Speri and G R Patrick, Poly Eng Sci, 15,608(1975)
- 280 W M Barentsen, D Heikens and P Piet, Polymer 1974, 15, February,119

- 281 W M Barentsen, D Heikens and P Piet, *Polymer*, 1974, 15, February, 119
- 282 W M Barentsen and D Heikens, *Polymer*, 1977, 18, January 69
- 283 R A M Arie Moshe Narkis and J Kost, *Poly Eng Sci*, April 1977, 17, No 4
- 284a K Ziegel, J Romanoff, *J App Poly Sci*, 1973, 17, (4) 1133
- 284b J A Kerr, *Chem Rev*, 66, 465 (1966)
- 285 A Scott and G Scott, PhD Thesis, Univ of Aston (1976)
- 286 Ref 148, p 250
- 287 Plant and Scott *Eur Poly J*, 7, 1173 (1971)
- 288 Instruction Manual for Rheovibron DDVII Toyo Measuring Instruments Co Ltd, Tokyo (1969)
- 289 K B Chakraborty and G Scott, PhD Thesis, Univ of Aston (1977)
- 290 R W Gray and N G McCrum, *J Poly Sci A2*, 7, 1329 (1969)
- 291 J Vyvoda and G Scott, PhD Thesis, Univ of Aston (1976)
- 292 G Scott, M Tahan, J Vyvoda, *Eur Poly J*, 14, 1021 (1978)